

Investigation of plastic related organic chemicals in the marine environment

Dissertation

with the aim of achieving a doctoral degree

at the Faculty of Mathematics, Informatics and Natural Sciences

Department of Earth Sciences

at Universität Hamburg

submitted by

Lijie Mi

Hamburg, 2024

Department of Earth Sciences

*Date of Oral Defense: 06.12.2024

Reviewers: PD Dr. Thomas Pohlmann
Dr. Zhiyong Xie

Members of the examination commission: Chair PD Dr. Thomas Pohlmann
Dr. Zhiyong Xie
PD Dr. Birgit Gaye
Prof. Dr. Bernd Leidl
Prof. Dr. Gerhard Schmiedl

Chair of the Subject Doctoral Committee

Earth System Sciences: Prof. Dr. Hermann Held

Dean of Faculty MIN: Prof. Dr.-Ing. Norbert Ritter

Eidesstattliche Versicherung | Declaration on Oath

Hiermit erkläre ich an Eides statt, dass ich die vorliegende Dissertationsschrift selbst verfasst und keine anderen als die angegebenen Quellen und Hilfsmittel benutzt habe.

I hereby declare upon oath that I have written the present dissertation independently and have not used further resources and aids than those stated.

A handwritten signature in black ink, appearing to read 'Lijie Mi', written in a cursive style.

Ort, den | City, date

Geesthacht, 06.07.2024

Unterschrift | Signature

Lijie Mi

Abstract

Phthalate esters (PAEs) and organophosphate esters (OPEs) are widely used as plasticizers and flame retardants in various industrial and consumer products, making them ubiquitous in the environment. Both PAEs and OPEs persist in the environment and can accumulate in organisms. They are currently of environmental concern due to their toxicity and endocrine-disrupting effects. Understanding their distribution and transport in marine environments is very important for assessing their environmental impact and developing mitigation strategies. This study aims to enhance our understanding of the distribution patterns and transport mechanisms of PAEs and OPEs in the Chinese marginal seas, with a particular focus on the roles of air-sea exchanges in these processes.

In the South China Sea, atmospheric concentrations of OPEs ranged from 66 to 550 pg/m^3 , while seawater concentrations averaged $1180 \pm 910 \text{ pg/L}$. Air-sea exchange fluxes indicated volatilization of some OPEs and deposition of others. Atmospheric particle deposition fluxes ranged from 5 to 71 $\text{ng/m}^2/\text{day}$. The input of ΣOPEs via atmospheric deposition was estimated at $22 \pm 19 \text{ tons/year}$, with net fluxes indicating volatilization from seawater to air at $44 \pm 33 \text{ tons/year}$.

PAEs were measured in the air and seawater of the Bohai and Yellow Seas in spring 2019. Atmospheric PAE concentrations ranged from 9.59 to 51.3 ng/m^3 , with seawater concentrations averaging $466 \pm 268 \text{ ng/L}$. In summer 2019, PAEs in the South China Sea showed atmospheric concentrations ranging from 2.84 to 24.3 ng/m^3 and seawater concentrations averaging 3.05 ng/L . Monsoon currents and cyclones significantly influence their concentrations and transport. The input of ΣPAEs via atmospheric deposition was about $579 \pm 222 \text{ tons/year}$, with net fluxes showing a predominance of PAEs moving from seawater to air at $1540 \pm 1430 \text{ tons/year}$ in the Bohai and Yellow Seas. In the South China Sea, net atmospheric depositions were 3740 tons/year for DMP, DEP, DiBP, and DnBP, and DEHP volatilization was 900 tons/year . Additionally, sedimentation has been identified as a significant sink for PAEs in the Bohai and Yellow Seas, with an inventory of 20.73 tons/year in the Bohai Sea and 65.87 tons/year in the Yellow Sea. These results suggest that air-sea exchange and atmospheric deposition are important processes in the transport of PAEs and OPEs in the Chinese marginal seas.

Zusammenfassung

Phthalatester (PAEs) und Organophosphatester (OPEs) werden häufig als Weichmacher und Flammschutzmittel in verschiedenen Industrie- und Konsumgütern verwendet, was sie zu allgegenwärtigen Umweltverschmutzern macht. Sowohl PAEs als auch OPEs persistieren in der Umwelt und können sich in Organismen anreichern. Aufgrund ihrer Toxizität und endokrinen Disruptionswirkung stellen sie derzeit ein Umweltrisiko dar. Das Verständnis ihrer Verteilung und ihres Transports in marinen Umgebungen ist entscheidend, um ihre Umweltauswirkungen zu bewerten und Minderungsstrategien zu entwickeln. Diese Studie zielt darauf ab, unser Verständnis der Verteilungsmuster und Transportmechanismen von PAEs und OPEs in den chinesischen Randmeeren zu verbessern, mit einem besonderen Fokus auf die Rolle des Luft-See-Austauschs in diesen Prozessen.

Im Südchinesischen Meer lagen die atmosphärischen Konzentrationen von OPEs zwischen 66 und 550 pg/m^3 , während die Konzentrationen im Meerwasser durchschnittlich $1180 \pm 910 \text{ pg/L}$ betragen. Die Flüsse des Luft-See-Austauschs zeigten die Verdampfung einiger OPEs und die Ablagerung anderer. Die Flüsse der atmosphärischen Partikelablagerung lagen zwischen 5 und 71 $\text{ng/m}^2/\text{Tag}$. Der Eintrag von $\sum\text{OPEs}$ durch atmosphärische Ablagerung wurde auf 22 ± 19 Tonnen/Jahr geschätzt, wobei die Nettoflüsse eine Verdampfung aus dem Meerwasser in die Luft von 44 ± 33 Tonnen/Jahr anzeigten.

PAEs wurden im Frühjahr 2019 in der Luft und im Meerwasser des Bohai- und Gelben Meeres gemessen. Die atmosphärischen PAE-Konzentrationen lagen zwischen 9,59 und 51,3 ng/m^3 , mit Meerwasserkonzentrationen von durchschnittlich $466 \pm 268 \text{ ng/L}$. Im Sommer 2019 zeigten PAEs im Südchinesischen Meer atmosphärische Konzentrationen zwischen 2,84 - 24,3 ng/m^3 und Meerwasserkonzentrationen von durchschnittlich 3,05 ng/L . Monsunströme und Zyklone beeinflussen ihre Konzentrationen und ihren Transport erheblich. Der Eintrag von $\sum\text{PAEs}$ durch atmosphärische Ablagerung betrug etwa 579 ± 222 Tonnen/Jahr, wobei die Nettoflüsse zeigten, dass PAEs überwiegend vom Meerwasser in die Luft transportiert wurden, und zwar mit 1540 ± 1430 Tonnen/Jahr im Bohai- und Gelben Meer. Im Südchinesischen Meer betragen die Netto-Atmosphärenablagerungen 3740 Tonnen/Jahr für DMP, DEP, DiBP und DnBP, während die DEHP-Verdampfung 900 Tonnen/Jahr betrug. Darüber

hinaus wurde die Sedimentation als ein bedeutender Senken Prozess für PAEs im Bohai- und Gelben Meer identifiziert, mit einem Bestand von 20,73 Tonnen/Jahr im Bohai-Meer und 65,87 Tonnen/Jahr im Gelben Meer. Diese Ergebnisse deuten darauf hin, dass der Luft-See-Austausch und die atmosphärische Ablagerung wichtige Prozesse beim Transport von PAEs und OPEs in den chinesischen Randmeeren sind.

Acknowledgements

I express my sincere gratitude to the China Scholarship Council and Helmholtz-Zentrum Hereon for their financial support, which made this meaningful work possible.

It is my genuine pleasure to express my deep gratitude to my supervisor, Dr. Thomas Pohlmann, who provided reliable and efficiency supervision and guidance on my work.

Several members of Helmholtz-Zentrum Hereon played crucial roles in helping me get to where I am today, and a few deserve special mention.

In particular, I extend my heartfelt thanks to my supervisor, Dr. Zhiyong Xie, who supported my research interests, connected me with collaborators, provided timely feedback, and guided my research to a comprehensive level. Over the past eight years, I have been extremely honoured to have him as a role model for a scientist and a mentor.

Thank Prof. Ralf Ebinghaus, Dr. Jürgen Gandraß, Dr. Hanna Joerss and Danijela Koetke for their kind support in completing this work. Thank Rui Shen for patiently taking care of me when we were in the cruise at the North Sea and also for her smart advice and novel perspectives. Many thanks to my colleagues at Hereon, Doris Schnalke, Andreas Wittmann, Freya Debler, Koketso Michelle Molepo and Frank Menger, who were brilliant companions on this journey. I received much help from them. Thank Mr. Uwe Benn, Ms. Anne Hartlich and Angela Kiehn-Kupke from the Welcome Office for their kindness and selfless help towards international students.

I would like to give special mention to Dr. Jianhui Tang from the Yantai Institute of Coastal Zone Research. I am thankful for his support of my decision to pursue a Ph.D. in the ocean science, which led me here. He assisted me securing funding from the CSC and facilitated my participation on board the China research vessel Beidou for the investigation of the Bohai and Yellow Seas, which is a significant part of my Ph.D. work.

I am grateful to Dr. Weihai Xu, Lulu Zhang from South China Sea Institute of Oceanology Chinese Academy of Sciences, Prof. Dr. Joanna J. Waniek from Leibniz Institute for Baltic Sea Research. Thanks for the field assistance and the excellent work onboard the research vessel SONNE, as well as constructive suggestions during our collaboration on papers.

I also appreciate the long-term support from my relatives, especially my parents, and all my friends. They have been a special pillar of support that has shaped this achievement. During those tough pandemic times, the unconditional support of family has never felt more important. They helped me remain strong through all the difficulties. Without their company, I could not have put together this thesis.

Acronym list

Acronym	Definition
BBP	butylbenzyl phthalate
BTs	back trajectories
BYSs	Bohai and Yellow Seas
DCHP	dicyclohexyl phthalate
DCM	dichloromethane
DEHP	di(2-ethylhexyl) phthalate
DEP	diethyl phthalate
DiBP	diisobutyl phthalate
DMP	dimethyl phthalate
DnBP	di-n-butyl phthalate
DnNP	dinonyl phthalate
DnOP	dioctyl phthalate
EHDPP	2-ethylhexyl diphenyl phosphate
EPA	Environmental Protection Agency
EU	European Union
GC	gas chromatograph
GFF	glass fiber filter
LOQ	limit of quantification
LRAT	long-range atmospheric transport
MDLs	method detection limits
MS	mass spectrometer
OPEs	organophosphate esters
PAEs/PEs	phthalate esters
PAH	polyaromatic hydrocarbons
PBDEs	polybrominated diphenyl ethers
PCBs	polychlorinated biphenyls
QFF	quartz fiber filter
SCSs	South China Sea
SPM	suspended particulate matter
TBEP	tris(2-butoxyethyl) phosphate
TCEP	tris(2-chloroethyl) phosphate
TCIPP	tris(2-chloroisopropyl) phosphate
TDCIPP	tris(1,3-dichloro-2-propyl) phosphate
TEHP	tris(2-ethylhexyl) phosphate
TEP	triethyl phosphate
TIBP	tri-iso-butyl phosphate
TNBP	tri-n-butyl phosphate
TOCs	total organic carbons
TPHP	triphenyl phosphate
TPrP	tripropyl phosphate

Contents

Abstract.....	III
Zusammenfassung.....	IV
Acknowledgements.....	VI
Acronym list.....	VIII
Contents	1
List of Figures	5
List of Tables	7
1 Introduction.....	10
1.1 Application of Phthalate Esters and Organophosphate Esters	10
1.2 Transport Pathways of PAEs and OPEs to the Marginal Seas.....	12
1.3 Riverrun Transport of PAEs and OPEs from Land to the Marginal Seas.....	17
1.4 Atmospheric Transport.....	18
1.5 Air-Sea Exchange.....	19
1.6 Occurrences of PAEs and OPEs in the Marine Environment	20
1.6.1 Occurrences of PAEs and OPEs in Seawater	20
1.6.2 Occurrences of PAEs and OPEs in Air.....	23
1.6.3 Occurrences of PAEs and OPEs in Sediment	26
1.7 Photo- and Biodegradation Processes of PAEs and OPEs.....	29
1.8 Objectives of This Work	31
1.9 Summary	32
1.10 Prospectives for Future Work.....	34
2 Air–Sea Exchange and Atmospheric Deposition of Phthalate Esters in the South China Sea	36
2.1 Introduction	37
2.2 Materials and Methods	38

2.2.1	Collection of Samples	38
2.2.2	Sample Preparation and Instrument Analysis.....	39
2.2.3	Quality Assurance and Quality Control.....	40
2.2.4	Air Mass Back Trajectory	41
2.2.5	Data Analysis	41
2.3	Results and Discussion.....	41
2.3.1	PAEs in Air	41
2.3.2	Spatial Distribution of PAEs in Air	42
2.3.3	Gas/Particle Partitioning	43
2.3.4	Washout Ratio.....	44
2.3.5	PAEs in Seawater.....	45
2.3.6	Water-Suspended Particular Matter Partitioning	46
2.3.7	Environmental Source of PAEs	47
2.3.8	Air-Sea Exchange	49
2.3.9	Atmospheric Particle Deposition	51
2.3.10	Atmospheric Dry Flux	52
2.4	Implications.....	53
	Supporting Information.....	53
3	Organophosphate Esters in Air and Seawater of the South China Sea: Spatial Distribution, Transport, and Air–Sea Exchange.....	84
3.1	Introduction	85
3.2	Materials and Methods	86
3.2.1	Research Area and Sample Collection.....	86
3.2.2	Chemicals and Reagents	87
3.2.3	Sample Preparation and Instrumental Analysis	88
3.2.4	Quality Assurance/ Quality Control.....	88
3.2.5	Data Analysis	89

3.2.6	Air Mass Back Trajectories (BTs)	89
3.3	Results and Discussion.....	89
3.3.1	Spatial Distribution of OPEs in Air	89
3.3.2	OPE Composition Profile in Air	91
3.3.3	Gas-Particle Partitioning.....	92
3.3.4	OPEs in Seawater.....	93
3.3.5	Spatial Distribution of OPEs in Seawater	95
3.3.6	Suspended Particulate Matter (SPM) Bound OPEs	95
3.3.7	Source Identification	96
3.3.8	Air-Sea Exchange	98
3.3.9	Atmospheric Particle Dry Deposition Fluxes	101
3.4	Implications.....	104
	Supporting Information.....	105
4	Occurrence and Spatial Distribution of Phthalate Esters in Sediments of the Bohai and Yellow Seas.....	130
4.1	Introduction	131
4.2	Materials and Methods	133
4.2.1	Sample Collection.....	133
4.2.2	Extraction, Clean-Up, and Analysis.....	133
4.2.3	Quality Assurance and Quality Control.....	134
4.2.4	Total Organic Carbon (TOC) and Total Inorganic Carbon (TIC) Analysis 135	
4.2.5	Data Analysis	135
4.3	Results and Discussion.....	136
4.3.1	Occurrences and Levels	136
4.3.2	Spatial Distributions.....	137
4.3.3	Comparison to Previous Studies	141
4.3.4	Correlation between PEs and Total Organic Carbon.....	142

4.3.5	Source Identification of PEs	143
4.3.6	Inventory of PEs in the Marine Sediments	144
4.4	Conclusion.....	146
	Supporting Information.....	147
5	Air – Sea Exchange of Phthalate Esters in the Bohai and Yellow Seas	153
5.1	Introduction	154
5.2	Materials and Methods	156
5.2.1	Research Area and Sample Collection.....	156
5.2.2	Sample Preparation and Instrumental Analysis	157
5.2.3	Quality Assurance and Quality Control.....	157
5.2.4	Data Analysis	158
5.2.5	Air Mass Back Trajectories (BTs).....	158
5.3	Result and Discussion	158
5.3.1	PAEs in Air.....	158
5.3.2	PAE Composition Profile	160
5.3.3	Gas-Particle Partitioning.....	161
5.3.4	PAEs in Seawater.....	162
5.3.5	Spatial Distribution of PAEs in Seawater	164
5.3.6	Source Identification.....	164
5.3.7	Air-sea Exchange	166
5.3.8	Atmospheric Particle Dry Deposition Fluxes	168
5.4	Implication	170
	Supporting Information.....	172
	References.....	191

List of Figures

Figure 1-1 Major environmental sources, processing and pathways of organic pollutants in the coastal and open seas	12
Figure 1-2 Comparison of PAEs concentrations in water from different sea areas (ng/L)	20
Figure 1-3 Comparison of OPEs concentrations in surface water from different areas (ng/L)	22
Figure 1-4 Comparison of OPEs concentrations in air from different regions (pg/m ³)	24
Figure 1-5 Comparison of PAEs concentrations in air from different regions (ng/m ³)	26
Figure 1-6 Comparison of PAEs concentrations in sediment from different marine areas (ng/g, dw).....	27
Figure 1-7 Comparison of OPEs concentrations in sediment from different marine areas (ng/g, dw).....	29
Figure 2-1 Spatial distribution of PAEs in the atmosphere (ng/m ³) over the South China Sea. DiBP and DnBP are the predominant PAEs in air samples from A3 to A22, while DEHP prevails in air samples A1 and A2.....	42
Figure 2-2 (A) Spatial distribution of PAEs in seawater of the South China Sea; (B) concentration ranges of individual PAEs (ng/L); and (C) profile of PAEs in individual water samples.....	45
Figure 2-3 Air-sea exchange fluxes of PAEs (ng/m ² /day) are calculated with two-film fugacity mode using paired air-seawater concentrations. The positive (+) value indicates water-to-air volatilization, and negative (-) value means air-to-water deposition. (A) DMP, (B) DEP, (C) DiBP, (D) DnBP, (E) DEHP, and (F) the range of the air-sea exchange fluxes of individual PAEs.....	49
Figure 2-4 Dry deposition fluxes of particle-bound PAEs (ng/m ² /day) to the South China Sea, which were dominated by DiBP and DnBP.	51
Figure 2-5 (A) Annual net dry deposition of particle-bound PAEs (t/y) and (B) the net air-sea exchange fluxes in the South China Sea (t/y). It should be noted that DEHP and DCHP showed net volatilization from water to air.....	52
Figure 3-1 (A) Concentrations of OPEs in the atmosphere (ng/m ³) over the South China Sea. (B) Box chart of OPEs. (C) Composition profile of OPEs. (D) Gas/particle partitioning of OPEs. Air masses originating from the Pacific Ocean and Southeast Asia dominated at the research area.....	90
Figure 3-2 (A) Concentrations of OPEs (without TEP) in seawater of the South China Sea, measured with high-volume water samples. (B) Box chart of OPEs. (C) Distribution of TEP in seawater of the South China Sea, determined with I L water samples using liquid-liquid extraction. (D) Box chart of TEP.	94
Figure 3-3 (A) Heat map for the correlation analysis of OPEs and salinity. (B) Source appointment based on the gradient of the salinities of seawater samples.....	97

Figure 3-4 Air-sea exchange fluxes of OPEs (ng/m ² /day) calculated with two-film fugacity mode using paired air/seawater concentrations. Positive (+) values indicate water to air volatilization, and negative (-) values mean air to water deposition.	101
Figure 3-5 Dry deposition fluxes of particle-bound OPEs (ng/m ² /day) to the South China Sea.	102
Figure 3-6 (A) Annual net dry deposition of particle-bound OPEs (tons/year). (B) Net air-sea deposition in the South China Sea (tons/year). TEP showed net deposition from air to water, while all other OPEs were dominated by water to air volatilization.	103
Figure 4-1 Spatial distribution of Σ ₆ PEs (ng/g) in the surface sediment of the Bohai, Northern and Southern Yellow seas (BS, NYS and SYS).....	137
Figure 4-2 Distributions of DEP, DiBP, DnBP, BBP, DCHP and DEHP (ng/g) in sediment of the Bohai and Yellow seas	139
Figure 4-3 Distribution of PEs comparable to that of TOC in sediment of Bohai and Yellow seas	142
Figure 4-4 Inventory of PEs (ton) in sediment of Bohai (left) and Yellow (right) seas	145
Figure 5-1 Spatial distribution of PAEs in the atmosphere (ng/m ³) over the Bohai and Yellow Seas	159
Figure 5-2 Spatial distribution of PAEs in seawater of the Bohai and Yellow Seas .	163
Figure 5-3 Heat map for the correlation analysis of PAEs and the salinity in seawater (A) and air (B).....	165
Figure 5-4 Air-sea exchange fluxes of PAEs (ng/m ² /day) calculated with two-film fugacity mode using paired air/seawater concentrations. The positive (+) value indicates water to air volatilization and the negative (-) value means air to water deposition.....	167
Figure 5-5 The dry deposition fluxes of particle bound PAEs (ng/m ² /day) to the Bohai and Yellow Seas.....	169
Figure 5-6 A: The annual net dry deposition of particle bound PAEs (ton/year), and B: the net air-sea deposition in the Bohai and Yellow Seas (ton/year)	170
Figure S 2-1 Air sampling stations in the South China Sea, with the blue dots marked at the starting position of each air sample.....	56
Figure S 2-2 (A) Seawater sampling stations in the South China Sea, with the black dots marked at the starting position of each water sample. The color map shows the salinity profile in surface seawater; (B) general water mass circulation in the research area in summer.....	57
Figure S 2-3 A. High-volume air sampler is equipped with quartz fiber filter for atmospheric particles and a PUF/XAD-2 column for gaseous phase. The air sampler is placed at the upper deck and operated with headwind. The Filter and PUF-XAD-2 column are changed at sampling site. The PUF/XAD-2 column can be sealed with glass caps immediately after disconnected from the sampler to eliminate exposure time to the indoor air. The Quartz fiber filter is wrapped in a clean aluminum. PUF/XAD2 columns and filters are stored at -20°C;	58
Figure S 2-4 Air mass back trajectories of air samples. Colors indicate the origin of the air mass parcels	59

Figure S 2-5 The schematic diagrams of the flow field of the South China Sea in 7 th (A) 13 th (B), 19 th (C) and 25 th (D) of August 2019	65
Figure S 3-1 Air sampling stations in the South China Sea, with the blue dots marked at the end position of each air sample	105
Figure S 3-2 High-volume Seawater sampling stations in the South China Sea, with the black dots marked at the starting position of each water sample.....	106
Figure S 3-3 Sampling station for 1-L seawater samples	107
Figure S 3-4 Air mass back trajectories of air samples. Colors indicate the origin of the air mass parcels and their contribution to the air mass	108
Figure S 3-5 The schematic diagrams of the flow field of the South China Sea on 10 th August 2019	111
Figure S 4-1 Correlations between Σ PEs and TOC in research areas	151
Figure S 4-2 Correlation between individual PEs and TOC in research areas	152
Figure S 5-1. Air sampling sites in the Bohai and Yellow Seas are indicated by black dots, representing the initial location for each air sample collection. The voyage commenced from the ports Qingdao-Shanghai-Qingdao, proceeded to the Yellow Sea, and then continued north towards the Bohai Sea.....	172
Figure S 5-2. Seawater collection points in the Bohai and Yellow Seas are denoted by black dots, marking the initial location of each water sample	173
Figure S 5-3. Air mass back trajectories delineate the paths of air samples. Colors denote the source regions of the air mass parcels	174
Figure S 5-4 The salinity of surface seawater in the Bohai and Yellow Seas during the cruise	175

List of Tables

Table 1-1 Physiochemical properties of phthalate esters.....	14
Table 1-2 Physiochemical properties of Organophosphate esters	16
Table 4-1 Concentrations of PEs (ng/g) in sediment of Bohai, northern and southern Yellow Seas.	136
Table 4-2 Comparison of PEs concentrations (ng/g) in this study with those measured in global estuaries and coastal seas	141
Table S 2-1. Detail information for air sampling.....	66
Table S 2-2. Detail information for seawater sampling.....	67
Table S 2-3. Physiochemical properties of seven phthalate esters(Cousins and Mackay, 2000)	68
Table S 2-4. Information about the chemicals and material applied in this work	69
Table S 2-5. Agilent 7890 GC-MS/MS conditions.....	69
Table S 2-6 Detail information for the determination of PAEs using GC-MS/MS.....	70

Table S 2-7. The field blanks and the method detection limits of PAEs in PUF/XAD-2, XAD-2 columns, QFF and GFF filters	71
Table S 2-8. Concentrations of PAEs in the atmosphere over the South China Sea. The MDLs of PAEs calculated with individual sampling volumes are given in brackets for the calculated concentrations less than MDLs.....	72
Table S 2-9. Particle-bound fractions (ϕ) of PAEs in air samples from the South China Sea. The particle-bound fractions are quite uncertain because BBP and DCHP were below MDLs in most particle samples.....	74
Table S 2-10. Washout ratio (W) calculated with particle bound fraction following eq. $W = (1-\phi)(RT/H) + \phi W_p$. BBP and DCHP were excluded because of low detection frequency.....	75
Table S 2-11. Concentrations of PAEs in the seawater from the South China Sea. The MDLs of PAEs calculated with individual sampling volumes are given in brackets for the calculated concentrations less than MDLs.....	76
Table S 2-12. Comparison with previous studies for the concentrations of seven PAEs in seawater (ng/L)	79
Table S 2-13. Particle-bound fractions (ϕ) of PAEs in seawater from the South China Sea.....	80
Table S 2-14. Correlation analysis of PAEs in air	81
Table S 2-15. Correlation analysis of PAEs in seawater	81
Table S 2-16. Air-sea exchange fluxes of PAEs in the South China Sea. Positive value indicates water to air volatilization and negative value indicates air to water deposition	82
Table S 2-17. Particle dry deposition of PAEs in the South China Sea.....	83
Table S 3-1. Detail information for air sampling.....	112
Table S 3-2. Detail information of high-volume seawater samples collected during the cruise SO269 in the South China Sea. Samples were collected through ship-intake system made with stainless steel.....	113
Table S 3-3. Detail information of 1-L seawater samples collected in the South China Sea during the cruise SO269. Water samples were collected from ship intake system and from CTD stations.....	114
Table S 3-4. Physiochemical properties of organophosphate esters.....	115
Table S 3-5. Agilent 7890 GC-MS/MS conditions.....	116
Table S 3-6. The information for determination of OPEs using GC-MS/MS	116
Table S 3-7. The field blanks and the method detection limits of OPEs in PUF/XAD-2, XAD-2 columns, QFF and GFF filters	117
Table S 3-8. Concentrations of OPEs in the atmosphere over the South China Sea .	118
Table S 3-9. Particle-bound fractions (ϕ) of OPEs in air samples from the South China Sea.....	120
Table S 3-10. Concentrations of OPEs in the seawater from the South China Sea...	121
Table S 3-11. Concentrations of OPEs in air of the marine environment (pg/m ³)	123
Table S 3-12. Concentrations of OPEs in surface seawater from previous studies (pg/L)	124

Table S 3-13. Correlation analysis of OPEs in air	126
Table S 3-14. Correlation analysis of OPEs in seawater	127
Table S 3-15. Air-sea exchange fluxes of OPEs in the South China Sea. Positive value indicates water to air volatilization and negative value indicates air to water deposition	128
Table S 3-16. Particle dry deposition of OPEs in the South China Sea.....	129
Table S 4-1 Physicochemical properties of PEs	147
Table S 4-2 PE concentration, TOC and TIC in the sediment of the Bohai, Northern Yellow and Southern Yellow seas	148
Table S 4-3 Correlation between TOC and PE compounds	150
Table S 4-4 Correlations between different PE compounds.....	150
Table S 5-1. Detail information for seawater sampling Detail information for air sampling.....	176
Table S 5-2. Detail information for air sampling (T: air temperature; WS: wind speed; WD: wind direction)	177
Table S 5-3. Physicochemical properties of eight phthalate esters(Cousins and Mackay, 2000)	178
Table S 5-4. Agilent 7890 GC-MS/MS conditions.....	179
Table S 5-5. The detail information for determination of PAEs using GC-MS/MS .	179
Table S 5-6 The field blanks and the method detection limits of PAEs in PUF/XAD-2, XAD-2 columns, QFF and GFF filters	180
Table S 5-7. Concentrations of PAEs in the atmosphere over the Bohai and Yellow Seas.	181
Table S 5-8. Particle-bound fractions (ϕ , %) of PAEs in air samples from the Bohai and Yellow Sea.....	183
Table S 5-9. Concentrations of PAEs in the seawater from the South China Sea. The MDLs of PAEs calculated with individual sampling volume are given in blankets for the calculated concentrations less than MDLs.....	184
Table S 5-10. Comparison with previous studies for the concentrations of 8 PAEs in seawater (ng/L)	187
Table S 5-11 Particle-bound fractions (ϕ) of PAEs in seawater from the Bohai and Yellow Seas	188
Table S 5-12. Air-sea exchange fluxes of PAEs in the Bohai and Yellow Seas. Positive value indicates water to air volatilization and negative value indicates air to water deposition.....	189
Table S 5-13. Particle dry deposition of PAEs in the Bohai and Yellow Seas.....	190

1 Introduction

1.1 Application of Phthalate Esters and Organophosphate Esters

Phthalate esters (PAEs) and organophosphate esters (OPEs) are two classes of chemical compounds with widespread industrial applications, each playing a pivotal role in modern manufacturing and consumer goods. (Schmidt et al., 2020) Their utility areas from the enhancement of material properties to serving as key ingredients in various products, underpinning their global production and usage.(Net et al., 2015; van der Veen and de Boer, 2012)

PAEs, developed in the early 20th century, have been primarily utilized as plasticizers in the production of flexible polyvinyl chloride (PVC). PVC, in its rigid form, is known for its durability and resistance to environmental factors, but it lacks the flexibility required for many applications. The incorporation of PAEs into PVC transforms its physical properties, making it softer and more pliable.(Net et al., 2015) This application is critical in a vast array of products including, but not limited to, medical devices such as blood bags and tubing, consumer goods like toys and packaging, automotive parts, floorings, and wall coverings. Beyond their role in plastics, PAEs find applications in personal care products (as solvents and fixatives in cosmetics and fragrances), adhesives, and coatings, showcasing their versatility and integral role in everyday products.(Staples et al., 1997b) Organophosphate esters have carved their niche primarily as flame retardants and plasticizers in various polymers. Introduced to improve fire safety standards, OPEs are incorporated into electronic devices, furnishings, textiles, and building materials to inhibit or delay the spread of fire. Their mechanism involves altering the chemical reactions occurring during combustion, thus reducing flammability and contributing to fire safety. Besides their use as flame retardants, OPEs are employed in hydraulic fluids as lubricants and in textiles to enhance durability and fire resistance.(Marklund et al., 2003; Möller et al., 2012)

The production of PAEs and OPEs is a testament to the advances in chemical engineering and synthesis. Manufacturers tailor these compounds to exhibit specific characteristics such as molecular weight and plasticizing efficiency, ensuring their efficacy and performance in various applications. The global demand for PEs and OPEs

is driven by the expanding plastic industry, increased safety regulations, and the continuous search for materials that combine performance with safety.(Marklund et al., 2003; Net et al., 2015)

However, the extensive use of these chemicals has raised concerns regarding their impact on human health and the environment. Studies have shown that certain phthalates and organophosphate esters can leach out from products into the environment, leading to their detection in water bodies, soil, and even human tissues.(Armstrong et al., 2018; Gholaminejad et al., 2024; Han et al., 2020; Latini, 2005; Li et al., 2019a; Meyer and Bester, 2004; Zhang et al., 2020a) Concerns include potential endocrine-disrupting effects, toxicity to aquatic life, and bioaccumulation. These issues have prompted regulatory bodies worldwide to assess and, in some cases, restrict the use of specific compounds within these classes. Their ubiquity and persistence raise concerns about potential toxicological impacts on wildlife and human health. Many laboratories' studies have been carried out to explore the toxicity of PAEs and OPEs, shedding light on the mechanisms through which they exert adverse effects and the implications of their pervasive presence. (Staples et al., 1997a; van der Veen and de Boer, 2012; Wang et al., 2019c)

PAEs include a diverse group of chemicals. Their primary route of human exposure is through ingestion, inhalation, and dermal contact, leading to their detection in human blood, breast milk, and urine.(Choi et al., 2021) Concerns regarding PAEs center on their potential as endocrine-disrupting chemicals (EDCs). Research indicates that certain phthalates may interfere with hormone function, particularly affecting reproductive health. Studies have linked high exposure levels to developmental issues, reduced fertility, and anomalies in reproductive organ development in both wildlife and humans. Additionally, some phthalates have been associated with obesity, insulin resistance, and cardiovascular diseases, highlighting the systemic effects of endocrine disruption.(Wang et al., 2019c)

OPEs are prevalent in indoor environments, consumer electronics, furnishings, and building materials.(Zhong et al., 2017) Like PAEs, exposure to OPEs occurs through ingestion, inhalation, and dust ingestion.(Bekele et al., 2021) The toxicological profile of OPEs includes neurotoxicity, with several studies indicating potential adverse effects on the nervous system, particularly during critical periods of development. Moreover, there is emerging evidence of OPEs acting as EDCs, with potential impacts on thyroid

function, reproductive health, and metabolic processes. The specific mechanisms through which OPEs exert these effects are under investigation, but their ability to disrupt normal hormonal signaling is of particular concern.(Chen et al., 2022; Yang et al., 2022)

Both PAEs and OPEs have been detected in various ecosystems, leading to exposure in non-target organisms. In the marine environment, aquatic species are particularly vulnerable, with evidence of bioaccumulation and subsequent effects on reproduction, growth, and survival. The environmental persistence of these compounds, coupled with their ability to travel long distances, complicates the toxicological landscape, affecting species in remote areas.(Huang et al., 2008; Qadeer et al., 2024)

Addressing the toxicity of PAEs and OPEs is challenging due to the diversity within each class and the variability in individual susceptibility. Regulatory efforts have focused on identifying the most harmful phthalates and organophosphate esters, leading to bans or restrictions on their use in certain applications. However, the continued detection of these chemicals in the environment and biota underscores the need for ongoing monitoring, research, and development of safer alternatives.

1.2 Transport Pathways of PAEs and OPEs to the Marginal Seas

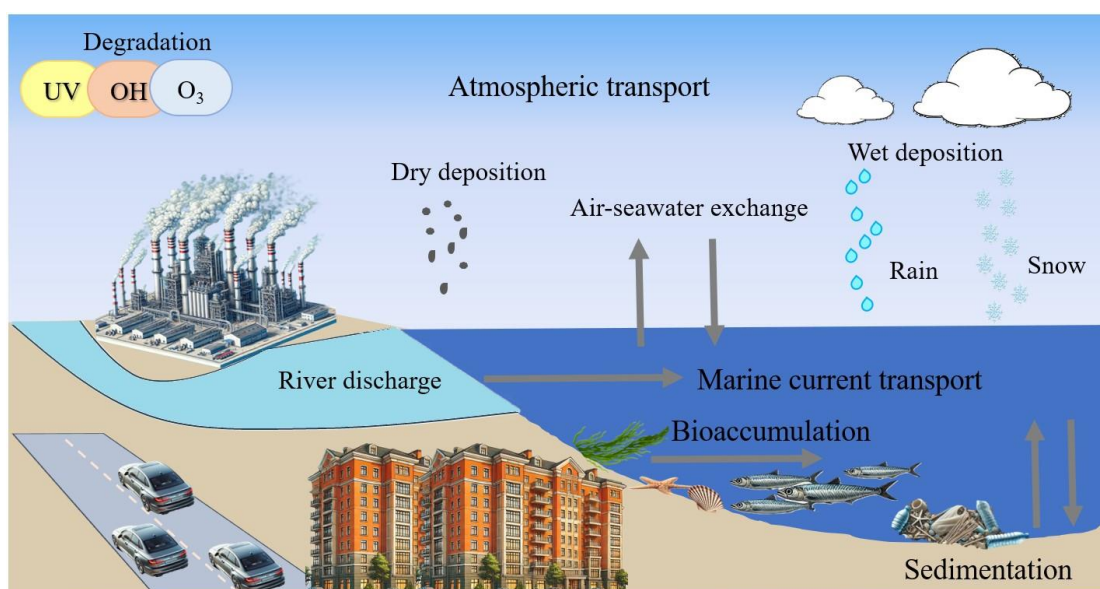
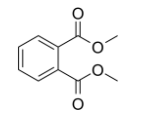
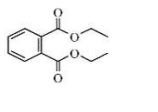
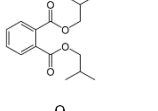
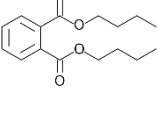
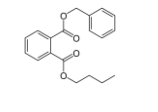
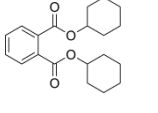
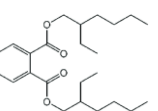


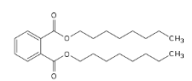
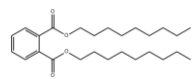
Figure 1-1 Major environmental sources, processing and pathways of organic pollutants in the coastal and open seas

PAEs and OPEs originate from various concurrent land-based sources which significantly contribute to their presence in marine environments. These sources primarily include the emission of vapors from consumer products, such as discarded electronic items, into the atmosphere, along direct discharges from rivers. Within river systems, a plethora of origins such as wastewater from sewage treatments, industrial leaks, runoff from waste sites containing plastics and electronics, and atmospheric deposition contribute to the riverine input of PAEs and OPEs. These terrestrial sources facilitate the accumulation of PAEs and OPEs in coastal and offshore zones through mechanisms of atmospheric transport and deposition, as well as waterborne movements driven by ocean currents.(Li et al., 2018a; Li et al., 2017a; Möller et al., 2012; Xie et al., 2005; Xie et al., 2007)

Moreover, PAEs and OPEs are consistently detected across diverse water bodies including wastewater, inland surface waters, groundwater, and seawater across continents like Europe, North America, and Asia.(Fernandez et al., 2007; Pantelaki and Voutsas, 2022; Schmidt et al., 2020; Schmidt et al., 2021; Wolecki et al., 2021; Xu et al., 2022; Yin et al., 2022) The interaction between these compounds and oceanic plastic debris further enhances their distribution, with significant amounts of PAEs leaching from marine debris such as polyethylene plastic bags and PVC cables as per laboratory findings. Interestingly, surface ocean waters have been identified as more potent zones for the release of these additives compared to deeper waters, which typically carry the bulk of plastic waste to sediment layers. This surface activity is often augmented by marine microorganisms, which play a crucial role in facilitating the release of these chemicals. Once introduced into the marine ecosystem, PAEs and OPEs tend to accumulate in the biological tissues of aquatic life forms, including fish and marine mammals.(Shore et al., 2022)

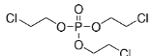
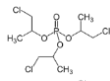
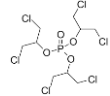
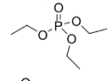
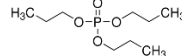
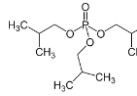
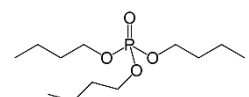
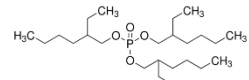
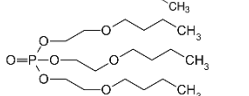
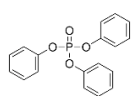
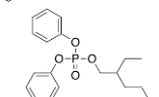
Table 1-1 Physicochemical properties of phthalate esters

Chemical Name	Abbreviation	CAS	MW	Chemical formula	V _p (Pa)	S (mg/L)	H (pa.m ³ /mol)	logK _{ow}	logK _{oa}	logK _{aw}	Half-life time in air (d)	Chemical structure
Dimethyl phthalate	DMP	131-11-3	194.19	C ₁₀ H ₁₀ O ₄	0.263	5220	9.78x10 ⁻³	1.61	7.01	-5.4	14.4	
Diethyl phthalate	DEP	84-66-2	222.24	C ₁₂ H ₁₄ O ₄	6.48x10 ⁻²	591	2.44x10 ⁻²	2.54	7.55	-5.01	2.39	
Diisobutyl phthalate	DiBP	84-69-5	278.35	C ₁₆ H ₂₂ O ₄	4.73x10 ⁻³	9.9	0.13	4.27	8.54	-4.27	0.58	
Dibutyl phthalate	DnBP	84-74-2	278.34	C ₁₆ H ₂₂ O ₄	4.73x10 ⁻³	9.9	0.13	4.27	8.54	-4.27	0.89	
Benzylbutyl phthalate	BBP	85-68-7	312.37	C ₁₉ H ₂₀ O ₄	2.49x10 ⁻³	3.8	0.205	4.70	8.78	-4.08	0.75	
Dicyclohexyl phthalate	DCHP	84-61-7	330.42	C ₂₀ H ₂₆ O ₄	6.1x10 ⁻⁴	4.1x10 ⁻²	4.92	6.2	11.59	-5.39	0.22	
Bis(2-ethylhexyl) phthalate	DEHP	117-81-7	390.56	C ₂₄ H ₃₈ O ₄	2.52x10 ⁻⁵	2.49x10 ⁻³	3.95	7.73	10.53	-2.80	0.38	

Diocetyl phthalate	DnOP	117-84-0	390.56	C ₂₄ H ₃₈ O ₄	2.52x10 ⁻⁵	2.49x10 ⁻³	3.95	7.73	10.53	-2.80	0.52	
Dinonyl phthalate	DnNP	84-76-4	418.6	C ₂₆ H ₄₂ O ₄	6.81x10 ⁻⁶	3.08x10 ⁻⁶	9.26	8.60	11.03	-2.43	0.46	

V_p: vapor pressure at 25°C; S: water solubility at 25°C; H: Henry's law constants at 25°C; logK_{ow}: log Octanol-Air coefficient at 25°C; logK_{oa}: log Octanol-Air coefficient at 25°C; logK_{aw}: log air-water transfer coefficient; Half-life time in air (d) (exclude DiBP)(Perterson, 2003); Half-live time in air for DiBP: (Calculated by EPIWEB 4.1).

Table 1-2 Physicochemical properties of Organophosphate esters

Chemical Name	Abbreviation	CAS	MW	Vp (Pa)	S (mg/L)	H (pa.m ³ /mol)	logKow	logKoa	logKaw	Half-life time (Air, h)	Chemical structure
Tris(2-chloroethyl) phosphate	TCEP	115-96-8	285.49	8.17	7000	0.333	1.44	5.311	-3.871	5.84	
Tris(2-chloroisopropyl) phosphate	TCIPP	13674-84-5	327.57	7.53 x 10 ⁻³	51.85	0.0475	2.59	8.203	-5.613	2.87	
Tris(1,3-dichloro-2-propyl) phosphate	TDCIPP	13674-87-8	430.91	3.82 x 10 ⁻⁵	1.5	1.095 x 10 ⁻²	3.65	10.662	-6.972	7.098	
Triethyl phosphate	TEP	78-40-0	182.16	52.4	1.12 x 10 ⁴	0.359	0.80	6.632	-5.832	2.215	
Tripropyl phosphate	TPrP	513-08-6	224.24	3.08	827	0.0689	1.87	6.426	-4.556	1.721	
Tri-iso-butyl phosphate	TIBP	126-71-6	266.32	1.71	16.22	0.323	3.60	7.485	-3.885	1.629	
Tri-n-butyl phosphate	TNBP	126-73-8	266.32	0.151	280	0.143	4.0	8.239	-4.239	1.628	
Tris(2-ethylhexyl) phosphate	TEHP	78-42-2	434.65	1.1 x 10 ⁻⁵	1.46 x 10 ⁻⁵	9.69	9.49	14.983	-5.493	1.312	
Tris(2-butoxyethyl) phosphate	TBEP	78-51-3	398.48	1.65 x 10 ⁻⁴	1.96	0.0333	3.75	-9.309	13.059	0.997	
Triphenyl phosphate	TPHP	115-86-6	326.29	8.37 x 10 ⁻⁴	1.9	0.335	4.59	-3.869	8.459	11.838	
2-Ethylhexyl diphenyl phosphate	EHDPP	1241-94-7	362.41	6.67 x 10 ⁻³	0.0666	5.49	5.73	-2.654	8.384	3.22	

1.3 Riverrun Transport of PAEs and OPEs from Land to the Marginal Seas

The transport of PAEs and OPEs from terrestrial sources to the marginal seas via river runoff is an environmental issue of increasing concern.(Mi, 2023; Mi et al., 2023) The journey of PAEs and OPEs begins with their release into the environment through industrial effluents, sewage discharges, urban runoff, and atmospheric deposition.(Xie et al., 2022a; Zhang et al., 2018b) Once introduced into a river system, these chemicals can be transported in the water column, either dissolved or adsorbed onto particulate matter. The fate of these compounds during river transport is influenced by their physicochemical properties, such as water solubility and affinity for particulate matter, which determine their distribution between the dissolved and particulate phases.(Addis et al., 2023) Upon reaching estuarine areas, the mixing of freshwater and seawater can further impact the behavior and fate of PAEs and OPEs. Estuarine processes, including adsorption-desorption dynamics and sedimentation, play critical roles in the transport and transformation of these contaminants.(Lao et al., 2022) For example, changes in salinity can affect the solubility and partitioning of PAEs and OPEs, potentially leading to their release from particles and increased bioavailability or, conversely, to their adsorption onto particles and removal from the water column through sedimentation.(Du et al., 2013; Mi et al., 2023; Zhang et al., 2022a)

Marginal seas, often located at the receiving end of riverine inputs, are particularly vulnerable to contamination by PAEs and OPEs.(Simcock et al., 2016) These semi-enclosed bodies of water can act as sinks for pollutants, where they may accumulate in the water column and sediments, posing risks to marine organisms and ecosystems. The environmental behavior of PAEs and OPEs in marginal seas is influenced by a combination of physical, chemical, and biological processes, including dilution, degradation (biotic and abiotic), and bioaccumulation.(Schmidt et al., 2021) These processes can affect the persistence, distribution, and toxicity of these contaminants in marine environments.(Xie et al., 2022b)

The Bohai Sea, Yellow Sea, and the South China Sea are particularly interesting in the context of PAE and OPE transport due to their proximity to densely populated and industrially active regions.(Mi et al., 2023; Mi et al., 2019) These marginal seas receive substantial riverine inputs from major rivers like the Yangtze, Yellow River, and Pearl

River, which are heavily laden with pollutants from upstream sources.(Waniek, 2021) The unique hydrodynamic and biogeochemical conditions of each sea influence the transport, distribution, and eventual fate of PAEs and OPEs. For instance, the Bohai Sea, being semi-enclosed, has limited water exchange with the Yellow Sea, potentially leading to higher concentrations of pollutants.(Ju et al., 2020; Liang et al., 2023) In contrast, the South China Sea, with its broader connection to the Pacific Ocean, may demonstrate different dispersal and dilution patterns for these compounds.(Liu et al., 2023b)

1.4 Atmospheric Transport

Furthermore, air mass flow and circle also contribute to the transport of PAEs and OPEs to these seas, especially in aerosols and dust particles. This pathway introduces an additional layer of complexity to understanding how these pollutants are distributed across marine environments. Although the atmospheric half-lives of PAEs and OPEs generally fall below two days—shorter than the threshold for LRAT as defined by the Stockholm Convention on POPs, these substances are still found ubiquitously throughout the global atmosphere.(Mi et al., 2023; Xie et al., 2022a) Initially, it was believed that the rapid degradation of PAEs and OPEs would limit their capacity for long-distance dispersal. Contrary to this assumption, significant levels of PAEs and OPEs have been detected in air across a vast range of geographical locations. These include the North Sea, the Great Lakes of North America, the Mediterranean Sea, and extensive oceanic and polar regions such as the Arctic, and the Pacific, Indian, Atlantic, and Southern Oceans.(Xie et al., 2005; Xie et al., 2022a) These findings indicate that PAEs and OPEs do indeed participate in long-range atmospheric transport, challenging earlier perceptions of their environmental persistence and mobility.

Liu et al. conducted research that provided estimated rate constants for heterogeneous reactions involving OPEs in the air, showing that these compounds, when bound to particles, demonstrate significant atmospheric persistence.(Liu et al., 2014b) The primary degradation mechanism for OPEs in the atmosphere was thought to be their reaction with OH radicals, with estimated atmospheric lifetimes for gaseous OPEs being under 1.3 days.(Xie et al., 2022a) Nevertheless, many OPEs are found predominantly attached to airborne particles, which could slow down their atmospheric degradation. Further studies on heterogeneous oxidation initiated by OH radicals

revealed longer atmospheric lifetimes of 5.6, 4.3, and 13 days for particle-bound TPhP, TEHP, and TDCIPP respectively. These durations suggest that particle-bound OPEs could indeed have the potential for medium to long-range atmospheric transport. (Liu et al., 2014b; Liu et al., 2014c) Consistent detection of OPEs in remote oceanic and polar regions supports their capability for LRAT.

Like OPEs, the atmospheric half-lives of PAEs are influenced by factors such as sunlight exposure, temperature, and reactions with atmospheric oxidants like OH and O₃. (Li et al., 2018d) These reactions primarily dictate the degradation of PAEs in the atmosphere. (Perterson, 2003) Studies suggest that the half-lives of PAEs can vary widely, typically ranging from hours to a few days under typical environmental conditions. The half-life estimates for various phthalates, such as DEHP (0.38 days), BBP (0.75 days), DnBP (0.89 days), DEP (2.39 days), and DMP (14.41 days), indicate that DEHP, BBP, and DnBP degrade more swiftly during atmospheric transport, while DEP and DMP exhibit greater persistence. Furthermore, the presence of phthalates with higher molecular weights, like DCHP and DEHP, in particulate matter may slow down their photolysis, consequently prolonging their atmospheric duration. (Perterson, 2003) This variability allows PAEs to remain in the atmosphere long enough to be transported over considerable distances before deposition occurs through processes like rainout or dry settling.

1.5 Air-Sea Exchange

During moving from their source regions to remote oceanic areas, OPEs and PAEs undergo exchanges across various environmental interfaces. Significant in shaping the fate of OPEs and PAEs in the environment, atmospheric deposition processes contribute to the burden on aquatic ecosystems and facilitate the accumulation of OPEs and PAEs within marine food chains. (Xie et al., 2007) Key mechanisms for these transfers include dry deposition, wet deposition, and gas exchange between air and water. (Li et al., 2018a; Mi et al., 2023)

C_A , C_G , C_W , and C_{Rain} represent the concentrations of a chemical in aerosols, the gas phase, water (dissolved phase), and rain, respectively. H' denotes the dimensionless Henry's law constant, v_D is the velocity at which aerosols deposit, p indicates the rate of rainfall, and K_{AW} is the coefficient for mass transfer between air and water. (Schwarzenbach et al., 2016; Xie et al., 2007) The extent of atmospheric

deposition or volatilization of PAEs and OPEs mainly depends on their physicochemical properties, particularly the Henry's law constant, and their concentrations in the air and water. These processes are also influenced by environmental factors such as wind speed, temperature, salinity, and the frequency and intensity of precipitation. (Xie et al., 2007; Xie et al., 2022a)

1.6 Occurrences of PAEs and OPEs in the Marine Environment

1.6.1 Occurrences of PAEs and OPEs in Seawater

A few studies have identified significant presence of PAEs in ocean water samples collected from numerous global locations (Benson and Fred-Ahmadu, 2020; Gholaminejad et al., 2024; Li et al., 2017c; Xie et al., 2007; Zhang et al., 2018a; Zhang et al., 2018b). Figure 1-1 provides range data on the presence of PAEs in seawater. 23 PAEs have been detected in global ocean predominantly around the Chinese coastal areas such as the Yellow Sea, Bohai Sea, and East China Sea. Among them, DEHP, DnBP, and DiBP were found to have the highest concentrations and detection rates in several studies.

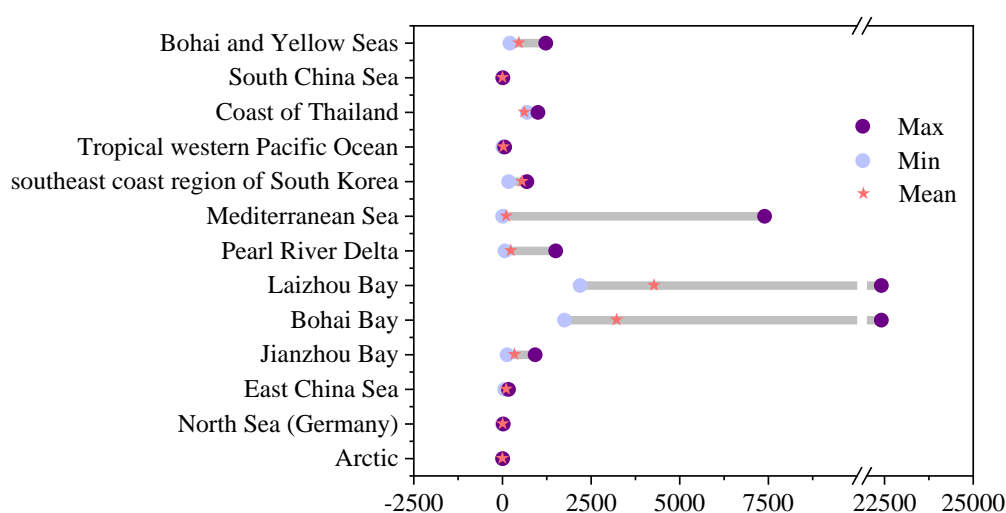


Figure 1-2 Comparison of PAEs concentrations in water from different sea areas (ng/L)

For instance, the maximum concentration of DEHP, reaching 168 $\mu\text{g/L}$, was observed off the coast of Mahdia in Tunisia, with a detection frequency of 93% (Gugliandolo et al., 2020b). Sampling in this area occurred near various pollution sources, including industrial zones and populated urban areas. Another notable finding was in Hangzhou

Bay, China, where DEHP levels reached 9738 ng/L with a detection frequency of 100%, with samples taken near Shanghai, China's largest city(Wang et al., 2021). Although lower, significant DEHP concentrations were also reported in the Gulf of Thailand and the North Sea along the Belgian coast, where levels were 1160 ng/L and 766 ng/L respectively, with sampling near densely populated zones(Huysman et al., 2019; Malem et al., 2019). While, the lower DEHP concentrations were measured in the tropical Western Pacific Ocean (9.2 ng/L) and high Arctic, a location remote from human activities(Xie et al., 2007; Zhang et al., 2019a). Similar trends were observed for DnBP and DiBP, with the highest concentrations recorded again in Tunisia (30.5 µg/L for DnBP and 106 µg/L for DiBP), and substantial amounts also found in Hangzhou Bay, China (17.952 µg/L for DnBP and 17.256 µg/L for DiBP), reflecting high urban influence on water quality(Jebara et al., 2021; Wang et al., 2021).

Sixteen OPEs have been detected across various river-sea adjacent areas(Cao et al., 2017; Lian et al., 2021; Sun et al., 2024; Wang et al., 2015). The concentration of OPEs in seawater exhibits a clear gradient distribution from river mouths to coastal waters to the open ocean, with concentrations gradually decreasing.(Xie et al., 2024) In the Pearl River estuary, OPE concentrations were found to range from 15-1790 ng/L, while the concentrations in the surface waters of the South China Sea were between 1-147 ng/L(Cao et al., 2017; Guo et al., 2017; Lai et al., 2019a). In Europe, concentrations of OPEs in the water at the estuaries of the Elbe, Weser, Ems, Rhine rivers in Germany and the Scheldt river in the Netherlands ranged from 58.3-485 ng/L, and in the German Bay and the North Sea, the concentrations were 5-50 ng/L (Greaves and Letcher, 2017). In the Bohai Sea, 40 rivers flowing into the sea showed OPE concentrations ranging from 9.6-1549 ng/L,(Wang et al., 2015) while in the Yellow and Bohai Seas, the concentrations were 8.12-98.04 ng/L(Zhong et al., 2017). The results indicate that the concentrations of OPEs in the waters of river estuaries are 1-2 orders of magnitude higher than in the adjacent marine areas. The freshwater mixing with seawater in estuaries effectively dilutes and dissolves the high concentrations of OPEs from river water.

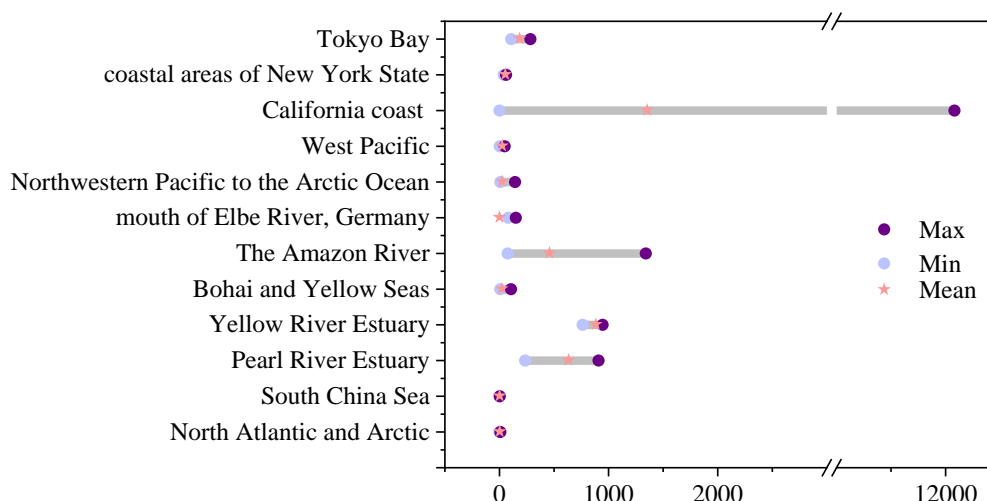


Figure 1-3 Comparison of OPEs concentrations in surface water from different areas (ng/L)

Lower concentrations of OPEs were also detected in various remote regions: around 36.5 ng/L in the Antarctic Fildes Peninsula,(Li et al., 2023a) 0.2-18 ng/L in the Canadian Arctic seas,(McDonough et al., 2018) 0.3-8.4 ng/L in the North Atlantic and Arctic oceans,(Li et al., 2017a) and 6.91-16.3 ng/L in the Fram Strait and the Arctic Ocean(McDonough et al., 2018). Apart from surface waters, varying depths of seawater in the Fram Strait (from 0 to 3000 meters) had OPE concentrations ranging from 6.3-440 pg/L, which supports the idea of the Fram Strait acting as a channel for the exchange of OPEs between the Arctic and Atlantic oceans(Cristale et al., 2017; McDonough et al., 2018).

Generally, chlorinated OPEs are the most abundant in the open ocean surface waters. In the Canadian Arctic surface waters, the concentration of chlorinated OPEs (6.2-430 pg/L) was higher than that of other OPE compounds (0.1-66 pg/L)(McDonough et al., 2018). In the North Atlantic to Arctic Ocean waters, the reported concentrations of OPEs were in the order: TCPP (257-5773 pg/L) > TCEP (MDL-2401 pg/L) > TiBP (39-638 pg/L) > TnBP (MDL-412 pg/L)(Li et al., 2017a). The highest concentration of OPEs reported in the Atlantic surface waters was TCIPP(Wang et al., 2017a). Chlorinated OPEs are characterized by their resistance to degradation, indirect photodegradation and hydrolyzation in water(Cristale et al., 2017; Wang et al., 2017a; Zhong, 2018), which enables their mid/long-range transport to the open oceans. The most abundant OPEs in estuaries, coastal, and open ocean waters are generally consistent. Different regional emission sources are the primary cause for the variation of OPE compositions in estuarine waters.

1.6.2 Occurrences of PAEs and OPEs in Air

OPEs have been reported in the air over the global ocean, including the Pacific, Indian, Atlantic, and Arctic Oceans (Castro-Jiménez et al., 2016; Li et al., 2017a; Song et al., 2018). The concentrations of OPEs in global marine aerosol samples range from picograms per cubic meter to several nanograms per cubic meter, as illustrated in Figure 1-3. OPE concentrations ranged 29-180 pg/m³ in the central Arctic, while it was approximately 600 pg/m³ near Russia and the United States in the Arctic Ocean (Diss_Dreyer, 2009; Li et al., 2017a). In mid-latitude regions such as the North Sea, Mediterranean, and Black Sea, concentrations can reach nanograms per cubic meter. For instance, OPE were observed in the air of the European seas with concentrations ranging 0.11-1.4 ng/m³ in German North Sea in 2010 (Moller et al., 2011), 0.4-6 ng/m³, in the Mediterranean and Black Sea from 2006-2007 (Castro-Jiménez et al., 2014). In subtropical and tropical oceans, the concentrations of OPEs are comparable across the Southern and Northern Hemispheres, with observed concentrations in total suspended particulate (TSP) samples from 2010-2011 in the North Atlantic, North Pacific, South Atlantic, and South Pacific respectively ranging from 0.7-3.93, 0.50-4.43, 0.87-4.31, and 1.11-3.16 ng/m³, slightly lower concentrations were observed in the Southern Indian Ocean, ranging from 0.36-3.22 ng/m³ (Li et al., 2018a). In general, concentrations of OPEs along the coastlines of the Northern Hemisphere are higher than those in the Southern Hemisphere, for instance, concentrations from the Sea of Japan to the Arctic (230-2900 pg/m³) (Möller et al., 2012) were higher than those observed in East Asia—Indian Ocean—Antarctic aerosol samples (120-1700 pg/m³). Observations also vary within the same marine areas. For example, OPE concentrations in marine aerosol samples ranged from 47.1-161 pg/m³ measured in the northern South China Sea in 2013, and 1510 -1970 pg/m³ at Yongxing Island in the South China from 2018-2019 (Lai et al., 2015; Zhang et al., 2022d).

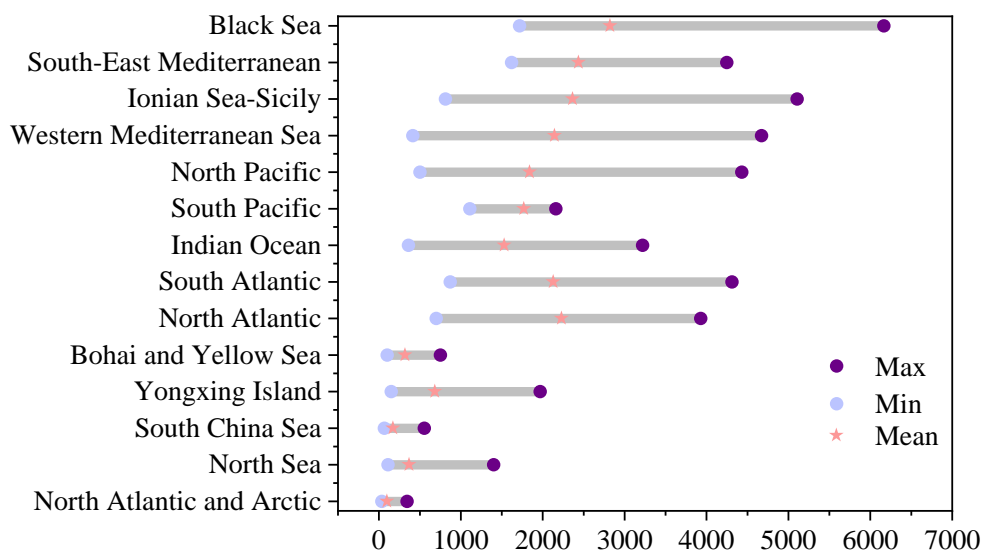


Figure 1-4 Comparison of OPEs concentrations in air from different regions (pg/m³)

Remote areas and polar aerosol samples showed OPE concentrations comparable to those observed in the open ocean (Figure 1-3). From 2012-2014, OPE concentrations in atmospheric samples from the Great Lakes in the USA were observed at 120-414 pg/m³(Salamova et al., 2016), with higher concentrations near the industrial cities of Chicago and Cleveland at 6080 pg/m³(Salamova et al., 2014). Between 2012-2013 in the European Arctic and 2007-2013 in the Canadian Arctic, reported OPE concentrations were 430 and 237 pg/m³ respectively (Li et al., 2017a; Sühling et al., 2016). From 2014-2018 in the western Antarctic Peninsula, particulate OPE concentrations were reported between 5.8-238 pg/m³(Li et al., 2023a). Generally, OPE concentrations in aerosol samples collected at coastal station are higher than those in open ocean samples. For example, in 2020, OPE concentrations along the coast of the Yellow and Bohai Seas were observed at 426-3930 pg/m³(Wu et al., 2022), whereas in 2015-2016, concentrations in the Yellow and Bohai Seas and near Daicheng Island were 44-520 pg/m³(Li et al., 2018a). In 2017, winter and summer aerosol samples from the coast of Izmir, Turkey, showed OPE concentrations of 1.2 and 2.0 ng/m³ respectively(Kurt-Karakus et al., 2018). However, from 2015-2016, OPE concentrations in coastal TSP samples from Bizerte, Tunisia, in the Mediterranean were lower than in the open Mediterranean Sea, possibly due to high solar radiation intensities in the city of Bizerte accelerating the degradation of atmospheric OPEs(Castro-Jiménez and Sempéré, 2018).

Besides a significant proportion of OPEs were measured in the gas phase in atmospheric samples of the marine environment. In German coastal regions, the proportion of gas-phase OPEs observed was 55%(Li et al., 2017a). In Beihuangcheng Island, the Yellow and Bohai Seas, and from the North Atlantic to the Arctic, the proportions of gas-phase OPEs were somewhat lower, at 18%, 49%, and 33% respectively(Li et al., 2018a; Li et al., 2017a). In the western Antarctica and Yongxing Island, reported proportions of gas-phase OPEs were slightly higher at 55% and 60.4% respectively(Zhang et al., 2022d). In the USA's Great Lakes, the proportion of gas-phase OPEs was slightly higher in summer than in winter (41% > 35%), but there was no significant seasonal variation(Wu et al., 2020). It is suggested that the partitioning of the OPEs between gaseous and particles are determined by their physicochemical behaviors, and could be affected by the ambient temperature, humidity, the character of the particle(Liu et al., 2023a). While, the measurements of the gaseous and particle concentrations might be influenced by the sampling techniques, such as flowrate and different pore size of the filters.

PAEs have been reported for various regions worldwide (Figure 1-4), showing DEHP, DiBP and DnBP are typically the predominant PAE detected in outdoor air, particularly in urban environments. The concentrations of PAEs in urban atmospheres are notably higher in Asia compared to Europe and North America(Zhang et al., 2019b). Netherlands exhibits the lowest urban concentrations of PAEs, significantly lower than rural concentrations in other countries. However, the specific composition of PAEs in rural areas varies. Investigations into specialized sites, like those surrounding e-waste dismantling facilities, indicate elevated PAE concentrations in such areas (India, China), with DINP being notably prominent, suggesting its potential as an indicator of e-waste activities(Yadav et al., 2017). However, current research on PAEs near e-waste disposal sites predominantly focuses on China, warranting future studies in other regions like Southeast Asia, Africa, and Europe(Ma et al., 2013).

Moreover, PAEs have been detected in oceanic and remote polar atmospheres, indicating their atmospheric persistence and long-range transport capabilities to remote oceans.(Mi et al., 2023; Xie et al., 2007) Arctic studies display variations in the relative abundance of PAEs, with most studies identifying DEHP, DnBP and DiBP as the predominant species, suggesting meteorological conditions influence PAE distribution(Xie et al., 2007).

Seasonal variation studies of PAEs in outdoor air primarily focus on China, requiring further investigations in other regions. Seasonal fluctuations in PAE concentrations have been observed, particularly in urban areas, with higher levels during warmer periods.(Huo et al., 2023) These fluctuations are attributed to changes in primary emissions, with higher concentrations typically occurring in summer and autumn compared to winter and spring. Temperature appears to significantly influence PAE distribution, with higher temperatures favoring volatilization due to the strong correlation between octanol-air partition coefficients (KOA) and vapor pressures with temperature. Specifically, DEHP, DEP, and DnBP concentrations exhibit a notable association with temperature, indicating their significance in seasonal PAE variations.(Huo et al., 2023)

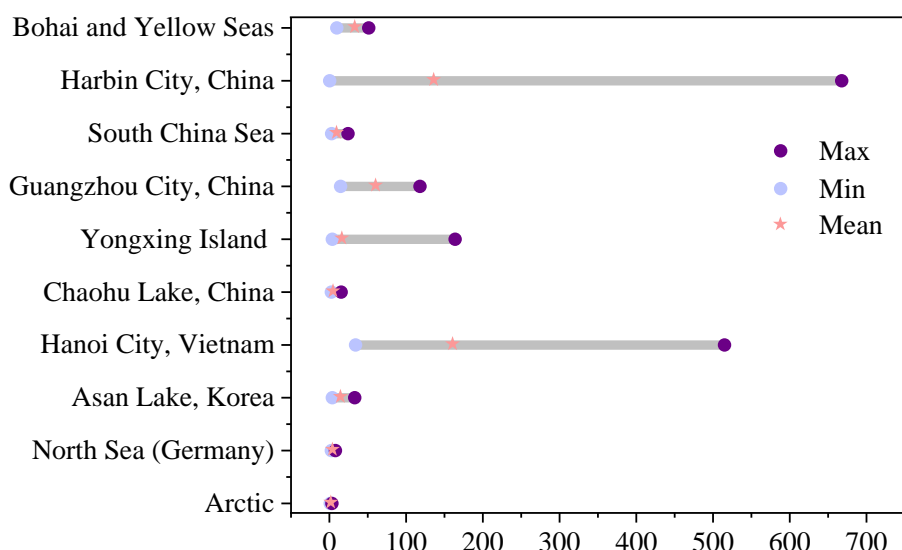


Figure 1-5 Comparison of PAEs concentrations in air from different regions (ng/m³)

1.6.3 Occurrences of PAEs and OPEs in Sediment

Research on marine sediments from around the world has detected a range of phthalate esters (PAEs), with significant findings emerging from various geographic areas.(Mi et al., 2019) Investigations have identified 21 different PAEs, with DEHP, DnBP, and DiBP being the most commonly observed. Additional compounds like DMP and DEP are primarily detected in coastal areas and are associated with personal care products(Hidalgo-Serrano et al., 2022). One notable observation was a particularly high concentration of 35 µg/g for DEHP in sediment samples from Asalouyeh, a town near an industrial area in the Persian Gulf(Arfaeinia et al., 2019). Similarly, near Hangzhou

Bay in the East China Sea, the sediment showed the second highest DEHP concentration at 22 $\mu\text{g/g}$, and DEHP accounting for 59% of the total PAE concentrations found(Wang et al., 2021). Conversely, lower levels of DEHP were recorded in Tunisia (5240 ng/g)(Souaf et al., 2023) and the Gulf of Thailand (1650 ng/g)(Malem et al., 2019). The highest levels of DnBP and DiBP were also recorded in the East China Sea at 15.1 $\mu\text{g/g}$ and 8.0 $\mu\text{g/g}$ respectively(Hidalgo-Serrano et al., 2022), with the Persian Gulf showing the second highest concentrations(Arfaenia et al., 2019). The lipophilic nature of PAEs, particularly those with higher molecular weights, facilitates their accumulation in carbon-rich sediments. According to Wang and colleagues, the distribution of PAEs between sediments and seawater varies by molecular weight: low-weight PAEs tend to migrate towards seawater, high-weight PAEs accumulate in sediments, and those of medium weight maintain a dynamic equilibrium(Wang et al., 2021). Spatial studies reveal that PAE levels are generally higher in coastal areas than offshore, largely due to significant land-derived pollutants transported by rivers and water discharges.(Mi et al., 2019) Arfaenia and colleagues explored the impact of land use on PAE concentrations in marine sediments, finding significantly higher levels in regions affected by industrial activities or close to agricultural lands, likely due to industrial wastewater and the use of agricultural plastics, respectively.(Arfaenia et al., 2019)

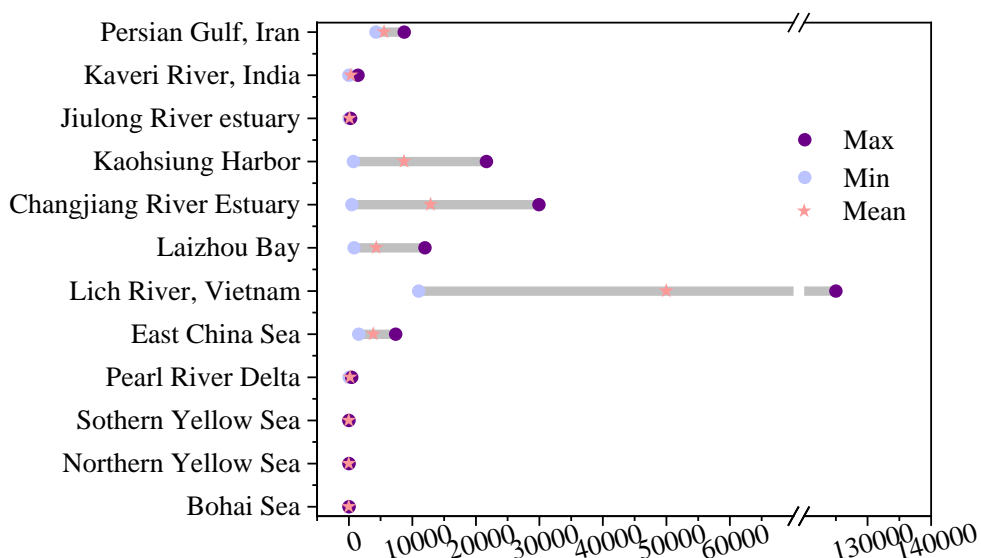


Figure 1-6 Comparison of PAEs concentrations in sediment from different marine areas (ng/g, dw)

Numerous analyses have been conducted on OPEs in marine sediments, revealing concentrations that vary widely.(Zhang et al., 2022a) These range from a few pg/g dw to tens of ng/g dw. In heavily polluted estuaries, sediment concentrations of OPEs can reach several hundreds ng/g dw. For example, the sediments of the Pearl River's urban and electronic waste recycling areas have reported OPE concentrations as high as 8.3-479 ng/g dw(Xie et al., 2022a). In contrast, concentrations in the Beibu Gulf of China, the Taiwan Strait, and Lion Bay in the northwest Mediterranean are lower, recorded at below the limit of quantification (LOQ) to 32.2 ng/g dw, 5.3-34.2 ng/g dw, and 4-227 ng/g dw, respectively(Alkan et al., 2021; Zeng et al., 2020a; Zhang et al., 2021b). Comparatively, OPE concentrations in the Bohai Sea sediments (1.42-52.9 ng/g dw)(Qi et al., 2021) are in line with those found in the Great Lakes (2.2-16.6 ng/g dw)(Cao et al., 2017), which are markedly higher than the concentrations detected in the Yellow Sea (0.08-4.6 ng/g dw) and from the North Pacific to the Arctic (0.2-4.7 ng/g dw)(Bekele et al., 2019). The Canadian Arctic sediments showed a range of 0.12 to 57 ng/g dw in OPE concentrations.(Xie et al., 2022b)

The primary components of OPEs in sediments vary by region and depth, generally dominated by more persistent congeners. The most prevalent OPEs from the North Pacific to the Arctic and the northern Gulf of Tonkin are chlorinated OPEs.(Xie et al., 2022a) The highest concentrations in the Yellow and Bohai Sea samples are of TCEP, TCPP, and TEHP.(Zhong et al., 2018) Canadian Arctic samples show comparable levels of both chlorinated and non-chlorinated OPEs(Xie et al., 2022a). Meanwhile, the dominant OPEs in Taiwan Strait samples are tributyl TNBP, TEHP, and TCPP(Zeng et al., 2020a).

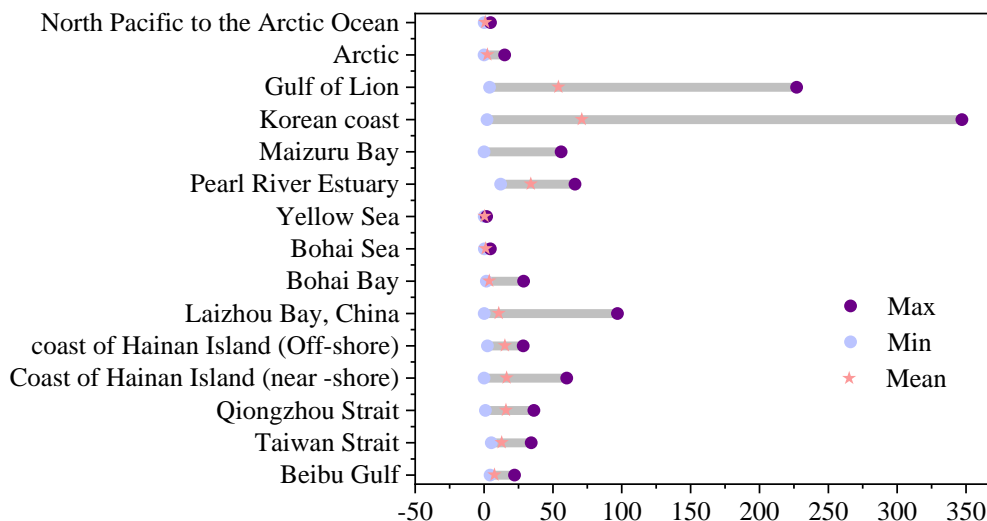


Figure 1-7 Comparison of OPEs concentrations in sediment from different marine areas (ng/g, dw)

TEHP, characterized by its high organic carbon-water partition coefficient and strong hydrophobicity, exhibits relatively high concentrations in samples from the Pearl River Delta (Zhang et al., 2020b), Yellow and Bohai Seas (Zhong et al., 2018), and Taiwan Strait (Zeng et al., 2020a). The compositional contributions of OPEs in Mediterranean and Great Lakes samples significantly differ from these regions (Cao et al., 2017). In the Mediterranean, the main components are TDCIPP, TEHP, and TiBP (Schmidt et al., 2021). The concentration of TCIPP in these samples is influenced by river discharge and decreases with distance from the source. In the Great Lakes, the primary OPEs are TBEP, TCP, and TPhP (Cao et al., 2017).

1.7 Photo- and Biodegradation Processes of PAEs and OPEs

The environmental fate of PAEs and OPEs is a subject of considerable interest due to their widespread use and persistence in various ecosystems. Photo- and biodegradation represent two critical natural processes that influence the breakdown and removal of these chemicals from the environment (Jansen et al., 2024). Understanding these mechanisms is essential for assessing the environmental impact of PAEs and OPEs, predicting their persistence, and developing strategies for their management and remediation.

Photo-degradation refers to the chemical breakdown of substances through exposure to light, primarily ultraviolet (UV) radiation. This process can lead to the transformation of PAEs and OPEs into less harmful substances or their complete mineralization into

carbon dioxide, water, and inorganic salts.(Zhang et al., 2021a) The efficiency of photo-degradation depends on various factors, including the chemical structure of the pollutants, the intensity and wavelength of the UV light, and the presence of photosensitizers in the environment.(Guo et al., 2023) The aromatic ring structures in the molecules of PAEs can absorb UV light, initiating photochemical reactions that break down the ester bonds. These reactions can lead to the formation of monoesters and other breakdown products with reduced plasticizing abilities and, potentially, lower toxicity.(Wang et al., 2019b) However, the intermediate products of photo-degradation can sometimes exhibit higher toxicity than the parent compounds, raising concerns about the environmental implications of this process.(Feng et al., 2022)

OPEs, with their diverse chemical structures, also undergo photo-degradation, although the pathways and products vary significantly among different OPEs. The presence of phosphate groups in these compounds influences their absorption of UV light and the efficiency of photo-degradation.(Konstas et al., 2019; Sun et al., 2020) The breakdown of OPEs through photochemical processes can result in the formation of alkyl or aryl phosphates, as well as other transformation products with unknown environmental and health impacts.(Liu et al., 2021b)

Biodegradation involves the breakdown of organic pollutants by microorganisms, such as bacteria and fungi, into simpler, non-toxic compounds. This process is influenced by a variety of environmental conditions, including temperature, oxygen availability, and the presence of suitable microbial communities.(F. Mohanty, 2017) PAEs are subject to biodegradation, with certain microbial species capable of utilizing these compounds as carbon and energy sources. The biodegradation process typically involves the hydrolysis of the ester bonds, leading to the formation of phthalic acid and its subsequent breakdown into CO₂ and water.(Billings et al., 2024) The rate of biodegradation varies among different PAEs, with lower molecular weight phthalates generally being degraded more rapidly than their higher molecular weight counterparts.(Kanaujiya et al., 2023) Biodegradation of OPEs is less understood compared to PAEs, with limited studies indicating variable degradation rates among different OPEs.(Liang and Liu, 2016) Certain bacteria and fungi have been identified that can metabolize OPEs, leading to the removal of alkyl or aryl groups and the breakdown of the phosphate ester bond. However, the efficiency of biodegradation is

highly dependent on the specific OPE structure and the environmental conditions.(Xie et al., 2022a)

The photo- and biodegradation of PAEs and OPEs are crucial natural processes that contribute to the attenuation of these pollutants in the environment. Understanding these processes can help in assessing the long-term fate of PAEs and OPEs and in developing effective strategies for mitigating their impact on ecosystems and human health. Further research is needed to elucidate the mechanisms, pathways, and products of photo- and biodegradation, as well as the factors influencing these processes, to better manage the environmental risks associated with these widespread pollutants.

1.8 Objectives of This Work

Observations of PAEs and OPEs in coastal waters are primarily focused on river estuaries, such as those of the Yangtze River, Yellow River, Elbe, and Amazon River. However, there is a significant gap in research and observations regarding the runoff from these estuaries to nearshore and open seas. PAEs and OPEs released from land-based pollution sources can reach remote areas and open seas through long-range atmospheric transport. Despite this, atmospheric observations and studies in the Chinese marginal seas are still lacking. Consequently, there is an insufficient systematic understanding of the sources, long-range transport mechanisms, and key influencing factors of PAEs and OPEs from rivers to nearshore and offshore of the marine environment.

In the Chinese marginal seas, PAEs and OPEs discharged into rivers by anthropogenic sources directly enter the coastal and marine environments through runoff and involve in biogeochemical processes. The complex ecological environment from nearshore to open seas, including variations in marine environmental factors such as salinity, water renewal, suspended matter load, sediment mobility, river runoff, and monsoons, significantly impacts the distribution, diffusion, and transport of PAEs and OPEs. Therefore, investigating PAEs and OPEs in nearshore and open sea surface waters and air will help elucidate their concentration characteristics, sources, transport processes, and influencing factors in the marine environment. This research will also provide reliable data for further studies on the toxicity and ecological health effects of PAEs and OPEs in the marine environment.

This research aims to enhance our understanding of the occurrence, spatial distribution, and transport mechanisms of plastic-related chemicals, specifically PAEs and OPEs, in the Chinese marginal seas, including the South China Sea, Bohai Sea, and Yellow Sea. Particular focus is given to the roles of air-sea exchange and atmospheric deposition in these processes. The specific objectives of this thesis are:

- Investigating PAEs and OPEs in surface waters and sediments of nearshore waters and open seas to elucidate their characteristics, sources, transmission processes, and ecological impacts in the marine environment
- Observing PAEs and OPEs in the air over the Chinese Marginal Seas to gain a comprehensive understanding of their sources, transport, and atmospheric processes in the marine environment
- Estimating the air-sea exchange fluxes of PAEs and OPEs and calculating atmospheric particle-bound depositions into the Chinese Marginal Seas.

1.9 Summary

PAEs were examined in the air and seawater of the Bohai and Yellow Seas during the spring of 2019. The concentrations of Σ_8 PAEs in the atmosphere ranged from 9.59 to 51.3 ng/m³, predominantly comprising DnBP, DiBP, and DEHP. The Σ_8 PAEs in seawater ranged from 210 to 1220 ng/L, averaging 466 ± 268 ng/L. PAEs associated with total suspended matter constituted about $40 \pm 13\%$ of the total PAE concentration in seawater. Air-sea exchange fluxes indicated that DMP, DEP, DiBP, DnBP, and BBP tended to volatilize, while DEHP, DOP, and DNP primarily underwent deposition. Atmospheric particle deposition fluxes ranged from 1540 to 5580 ng/m²/day, averaging 3470 ± 1430 ng/m²/day. The input of Σ PAEs to the Bohai and Yellow Seas via atmospheric particle deposition was estimated at approximately 579 ± 222 tons/year, while the net air-sea exchange fluxes of PAEs were predominantly from seawater to air, averaging around 1540 ± 1430 tons/year.

PAEs and OPEs were investigated in paired air and seawater samples collected on board the research vessel SONNE in the South China Sea in summer 2019. The concentrations of Σ_7 PAEs ranged from 2.84 to 24.3 ng/m³ with a mean of 9.67 ± 5.86 ng/m³ in the air, and from 0.96 to 8.35 ng/L with a mean of 3.05 ng/L in seawater. Net air-to-seawater deposition dominated air-sea exchange fluxes of DiBP, DnBP, DMP, DEP, and BBP, while strong water-to-air volatilization was estimated for DEHP. The estimated net

atmospheric depositions were 3000 tons/year for the sum of DMP, DEP, DiBP, DnBP, and BBP, but DEHP and DCHP volatilized from seawater to air at an average of 990 tons/year. The seasonally changing monsoon circulation, currents, and cyclones in the Pacific can significantly influence the concentration of PAEs and alter the direction and magnitude of air-sea exchange and particle deposition fluxes.

The concentrations of Σ_{10} OPEs in the atmosphere ranged from 66 to 550 pg/m³, with TCIPP, TNBP, TPhP, and TEP predominating in the air. The total dissolved OPE concentrations (Σ_{10} OPEs without TEP) measured in high-volume water samples ranged from 300 to 3600 pg/L, with mean concentrations of 1180 ± 910 pg/L. TEP, measured with liquid-liquid extraction (LLE), showed the highest concentration (average: 2000 ± 1450 pg/L) among the selected OPEs. Total suspended matter associated OPEs accounted for less than 4.7% of the sum OPE concentration in seawater. Fugacity fractions and air-sea exchange fluxes showed that TCEP, TCIPP, TIBP, TEHP, TPhP, and EHDPP favored volatilization, TEP dominated deposition, while TPrP and TNBP varied between volatilization and deposition. Atmospheric particle deposition fluxes ranged from 5 to 71 ng/m²/day, averaging 17 ± 15 ng/m²/day. The input of Σ OPEs to the entire South China Sea via atmospheric particle deposition was estimated to be 22 ± 19 tons/year, while the net air-sea exchange fluxes of OPEs were volatilization from seawater to air, averaging 44 ± 33 tons/year.

PAEs have been analyzed in sediment samples collected in the Bohai and Yellow Seas in 2009. The sum concentrations of six PAEs ranged from 1.4 to 24.6 ng/g, with an average of 9.1 ng/g. The highest concentrations of PAEs in the sediment samples were those of DEHP, with a median concentration of 3.77 ng/g, followed by DiBP (median: 1.60 ng/g), DnBP (0.91 ng/g), DEP (0.32 ng/g), BBP (0.03 ng/g), and DCHP (0.01 ng/g). Generally, concentrations of PEs in the Bohai Sea were higher than those in the Yellow Sea. The varying spatial distributions of individual PEs can be attributed to discharge sources, regional ocean circulation patterns, and mud areas in the Bohai and Yellow Seas. Significant positive correlations were found between total organic carbon content and the concentrations of DiBP, DnBP, and DEHP. It is estimated that the inventories of Σ_6 PEs were 20.73 tons in the Bohai Sea and 65.87 tons in the Yellow Sea. Both riverine discharge and atmospheric deposition are major input sources for PE sedimentation, while massive plastic litter and microplastics sinking to the ocean floor can directly release PAEs into sediment.

1.10 Prospectives for Future Work

This study demonstrated that a significant amount of PAEs and OPEs has been transported from continental sources to the South China Sea via ocean currents and atmospheric deposition. The dynamic air-sea exchange process drives the movement of PAEs and OPEs from land sources and polluted marginal seas and estuaries to remote marine environment, playing an important role in their global environmental transport and cycling. Changing meteorological conditions, particularly seasonal monsoons, significantly impact the variability of this air-sea exchange. Although the half-lives of both PAEs and OPEs do not typically support long-range transport, their extensive industrial, agricultural, and household use results in high emissions, making PAEs and OPEs more prevalent than many legacy persistent organic pollutants in various environmental compartments.

Given that the environmental behavior of organic pollutants is influenced by temperature, it is essential to ascertain the gas-particle partitioning coefficients of PAEs and OPEs and their Henry's Law Constants across different ambient temperatures. Understanding the transport mechanisms of PAEs and OPEs through the atmosphere and their air-sea exchange fluxes can be greatly enhanced by accurately evaluating these properties.

To better understand the sources, distribution, and fate of PAEs and OPEs in vast marine areas and to improve long-distance transport model data, future work should include sampling and research over a broader region. Additionally, investigation into the vertical distribution of PAEs and OPEs within the water column and sediment of the continental shelf is needed to assess transportation via ocean currents and bioaccumulation in various marine organisms. The absence of seasonal data limits understanding of seasonal effects, such as river runoff and monsoon impacts, on input to research areas and other seas and oceans. Therefore, long-term sampling is essential. Furthermore, the partitioning of PAEs and OPEs into particulate matter in the atmosphere and seawater significantly slows photo- and bio-degradation processes, increasing their environmental persistence and potential hazard to marine organisms. Few regulations currently limit the applications of PAEs and OPEs. Plastic debris or microplastics serve as intermediate storage and transport media for PAEs, releasing them into local environments throughout their lifecycle. The greatest toxic risk of

microplastics to marine organisms arises from chemical additives such as PAEs, softeners, antioxidants, and flame retardants. Therefore, future studies should strengthen research on the interaction between microplastics and plastic-related chemicals in the marine environment, including interface interactions, sedimentation, and bioaccumulation in organisms.

2 Air–Sea Exchange and Atmospheric Deposition of Phthalate Esters in the South China Sea

This chapter has been published as:

Lijie Mi, Zhiyong Xie, Weihai Xu, Joanna J. Waniek, Thomas Pohlmann, and Wenying Mi, 2023a. Air-Sea Exchange and Atmospheric Deposition of Phthalate Esters in the South China Sea. *Environmental Science & Technology* 57 (30), 11195-11205.

DOI: 10.1021/acs.est.2c09426

The section includes the full manuscript of the published paper except for some editorial changes. Layout and numbering have been changed to this thesis document. Abstract is deleted. References and acknowledgements have been integrated into the separate chapters of this thesis document.

2.1 Introduction

Phthalates esters (PAEs) are synthesized organic chemicals and have been used on a large scale as plasticizers and additives for more than 80 years. Owing to their versatility, PAEs are extensively used in the manufacturing of resin and polymer products, building materials, personal care products, medical devices, food and water packages, and pharmaceuticals, which account for more than 80% of worldwide plasticizers production. (Latini, 2005; Staples et al., 1997a; Xie et al., 2007) The annual global production of phthalates was 4.7 million tons in 2006 and increased to about 8 million tons in 2015. (Net et al., 2015) Previous studies have shown that phthalates are reproductive and developmental toxicants; hence, PAEs are considered endocrine-disrupting chemicals (EDCs) and pose a toxic risk to organisms. (Kwan et al., 2021; Liu et al., 2009; Wang et al., 2019c) Six-PAEs, e.g., dimethyl phthalate (DMP), diethyl phthalate (DEP), di-n-butyl phthalate (DnBP), butyl benzyl phthalate (BBP), bis(2-ethylhexyl) phthalate (DEHP), and di-n-octyl phthalate (DnOP), have been listed as priority control pollutants by the US Environmental Protection Agency (EPA), the European Union, and China. (Keith and Telliard, 1979; Net et al., 2015)

As PAEs are physically added to the products, they can leach out during production and application, especially from the disposal of plastic waste. (Lange, 2021) Continuous emissions of PAEs have led to their ubiquitous distribution and abundance in the global environment. For example, PAEs have been determined in wastewater, river water, seawater, air, sediment, and fish. (Armstrong et al., 2018; Cao et al., 2022b; Fatoki and Noma, 2001; Hu et al., 2016; Kim et al., 2020; Turner and Rawling, 2000) Both atmospheric and aquatic transport pathways play an important role in the presence of PAEs in the marine environment. (Alkan et al., 2021; Cao et al., 2022e; Xie et al., 2005; Zhang et al., 2018b) When PAEs enter the marine environment, they can redistribute in the different environmental compartments and exchange, crossing the interface between gas/particle, air/water, water/sediment, and water/organism. (Wang et al., 2021; Xie et al., 2005; Xu and Li, 2009) Furthermore, it has been proven that sediments are important sinks and sources for PAE distribution and bioaccumulation in the marine environment. (Mohammadian et al., 2016; Paluselli and Kim, 2020; Zhu et al., 2022b) Besides, photo- and biological degradation may interfere with their levels in the air and aquatic environments. (Dong et al., 2020; Wolecki et al., 2021) However, the transformed products of PAEs can be more toxic than their parent substances. (Scholz,

2003)Consequently, air-sea exchange processes may significantly interfere with the biogeochemical cycle of PAEs in the marine environment. (Xie et al., 2007)

The South China Sea is one of largest marginal seas in the world, which is surrounded by China and several countries in Southeast Asia within the tropical-subtropical climate realm. Previous studies have highlighted that riverine discharges are important vectors for various classes of organic contaminants in the South China Sea, such as from the Pearl River and the Mekong.(Fu et al., 2003; Minh et al., 2007) Several classes of organic contaminants have been measured in air, seawater, sediments and fish species, indicating that the South China Sea serves as a sink for emerging and legacy organic contaminants.(Cai et al., 2018; Ding et al., 2020; Hou et al., 2022; Zhang et al., 2022d; Zhang et al., 2021d)

To the best of our knowledge, there is no relevant report for PAEs offshore of the South China Sea. Hence, it is requested that the levels and environment fate of PAEs in the South China Sea be thoroughly investigated so as to close the gap. In this work, we aim to (1) determine the concentrations, congener profiles, and spatial distributions of major PAEs in air and sea water obtained from a research ship campaign across the south-to-north transect in the South China Sea, (2) estimate air-sea exchange fluxes of PAEs, and (3) calculate atmospheric particle-bound PAE depositions into the South China Sea. This work provides a consistent unique dataset for evaluating the risk of PAEs to the ecosystem of the South China Sea.

2.2 Materials and Methods

2.2.1 Collection of Samples

Ship-bound sampling was carried out on board the German research vessel SONNE(SO269) along a transect from Singapore to Hong Kong in 2.8-2.9.2019. Air and water samples were collected intensively offshore of the South China Sea (Figure S2-1 and S2-2).

In summary, an actively high-volume air sample was deployed at the Monkey deck (15m above sea level) and run at 15m³/h for 24-h samples. A quartz fiber filter (QFFs, diameter:150mm, pore size: 1.0µm) was used to trap particle-phase PAEs, and the gaseous PAEs were collected by a follow-up PUF/XAD-2 resin glass column. As reported by Lohmann et al.,(Lohmann et al., 2004) there is always potential for contamination by air from shipboard samples. Therefore, the air sampler was usually

running continually in the headwind, with wind speed > 3m/s. sometimes, the pump was stopped when air masses came from the backside to avoid combustion emission. Air sample blanks (column and filter) were prepared by briefly opening the PUF/XAD-2 column and filters next to the air sampler. Air samples were stored at 5°C in the cooling room, and QFF filters were stored at -20 °C.

Seawater sampling was performed in the water lab via a seawater intake system, which is built with stainless-steel tubing for the whole system; the inlet is located at 1m underneath the keel (8m depth). High-volume seawater samples were collected with a glass fiber filter (GFF, 1.2µm, 140mm) for the particles and XAD-2 resin column for the dissolved PAEs. The volumes of seawater samples ranged from 36 to 310L. all samples were transported with cooling containers from Hong Kong back to Helmholtz-Zentrum Hereon, Germany, in December 2019. Detailed information on air and water samples is provided as summarizes in Table S2-1 and S2-2.

2.2.2 Sample Preparation and Instrument Analysis.

The air and seawater samples were treated in a clean laboratory, as described in previous work.(Xie et al., 2007) In brief, PUF/XAD-2 columns (vapor phase) and XAD-2 columns (dissolved phase) were spiked with internal standards (d4-DMP, d4-DEP, d4-DiBP, and d4-DEHP: 50µL * 100 ng/mL, LGC, Wesel) and extracted using a modified Soxhlet system with dichloromethane (DCM, Promochem, Wesel) for 16h. QFF and GFF samples were extracted in that way as well. The extracts were concentrated and cleaned up with column chromatography packed with 2.5g of silica gel (Macherey Nagel, Düren, Germany) and 3g of anhydrous sodium sulfate (99%, Merck, Darmstadt, Germany) on the top. The extracts were blown down to 190 µL under a gentle nitrogen stream (purity: 99.999%) and spiked with 10 µL of 50pg/ µL isotope-labeled poly (chlorinated biphenyl) 208 (¹³C₁₂-PCB 208, Cambridge Isotope Laboratories) as an injection standard. The samples were determined for 7PAEs, including DMP, DEP, DiBP, DnBP, BBP, DCHP and DEHP, which are supplied by LGC (Wesel). The physicochemical properties of PAEs are listed in Table S2-3, and the information on the chemicals and materials is given in Table S2-4.

Analysis was performed with a gas chromatograph (Agilent 8890A) coupled to a triple quadrupole mass spectrometer (Agilent 7010B, GC-MS/MS) equipped with a programmed temperature vaporizer (PTV) injector (Agilent Technologies). The MS

transfer line and high-sensitivity electron impact ionization source (HSEI) were held at 280 and 230°C, respectively. The MS/MS was operated in multiple reaction monitoring (MRM) mode. Two HP-5MS columns (15m * 0.25mm i.d. 0.25µm film thickness, J&W Scientific) were connected in tandem for separation. The details for the instrumental method and the quantifier ions are listed in Table S2-5 and S2-6.

2.2.3 Quality Assurance and Quality Control

It is very critical to determine trace concentrations of PAEs in environmental samples, as relatively high concentration of PAEs might be present in the sampling material, equipment and the surrounding environment. To eliminate the PAE concentration, the sampling materials, e.g., PUF/XAD-2 and XAD-2 columns, were cleaned with methanol, acetone and n-hexane, in turn for 72h, and all organic solvents were distilled prior to use. QFFs and GFFs were, respectively, baked out at 600 and 450 °C. Besides, dust, fibers and microplastics present in the laboratory air and the research vessel may cause significant PAE contamination during the sampling process.(Leistenschneider et al., 2021) In this work, self- designed columns and samplers were applied for air and seawater sampling (Figure S2-3), which reduced the exposure time to indoor air, thus eliminating contamination onboard the research vessel and in the analytical laboratory.(Xie et al., 2006) Moreover, an artificial aspect often occurs for particles with QFF or GFF for high-volume air and water sampling. Fine particles might penetrate the filters and be trapped by PUF or XAD-2, and the particle-bound PAEs will be extract as a gaseous phase or dissolved phase, especially for high molecular PAEs. However, the analysis of concentrations of PAEs in air and seawater is usually not impacted significantly.(Xie et al., 2006) The effects of sampling volumes on the recoveries for air and seawater sampling were studies by field spiking of deuterated PAEs.(Xie, 2005) The recoveries for sampling 500L seawater were 48% for d4-DMP, 52% for d4-DEP, 88% for d4-DnBP and 100% for d4-DEHP, respectively. The losses of d4-DMP and d4-DEP may result from their relatively high solubility in water, which suggests the concentrations of DMP and DEP in seawater might be underestimated. The recoveries of deuterated PAEs in spiked air samples ranged from 80 to 140%, suggesting that PUF/XAD-2 columns are efficient for sampling trace PAEs in air and losses of PAEs during storage are not significant. Besides, the recoveries of breakthrough test showed that 80% PAEs retained on the first column, indicating that no significant breakthrough happens for PAEs. (Xie, 2005)

DMP, DEP, DiBP, DnBP, BBP and DEHP were detectable in the field blank of PUF/XAD-2, XAD-2 columns, and QFF filters. The method detection limits (MDLs) were defined by the mean concentrations in blanks plus three standard deviations of the blanks. The MDLs ranged from 0.002ng/m³ for DCHP to 0.15ng/m³ for DEHP in the gaseous phase, from 0.001ng/m³ for DCHP to 0.072 ng/m³ for DEHP in the particle phase, from 0.001ng/L for DCHP to 0.17ng/L for DEHP in the dissolved water phase, and from 0.001ng/L for DCHP to 0.47 ng/L for DEHP in GFF (particle matter) (Table S2-7). It is noted that the MDLs were calculated with an average volume of 370 m³ for PUF/XAD-2, 180 m³ for the particle phase and 170L for seawater. The concentrations of PAEs reported in this work were not corrected with their blanks.

2.2.4 Air Mass Back Trajectory

The air mass origins of the air samples were assessed using air mass back trajectories (BTs), calculated by the Hybrid Single-Particle Lagrangian Integrated Trajectory model (HYSPLIT).(Stein et al., 2015c) Air mass back trajectories traced back the air masses for 120h with 6h steps at the heights of 10m above the sea level, which are shown in Figure S2-4.

2.2.5 Data Analysis

The data of GC-MS/MS were analyzed using MassHunter B10 (Agilent). Statistical analyses were performed with Excel 2016 and Origin 2020 (OriginLab). Geographic maps were plotted with Ocean Data View 4.0.(Schlitzer) The washout ratio, air-sea exchange, and atmospheric particle deposition were calculated on the basis of the equations previously reported.(Xie et al., 2005; Xie et al., 2007) The details of the calculation methods are presented in the Supporting Information.

2.3 Results and Discussion

2.3.1 PAEs in Air

Seven PAEs were detected in gaseous and particle phase of ship-bound air samples collected in the South China Sea, which are summarized in Table S2-8 in detail. The concentrations of Σ_7 PAEs varied between 2.83 and 58.9 ng/m³, with a mean of 11.6±11.3 ng/m³. DiBP, DnBP and DEHP were the predominant PAEs, with average concentrations of 5.18±5.92, 3.94±3.62, and 1.47±1.37 ng/m³ respectively, accounting for 89.2% of the Σ_7 PAEs. Other PAEs, such as DMP (mean: 0.74±0.95 ng/m³), DEP

(mean: $0.23 \pm 0.14 \text{ ng/m}^3$), BBP (mean: $0.04 \pm 0.02 \text{ ng/m}^3$), and DCHP (mean: $0.01 \pm 0.01 \text{ ng/m}^3$) showed relatively low levels in air. As compared with recent studies for PAEs in air, the concentrations of PAEs in air samples from this work were slightly lower than those measured in fine particulates at Yongxing Island ($\Sigma_5\text{PAEs}$: $3.8\text{-}160 \text{ ng/m}^3$, mean: 16.6 ng/m^3) (Liu et al., 2022), 1-2 orders of magnitude lower than those measured in urban areas (Fang et al., 2022; Zhang et al., 2019b), comparable to the levels, in the Asan Lake of Korea ($\Sigma_{14}\text{PAEs}$: $3.92\text{-}33.09 \text{ ng/m}^3$) (Lee et al., 2019) and the Chao Lake of China ($\Sigma_6\text{PAEs}$: $2.0\text{-}14.8 \text{ ng/m}^3$) (He et al., 2019), and higher than those reported for the North Sea ($\Sigma_6\text{PAEs}$: $2.57\text{-}7.82 \text{ ng/m}^3$) (Xie et al., 2005) and the Arctic ($\Sigma_6\text{PAEs}$: $1.11\text{-}3.34 \text{ ng/m}^3$) (Xie et al., 2007). The composition profile of PAEs in gaseous and particle phases varied in comparison with those from the urban sites; for instance, low proportions of DMP and DEP were found in air, although they are very volatile. We suppose the distribution pattern of PAEs in air could be caused by the origin of air masses, metrological conditions, and physicochemical behavior of PAEs, which are discussed in the context.

2.3.2 Spatial Distribution of PAEs in Air

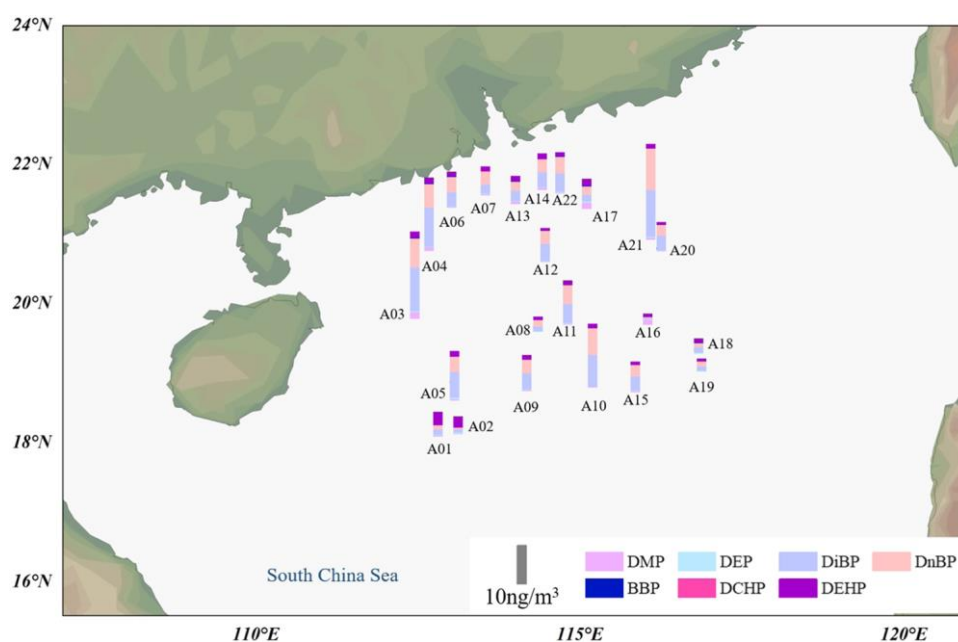


Figure 2-1 Spatial distribution of PAEs in the atmosphere (ng/m^3) over the South China Sea. DiBP and DnBP are the predominant PAEs in air samples from A3 to A22, while DEHP prevails in air samples A1 and A2.

The spatial distribution of PAEs in the air of the South China Sea is shown in Figure 2-1. The highest concentration of $\Sigma_7\text{PAEs}$ (24.3 ng/m^3) was present in the air sample A21, which is almost in the range of PAE concentrations measured in urban environment.

(Fang et al., 2022; Zhang et al., 2019b) The BTs (Figure S2-4) show that 50% of air masses are from the coastal region of Vietnam, other 31% are from southwestern Asia, and 19% are from the East China Sea. Typically for the summer season, the trade wind transports the air masses mainly over South Asian countries such as Malaysia, Singapore and Indonesia. Other high concentrations were presented in air samples collected along the Chinese coast, such as A3(22.1 ng/m³), A4(18.5 ng/m³) and A10(16.1 ng/m³). BTs showed that important sources of air masses were from the Chinese coastal areas of Fujian and Guangdong provinces, with contributions of 55 and 71% for A3 and A4. Another major air mass source was in Southeast Asia; it swept through Vietnam and its east coast region. Relatively low PAE concentrations were measured in air samples from offshore (A16, A18 and A19), which are influenced by the summer monsoon with the air masses mainly from the open South China Sea, the Indian Ocean, and the Pacific Ocean. Besides, the atmospheric concentrations of PAEs measured in this work have also shown the impacts of weather conditions in the South China Sea. For instance, the rainfall precipitation could significantly deplete the PAE concentrations in air, which led to low levels in A1 and A2. Furthermore, several tropical cyclones, e.g., Lekima, Krosa, Bailu and Podul, were formed in the North Pacific Ocean in August 2019 and moved northward during the sampling campaign(Yong et al., 2022). The tropical air masses and rainfall caused by cyclones strongly influenced the South China Sea and Southeast China. Thus, relatively low concentrations of PAEs were measured in nearshore air samples A6, A7, A13 and A14. Nevertheless, the origin of the air masses and weather conditions can significantly affect the PAE concentrations in the South China Sea.

2.3.3 Gas/Particle Partitioning

PAEs have been determined separately in gaseous and particle phase that allow evaluation of the gas/particle processes (Table S2-9). The particle-bound fractions (ϕ) showed that DMP (0.06±0.04) and DEP (0.32±0.19) were predominantly in the gas phase, whereas DiBP (0.47±0.37), DnBP (0.49±0.35) and DEHP (0.48±0.16) were more present in particle phase. In comparison to the particle-bound fraction values calculated in other regions, DMP is quite comparable to the city of Paris (DMP: 0.07), but DEP, DnBP and DEHP are much higher (DEP: 0.06, DnBP: 0.13, DEHP: 0.35).(Teil et al., 2006) The fraction values of DnBP and DEHP are similar to those determined in the Gulf of Mexico (0.32 for DnBP and 0.43 for DEHP).(Giam et al.,

1980) In the north Atlantic and the Arctic, the particle-associated fraction of DnBP (0.46) is similar to this study, but DEHP (0.78)(Xie et al., 2007) is much higher than in this work.

Indirect photolysis in air, caused by hydroxyl radical attack in both gaseous phase and particle-bound phthalates, may play a significant role in removal of PAEs. The estimated half-lives of PAEs were 0.38, 0.75, 0.89, 2.39 and 14.41 days for DEHP, BBP, DnBP, DEP and DMP,(Perterson, 2003) suggesting the DEHP, BBP and DnBP should be degraded more rapidly during atmospheric transport and that DEP and DMP are rather persistent during atmospheric transport. As atmospheric reactions often deplete compounds in the gaseous phase, the partitioning of high molecular weight PAEs to particles, e.g., DEHP, might reduce their photolysis rates and thereby increase their persistence in the atmosphere.

2.3.4 Washout Ratio

The washout ratio (WR) estimated is $240,000 \pm 9900$ for DMP, $75,200 \pm 15,800$ for DEP, $19,300 \pm 510$ for DiBP, $19,300 \pm 480$ for DnBP, and 9780 ± 3260 for DEHP (Table S2-10), showing that DMP and DEP can be easily scavenged from air than other PAEs. DEHP has relatively low WR values, suggesting they are more persistent in the atmosphere. These findings are proved by varying PAE profiles presented in air samples A1 and A2, which were collected when it was raining. The concentrations of DMP, DiBP and DnBP in A1 and A2 decreased by a factor of 2-5 in comparison to A3 and A4. Given the high intensity of rainfall in the summer, precipitation scavenging is a significant process to remove DMP and DEP from the atmosphere in the South China Sea, which is consistent with the model prediction for wet deposition of other semi volatile organic compounds in the tropic ocean.(He and Balasubramanian, 2009) compared with the WR values reported for DnBP and DEHP in the North Sea, the variations in WR are highly influenced by both environmental temperatures and particle-bound fractions. Although DMP and DEP are relatively volatile and resistant to photodegradation in air, their high washout ratios suggest that they are limited for long-range atmospheric transport (LRAT) and turn to deposit in water column. While DiBP, DnBP and DEHP can undergo medium LRAT, and their particle-bound fractions might be favored for LRAT.

2.3.5 PAEs in Seawater

The concentrations of PAEs in seawater in the South China Sea are shown in Figure 2-2, and detailed information is summarized in Table S2-11. The concentrations of the Σ_7 PAE in seawater ranged from 1.08 to 9.82 ng/L with a mean of 3.48 ± 1.89 ng/L. DEHP was the dominant PAE in seawater with a mean concentration of 1.79 ± 1.11 ng/L, followed by DMP (0.51 ± 0.52 ng/L), DEP (0.46 ± 0.26 ng/L), DnBP (0.46 ± 0.36 ng/L) and DiBP (0.24 ± 0.22 ng/L). Concentrations of BBP and DCHP are only detectable in a few seawater samples with a mean concentration of 0.020 ± 0.021 and 0.003 ± 0.003 ng/L, respectively. Given the high water solubility of DMP (5200 mg/L) and DEP (591 mg/L), breakthrough might occur for large-volume seawater samples; thus, the concentrations of DMP and DEP might be underestimated on account of limitations of the high-volume sample collection.

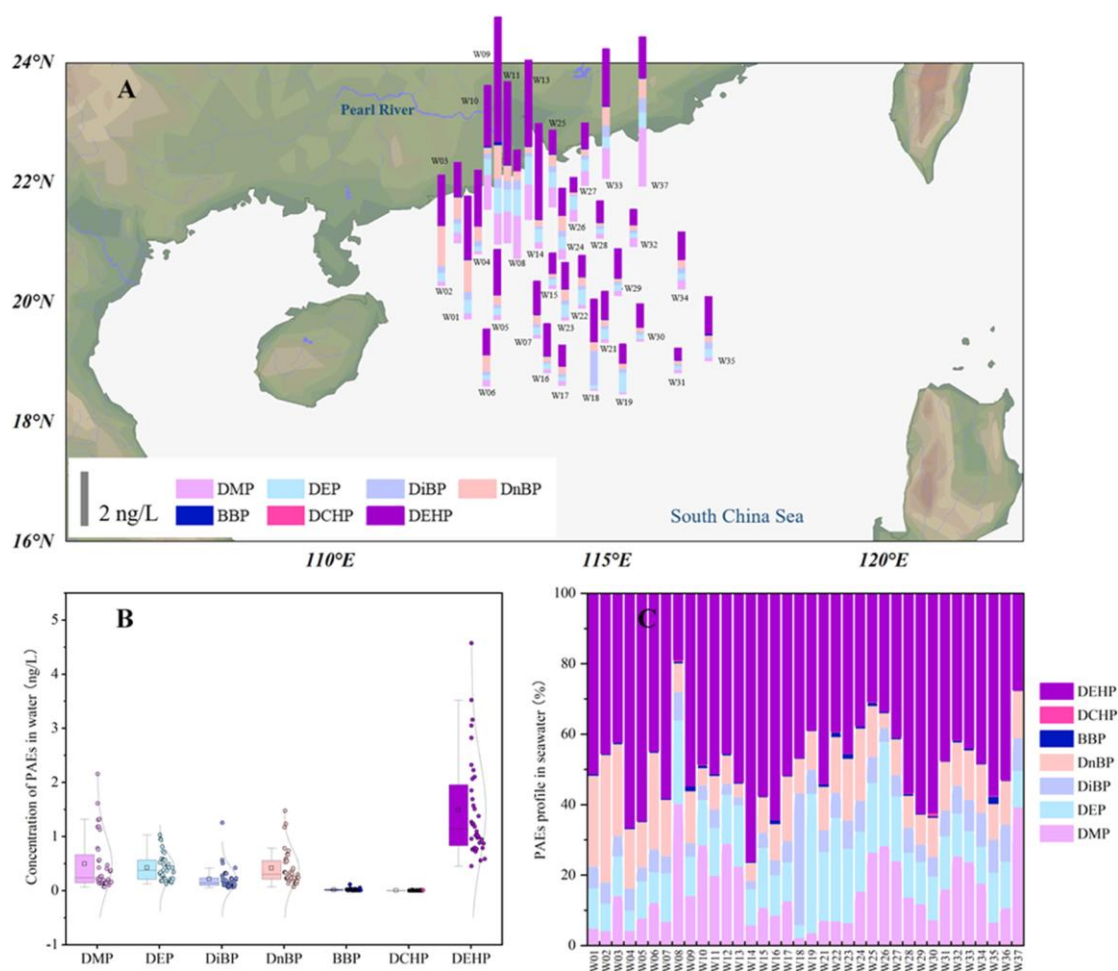


Figure 2-2 (A) Spatial distribution of PAEs in seawater of the South China Sea; (B) concentration ranges of individual PAEs (ng/L); and (C) profile of PAEs in individual water samples.

The PAE concentrations clearly showed spatial distribution, which is higher near the coast, the decline from nearshore to offshore. The high levels were presented in water plume of Pearl River (Figure S2-5). Recently, PAEs were measured in the Pearl River, with Σ_6 PAEs (DMP, DEP, BBP, DnBP, DEHP, DOP) ranging from 500 to 28,100 ng/L, which are 2-3 orders of magnitude higher than this study.(Li et al., 2016) Evidently, the river discharge of Pearl River could be a major input vector for PAEs in the Pearl River Delta and the South China Sea.(Cao et al., 2022a) Compared with other coastal regions of East Asia (Table S2-12), the PAE concentrations are 1-3 orders of magnitude lower than those in the Bohai Sea and the Yellow Sea (Σ_{16} PAEs: 2880 and 1600 ng/L)(Zhang et al., 2018c), in the Yangtze River Estuary (Σ_{16} PAEs: 180-3421 ng/L)(Zhang et al., 2018b), and in the East China Sea and Korean South Sea (Σ_7 PAEs (DMP, DEP, DiBP, DnBP, BBP DEHP, DOP): 63-169 ng/L)(Paluselli and Kim, 2020). In comparison with global oceans (Table S2-12), the PAE concentrations in South China Sea are also at lower levels. They are 2-3 orders of magnitudes lower than those from Pradu Bay, Thailand (Malem et al., 2019), Chabahar Bay, Iran (Ajdari et al., 2018), and Marseille Bay (NW Mediterranean Sea)(Schmidt et al., 2021) and in the surface microlayer and sea surface water in the Antarctic (77-406 ng/L). While the concentrations of PAEs are about 5-10 times lower than those reported from Pacific Ocean(Zhang et al., 2019a), and in good agreement with those measured in the North Sea(Xie et al., 2005), the North Atlantic and the Arctic (0.03-5.03 ng/L)(Xie et al., 2007). Oceanic current dilution (Figure S2-5), as well as enhanced photodegradation and biodegradation under the tropical climate, may be responsible for the large differences in concentration between the open South China Sea and other coastal areas.(Net et al., 2015; Paluselli and Kim, 2020).

2.3.6 Water-Suspended Particular Matter Partitioning

PAEs have also been detected in suspended particular matters (SPMs) in seawater. The detection frequencies of PAEs in SPMs were 97% for DnBP, followed by BBP (75%), DEP (69%), DMP (53%) and DEHP (47%), while only 8% for DiBP and DCHP (Table S2-11). As shown in Table S2-13, SPM-bound PAE fractions were 0.34 ± 0.16 for DEHP, followed by 0.25 ± 0.14 for DiBP, 0.23 ± 0.14 for DnBP, 0.19 ± 0.09 for DEP and 0.08 ± 0.07 for DMP. Compared with other studies, the total suspended matter (TSM) fraction of DEHP is in line with the values determined in the North Sea (0.42) (Xie et al., 2005), whereas it is lower than those determined in the Lake Yssel and the Rhine

(0.67)(Ritsema et al., 1989). However, the TSM fractions of DnBP and DiBP are higher than the North Sea (0.02) and Rhine (0.02) but similar to the fractions (0.14-0.34) measured in the River Mersey Estuary in the U.K.(Preston and Alomran, 1986). The differences might be caused by the seawater sampling technique, the character of different SPMs, and water chemistry. The elevated seawater temperature in the tropical ocean usually lowers the SPM fractions of PAEs. However, the competition between absorption and degradation may lead to complicated water-SPM partitioning. Nevertheless, SPM-bound PAEs are expected to be accumulated in the sediment undergo slow degradation processes.(Mackintosh et al., 2006)

2.3.7 Environmental Source of PAEs

PAEs in the South China Sea are usually transported from terrestrial sources, such as volatilization during the production of plastic products, waste treatment, and riverine input from surrounding countries, which have been evidenced by the high PAE levels measured in indoor air, urban air and adjacent rivers. (Cao et al., 2022c; Huang et al., 2022; Newton et al., 2015; Zhang et al., 2022b) For instance, the sum concentrations of DMP, DEP, DnBP and DEHP were measured in fine atmospheric particles ($PM_{2.5}$) of metropolitan areas of Guangzhou (32.5-76.1 ng/m^3), Shanghai (10.1-101 ng/m^3), Beijing (8.02-107 ng/m^3) and Harbin (13.5-622 ng/m^3),(Zhang et al., 2019b) and 13 PAEs (range: 2.6-15.3 ng/m^3) were measured in atmospheric particles over the inland lake Chaohu.(He et al., 2019) Fang et al. reported DnBP and DEHP in atmospheric particles from various sites in central Taiwan, with respective mean concentrations of 33.94 and 109.7 ng/m^3 . (Fang et al., 2021; Latini, 2005) These concentrations of PAEs over land or island are usually 1-2 orders of magnitude higher than those reported in the South China Sea.

The river-run discharge from the Pearl River is an important vector for the occurrence of PAEs in the South China Sea. (Cao et al., 2022c; Zhang et al., 2020b) In addition, PAE concentrations accumulated in neighboring marginal seas could also be transported into South China Sea by the Chinese coastal current. In addition, PAE contaminations accumulated in neighboring marginal seas could also be transported into the South China Sea by the Chinese coastal current.(Zhu et al., 2022a) For instance, PAEs discharged from the Yangtze River are an important source for the East China Sea, which can be further transported to the South China Sea via Taiwan Strait. Besides, the Kuroshio Current has important effects on both physical and biological processes

of the North Pacific, including nutrient, sediment, and pollution transport.(Liu et al., 2021a; Shaw and Chao, 1994) Hence, PAEs discharged into the coastal areas could be partially transported to the South China Sea with the ocean currents. During the sampling cruise, the basin-wide circulation of the South China Sea was influenced by the South and East Asian summer monsoons in August,(Jan et al., 2021) and several cyclones occurred in the western Pacific Ocean. The cyclonic gyres significantly accelerate the matter exchange between the continental runoff and the Pacific oceanic water masses, which led to a strong dilution of the PAE concentrations observed in this study.

In addition, terrestrial wastes and matters, e.g., plastic litter or microplastics, could be transported to the South China Sea and release PAEs into air and seawater.(Harris et al., 2021; Jambeck et al., 2015; Schmidt et al., 2017) It is estimated that up to 300,000 t/y of plastic are discharged from the surrounding rivers into the South China Sea,(Lebreton et al., 2019) and as many as 2.56-7.08 million tons of plastic pollution to the ocean every year from the countries bordering the South China Sea.(Jambeck et al., 2015) Besides, about 1400 t microplastics entered the South China Sea by means of dry deposition.(Ding et al., 2021) As PAEs are the major plasticizers physically added to plastic matter, they can leach out from plastic materials and release into the water columns. DiBP and DnBP are the two main PAEs released from polyethylene bags, while DMP and DEP are mainly discharged from poly (vinyl chloride) products.(Paluselli et al., 2019) Microplastics in the ocean could efficiently release plastic additives, including PAEs, while the leaching process could be slowed down when microplastics are covered by a biofilm or buried in deep-sea sediment. (Fauvelle et al., 2021)

2.3.8 Air-Sea Exchange

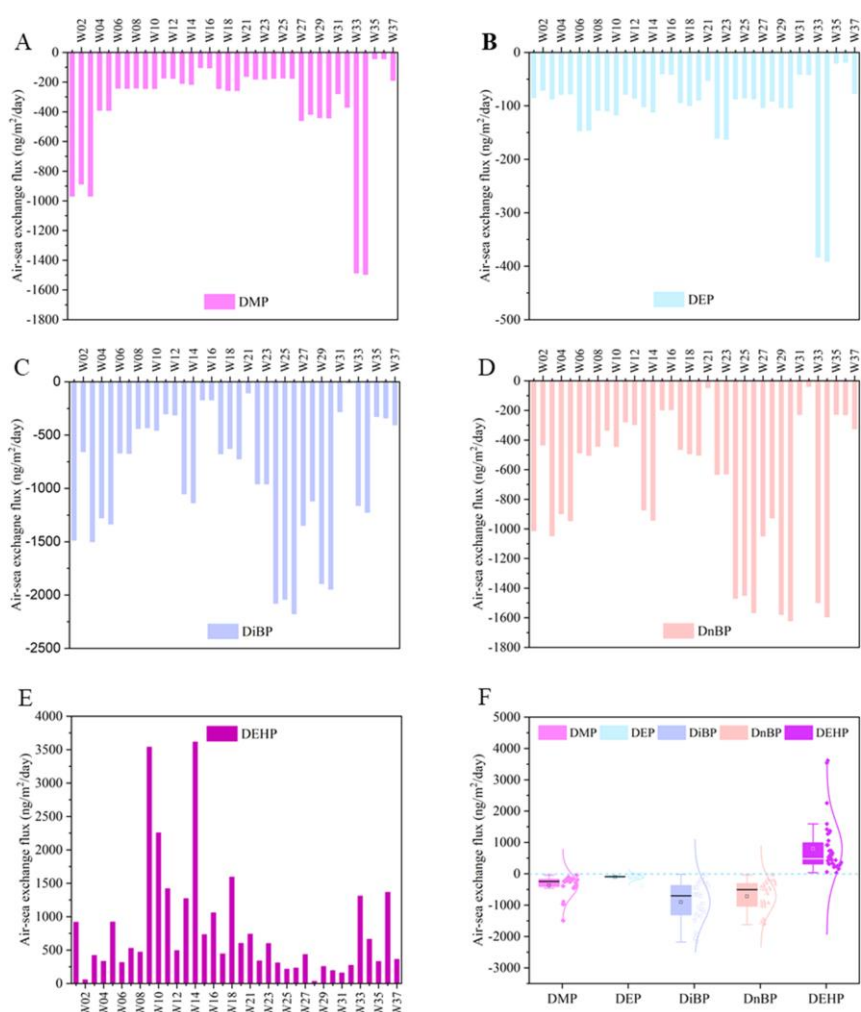


Figure 2-3 Air-sea exchange fluxes of PAEs ($\text{ng}/\text{m}^2/\text{day}$) are calculated with two-film fugacity mode using paired air-seawater concentrations. The positive (+) value indicates water-to-air volatilization, and negative (-) value means air-to-water deposition. (A) DMP, (B) DEP, (C) DiBP, (D) DnBP, (E) DEHP, and (F) the range of the air-sea exchange fluxes of individual PAEs.

The estimated air-sea exchange fluxes of PAEs in the South China Sea are shown in Figure 2-3; the details are summarized in Table S2-16. BBP and DCHP are excluded due to their low detection frequencies and low concentrations. Net volatilization dominated the air-sea exchange fluxes of DEHP, with an average of $+800 \pm 360$ $\text{ng}/\text{m}^2/\text{day}$, which is about 5-20 times higher than those estimated for the North Sea ($+53 \pm 24$ $\text{ng}/\text{m}^2/\text{day}$) (Xie et al., 2005) and for seawater off the Norwegian coast ($+212$ $\text{ng}/\text{m}^2/\text{day}$) (Xie et al., 2007), while it changed to air-to-water deposition in the open ocean and the high Arctic (Xie et al., 2007). In the South China Sea, the higher net volatilization fluxes of DEHP were estimated for the water/air sample pairs W9/A9, W14/A10 and W10/A9, which are consistent with the high concentrations of dissolved DEHP in seawater from the offshore. Although the lower molecular weight PAEs are

avored to partition to the gaseous phase, once they deposit into seawater, their high solubility in water and very low K_{AW} values limit their volatilization ability from the aquatic phase to air.(Cousins and Mackay, 2000) On the other hand, the air-water partition coefficients (K_{AW}) increase with growing molecular weight; hence, PAEs with higher molecular weight, such as DEHP, can potentially vaporize more rapidly from water to air, which aligns with the air-sea exchange fluxes of DEHP estimated in this work and other existing literature. (Xie et al., 2005; Xie et al., 2007) These findings suggest that PAEs are favored for both atmospheric and oceanic transport. Nevertheless, the air-sea exchange of PAEs from the marginal seas to remote oceans following the mode of “grass hopping”.(Wania and Mackay, 1996)

Though the concentrations of PAEs in the gaseous and dissolved phases and the physiochemical behaviors determine the direction and intensity of the air-sea exchange, several other important factors can affect the air-sea exchange fluxes of PAEs. Air mass circling in the South China Sea during the sampling period are dominated by summer monsoons. The clean oceanic air may dilute the PAEs emissions from terrigenous origins and decrease the air concentration gradients for the entire South China Sea. Consequently, the potential for water-to-air volatilization can be increased. Winter monsoons might intensify air-to-water deposition because the air masses originating from East Asia can significantly transport land emissions of PAEs to the South China Sea. Besides, the loss of PAEs through the sinking of sediment might cause a decline of dissolved PAE concentrations in seawater and lead to the tendency of air-water exchange of PAEs from air to water, especially for high molecular weight of PAEs. Furthermore, microbial degradation and adsorption of PAEs by phytoplankton in seawater could also eliminate dissolved PAE concentrations,(Paluselli et al., 2019) thereby increasing the air-to-water deposition potential. Other meteorological parameters, such as both temperature and wind speed, can also influence the air-water exchange fluxes by altering the total mass transfer coefficient.(Wanninkhof, 2014) For instance, the net volatilization fluxes of DEHP were estimated at 57 ng/m²/day for water sample W2 (wind speed: 1.1 m/s) and 33 ng/m²/day for W28 (wind speed:1.5 m/s), which are 20 times lower than the average of 800 ng/m²/day. This fits previous studies for PCBs in the South ChinaSea and Pacific Ocean.(Zhang and Lohmann, 2010)

2.3.9 Atmospheric Particle Deposition

As shown in figure 2-4 the dry deposition fluxes of total PAEs ranged from 34 to 3620 ng/m²/day with an average of 920±990 ng/m²/day (Table S2-17). The dry deposition fluxes of individual PAEs were dominated by DiBP (440±550 ng/m²/day), DnBP (370±430 ng/m²/day) and DEHP (91±42 ng/m²/day), which is consistent with the composition profile of PAEs in the particle phase. The highest dry deposition fluxes were determined near the coastal area of Southeast Asia, followed by several higher values along the coastal area of Southeast China. The lower dry deposition fluxes were estimated for air samples collected during rainfall since precipitation has significantly decreased the particle dry deposition. In addition, atmospheric circulation and continental or oceanic air masses are considered the main factors that influence the dry deposition fluxes of PAEs. The air masses off inland may bring high particle load into the coastal region, thereby increasing the dry deposition of PAEs in the marine environment. As the continental air masses prevail in fall and winter over the study area, it is suggested that dry deposition may play an important role in winter months in the South China Sea. In comparison with other classic organic contaminants, particle deposition fluxes of PAEs are less than that of decabromodiphenyl ether (BDE-209) OF 1670±1940 ng/m²/day in the Pearl River Delta,(Li et al., 2010) 3 times higher than that of polycyclic aromatic hydrocarbon (PAH) of 260±190 ng/m²/day observed near coast of the South China Sea,(Liu et al., 2013a) and 2 orders of magnitude higher than those of organochlorine pesticides (OCPs).(Li et al., 2010)

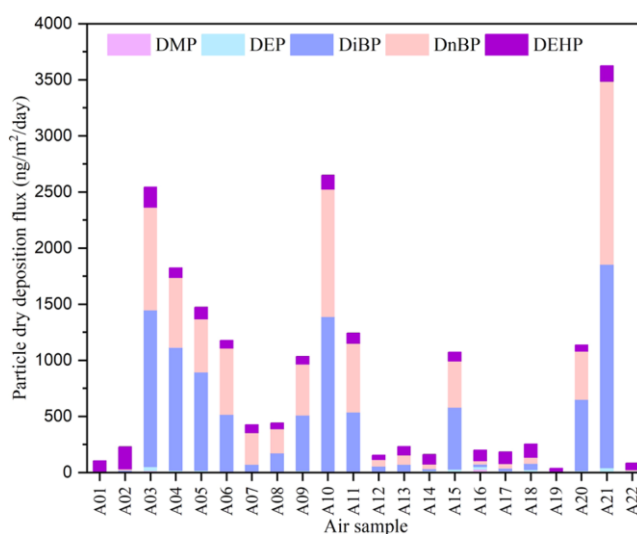


Figure 2-4 Dry deposition fluxes of particle-bound PAEs (ng/m²/day) to the South China Sea, which were dominated by DiBP and DnBP.

2.3.10 Atmospheric Dry Flux

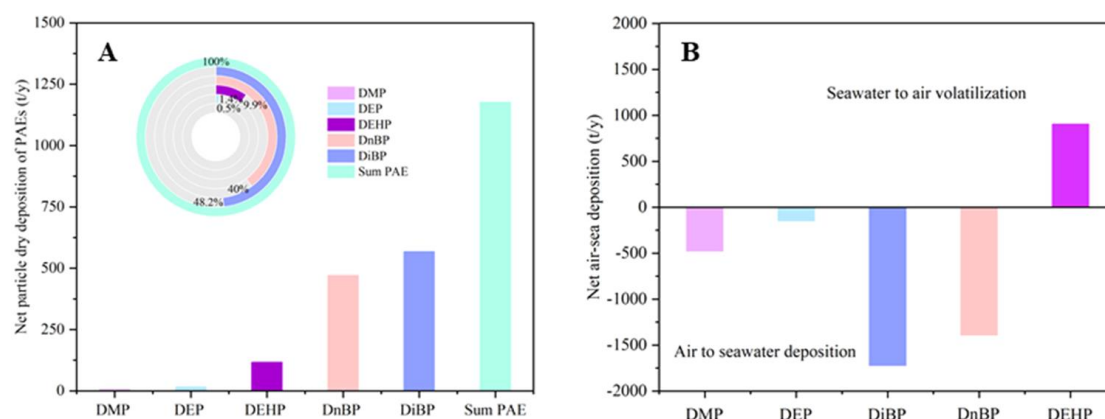


Figure 2-5 (A) Annual net dry deposition of particle-bound PAEs (t/y) and (B) the net air-sea exchange fluxes in the South China Sea (t/y). It should be noted that DEHP and DCHP showed net volatilization from water to air.

Given a surface area of approximately 3,500,000 km² for the South China Sea, (Liu, 2013) the atmospheric particle deposition fluxes of Σ_5 PAEs ranged from 46 to 4630 t/y, with a mean of 1180±1260 t/y (Figure 2-5A). DiBP, DnBP and DEHP accounted for 48.1, 40.0 and 9.9% of total particle deposition of PAEs, respectively. Once deposited in the sea, PAEs may repartition between dissolved and particle phase in the water column and sink to the bottom of the ocean. (Wang et al., 2021) PAEs have been measured in the sediment of the Indian Ocean with concentrations ranging from 823 to 1615 ng/g dw. (Cong et al., 2022) The atmospheric particle deposition can be an important source of PAEs in the oceanic sediment. (Cong et al., 2022) Nevertheless, the occurrences and inventories of PAEs in the sediment of the South China Sea request further research.

Based on the air-sea exchange fluxes of PAEs, the net depositions were dominated by DiBP and DnBP as well, with an average of 1150 and 920 t/y, followed by 470 t/y for DMP and 140 t/y for DEP (Figure 2-5B). the net volatilization of DEHP was estimated to be 1020 t/y from the South China Sea, which can be transported further to remote oceans via the atmosphere. The air-sea exchange fluxes of PAEs in this work were significantly higher than those estimated for the North Sea and the European Arctic. (Xie et al., 2005; Xie et al., 2007) The overall net fluxes are 3740 t/y deposition for DMP, DEP, DiBP and DnBP, and 900 t/y volatilization for DEHP in the South China Sea.

2.4 Implications

This study showed the dynamic air-sea exchange process may drive the transport of PAEs from contaminated marginal seas and estuaries toward remote marine environments, which can play an important role in the environmental transport and cycling of PAEs in the global ocean. The changing meteorological conditions, especially through the seasonality of the monsoon, have a strong impact on the variability of the air-sea exchange. So far, only a few regulations have been implemented to limit the applications of PAEs. Indeed, plastic debris or microplastics are a kind of intermediate storage and transport media for PAEs from sources to remote areas, and these release them into the local environment during life. On the other hand, the most toxic risk of microplastics to marine organisms can be attributed to the chemical additives such as PAEs, softeners, antioxidants and flame-retardants. Therefore, research on the interaction of microplastics and synthetic organic plastic additives in the marine environment including the interface interaction, sedimentation and bioaccumulation in the organisms needs to be strengthened in future studies.

Supporting Information

Text S2-1. Chemicals and materials

PAEs standard mixture, containing Dimethyl phthalate (DMP), Diethyl phthalate (DEP), Diisobutyl phthalate (DiBP), Di-n-butyl phthalate (DnBP), Butylbenzyl phthalate (BBP), Dicyclohexyl phthalate (DCHP) and Di(2-ethylhexyl) phthalate (DEHP) at 1000 $\mu\text{g}/\text{mL}$ each, and surrogate standards, e.g. deuterated dimethyl phthalate (DMP d4), diethyl phthalate (DEP d4), n-dibutyl phthalate (DnBP d4) and di(2-ethylhexyl) phthalate (DEHP d4), were supplied by LGC (Wesel, Germany).

Picograde® solvents, e.g. methanol, acetone, n-hexane and dichloromethane (DCM) were purchased from Promochem (Germany). Neutral silica gel (0.063-0.2 mm) was supplied by Macherey Nagel (Düren, Germany) and anhydrous sodium sulphate (99%) and XAD-2 resin was obtained from Merck (Darmstadt, Germany).

Text S2-2. Washout ratio

Considering both vapor and particle scavenging mechanism, washout ratio (W) can be expressed as equation 2-1, (Bidleman, 1988)

$$W = (1-\phi) (RT/H) + \phi W_p \quad (2-1)$$

where ϕ is the particle-bound fraction of the chemical, RT/H is the dimensionless Henry's law constant at the ambient temperature (298 K), and W_p is the particle scavenging coefficient. A representative W_p value of 20,000 is used for the calculation in this work. (Ligocki et al., 1967)

Text S2-3. Air-sea exchange

During the transport from continental sources to the South China Sea, PAEs may undergo several processes at the interface between air and seawater. The direction and fluxes of air-sea exchange of PAEs are mainly controlled by their physicochemical parameters such as Henry's Law Constants and the concentrations in air and seawater, and are influenced by metrological conditions. In this work, air-sea exchange fluxes of PAEs were calculated using the modified version of Whitman's two-film fugacity model, which has been extensively applied for the evaluation of PAHs, PCBs and PAEs in the marine environment, (Bamford et al., 2002; Bamford et al., 1999; Xie et al., 2005) The volatilization and deposition fluxes (F_{vol} and F_{dep} , ng/m²/day) are calculated as in equation 2-3 and 2-4,

$$K_{OL} = \left(\frac{1}{K_w} + \frac{1}{K_a * H} \right)^{-1} \quad (2-2)$$

$$F_{vol} = K_{OL} C_w \quad (2-3)$$

$$F_{dep} = K_{OL} C_a / H' \quad (2-4)$$

The net diffusive gas exchange flux (F , ng/m²/day) is then calculated by subtracting the volatilization flux from the deposition flux, which is described as equation 2-5,

$$F = K_{OL} \left(C_w - \frac{C_a}{H'} \right) \quad (2-5)$$

where C_w (ng/m³) and C_a (ng/m³) are the dissolved- and gas-phase concentrations, $(C_w - C_a/H')$ describes the concentration gradient (ng/m³), H' is the dimensionless Henry's law constant. The K_{OL} (m/s) is the overall mass transfer coefficient, which contains contributions from the mass transfer coefficients of the water phase (k_w) and the air phase (k_a). The calculation of K_w and K_a for PAEs refer to the equations recommended by Schwarzenbach et al. (Schwarzenbach et al., 2016) and Wanninkhof's quadratic relationship. (Wanninkhof, 1992) H' of PAEs are corrected with temperature of seawater (T_w , K) and averaged salt concentration (C_s , 0.5 mol/L). The total propagation

error in F was 45%, which is derived from an error propagation analysis from previous studies.(Xie et al., 2005) A positive F value indicates seawater to air volatilization, while a negative F means that deposition is dominating air-sea exchange flux.

Text S2-4. Atmospheric particle deposition

Atmospheric deposition is one of the key processes that remove pollutants from air and is considered the major source of organic matter and chemical pollutants into the marine environment. Based on the concentrations of PAEs measured in the particle phase, the particle-bound dry deposition fluxes (F_D , ng/m²/day) were calculated via equation 2-6 (Schwarzenbach et al., 2016):

$$F_D = C_p \times V_d \quad (2-6)$$

where C_p is the concentrations of particle phase PAEs (ng/m³), and V_d is the deposition velocity (cm/s), which can be used to estimate the deposition fluxes of air pollutants. In this work, we used the dry deposition velocity of 0.5 cm/s, which was estimated for pollutants concentrated in fine particles over the South China Sea.(Gao et al., 2020)

Text S2-5. Pearson correlation analysis

Correlation analysis of PAEs in air and seawater was conducted. Pearson correlation coefficient values of DiBP and DnBP ($p < 0.01$, $r \geq 0.951$), and DMP and DEP ($p < 0.01$, $r \geq 0.647$) (Table S2-14) indicated the significant correlations in between, and attributed to similar sources and transport pathways. While DEHP did not show any correlation with other PAEs. In seawater, DEP was highly correlated with DMP ($p < 0.01$, $r \geq 0.659$), BBP ($p < 0.01$, $r \geq 0.578$) and DEHP ($p < 0.01$, $r \geq 0.578$) (Table S2-15), and DEHP were correlated with most other PAEs, except from DCHP. We suppose PAEs have uniform sources for the seawater, while PAEs in air might be affected by their original sources, monsoon, and atmospheric degradation and precipitation.

Figure S 2-1 Air sampling stations in the South China Sea, with the blue dots marked at the starting position of each air sample

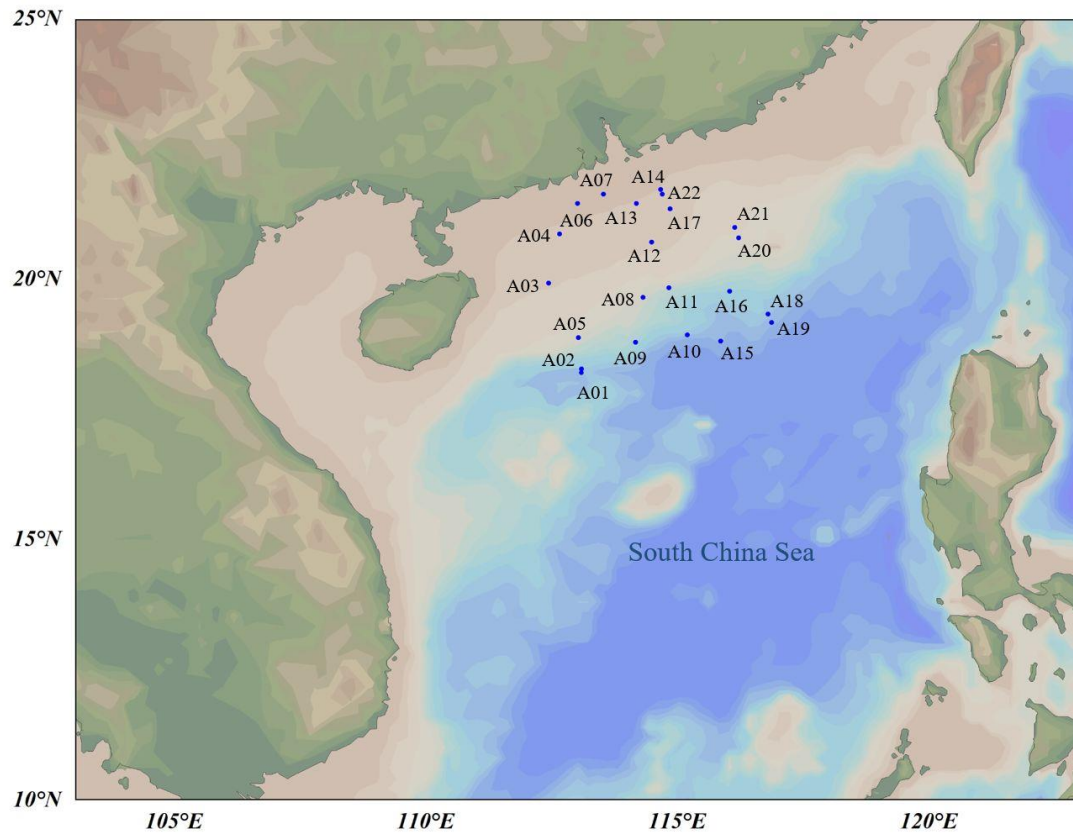


Figure S 2-2 (A) Seawater sampling stations in the South China Sea, with the black dots marked at the starting position of each water sample. The color map shows the salinity profile in surface seawater; (B) general water mass circulation in the research area in summer

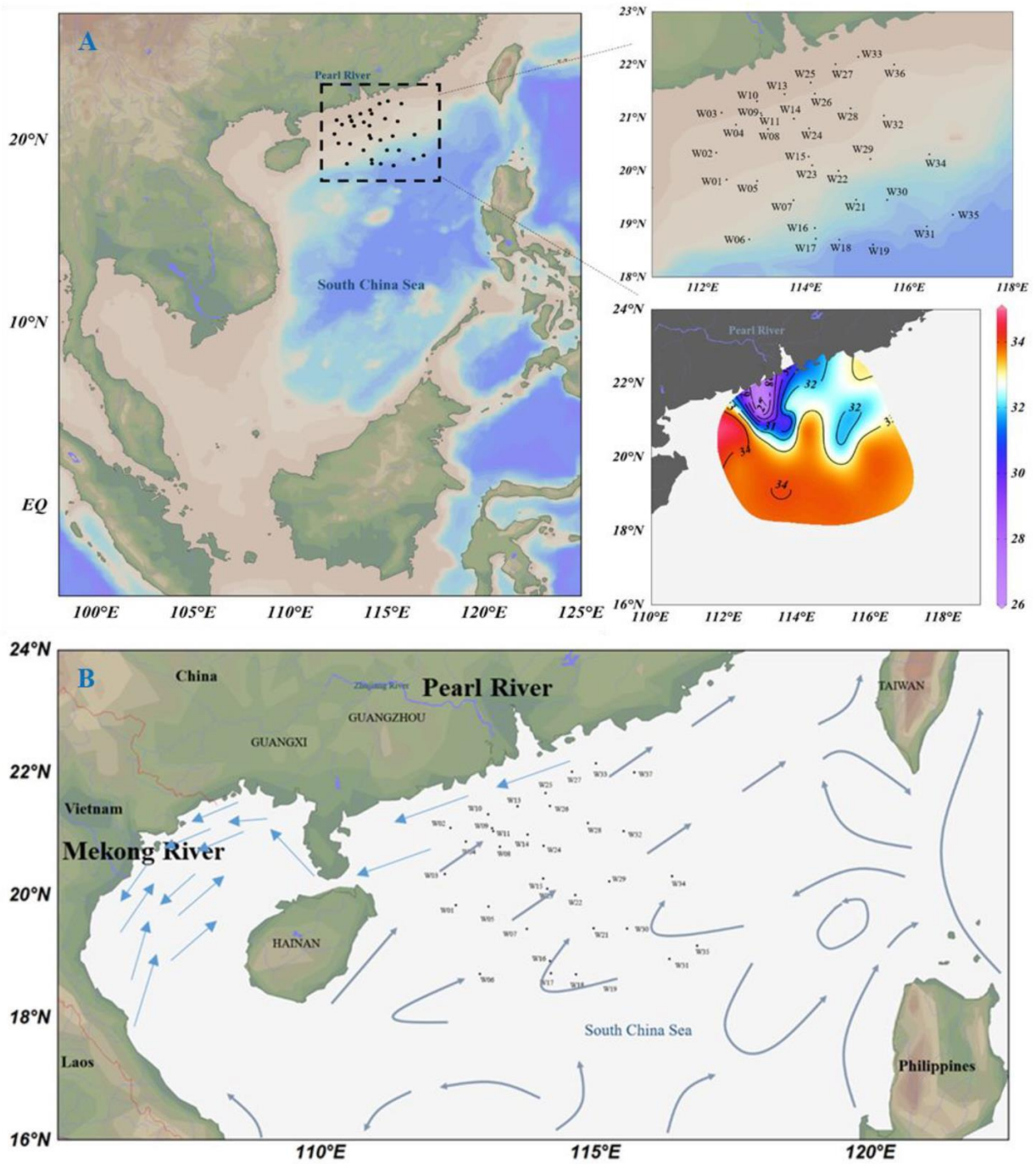


Figure S 2-3 **A.** High-volume air sampler is equipped with quartz fiber filter for atmospheric particles and a PUF/XAD-2 column for gaseous phase. The air sampler is placed at the upper deck and operated with headwind. The Filter and PUF-XAD-2 column are changed at sampling site. The PUF/XAD-2 column can be sealed with glass caps immediately after disconnected from the sampler to eliminate exposure time to the indoor air. The Quartz fiber filter is wrapped in a clean aluminum. PUF/XAD2 columns and filters are stored at -20°C ;

B: The set-up of high-volume water sampler equipped with glass fiber filter and a XAD-2 column. The high-volume water sampler is connected to the ship-intake system with metal tubing. A glass fiber filter is closed in the filter holder to collect suspended particular matters and a XAD-2 column to retain organic chemicals in the dissolved phase. The seawater flows over the entire system at a flow rate of 0.2-1 L/min. The XAD-2 column is sealed with clips immediately after the sampling, and stored at 5°C . Glass fiber filter is wrapped in a clean aluminum foil and stored at -20°C

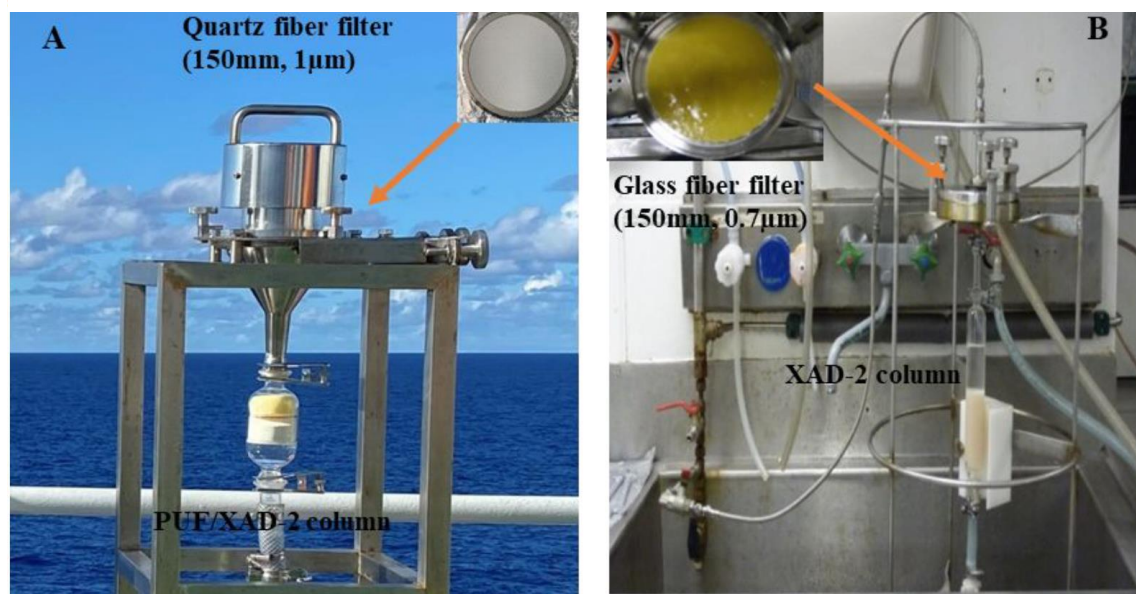
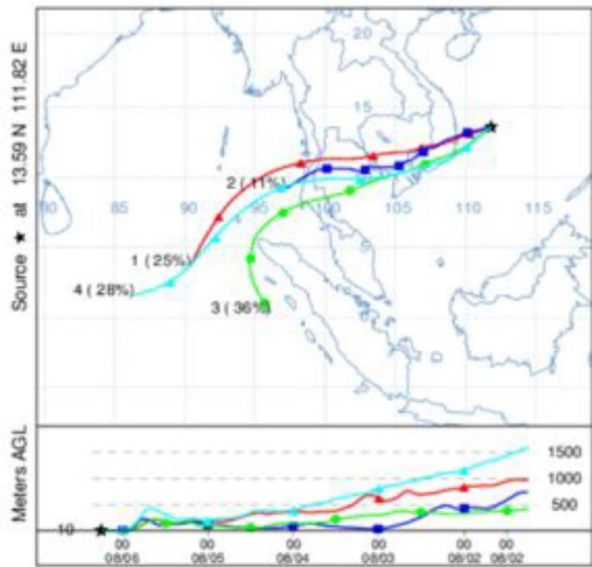
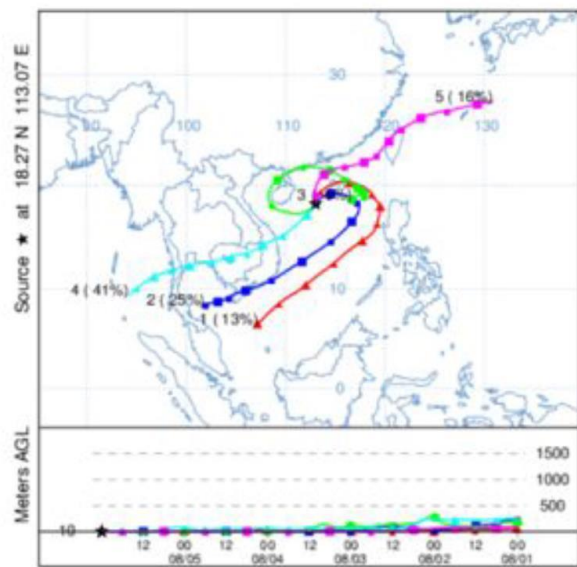


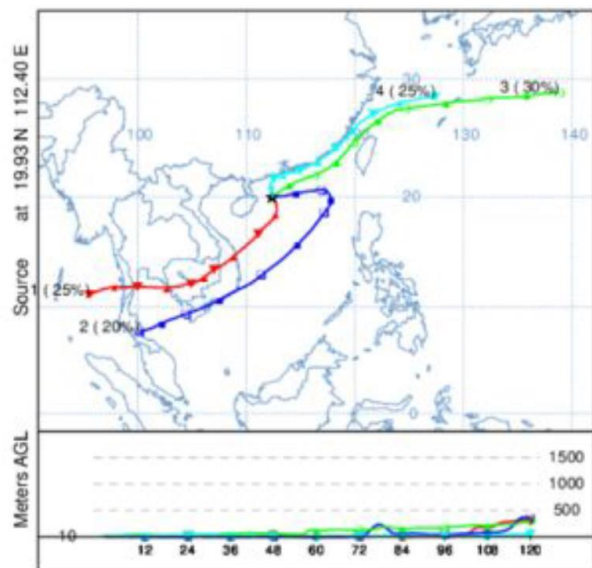
Figure S 2-4 Air mass back trajectories of air samples. Colors indicate the origin of the air mass parcels



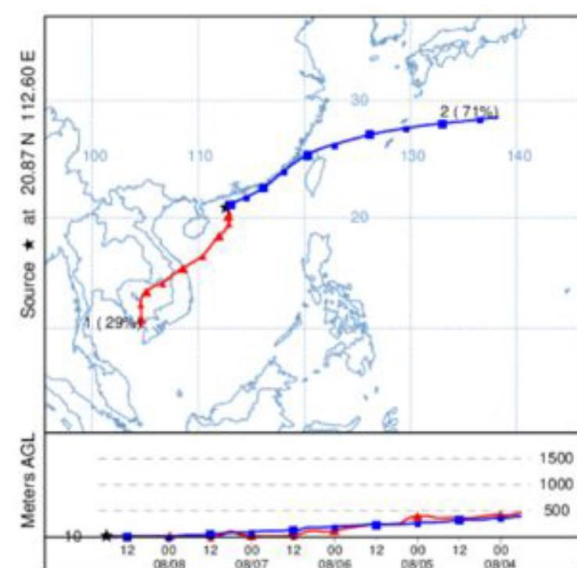
A01



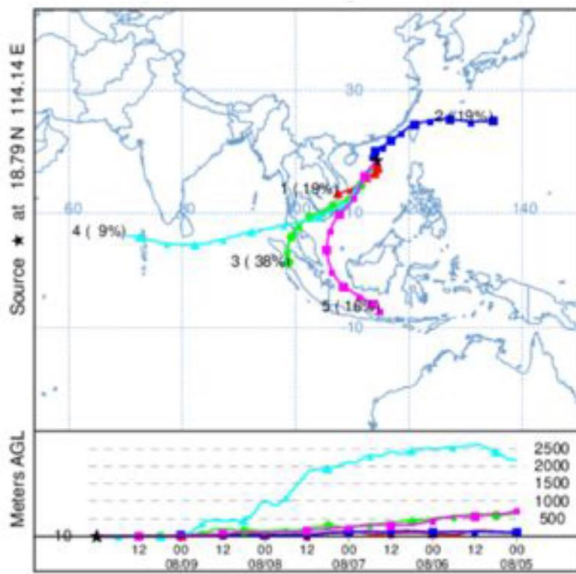
A02



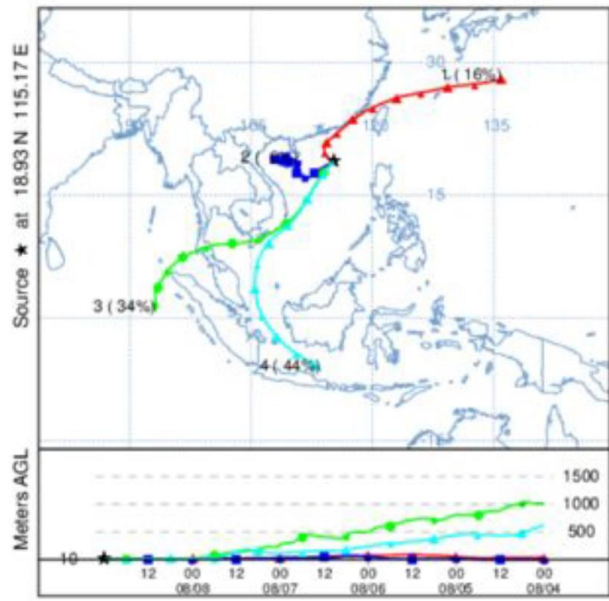
A03



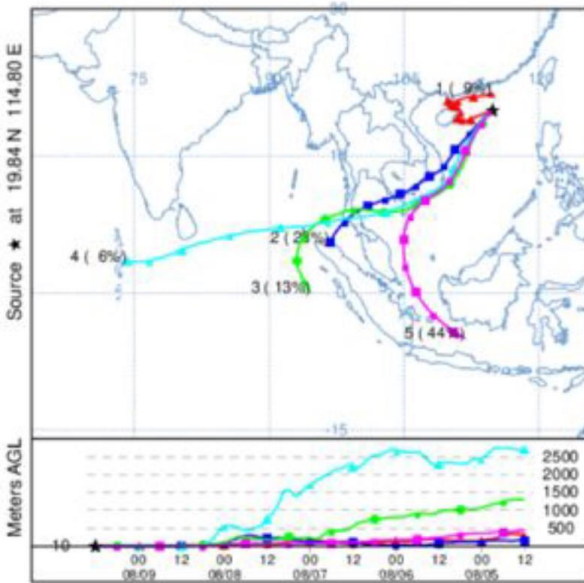
A04



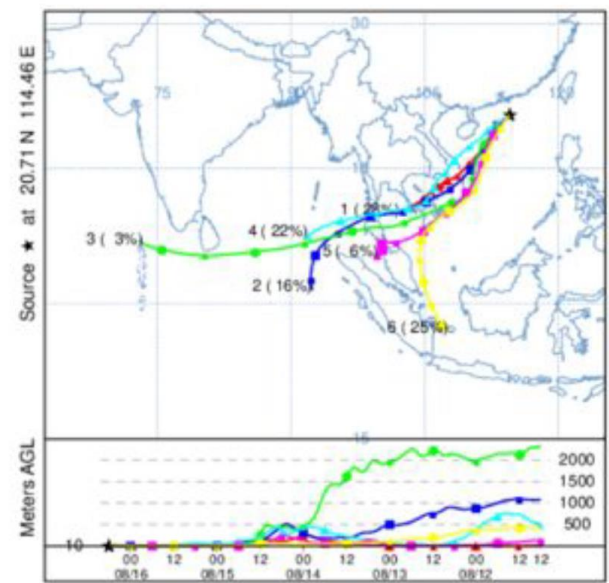
A09



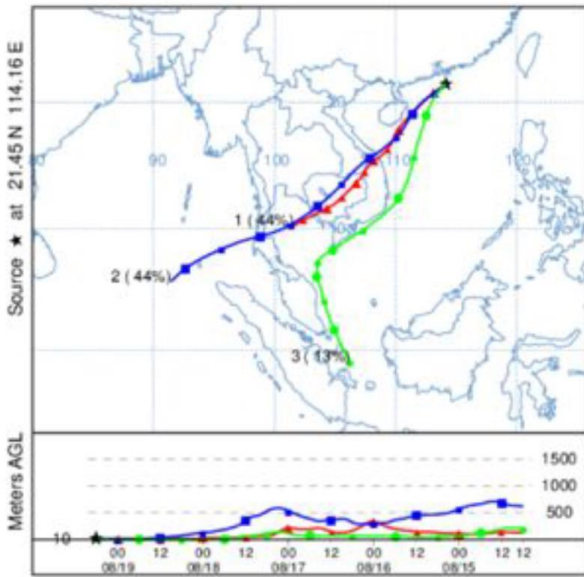
A10



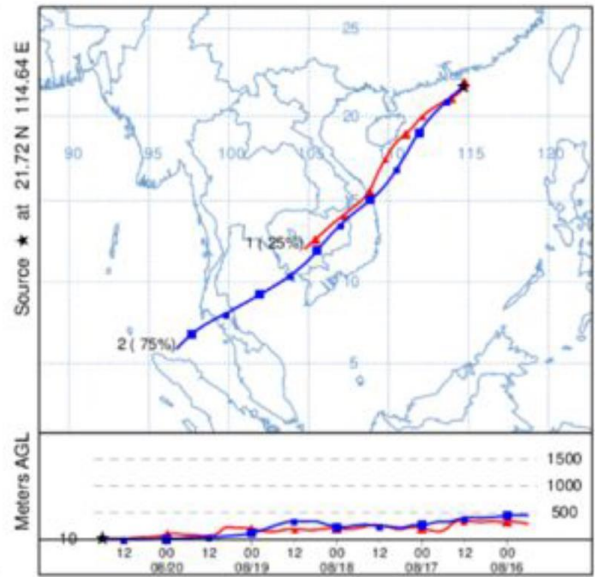
A11



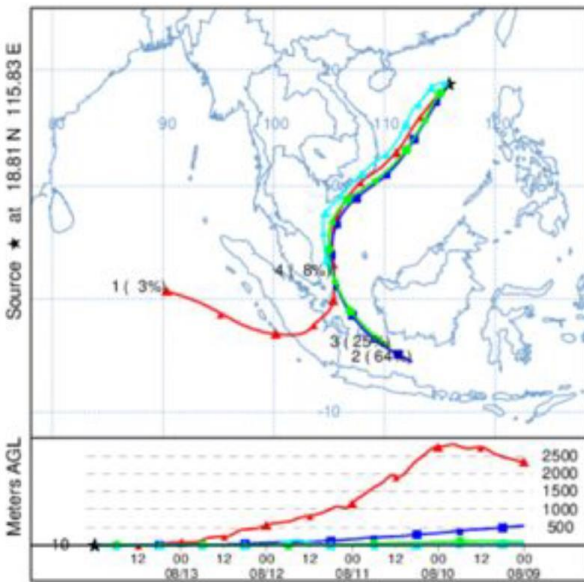
A12



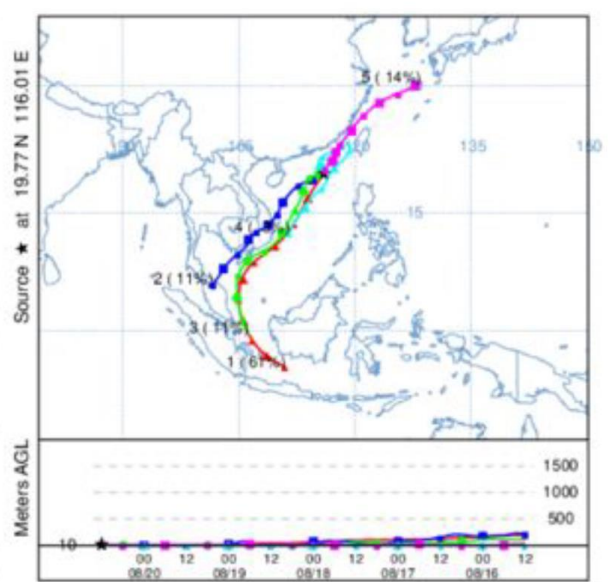
A13



A14



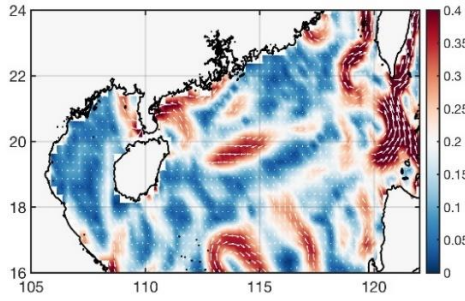
A15



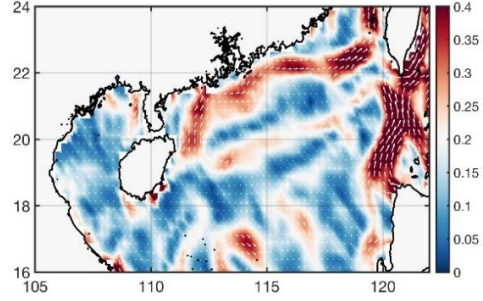
A16

Figure S 2-5 The schematic diagrams of the flow field of the South China Sea in 7th (A) 13th (B), 19th (C) and 25th (D) of August 2019

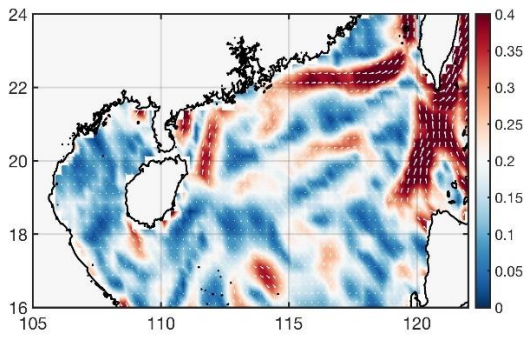
A



B



C



D

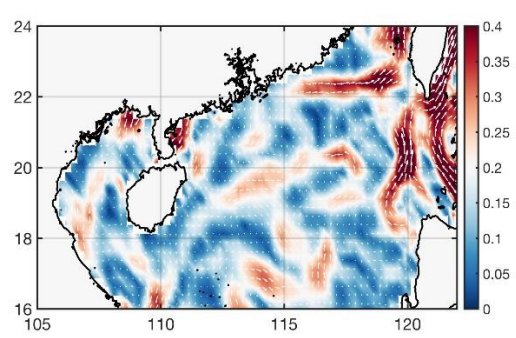


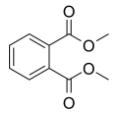
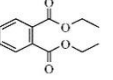
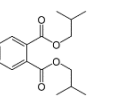
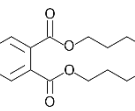
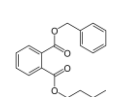
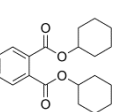
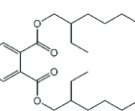
Table S 2-1. Detail information for air sampling

Air sample	Latitude (North, degree)	Longitude (East, degree)	Sampling Date	Time	Volume (m³)	Air temperature (°C)	Humidity (%)	Wind speed (m/s)	Wind direction (degree)
A01	13.589	111.820	5-Aug-2019	0:37	382	29.1	73.8	11.3	244.5
A02	18.278	113.070	6-Aug-2019	7:30	373	29	82.4	9.9	336.8
A03	19.927	112.414	7-Aug-2019	11:08	293	28.8	83.7	7.2	50.2
A04	20.867	112.632	8-Aug-2019	10:37	269	29.2	80.8	4.8	232.2
A05	18.875	112.997	9-Aug-2019	11:28	326	29.5	82.7	6.3	205
A06	21.453	112.986	11-Aug-2019	11:03	341	29.6	83.4	8.2	219.5
A07	21.631	113.505	12-Aug-2019	11:03	348	29.6	84.5	8.2	221.6
A08	19.651	114.290	13-Aug-2019	10:12	344	29.6	84.2	8.4	219.1
A09	18.787	114.142	14-Aug-2019	10:54	280	29.7	75.3	8.9	229.6
A10	18.926	115.167	15-Aug-2019	10:54	316	29.2	82.8	11.1	201.3
A11	19.839	114.797	16-Aug-2019	10:54	278	29.6	83	7.5	198.8
A12	20.708	114.456	17-Aug-2019	11:05	645	29.4	83.8	7.6	214.4
A13	21.452	114.160	19-Aug-2019	10:39	290	29.4	74.8	6	223
A14	21.720	114.644	20-Aug-2019	11:00	535	28.6	74.4	8.3	94.3
A15	18.813	115.830	22-Aug-2019	10:39	339	26.6	87	9.7	314.9
A16	19.766	116.008	23-Aug-2019	11:46	356	28.9	80.3	3.4	26
A17	21.351	114.831	24-Aug-2019	11:46	504	30.3	79.9	12.5	242.3
A18	19.332	116.770	26-Aug-2019	11:00	310	29.2	81.7	3.9	141.6
A19	19.166	116.840	27-Aug-2019	11:00	531	28.7	81.7	7.2	35.3
A20	20.791	116.190	29-Aug-2019	11:00	345	28.5	81.3	7.8	124.7
A21	20.993	116.111	30-Aug-2019	11:06	313	28.5	78.1	4.6	108.8
A22	21.630	114.665	31-Aug-2019	11:15	300	28.7	79.4	7.9	81.5

Table S 2-2. Detail information for seawater sampling

Seawater Sample	Latitude (North, degree)	Longitude (East, degree)	Sampling Date	Volume (L)	Ta (°C)	Tw (°C)	Conductivity (S/m)	Depth (m)
W01	19.83	112.45	7-Aug-2019	100	28.8	29.9	5.64	113.2
W02	20.34	112.25	7-Aug-2019	135	28.5	29.6	5.65	83.4
W03	21.09	112.35	8-Aug-2019	171	29	29.4	5.64	48.8
W04	20.87	112.63	8-Aug-2019	178	29.4	29.6	5.67	60
W05	19.81	113.04	9-Aug-2019	193	29.4	30	5.67	154
W06	18.71	112.89	9-Aug-2019	177	29.4	30	5.67	900
W07	19.45	113.75	10-Aug-2019	244	29.8	29.8	5.67	472.5
W08	20.78	113.25	10-Aug-2019	196	29.3	30	5.4	81.1
W09	21.09	113.12	11-Aug-2019	36	29.8	30.3	4.74	60
W10	21.31	113.04	11-Aug-2019	169	29.8	29.8	4.57	42
W11	21.04	113.13	12-Aug-2019	84	30.3	30.4	4.98	44.3
W12	21.04	113.13	12-Aug-2019	119	30.3	30.4	4.98	44.3
W13	21.44	113.57	12-Aug-2019	68	29.7	29.6	5.18	42.2
W14	20.98	113.75	12-Aug-2019	105	29.7	30.4	4.83	85.6
W15	20.27	114.04	13-Aug-2019	310	29.8	29.6	5.58	121.4
W16	18.92	114.16	13-Aug-2019	199	29.5	29.8	5.66	1348.3
W17	18.72	114.18	14-Aug-2019	198	29.5	29.8	5.66	1859.1
W18	18.70	114.64	14-Aug-2019	126	29.2	29.7	5.65	3510
W19	18.61	115.29	15-Aug-2019	247	29.2	29.4	5.62	3694.5
W20	19.02	115.13	15-Aug-2019	108	29.2	29.6	5.63	2276.6
W21	19.45	114.96	16-Aug-2019	195	29.9	29.7	5.62	1469.2
W22	20.00	114.62	16-Aug-2019	195	27.7	29.7	5.58	1469.2
W23	20.10	114.11	17-Aug-2019	165	29.6	29.8	5.61	187.5
W24	20.80	114.05	18-Aug-2019	165	29.6	30	5.68	89
W25	21.66	114.08	18-Aug-2019	217	27.7	29.6	5.45	51
W26	21.45	114.16	19-Aug-2019	210	29.2	29.9	5.42	55
W27	22.01	114.56	20-Aug-2019	143	28.4	29.2	5.3	40
W28	21.17	114.85	20-Aug-2019	158	28.4	29.7	5.46	95
W29	20.22	115.24	21-Aug-2019	185	26.7	29.4	5.35	468
W30	19.45	115.56	22-Aug-2019	258	28.7	29.3	5.56	2490
W31	18.95	116.33	23-Aug-2019	240	28.8	29.4	5.61	2732
W32	21.04	115.5	24-Aug-2019	220	29.4	29.8	5.34	125
W33	22.14	115	25-Aug-2019	250	27.5	29.9	5.44	51.8
W34	20.31	116.38	26-Aug-2019	138	29.2	29.4	5.58	961
W35	19.17	116.84	26-Aug-2019	180	29.2	29.5	5.6	3339
W36	19.17	116.84	27-Aug-2019	35	29.5	29.6	5.6	3340
W37	22.00	115.7	31-Aug-2019	100	29.2	29.9	5.54	80

Table S 2-3. Physiochemical properties of seven phthalate esters(Cousins and Mackay, 2000)

Chemical Name	Abbreviation	CAS	MW	Chemical formula	V _p (Pa)	S (mg/L)	H (pa.m ³ /mol)	logK _{ow}	logK _{oa}	logK _{aw}	Half-life time in air (d)	Chemical structure
Dimethyl phthalate	DMP	131-11-3	194.19	C ₁₀ H ₁₀ O ₄	0.263	5220	9.78x10 ⁻³	1.61	7.01	-5.4	14.4	
Diethyl phthalate	DEP	84-66-2	222.24	C ₁₂ H ₁₄ O ₄	6.48x10 ⁻²	591	2.44x10 ⁻²	2.54	7.55	-5.01	2.39	
Diisobutyl phthalate	DiBP	84-69-5	278.35	C ₁₆ H ₂₂ O ₄	4.73x10 ⁻³	9.9	0.13	4.27	8.54	-4.27	0.58	
Dibutyl phthalate	DnBP	84-74-2	278.34	C ₁₆ H ₂₂ O ₄	4.73x10 ⁻³	9.9	0.13	4.27	8.54	-4.27	0.89	
Benzylbutyl phthalate	BBP	85-68-7	312.37	C ₁₉ H ₂₀ O ₄	2.49x10 ⁻³	3.8	0.205	4.70	8.78	-4.08	0.75	
Dicyclohexyl phthalate	DCHP	84-61-7	330.42	C ₂₀ H ₂₆ O ₄	6.1x10 ⁻⁴	4.1x10 ⁻²	4.92	6.2	11.59	-5.39	0.22	
Bis(2-ethylhexyl) phthalate	DEHP	117-81-7	390.56	C ₂₄ H ₃₈ O ₄	2.52x10 ⁻⁵	2.49x10 ⁻³	3.95	7.73	10.53	-2.80	0.38	

V_p: vapor pressure at 25°C; *S*: water solubility at 25°C; *H*: Henry's law constants at 25°C; *logK_{ow}*: log Octanol-Air coefficient at 25°C; *logK_{oa}*: log Octanol-Air coefficient at 25°C; *logK_{aw}*: log air-water transfer coefficient; Half-life time in air (d) (exclude DiBP and DCHP)(Perterson, 2003); Half-live time in air for DiBP and DCHP: (Calculated by EPIWEB 4.1). Physiochemical properties of DCHP were Calculated with EPIWEB 4.1.

Table S 2-4. Information about the chemicals and material applied in this work

Chemical and material	Description	Supplier
Dichloromethane	Pico grade	Promochem, Wesel, Germany
n-Hexane	Pico grade	Promochem, Wesel, Germany
Methanol	Pico grade	Promochem, Wesel, Germany
Acetone	Pico grade	Promochem, Wesel, Germany
Dimethyl phthalate-3,4,5,6-d4	Ring-d4, 98%, 100µg/mL	LGC, Wesel, Germany
Diethyl phthalate-3,4,5,6-d4	Ring-d4, 98%, 100µg/mL	LGC, Wesel, Germany
Dibutyl phthalate-3,4,5,6-d4	Ring-d4, 98%, 100µg/mL	LGC, Wesel, Germany
Bis(2-ethylhexyl) phthalate-3,4,5,6-d4	Ring-d4, 98%, 100µg/mL	LGC, Wesel, Germany
2,2',3,3',4,5,5',6,6'- Nonachlorobiphenyl (¹³ C ₁₂)	99%, 2µg/mL	Cambridge Isotope Laboratories, UK
Phthalate esters Analytes Mix 3 Content: DMP, DEP, DiBP, DnBP, BBP, DCHP, DEHP and other 10 PAEs	1000µg/mL	LGC, Wesel, Germany
Silica gel	0.063-0.2mm	Macherey Nagel, Düren, Germany
Anhydrous sodium sulphate	99%	Merck, Darmstadt, Germany
Amberlite XAD-2	20-60 mesh	Merck, Darmstadt, Germany

Table S 2-5. Agilent 7890 GC-MS/MS conditions

Parameter	Value
Analytical column	2 set Agilent HP5-ms, 250 µm × 15 m, 0.25 µm
Sample injection mode	1 µL Pulsed splitless using Multimode Inlet (MMI)
Injection port liner	Agilent 200 µL dimpled, single-taper liner
Injection temperature program	20 °C (0.2 minutes), 300 °C/min to 300 °C
Injection pulsed pressure	25 psi (1.9 minutes)
Purge flow to spit vent	50 mL/min (2.0 minutes)
Carrier gas	Helium
Carrier gas flow	1.2 mL/min
Oven temperature program	50 °C for 2 min, 20 °C/min to 80 °C, 5 °C/min to 250 °C, 15 °C/min to 300 °C (14 min)
Post run	310 °C for 3 min
Backflush	3.0 ml/min
Mass spectrometer	Agilent 7000C with electron impact ionization source operated in multiple reaction monitoring mode (MRM)
Ionization mode	Positive
Source temperature	280 °C
Quadrupole 1 and 2 temperature	150 °C
Transfer line temperature	280 °C

Table S 2-6 Detail information for the determination of PAEs using GC-MS/MS

PAE	Quantifier ions (m/z)	Qualifier ions (m/z)	Collision energy (eV)	Retention time (min)	Instrumental detection limit(pg)
DMP	163>77	163>135	15	16.963	0.02
DEP	149>93	149>121	15	20.258	0.03
DiBP	149>93	149>121	15	26.105	0.04
DnBP	149>93	149>121	15	27.956	0.04
BBP	149>93	149>121	15	34.854	0.1
DCHP	149>93	149>121	15	37.532	0.1
DEHP	149>93	149>121	15	37.955	0.2
d4-DMP	167>81	167>139	15	16.933	-
d4-DEP	153>97	153>125	15	20.232	-
d4-DnBP	153>97	153>125	15	27.937	-
d4-DEHP	153>97	153>125	15	37.943	-

Table S 2-7. The field blanks and the method detection limits of PAEs in PUF/XAD-2, XAD-2 columns, QFF and GFF filters

Sample material	PUF/XAD-2 column (gas)		QFF (particle)		XAD-2 column (dissolved phase)		GFF (particular matter)	
	Blank (mean±SD) (ng/m ³)	MDL (ng/m ³)	Blank (mean±SD) (ng/m ³)	MDL (ng/m ³)	Blank (mean±SD) (ng/L)	MDL (ng/L)	Blank (mean±SD) (ng/L)	MDL (ng/L)
DMP	0.017±0.006	0.036	0.002±0.001	0.004	0.002±0.001	0.004	0.005±0.002	0.011
DEP	0.014±0.002	0.022	0.008±0.004	0.021	0.008±0.004	0.021	0.021±0.008	0.045
DiBP	0.020±0.007	0.042	0.005±0.001	0.007	0.005±0.001	0.007	0.045±0.011	0.077
DnBP	0.037±0.011	0.068	0.006±0.002	0.011	0.006±0.002	0.011	0.015±0.001	0.017
BBP	0.060±0.010	0.090	0.001±0.000	0.001	0.001±0.000	0.001	0.001±0.001	0.002
DCHP	0.001±0.000	0.002	0.001±0.000	0.001	0.001±0.000	0.001	0.001±0.000	0.001
DEHP	0.14±0.002	0.15	0.074±0.031	0.166	0.074±0.031	0.17	0.17±0.099	0.47

Table S 2-8. Concentrations of PAEs in the atmosphere over the South China Sea. The MDLs of PAEs calculated with individual sampling volumes are given in brackets for the calculated concentrations less than MDLs.

Air sample	DMP	DEP	DiBP	DnBP	BBP(MDL)	DCHP (MDL)	DEHP	Σ_7 PAEs
Gaseous phase (C_g, ng/m³)								
A01	0.45	0.10	1.37	0.94	0.02 (0.09)	0.00 (0.002)	2.80	5.68
A02	0.26	0.25	0.74	0.34	0.06 (0.09)	0.00 (0.002)	1.42	3.07
A03	1.60	0.14	2.93	2.13	0.09(0.11)	0.002	0.47	7.36
A04	0.89	0.17	3.46	2.48	0.03(0.12)	0.024	0.86	7.91
A05	0.45	0.26	1.46	1.13	0.03(0.10)	0.005	0.68	4.00
A06	0.27	0.13	0.58	0.57	0.07(0.10)	0.001 (0.002)	0.67	2.28
A07	0.32	0.17	1.93	1.63	0.03(0.09)	0.003	0.70	4.78
A08	0.15	0.06	0.29	0.35	0.05(0.10)	0.001(0.002)	0.46	1.37
A09	0.35	0.13	1.15	0.82	0.02(0.12)	0.013	0.63	3.12
A10	0.19	0.06	0.15	0.09	0.03(0.10)	0.001 (0.002)	0.25	0.76
A11	0.29	0.26	1.76	1.19	0.01(0.12)	0.001 (0.003)	0.50	4.00
A12	0.28	0.14	4.02	2.90	0.08	0.006	0.36	7.79
A13	0.68	0.15	2.31	1.81	0.08(0.11)	0.002 (0.003)	0.85	5.88
A14	0.65	0.15	3.58	3.00	0.03(0.06)	0.004	0.79	8.21
A15	0.36	0.05	0.46	0.38	0.02(0.10)	0.002	0.31	1.58
A16	1.08	0.12	0.05	0.15	0.04(0.09)	0.001 (0.002)	0.22	1.68
A17	1.53	0.39	1.50	1.96	0.02(0.06)	0.002	1.08	6.48
A18	0.12	0.06	1.10	0.78	0.07(0.10)	0.001 (0.002)	0.19	2.32
A19	0.14	0.06	1.30	1.12	0.04(0.06)	0.003	0.34	3.00
A20	0.24	0.08	0.16	0.12	0.01(0.10)	0.00 (0.002)	0.22	0.83
A21	0.47	0.19	1.26	1.06	0.05(0.10)	0.002	0.30	3.33
A22	0.25	0.20	4.63	4.26	0.07(0.10)	0.012	0.55	9.98
Mean	0.50	0.15	1.64	1.33	0.04(0.09)	0.00 (0.002)	0.67	4.34
S.D.	0.42	0.08	1.33	1.10	0.03	0.01	0.57	2.70
Median	0.34	0.14	1.33	1.09	0.03(0.09)	0.00 (0.002)	0.52	3.67
Max	1.60	0.39	4.63	4.26	0.09(0.09)	0.02	2.80	9.98
Min	0.12	0.05	0.05	0.09	0.01(0.09)	0.00 (0.002)	0.19	0.76
Particle phase (C_p, ng/m³)								
A01	0.01	0.02	0.01	0.02	0.0002(0.001)	0.000(0.001)	0.54	0.60
A02	0.00	0.01	0.10	0.06	0.001	0.000(0.001)	1.15	1.32
A03	0.09	0.21	8.08	5.31	0.001	0.0013	1.04	14.72
A04	0.03	0.07	6.35	3.60	0.002	0.0102	0.49	10.56
A05	0.02	0.08	5.08	2.74	0.000(0.001)	0.0011	0.60	8.52
A06	0.02	0.04	2.94	3.41	0.003	0.000(0.001)	0.39	6.81
A07	0.01	0.04	0.36	1.65	0.005	0.0079	0.40	2.47
A08	0.01	0.04	0.96	1.24	0.002	0.0025	0.31	2.56
A09	0.02	0.07	2.87	2.63	0.005	0.0139	0.39	6.00
A10	0.02	0.05	7.97	6.57	0.005	0.0015	0.73	15.34
A11	0.01	0.05	3.05	3.54	0.003	0.0043	0.53	7.20
A12	0.01	0.02	0.31	0.33	0.002	0.0012	0.23	0.90
A13	0.03	0.03	0.36	0.48	0.001	0.0024	0.44	1.34
A14	0.02	0.07	0.10	0.24	0.004	0.0051	0.50	0.93
A15	0.02	0.14	3.20	2.38	0.008	0.0062	0.47	6.22
A16	0.16	0.14	0.13	0.17	0.003	0.001 (0.001)	0.55	1.16
A17	0.01	0.06	0.15	0.23	0.003	0.0010	0.60	1.06
A18	0.03	0.13	0.30	0.31	0.001	0.0005	0.68	1.46
A19	0.01	0.02	0.01	0.03	0.000(0.001)	0.0008	0.15	0.21
A20	0.03	0.07	3.67	2.49	0.002	0.001 (0.001)	0.32	6.58
A21	0.04	0.20	10.50	9.44	0.005	0.020	0.80	21.00
A22	0.01	0.03	0.04	0.06	0.000(0.001)	0.001 (0.001)	0.34	0.48
Mean	0.03	0.07	2.57	2.13	0.002	0.004	0.53	5.34
S.D.	0.03	0.06	3.17	2.47	0.002	0.005	0.24	5.73

Median	0.02	0.06	0.66	1.44	0.002	0.001	0.50	2.51
Max	0.16	0.21	10.50	9.44	0.008	0.020	1.15	21.00
Min	0.00	0.01	0.01	0.02	0.000(0.001)	0.000 (0.001)	0.15	0.21
Sum of C_g+C_p (ng/m³)								
A01	0.46	0.12	1.38	0.96	0.02	0.00	3.34	6.28
A02	0.26	0.26	0.84	0.40	0.06	0.00	2.57	4.39
A03	1.69	0.35	11.01	7.44	0.09	0.00	1.51	22.08
A04	0.92	0.24	9.81	6.08	0.03	0.03	1.35	18.47
A05	0.47	0.34	6.54	3.87	0.03	0.00	1.28	12.52
A06	0.29	0.17	3.52	3.98	0.07	0.00	1.06	9.09
A07	0.33	0.21	2.29	3.28	0.03	0.01	1.10	7.25
A08	0.16	0.10	1.25	1.59	0.05	0.00	0.77	3.93
A09	0.37	0.20	4.02	3.45	0.02	0.02	1.02	9.12
A10	0.21	0.11	8.12	6.66	0.04	0.00	0.98	16.10
A11	0.30	0.31	4.81	4.73	0.01	0.00	1.03	11.20
A12	0.29	0.16	4.33	3.23	0.08	0.01	0.59	8.69
A13	0.71	0.18	2.67	2.29	0.08	0.00	1.29	7.22
A14	0.67	0.22	3.68	3.24	0.03	0.01	1.29	9.14
A15	0.38	0.19	3.66	2.76	0.03	0.01	0.78	7.80
A16	1.24	0.26	0.18	0.32	0.04	0.00	0.77	2.84
A17	1.54	0.45	1.65	2.19	0.02	0.00	1.68	7.54
A18	0.15	0.19	1.40	1.09	0.07	0.00	0.87	3.78
A19	0.15	0.08	1.31	1.15	0.04	0.00	0.49	3.21
A20	0.27	0.15	3.83	2.61	0.01	0.00	0.54	7.41
A21	0.51	0.39	11.76	10.50	0.05	0.02	1.10	24.33
A22	0.26	0.23	4.67	4.32	0.07	0.01	0.89	10.46
Mean	0.53	0.22	4.21	3.46	0.05	0.01	1.20	9.67
S.D.	0.44	0.10	3.31	2.48	0.02	0.01	0.66	5.86
Median	0.35	0.20	3.67	3.23	0.04	0.00	1.05	8.24
Max	1.69	0.45	11.76	10.50	0.09	0.03	3.34	24.33
Min	0.15	0.08	0.18	0.32	0.01	0.00	0.49	2.84

Table S 2-9. Particle-bound fractions (ϕ) of PAEs in air samples from the South China Sea. The particle-bound fractions are quite uncertain because BBP and DCHP were below MDLs in most particle samples.

Sample	DMP	DEP	DiBP	DnBP	BBP	DCHP	DEHP	PEs
A01	0.01	0.17	0.01	0.02	0.01	0.02	0.16	0.10
A02	0.02	0.05	0.11	0.16	0.01	0.49	0.45	0.30
A03	0.05	0.59	0.73	0.71	0.01	0.42	0.69	0.67
A04	0.03	0.29	0.65	0.59	0.06	0.30	0.36	0.57
A05	0.03	0.24	0.78	0.71	0.01	0.19	0.47	0.68
A06	0.07	0.23	0.84	0.86	0.04	0.29	0.37	0.75
A07	0.03	0.18	0.16	0.50	0.13	0.72	0.36	0.34
A08	0.06	0.40	0.77	0.78	0.03	0.65	0.40	0.65
A09	0.06	0.35	0.71	0.76	0.09	0.52	0.38	0.66
A10	0.08	0.42	0.98	0.99	0.15	0.72	0.75	0.95
A11	0.05	0.16	0.63	0.75	0.18	0.79	0.52	0.64
A12	0.03	0.10	0.07	0.10	0.02	0.17	0.40	0.10
A13	0.04	0.18	0.13	0.21	0.02	0.54	0.34	0.19
A14	0.03	0.32	0.03	0.07	0.13	0.54	0.39	0.10
A15	0.05	0.72	0.87	0.86	0.28	0.76	0.60	0.80
A16	0.13	0.54	0.70	0.52	0.06	0.36	0.72	0.41
A17	0.01	0.14	0.09	0.11	0.12	0.37	0.36	0.14
A18	0.2	0.68	0.22	0.29	0.02	0.42	0.78	0.39
A19	0.05	0.24	0.01	0.02	0.01	0.21	0.30	0.07
A20	0.1	0.46	0.96	0.95	0.13	0.86	0.59	0.89
A21	0.08	0.52	0.89	0.90	0.09	0.91	0.73	0.86
A22	0.05	0.13	0.01	0.01	0.01	0.06	0.38	0.05
Mean	0.06	0.32	0.47	0.49	0.07	0.47	0.48	0.47
S.D.	0.04	0.19	0.37	0.35	0.07	0.26	0.17	0.30

Table S 2-10. Washout ratio (W) calculated with particle bound fraction following eq. $W = (1-\phi) (RT/H) + \phi W_p$. BBP and DCHP were excluded because of low detection frequency.

Washout ratio (W)	DMP	DEP	DiBP	DnBP	DEHP
A01	250001	88055	18650	18661	3784
A02	249049	97693	18794	18851	9284
A03	241086	53620	19638	19610	13992
A04	246568	77786	19520	19444	7669
A05	245343	81678	19696	19603	9745
A06	237432	83066	19777	19805	7783
A07	245799	86685	18854	19323	7621
A08	238486	69124	19680	19701	8411
A09	239887	73298	19610	19677	8006
A10	235434	67580	19975	19983	15097
A11	242910	88639	19502	19658	10631
A12	246794	93344	18734	18777	8327
A13	244920	86717	18820	18923	7234
A14	247213	75085	18674	18738	8111
A15	241118	42584	19830	19812	12229
A16	222975	57545	19594	19352	14479
A17	251596	90011	18759	18782	7559
A18	207786	46031	18934	19031	15690
A19	241474	82131	18647	18670	6495
A20	229263	64022	19945	19937	12013
A21	235419	59487	19854	19862	14700
A22	242384	91108	18649	18656	8038
Max	251596	97693	19975	19983	15690
Min	207786	42584	18647	18656	3784
Mean	240134	75241	19279	19312	9859
SD	9895	15795	510	480	3261
Median	241929	79732	19511	19398	8369

Table S 2-11. Concentrations of PAEs in the seawater from the South China Sea. The MDLs of PAEs calculated with individual sampling volumes are given in brackets for the calculated concentrations less than MDLs.

Sample	DMP	DEP	DiBP	DnBP	BBP	DCHP	DEHP	PAEs
PAE in dissolved phase (C _w , ng/L)								
W01	0.20	0.46	0.25	1.08	0.014	0.001(0.002)	1.53	3.54
W02	0.15	0.27	0.21	1.38	0.008	0.001(0.001)	1.39	3.40
W03	0.41	0.30	0.14	0.73	0.006	0.001(0.001)	0.77	2.36
W04	0.12	0.14	0.18	0.49	0.005	0.001(0.001)	0.93	1.85
W05	0.20	0.25	0.09	0.30	0.004	0.000(0.001)	1.32	2.16
W06	0.24	0.14	0.11	0.50	0.003	0.001(0.001)	0.63	1.64
W07	0.13	0.26	0.09	0.28	0.003	0.000(0.001)	0.98	1.74
W08	1.60	0.93	0.31	0.21	0.006	0.013	0.48	3.55
W09	1.14	0.84	0.25	1.02	0.107	0.001(0.005)	3.52	6.88
W10	1.30	0.57	0.13	0.17	0.027	0.007	2.03	4.23
W11	1.16	0.77	0.20	0.43	0.012	0.001(0.002)	2.68	5.25
W12	0.77	0.35	0.08	0.20	0.003	0.000(0.001)	1.01	2.42
W13	1.30	0.98	0.08	0.20	0.005	0.000(0.002)	2.87	5.43
W14	0.25	0.43	0.09	0.22	0.008	0.000(0.002)	3.30	4.30
W15	0.14	0.22	0.05	0.13	0.003	0.000(0.001)	0.70	1.23
W16	0.14	0.19	0.07	0.17	0.020	0.001(0.001)	1.04	1.62
W17	0.17	0.14	0.08	0.24	0.003	0.000(0.001)	0.65	1.29
W18	0.07	0.11	1.24	0.30	0.003	0.000(0.001)	1.48	3.20
W19	0.07	0.72	0.12	0.20	0.001 (0.001)	0.000(0.001)	0.66	1.76
W21	0.13	0.32	0.08	0.16	0.006	0.002	0.55	1.25
W22	0.13	0.53	0.09	0.24	0.018	0.003	0.46	1.48
W23	0.13	0.40	0.14	0.33	0.022	0.003	0.68	1.70
W24	0.40	0.40	0.20	0.49	0.009	0.001(0.001)	0.68	2.18
W25	0.75	0.52	0.18	0.37	0.020	0.004	0.59	2.44
W26	0.47	0.46	0.04	0.03	0.001 (0.001)	0.000(0.001)	0.39	1.40
W27	0.55	0.38	0.12	0.21	0.007	0.003	0.75	2.02
W28	0.18	0.14	0.08	0.10	0.005	0.002	0.62	1.12
W29	0.20	0.17	0.07	0.11	0.001 (0.001)	0.002	0.91	1.46
W30	0.10	0.15	0.06	0.13	0.004	0.012	0.66	1.12
W31	0.15	0.13	0.06	0.12	0.001 (0.001)	0.001(0.001)	0.38	0.83
W32	0.35	0.15	0.10	0.16	0.005	0.001(0.001)	0.49	1.26
W33	1.12	0.41	0.41	0.66	0.020	0.000(0.001)	1.84	4.46
W34	0.37	0.19	0.19	0.27	0.002	0.000(0.001)	0.89	1.91
W35	0.15	0.31	0.21	0.22	0.049	0.005	1.28	2.23
W36	0.47	0.56	0.49	0.58	0.007	0.007	2.32	4.44
W37	2.14	0.54	0.48	0.71	0.003	0.007	1.37	5.26
Mean	0.48	0.38	0.19	0.37	0.012	0.002	1.19	2.62
SD	0.51	0.24	0.21	0.30	0.019	0.003	0.83	1.52

Median	0.22	0.34	0.12	0.24	0.005	0.001(0.001)	0.90	2.09
Min	0.07	0.11	0.04	0.03	0.001 (0.001)	0.000(0.001)	0.38	0.83
Max	2.14	0.98	1.24	1.38	0.110	0.013	3.52	6.88
PAE in particle phase (C_{spm}, ng/L)								
W01	0.046	0.11	0.05(0.13)	0.18	0.010	0.000 (0.002)	1.58	1.97
W02	0.03	0.09	0.07(0.10)	0.20	0.011	0.000 (0.001)	0.92	1.32
W03	0.02	0.08	0.05(0.08)	0.11	0.015	0.000 (0.001)	0.99	1.27
W04	0.03	0.08	0.03(0.07)	0.07	0.008	0.000 (0.001)	2.28	2.50
W05	0.01	0.05	0.03(0.07)	0.07	0.005	0.000 (0.001)	0.74	0.91
W06	0.04	0.08	0.05(0.07)	0.16	0.009	0.000 (0.001)	0.64	0.98
W07	0.02	0.06	0.03(0.05)	0.11	0.006	0.000 (0.001)	0.49	0.73
W08	0.019	0.05	0.02(0.07)	0.23	0.026	0.002	0.57	0.92
W09	0.072	0.20(0.21)	0.13(0.36)	0.43	0.013	0.000 (0.005)	2.1(2.2)	2.94
W10	0.018	0.04(0.045)	0.11	0.11	0.015	0.001 (0.001)	0.39(0.47)	0.69
W11	0.04	0.09(0.09)	0.23	0.28	0.027	0.002(0.002)	0.74(0.95)	1.41
W12	0.02	0.04(0.06)	0.02(0.11)	0.03	0.018	0.003	0.43(0.67)	0.57(0.89)
W13	0.05	0.09(0.11)	0.10(0.19)	0.06	0.024	0.003	0.57(1.17)	0.91(1.55)
W14	0.040	0.08	0.03(0.12)	0.04	0.002(0.003)	0.000 (0.002)	0.44(0.76)	0.63(1.0)
W15	0.007	0.02(0.02)	0.01(0.04)	0.01	0.001 (0.001)	0.000 (0.001)	0.12(0.26)	0.17(0.34)
W16	0.035	0.05	0.02(0.07)	0.04	0.002(0.002)	0.000 (0.001)	0.28(0.40)	0.43(0.53)
W17	0.038	0.06	0.01(0.07)	0.08	0.001 (0.002)	0.000 (0.001)	0.28(0.40)	0.47(0.53)
W18	0.012(0.015)	0.03(0.06)	0.03(0.10)	0.06	0.001 (0.003)	0.000 (0.001)	0.18(0.63)	0.31(0.84)
W19	0.003(0.008)	0.01(0.03)	0.02(0.05)	0.01(0.01)	0.000 (0.001)	0.000 (0.001)	0.12(0.32)	0.16(0.43)
W21	0.007(0.010)	0.10	0.07(0.07)	0.14	0.020	0.000 (0.001)	0.94	1.27
W22	0.008(0.010)	0.09	0.09	0.13	0.017	0.000 (0.001)	0.61	0.95
W23	0.011(0.010)	0.11	0.06(0.08)	0.10	0.013	0.000 (0.001)	0.60	0.89
W24	0.011(0.010)	0.10	0.06(0.08)	0.10	0.013	0.000 (0.001)	0.61	0.89
W25	0.009(0.009)	0.09	0.06(0.06)	0.09	0.011	0.000 (0.001)	0.59	0.84
W26	0.004	0.06	0.04(0.06)	0.08	0.009	0.000 (0.001)	0.33(0.38)	0.52
W27	0.009(0.013)	0.09	0.04(0.09)	0.06	0.005	0.000 (0.001)	0.39(0.56)	0.59(0.74)
W28	0.012(0.012)	0.08	0.04(0.08)	0.06	0.006	0.000 (0.001)	0.33(0.50)	0.53
W29	0.011(0.010)	0.08	0.04(0.07)	0.07	0.006	0.000 (0.001)	0.37(0.43)	0.59
W30	0.005(0.007)	0.05	0.03(0.05)	0.04	0.004	0.000 (0.001)	0.43	0.55
W31	0.006(0.008)	0.03(0.03)	0.02(0.05)	0.03	0.002	0.000 (0.001)	0.16(0.33)	0.24(0.44)
W32	0.004(0.008)	0.04	0.02(0.06)	0.03	0.003	0.000 (0.001)	0.19(0.36)	0.28(0.48)
W33	0.005(0.007)	0.03(0.03)	0.02(0.05)	0.02	0.001 (0.001)	0.000 (0.001)	0.53	0.60
W34	0.013(0.014)	0.06	0.03(0.10)	0.04	0.003	0.000 (0.001)	0.26(0.58)	0.41(0.77)
W35	0.009(0.009)	0.06	0.02(0.07)	0.04	0.002(0.002)	0.000 (0.001)	0.20(0.44)	0.33(0.59)
W36	0.190	0.28	0.15(0.37)	0.15	0.004(0.01)	0.000 (0.005)	1.01(2.28)	1.79(3.02)
W37	0.034	0.05(0.05)	0.05(0.13)	0.05	0.005	0.000 (0.002)	0.27(0.80)	0.46(1.06)
Mean	0.025	0.076	0.052(0.077)	0.098	0.009	0.000 (0.001)	0.60	0.86
SD	0.032	0.049	0.045(0.077)	0.085	0.007	0.001 (0.001)	0.49	0.62(0.62)
Median	0.013	0.07	0.04(0.077)	0.074	0.006	0.000 (0.001)	0.47(0.47)	0.66
Min	0.003(0.011)	0.013	0.009(0.077)	0.011(0.017)	0.000(0.002)	0.000 (0.001)	0.12(0.47)	0.16(0.62)

Max	0.190	0.279	0.229	0.428	0.027	0.003	2.27	2.94
Sum of C_w + C_{SPM} (ng/L)								
W01	0.24	0.57	0.30	1.26	0.012	0.000 (0.003)	3.11	5.51
W02	0.18	0.36	0.27	1.58	0.009	0.000 (0.003)	2.31	4.73
W03	0.43	0.38	0.20	0.84	0.010	0.001 (0.002)	1.76	3.63
W04	0.15	0.22	0.21	0.56	0.006	0.000 (0.002)	3.20	4.35
W05	0.21	0.30	0.12	0.37	0.005	0.000 (0.002)	2.06	3.07
W06	0.28	0.23	0.16	0.67	0.006	0.001 (0.002)	1.28	2.62
W07	0.15	0.32	0.12	0.39	0.005	0.000 (0.001)	1.47	2.47
W08	1.62	0.98	0.33	0.44	0.016	0.008	1.05	4.47
W09	1.21	1.04	0.38	1.44	0.060	0.000(0.009)	5.62	9.82
W10	1.32	0.61	0.24	0.28	0.021	0.004	2.42	4.92
W11	1.20	0.85	0.43	0.71	0.020	0.002(0.004)	3.42	6.65
W12	0.79	0.40	0.09	0.23	0.011	0.002(0.003)	1.45	2.99
W13	1.34	1.08	0.18	0.26	0.014	0.002(0.005)	3.44	6.34
W14	0.29	0.51	0.12	0.26	0.005(0.005)	0.000(0.003)	3.74	4.93
W15	0.14	0.23	0.06	0.14	0.002(0.002)	0.000(0.001)	0.82	1.40
W16	0.17	0.24	0.09	0.21	0.011	0.000(0.002)	1.32	2.06
W17	0.21	0.20	0.10	0.32	0.002(0.003)	0.000(0.002)	0.93	1.76
W18	0.08	0.14	1.27	0.36	0.002(0.004)	0.000(0.003)	1.66	3.51
W19	0.07	0.74	0.13	0.21	0.001(0.002)	0.000(0.001)	0.78	1.93
W21	0.14	0.42	0.15	0.30	0.013	0.001(0.002)	1.49	2.52
W22	0.14	0.62	0.18	0.38	0.017	0.002(0.002)	1.07	2.43
W23	0.14	0.51	0.20	0.43	0.017	0.001(0.002)	1.27	2.59
W24	0.41	0.50	0.26	0.59	0.011	0.001(0.002)	1.29	3.07
W25	0.76	0.61	0.24	0.46	0.016	0.002(0.002)	1.18	3.28
W26	0.47	0.52	0.09	0.11	0.005	0.000(0.002)	0.72	1.92
W27	0.56	0.47	0.16	0.26	0.006	0.002(0.002)	1.14	2.61
W28	0.20	0.21	0.12	0.15	0.005	0.001(0.002)	0.95	1.65
W29	0.21	0.25	0.11	0.19	0.004	0.001(0.002)	1.28	2.05
W30	0.10	0.20	0.09	0.18	0.004	0.006	1.08	1.67
W31	0.16	0.16	0.08	0.15	0.001(0.002)	0.000(0.001)	0.53	1.08
W32	0.36	0.19	0.12	0.19	0.004	0.001(0.002)	0.68	1.54
W33	1.13	0.44	0.43	0.68	0.011	0.000(0.001)	2.36	5.06
W34	0.38	0.25	0.22	0.31	0.003(0.004)	0.000(0.002)	1.15	2.32
W35	0.16	0.37	0.23	0.26	0.025	0.002(0.002)	1.48	2.56
W36	0.66	0.84	0.64	0.74	0.005(0.015)	0.004(0.010)	3.33	6.23
W37	2.17	0.59	0.53	0.76	0.004(0.005)	0.004	1.64	5.72
Mean	0.51	0.46	0.24	0.46	0.02	0.003(0.002)	1.79	3.48
SD	0.51	0.26	0.22	0.36	0.02	0.003(0.002)	1.11	1.89
Median	0.26	0.41	0.18	0.34	0.01	0.000(0.002)	1.38	2.81
Min	0.07	0.14	0.06	0.11	0.002(0.003)	0.000(0.002)	0.53	1.08
Max	2.17	1.08	1.27	1.58	0.12	0.02	5.62	9.82

Table S 2-12. Comparison with previous studies for the concentrations of seven PAEs in seawater (ng/L)

Region	DMP	DEP	DiBP	DnBP	BBP	DCHP	DEHP
Arctic(Xie et al., 2007) (Xie et al., 2007)	n.d.- 0.3	n.d.-0.8	n.d.-0.2	0.008-0.3	n.d.-0.05	-	n.d.-3.3
North Sea (Germany) (Xie et al., 2005)	0.23	1.45	-	1.74	0.07	-	3.8
North Sea (Belgium) (Huysman et al., 2019)	-	< 25-753	-	< 5-2645	< 10-343	-	66-766
East China Sea, China(Wang et al., 2021; Zhang et al., 2018b; Zhang et al., 2020d)	0.08-830	0.25-2404	5-17256	11-17952	0.09-344	0.05-705	9- 9738
Bohai and Yellow Seas, China(Liu et al., 2020; Zhang et al., 2018c)	n.d.-160	1.18-85.9	89.3-2424	n.d.-2226	n.d.-7.8	1.34-3.12	51.4-3388
Pearl River Delta, China(Cao et al., 2022b)	1.7-13.6	< 5.1-34.8	< 30.2-70.3	< 33.2-358	n.d.	n.d.	12.7-1050
Mediterranean Sea(Castro-Jimenez and Ratola, 2020; Paluselli et al., 2018a; Sanchez-Avila et al., 2012)	1.4-140	6.9-870	56.5-383.4	63.4-466	1-100	-	30-5970
Bay of Biscay, Spain(Prieto et al., 2007)	7.5±0.4	33±3	-	83±7	8±1	64±4	-
Barkley Sound, Canada(Keil et al., 2011)	-	-	-	18-3000	-	-	10-950
Puget Sound, USA(Keil et al., 2011)	-	-	-	-	-	-	60-640
Klang River estuary, Australia(Tan, 1995)	-	-	-	-	-	-	3100-64300
South Korea(Heo et al., 2020)	20-100	20-150	-	40-360	-	-	30-300
Tropical western Pacific Ocean(Zhang et al., 2019a)	n.d.-7	n.d.-2.1	1.9-14	2.2-13	n.d.-5.5	1.1-7	2.0-9.2
Caspian Sea, Iran (Hadjmohammadi et al., 2011)	490	520	-	-	-	-	-
Thailand(Malem et al., 2019)	-	-	-	230-770	-	-	310-1160
Tunisia(Jebara et al., 2021)	-	< 10-17000	< 5-106000	< 29-30500	-	-	< 26-168000
This work	0.07-2.17	0.14-1.08	0.06-1.27	0.11-1.58	<n.d.-0.12	<n.d.-0.02	0.53-5.62

Table S 2-13. Particle-bound fractions (ϕ) of PAEs in seawater from the South China

Sea

Sample	DMP	DEP	DiBP	DnBP	BBP	DCHP	DEHP	PAE
W01	0.19	0.20	0.16	0.14	0.42	0.18	0.51	1.80
W02	0.16	0.26	0.24	0.13	0.58	0.14	0.40	1.90
W03	0.06	0.21	0.27	0.13	0.73	0.14	0.56	2.11
W04	0.20	0.35	0.15	0.13	0.63	0.12	0.71	2.30
W05	0.06	0.18	0.23	0.20	0.60	0.08	0.36	1.71
W06	0.14	0.36	0.31	0.24	0.76	0.17	0.50	2.48
W07	0.13	0.19	0.29	0.29	0.68	0.11	0.33	2.03
W08	0.01	0.05	0.07	0.52	0.80	0.13	0.55	2.14
W09	0.06	0.19	0.33	0.30	0.11	0.31	0.37	1.67
W10	0.01	0.07	0.46	0.39	0.36	0.07	0.16	1.54
W11	0.03	0.10	0.54	0.40	0.69	0.73	0.22	2.71
W12	0.02	0.11	0.18	0.15	0.84	0.88	0.30	2.48
W13	0.04	0.09	0.57	0.23	0.83	0.89	0.17	2.82
W14	0.14	0.15	0.21	0.16	0.22	0.26	0.12	1.26
W15	0.05	0.08	0.15	0.08	0.22	0.09	0.15	0.80
W16	0.20	0.22	0.21	0.21	0.09	0.04	0.21	1.19
W17	0.18	0.32	0.15	0.24	0.31	0.12	0.30	1.62
W18	0.15	0.24	0.02	0.16	0.19	0.07	0.11	0.94
W19	0.04	0.02	0.11	0.06	0.22	0.35	0.16	0.96
W21	0.05	0.23	0.47	0.45	0.78	0.04	0.63	2.65
W22	0.06	0.15	0.48	0.36	0.49	0.04	0.57	2.14
W23	0.07	0.21	0.29	0.24	0.37	0.04	0.47	1.69
W24	0.02	0.20	0.22	0.18	0.61	0.02	0.47	1.72
W25	0.01	0.14	0.24	0.19	0.35	0.08	0.50	1.51
W26	0.01	0.12	0.49	0.70	0.87	0.43	0.45	3.07
W27	0.02	0.19	0.26	0.22	0.43	0.05	0.34	1.50
W28	0.06	0.36	0.32	0.38	0.57	0.03	0.35	2.08
W29	0.05	0.33	0.38	0.39	0.82	0.04	0.29	2.30
W30	0.05	0.23	0.28	0.25	0.53	0.00	0.40	1.74
W31	0.04	0.20	0.23	0.18	0.78	0.07	0.29	1.80
W32	0.01	0.20	0.17	0.15	0.36	0.04	0.28	1.21
W33	0.00	0.06	0.04	0.03	0.06	0.13	0.22	0.56
W34	0.04	0.23	0.14	0.14	0.51	0.08	0.22	1.37
W35	0.05	0.15	0.09	0.14	0.04	0.01	0.14	0.62
W36	0.29	0.33	0.23	0.21	0.35	0.03	0.30	1.74
W37	0.02	0.09	0.10	0.06	0.64	0.05	0.17	1.11
Mean	0.08	0.19	0.25	0.23	0.50	0.17	0.34	1.76
SD	0.07	0.09	0.14	0.14	0.25	0.23	0.16	0.62

Table S 2-14. Correlation analysis of PAEs in air

	DMP	DEP	DiBP	DnBP	BBP	DCHP	DEHP
DMP	1(0.000***)	0.647(0.001***)	0.242(0.279)	0.168(0.455)	0.131(0.561)	0.046(0.837)	0.214(0.339)
DEP	0.647(0.001***)	1(0.000***)	0.385(0.077*)	0.398(0.067*)	0.012(0.958)	0.196(0.383)	0.199(0.375)
DiBP	0.242(0.279)	0.385(0.077*)	1(0.000***)	0.951(0.000***)	0.101(0.656)	0.508(0.016**)	-0.091(0.686)
DnBP	0.168(0.455)	0.398(0.067*)	0.951(0.000***)	1(0.000***)	0.09(0.689)	0.496(0.019**)	-0.148(0.512)
BBP	0.131(0.561)	0.012(0.958)	0.101(0.656)	0.09(0.689)	1(0.000***)	-0.203(0.366)	-0.057(0.800)
DCHP	0.046(0.837)	0.196(0.383)	0.508(0.016**)	0.496(0.019**)	-0.203(0.366)	1(0.000***)	-0.123(0.586)
DEHP	0.214(0.339)	0.199(0.375)	-0.091(0.686)	-0.148(0.512)	-0.057(0.800)	-0.123(0.586)	1(0.000***)

***, **, *means significant 0.01, 0.05, 0.1

Table S 2-15. Correlation analysis of PAEs in seawater

	DMP	DEP	DiBP	DnBP	BBP	DCHP	DEHP
DMP	1(0.000***)	0.659(0.000***)	0.27(0.112)	0.245(0.150)	0.371(0.026**)	0.497(0.002***)	0.354(0.034**)
DEP	0.659(0.000***)	1(0.000***)	0.174(0.311)	0.336(0.045**)	0.578(0.000***)	0.382(0.022**)	0.55(0.001***)
DiBP	0.27(0.112)	0.174(0.311)	1(0.000***)	0.324(0.054*)	0.095(0.582)	0.122(0.478)	0.296(0.080*)
DnBP	0.245(0.150)	0.336(0.045**)	0.324(0.054*)	1(0.000***)	0.471(0.004***)	-0.077(0.656)	0.611(0.000***)
BBP	0.371(0.026**)	0.578(0.000***)	0.095(0.582)	0.471(0.004***)	1(0.000***)	0.135(0.434)	0.606(0.000***)
DCHP	0.497(0.002***)	0.382(0.022**)	0.122(0.478)	-0.077(0.656)	0.135(0.434)	1(0.000***)	-0.053(0.759)
DEHP	0.354(0.034**)	0.55(0.001***)	0.296(0.080*)	0.611(0.000***)	0.606(0.000***)	-0.053(0.759)	1(0.000***)

***, **, *means significant 0.01, 0.05, 0.1

Table S 2-16. Air-sea exchange fluxes of PAEs in the South China Sea. Positive value indicates water to air volatilization and negative value indicates air to water deposition

F (ng/m²/day)	DMP	DEP	DiBP	DnBP	BBP	DCHP	DEHP
W01	-970	-85	-1488	-1015	-43	0	918
W02	-888	-71	-657	-435	-15	0	57
W03	-969	-88	-1502	-1048	-45	0	419
W04	-391	-79	-1278	-899	-9	-2	331
W05	-392	-78	-1337	-947	-10	-4	919
W06	-243	-147	-671	-489	-11	0	314
W07	-243	-146	-674	-505	-11	0	528
W08	-241	-109	-440	-444	-52	23	470
W09	-245	-110	-434	-335	-31	1	3538
W10	-244	-118	-457	-445	-47	11	2255
W11	-174	-79	-303	-279	-33	0	1419
W12	-176	-86	-313	-297	-34	0	492
W13	-210	-102	-1054	-874	-14	-0.1	1272
W14	-217	-112	-1138	-943	-16	-0.2	3616
W15	-104	-41	-172	-198	-27	0.3	733
W16	-106	-42	-172	-197	-25	0.7	1059
W17	-244	-94	-678	-465	-10	-2.2	444
W18	-258	-100	-628	-494	-11	-2.9	1593
W19	-258	-90	-726	-505	-11	-3.3	601
W21	-164	-53	-107	-48	-22	3.5	740
W22	-181	-161	-959	-634	-4	3.4	338
W23	-181	-163	-961	-631	-3	3.5	600
W24	-177	-88	-2080	-1470	-39	0.1	310
W25	-174	-86	-2042	-1451	-37	1.5	214
W26	-177	-87	-2178	-1568	-42	-0.7	233
W27	-460	-104	-1349	-1050	-43	2.7	435
W28	-419	-92	-1120	-927	-6	0.1	33
W29	-442	-104	-1896	-1579	-12	0.3	255
W30	-443	-105	-1948	-1622	-13	5.5	194
W31	-279	-42	-284	-230	-11	0.3	159
W32	-371	-42	-12	-40	-12	0.8	273
W33	-1487	-383	-1162	-1500	-14	0.0	1308
W34	-1497	-391	-1226	-1596	-19	0.0	663
W35	-44	-21	-328	-229	-17	1.5	329
W36	-44	-19	-342	-231	-22	5.5	1366
W37	-190	-77	-406	-326	-14	2.2	361
mean	-370	-105	-903	-721	-22	1.4	800

Table S 2-17. Particle dry deposition of PAEs in the South China Sea

F_D (ng/m ² /day)	DMP	DEP	DiBP	DnBP	BBP	DCHP	DEHP	PEs
A01	0.29	0.89	0.6	0.7	0.01	0.00	23.5	26.0
A02	0.21	0.55	4.1	2.7	0.04	0.02	49.5	57.2
A03	3.86	8.92	348.9	229.4	0.04	0.06	44.8	635.9
A04	1.17	3.10	274.3	155.7	0.07	0.44	21.2	456.0
A05	0.70	3.65	219.3	118.2	0.01	0.05	26.0	367.9
A06	0.85	1.67	127.1	147.5	0.11	0.02	16.9	294.0
A07	0.47	1.62	15.7	71.1	0.20	0.34	17.1	106.5
A08	0.46	1.76	41.3	53.5	0.07	0.11	13.4	110.6
A09	0.94	3.06	123.9	113.5	0.08	0.60	16.9	259.0
A10	0.67	1.99	344.5	283.8	0.23	0.07	31.4	662.7
A11	0.59	2.08	131.9	153.0	0.11	0.18	23.0	310.8
A12	0.36	0.69	13.2	14.2	0.07	0.05	10.1	38.7
A13	1.11	1.47	15.4	20.7	0.06	0.10	19.0	57.9
A14	0.77	3.13	4.3	10.3	0.17	0.22	21.6	40.4
A15	0.87	6.10	138.3	102.8	0.33	0.27	20.1	268.8
A16	7.03	6.09	5.6	7.3	0.11	0.03	23.9	50.0
A17	0.53	2.76	6.3	10.0	0.15	0.05	25.9	45.6
A18	1.25	5.61	13.1	13.6	0.05	0.02	29.4	63.1
A19	0.33	0.77	0.4	1.2	0.01	0.03	6.4	9.1
A20	1.18	2.85	158.6	107.6	0.09	0.02	13.8	284.1
A21	1.69	8.67	453.4	407.6	0.20	0.85	34.5	907.0
A22	0.54	1.30	1.6	2.6	0.02	0.03	14.6	20.7
Max	7.03	8.92	453.4	407.6	0.33	0.85	49.5	907.0
Min	0.21	0.55	0.4	0.7	0.01	0.00	6.4	9.1
Mean	1.18	3.12	111.0	92.1	0.10	0.16	22.9	230.6
SD	1.51	2.45	137.0	106.9	0.08	0.22	10.4	247.5
Median	0.73	2.42	28.5	62.3	0.08	0.06	21.4	108.6

3 Organophosphate Esters in Air and Seawater of the South China Sea: Spatial Distribution, Transport, and Air–Sea Exchange

This chapter has been published as:

Lijie Mi, Zhiyong Xie, Lulu Zhang, Joanna J. Waniek, Thomas Pohlmann, Wenying Mi and Weihai Xu, 2023b. Organophosphate Esters in Air and Seawater of the South China Sea: Spatial Distribution, Transport, and Air–Sea Exchange. *Environment & Health* 1(3), 191-202.

DOI: [10.1021/envhealth.3c00059](https://doi.org/10.1021/envhealth.3c00059)

The section includes the full manuscript of the published paper except for some editorial changes. Layout and numbering have been changed to this thesis document. Abstract is deleted. References and acknowledgements have been integrated into the separate chapters of this thesis document.

3.1 Introduction

Organophosphate ester (OPEs) are typical chemicals of emerging concern because of their ubiquity in the environment and adverse effects on living organisms.(Xie et al., 2022a) OPEs have been extensively used as flame retardants, plasticizers and antifoaming agents in a broad spectrum of products, including electronics, construction materials, furniture, textiles, plastics and food packaging.(van der Veen and de Boer, 2012) As brominated flame retardants, such as polybrominated diphenylethers (PBDEs), hexabromocyclododecane (HBCD), and hexabromobenzene (HBB), have been regulated globally by the Stockholm Convention (SC), the production and consumption of OPEs have been increasing dramatically driven by market demand. (Blum et al., 2019) in the past 20 years, the consumption of OPEs has increased from 1.86×10^5 tons in 2001 to 6.8×10^5 tons in 2015.(Xie et al., 2022a) along with their high usage, OPEs has been suspected to exercise toxic effects on humans and ecosystems.(Wei et al., 2015) As a consequence of the increasing concern for OPEs in the environment, organisms and human beings, the prevention of the use of chlorinated OPEs, such as tris(2-chlorethyl) phosphate (TCEP), tris(1,3-dichloroisopropyl) phosphate (TDCIPP) and tris(1-chloro-2-propyl) phosphate (TCIPP), has been proposed by the United States, Canada and the European Union (EU).(van der Veen and de Boer, 2012) China added isopropylated triphenyl phosphate (IPPP) and TCEP to the list of primarily controlled chemicals in 2020.(MEE, 2020)

OPEs have been detected in a variety of environmental areas, such as water,(Fu et al., 2020; Meyer and Bester, 2004; Zeng et al., 2014) soil,(Han et al., 2020) sediment,(Li et al., 2019a) air,(Li et al., 2018a) and organism.(Zhang et al., 2020a) These studies have shown that the concentrations of OPEs are already higher than those of classic persistent organic pollutants (POPs) regulated by the SC, such as polychlorinated biphenyls (PCBs), organochlorine pesticides (OCPs), and PBDEs.(Wang et al., 2020) OPEs have become the new pollutants of widespread public concern, requiring extensive research on their environmental fate, transport and potential toxic effects. OPEs can be released during the production of consumer and household products and continually re-emit to the environment by volatilization, abrasion and leaching during the lifespan.(Xie et al., 2022a) Emission from industrial inputs, wastewater treatment

facilities, and e-waste recycling activities are important sources for the urban and metropolitan environment.(Wei et al., 2015) In addition, leaching from plastic debris is also a speculated source for OPEs occurring in the environment.(Liu et al., 2019)

The South China Sea is one of the largest marginal seas in the world, with an area of about 3.5 million km² surrounded by some tropical-subtropical developing countries in Southeast Asia, such as China, Vietnam, Philippines, Thailand, Brunei, Singapore, Malaysia and Indonesia. These countries are becoming the world's factories due to dense populations, effective resources and economic development policies.(Wang et al., 2019a) Accompanying the blooming of industry, economy and metropolitan areas, the South China Sea is facing extensive anthropogenic pressure caused by increasing human activities.(Ding et al., 2020; Lai et al., 2019a) Large rivers such as the Pearl River and the Mekong act as important vectors for transporting numbers of chemicals into the South China Sea.(Bao et al., 2017; Sudaryanto et al., 2011; Tan et al., 2016) As the South China Sea is a semienclosed marginal sea of the Northwest Pacific, it is affected by frequent Pacific water intrusion, abundant runoff, and seasonally changing monsoon winds.(Zhu et al., 2022a) Previous studies have shown that atmospheric transport and deposition is a significant input process for OPEs in the South China Sea,(Lai et al., 2015; Liu et al., 2022; Zhang et al., 2022c) while diffusive fluxes of OPEs between the interface of air and sea are not well understood. Zhang et al. attempted to estimate air-sea exchange fluxes of OPEs using estimated gaseous OPE concentrations.(Zhang et al., 2022a) Given the complex gas/particle partitioning process of OPEs, such an estimation is highly uncertain.

In this work, the main objectives were to investigate the concentrations, composition profile, and spatial distribution of OPEs in the air and seawater of the South China Sea. This work provides a new data set for a better understanding of the transport and environmental fate of OPEs in the South China Sea.

3.2 Materials and Methods

3.2.1 Research Area and Sample Collection

Ship-bound sampling was carried out on board the German research vessel SONNE (SO269) along a transect from Singapore to Hong Kong, China in August 2 to September 2, 2019. Twenty-two active air samples, 37 high-volume seawater samples, and 23 1 L seawater samples were collected offshore the South China Sea (Figures S3-

1 to S3-3). Briefly, large volumes of air from 300 to 500 m³ were sucked with an active pump at a flow rate of ~ 15 m³/h. Atmospheric particles were collected on a quartz fiber filter (QFF; diameter 150mm, pore size 1.0 µm), and the gaseous phase was trapped by a PUF/XAD-2 resin glass column. Given the concern of ship-bound contamination (Lohmann et al., 2004), air sampling was only operated under a headwind to avoid contamination from ship combustion emissions. Air sample blanks (column and filter) were prepared by briefly opening the PUF/XAD-2 column and filter next to the air sampler. High-volume seawater samples were collected from the ship intake system in the web lab. A glass fiber filter (GFF; 1.2 µm, 140mm) was used to collect suspended particulate matter (SPM), and an XAD-2 column (40 g XAD-2 packed) was used to catch organic chemicals in the dissolved phase. It is noted that chemicals associated with SPM could be washed off the SPM during the sampling. Besides, 1 L seawater samples were collected in brown glass bottles from the seawater intake system and CTD-Rosette. PUF/XAD-2, QFF and GFF samples were stored at -20°C, and XAD-2 column and 1 L seawater samples were kept at 5°C on board. All samples were transported with cooling containers from Hong Kong back to Helmholtz-Zentrum Hereon, Germany, in December 2019. The detailed information on air and water samples is provided as summarises in Supporting Information (Table S3-1 to S3-3).

3.2.2 Chemicals and Reagents

All chemicals were of trace analysis grade. Picograde solvents, e.g., methanol, acetone, n-hexane and dichloromethane (DCM), were purchased from Promochem (Germany). Silica gel (60-200 mesh) was supplied by Macherey Nagel (Düren, Germany), and anhydrous sodium sulfate (99%) and XAD-2 resin were obtained from Merck (Darmstadt, Germany). Analytical standards, e.g., tris(2-chloroethyl) phosphate (TCEP), tris(chloro-2-propyl) phosphate (TCIPP), tris-(1,3-dichloro-2-propyl) phosphate (TDCIPP), triethyl phosphate (TEP), tri-n-propyl phosphate (TPrP), triisobutyl phosphate (TIBP), tri-n-butyl phosphate (TNBP), tris(2-ethylhexyl) phosphate (TEHP), tris(2-butoxyethyl) phosphate (TBEP), triphenyl phosphate (TPhP) and 2-ethylhexyldiphenyl phosphate (EHDPP), and deuterated OPEs, e.g., tris(2-chloroethyl)phosphate-d₁₂ (TCEP-d₁₂), tri-n-butyl phosphate-d₂₇ (TNBP-d₂₇), triphenyl phosphate-d₁₅ (TPhP-d₁₅) and tripropyl phosphate-d₂₁ (TPrP-d₂₁), were acquired from Willington Laboratories (Guelph, Canada). Isotope labeled

polychlorinated biphenyl 208 ($^{13}\text{C}_{12}$ -PCB 208) was supplied by Cambridge Isotope Laboratories.

3.2.3 Sample Preparation and Instrumental Analysis

The PUF/XAD-2 column, XAD-2 column, and GFF and QFF filters were extracted using an MX-Soxhlet extractor with DCM for 16 h. An 800 mL seawater sample was transferred in a 1000 mL separating funnel and liquid-liquid extracted with 50 mL of DCM three times. Before extraction, 20 ng (50 μL , 0.4 ng/ μL in acetone) of each labeled standard (TCEP-d₁₂, TNBP-d₂₇ and TPhP-d₁₅) was added to the sample for internal standard quantification by isotopic dilution. The extract was concentrated to 1 mL with a rotary evaporator and nitrogen evaporator before cleanup with column chromatography packed with 2.5 g of silica gel and 3 g of sodium sulfate anhydrous. The silica gel was baked out at 450 °C for 10h and conditioned with the addition of 10% Milli-Q water. The silica gel column was precleaned with 10 mL of acetone followed by 20 mL of n-hexane. After sample loading, the silica gel column was eluted in two separate fractions of (1) 20 mL of n-hexane and (2) 20 mL of acetone/DCM (1:1, v/v). fraction 2 was concentrated to 190 μL under gentle nitrogen and transferred to an injection vial (230 μL inner vial). A 10 μL $^{13}\text{C}_{12}$ - PCB 208 injection standard was added (0.05 ng/ μL in acetone) for instrumental analysis.

Analysis of the OPEs was performed on a gas chromatograph (Agilent 8890A) coupled to a triple quadrupole mass spectrometer (Agilent 7010B) equipped with a programmed temperature vaporizer (PTV) multifunction injector (GC-MS/MS, Agilent, USA). Separation was achieved on tandem connected HP-5MS columns (15m \times 0.25 μm \times 0.25mm) supported with backflush at the middle point. The MS/MS was operated in multiple reaction monitoring (MRM) mode. Detailed information on the GC-MS/MS and qualitative and quantitative transitions is listed in Tables S3-5 and S3-6.

3.2.4 Quality Assurance/ Quality Control

GFF and QFF filters were backed out respectively at 450 and 600 °C for 10h to remove any OPE contaminations. The PUF/XAD-2 and XAD-2 columns were pre-extracted using methanol, acetone and n-hexane in turn for 72h. After being dried with nitrogen (99.999%), the columns were closed with glass caps and sealed in an aluminum bag. The columns were only opened at the sampling site to avoid indoor air contamination. All organic solvents were distilled using a fully glass-made apparatus. Though great

efforts were dedicated to removing OPEs from the sampling material and minimizing their background levels, TCIPP, TNBP and TEP are often detectable in procedure blanks, which is consistent with levels reported in the ambient air.(Kim et al., 2019; Takeuchi et al., 2014) Other OPEs usually not detectable or with relatively low levels. The method detection limits (MDLs) were defined by the mean concentrations in blanks plus three standard deviations of the blanks. The blanks and MDLs are summarized in Table S3-7. The recoveries of internal standards TCEP-D12, TNBP-D27 and TPhP-D15 were $78.8 \pm 22.7\%$, $80.0 \pm 18.9\%$ and $94.9 \pm 26.4\%$ for LLE, $107 \pm 56.6\%$, $40.3 \pm 16.2\%$ and $73.8 \pm 33.5\%$ for XAD-2, $47.9 \pm 11.5\%$ and $59.2 \pm 22.3\%$ for PUF/XAD-2, $126 \pm 31.6\%$, $122 \pm 26.1\%$ and $263 \pm 86\%$ for GFF, respectively. The concentrations of OPEs reported in this work were not corrected with their blanks.

3.2.5 Data Analysis

The data of GC-MS/MS were analyzed using Mass Hunter B10 (Agilent). Statistical analyses were performed with Excel 2016 and Origin 2020 (Origin Lab). Geographic maps were plotted with Ocean Data View 4.0.(Schlitzer, 2023)

3.2.6 Air Mass Back Trajectories (BTs)

The air mass origins of the air samples were assessed using air mass back trajectories (BT), calculated by the Hybrid Single-Particle Lagrangian Integrated Trajectory model (HYSPLIT).(Stein et al., 2015a) Air mass back trajectories traced back the air masses for 120 h with 6 h steps at the heights of 10 m above sea level, which are shown in Figure S3-4.

3.3 Results and Discussion

3.3.1 Spatial Distribution of OPEs in Air

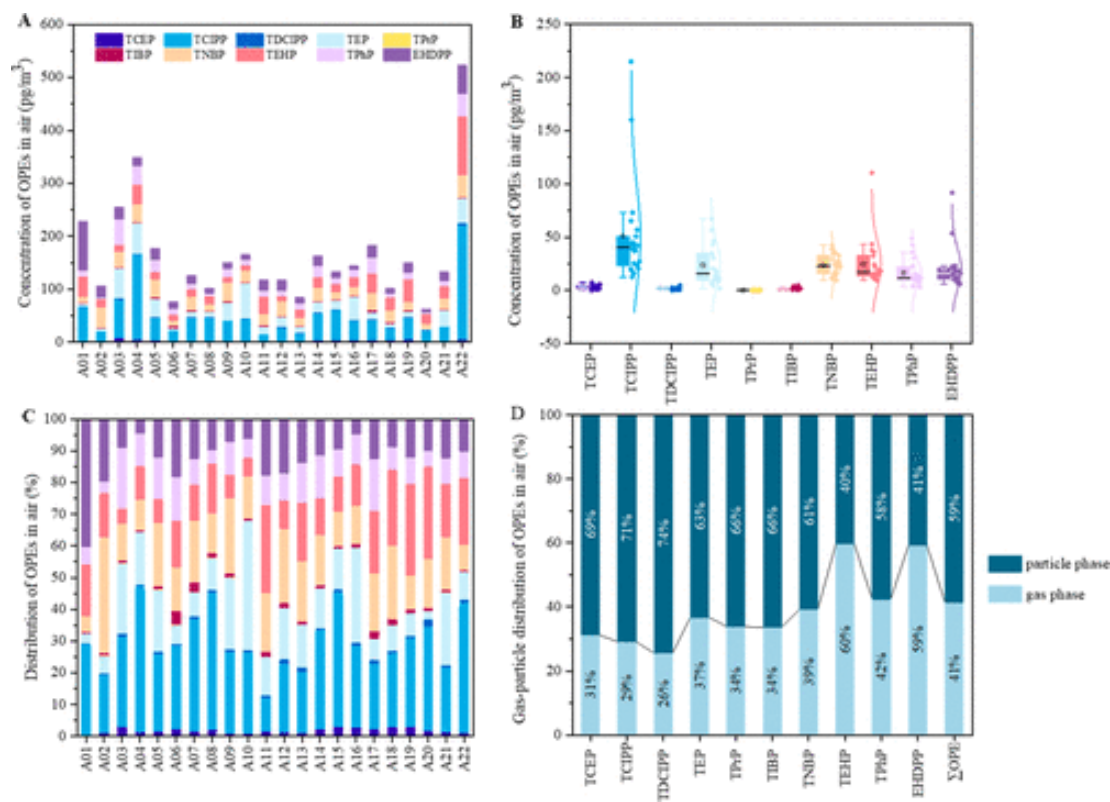


Figure 3-1 (A) Concentrations of OPEs in the atmosphere (ng/m^3) over the South China Sea. (B) Box chart of OPEs. (C) Composition profile of OPEs. (D) Gas/particle partitioning of OPEs. Air masses originating from the Pacific Ocean and Southeast Asia dominated at the research area.

OPEs have been detected in both gaseous and particle phases of the air samples. The concentrations of individual OPEs and their spatial distribution are shown in Figure 3-1, and summarized in Table S3-8. As TBEP is below the MDL in all air samples, we exclude it from the sum. The total concentrations of 10 OPEs ($\Sigma_{10}\text{OPE}$) varied between 66 and 550 pg/m^3 , which is consistent with concentrations determined in a yearly monitoring program at Yongxing Island in 2017-2018, indicating a “background” level of OPEs in the oceanic air of the South China Sea. The higher OPE concentrations were measured in air samples A22 and A04, which are collected nearshore. However, the OPE concentrations in the more nearshore samples, e.g. A06, A07 and A14 were just below the average. The concentrations of OPEs are highly influenced by the air mass origins and the weather conditions during sampling. Air mass back trajectories (Figure S3-4) showed that the air masses of A22 mainly originated from South Asia and Vietnam, and 9% from the coastal area of East China. Moreover, A22 was collected when SONNE sailed towards the harbor of Hong Kong. North and northeast wind could bring the urban emissions to the open area of the South China Sea and raise the contamination levels in the air. Besides, according to the report of the Ministry of

Ecology and Environment of China, 42% of electronic waste treatment companies were located in the coastal zones of North China (19%) and East China (33%) in 2017 (<http://www.mee.gov.cn/hjzl/sthjzk/>). The air masses passing through these areas could transport the emissions to remote areas and elevate OPE concentrations. By contrast, air samples with oceanic air mass origins showed relatively low levels of OPE, such as 79 pg/m³ for A6, 86 pg/m³ for A13 and 66 pg/m³ for A20, which are comparable with or even below those concentrations measured in the Pacific, Atlantic and the Arctic. Furthermore, the summer monsoon is dominant in August. Warm and mild trade winds from the tropic Pacific and Indian Ocean accelerate the exchange of the air masses in the South China Sea. OPE emissions from terrestrial sources could be diluted by the oceanic air and washed out with precipitation. Therefore, the atmospheric concentrations of OPEs reported in this work can represent the background level of OPEs in the summer season. As seasonal variations have been observed from Yongxing Island, OPE concentrations in winter and spring need to be investigated to discover the impact of terrestrial input when the winter monsoon dominates in the South China Sea.

3.3.2 OPE Composition Profile in Air

TCIPP was the dominant OPE (ranging from 13 to 215 pg/m³, median: 40 pg/m³), which accounts for 28% of the Σ_{10} OPE, followed by 16% for TNBP (9.5 - 43 pg/m³, median: 23 pg/m³), 15% for TEHP (9.8 - 110 pg/m³, median: 17 pg/m³), 14% for TEP and 13% for EHDPP. Surprisingly, TCEP was measured at very low levels in this work, with concentrations ranging from 1.7 to 7.6 pg/m³, and only accounted for 2.3% of the Σ_{10} OPE. TCIPP and TCEP are two major chlorinated OPEs, and have been often measured in air as the predominant OPEs in the global ocean.(Castro-Jimenez et al., 2016; Xie et al., 2022a) In the South China Sea, Lai et al. found that TCPE (14 - 110 pg/m³) exceeded TCIPP (15 - 38 pg/m³) in the particle samples collected in the northern South China Sea in 2012.(Lai et al., 2015), Zhang et al. measured concentrations of TCEP (40 - 741 pg/m³) slightly lower than those of TCIPP (19 - 973 pg/m³) in air samples collected at Yongxing Island from 2017-2018(Zhang et al., 2022c). Liu et al. reported higher TCEP concentration (39.2 - 8944 pg/m³) than TCIPP (63.9 - 1405 pg/m³) with a factor of 5 in PM_{2.5} at Yongxing Island from June 2018 to May 2019.(Liu et al., 2022) The varying ratios of TCEP/TCIPP and their concentration levels highlight the complexity of the investigation of OPEs in the remote environment. Indeed, both research vessel and stationary platform can act as emission sources during air sampling.

The warm temperature in the tropical ocean can enhance the leaching process for organic chemicals from surrounding buildings and infrastructures, e.g. flame-retardants, plasticizers and waterproof chemicals. The low concentrations of TCEP measured in this work can be attributed to the regulation of TCEP from industrial production and application, and to governmental control and reduction for e-waste treatment in China.(Yang et al., 2020b)

The mean concentrations of Σ alkyl-OPE (74 ± 37 pg/m³) are higher than Σ Cl-OPE (55 ± 49 pg/m³) and Σ aryl-OPE (37 ± 25 pg/m³). This is the first time that we observed Σ alkyl-OPE exceeding Σ Cl-OPE in air. Three alkyl-OPEs (TEP, TNBP and TEHP) and two aryl-OPEs (TPhP and EHDPP) showed comparable concentrations and were almost equally distributed in both gas and particle phases. The concentrations of TNBP (mean 24 ± 10 pg/m³) and TEHP (25 ± 21 pg/m³) were at a lower level in comparison with those measured in the Pacific, Atlantic and Indian Oceans and the European seas(Castro-Jimenez et al., 2014; Castro-Jimenez et al., 2016; Moller et al., 2011), while they are comparable to those measured in the Bohai and Yellow Sea(Li et al., 2018a) the Northern South China Sea (Lai et al., 2015) and Yongxing Island (Zhang et al., 2022c). TEP showed levels similar to those of TNBP and TEHP with concentrations ranging from 1.7 to 67 pg/m³ and an average of 24 ± 20 pg/m³, which are lower than those measured at Yongxing Island in 2017-2018(Zhang et al., 2022c) but 10 times higher than those measured in 2018 - 2019.(Liu et al., 2022) Data of TEP from other marine areas are rare for comparison. TPhP and EHDPP were detected in both gas and particle phases in all air samples. The concentrations of TPhP were consistent with those from other geographic areas, indicating that TPhP is a typical aryl-OPE contaminant in the marine environment.

3.3.3 Gas-Particle Partitioning

The fractions of particle bound OPEs (Φ , %) are shown in Table S3-9, which varies from $33.3 \pm 23.6\%$ for TEHP to $71.5 \pm 18.2\%$ for TDCIPP. OPEs range from $\log K_{OA}$ 6.63 for TEP to $\log K_{OA}$ 14.98 for TEHP. Light weigh OPEs such as TEP and TCEP have high volatility with vapor pressures 3-6 orders of magnitude higher than those of other OPEs (Table S3-6). Meanwhile, the Φ values of OPEs do not seem consistent with their $\log K_{OA}$ and vapor pressures (V_p) values. TEP is more volatile than light weight PAHs, e.g. naphthalene (V_p at 25 °C: 5.38 Pa), but with a Φ of $48.6 \pm 27.0\%$, which is higher than the Φ ($33.3 \pm 23.6\%$) of TEHP. The distribution patterns are

comparable to those determined in the Bohai Sea, Yellow Sea, and Yongxing Island but lower than in the Arctic. The partitioning of OPEs between gaseous and particle phases is interfered with not only by their physicochemical properties but also by the fast degradation process caused by light intensity and radicals, and scavenging process. Given the high reaction rates with heterogeneous OH- initiated oxidation of OPEs in air, the half-lifetimes of OPEs in the gaseous phase were estimated to just a few hours. Meanwhile, the approximate atmospheric lifetimes were estimated to be 5.6, 4.3 and 13 days for particle- bound TPhP, TEHP and TDCIPP.(Liu et al., 2014a; Liu et al., 2014b) Moreover, rain scavenging is more effective in removing gaseous OPEs,(Regnery and Puttmann, 2009) especially for OPEs with high solubilities, such as TEP, TCEP, TCIPP, TPrP and TNBP. Besides, the thin liquid film of water on the surface of the particles may also retain certain OPEs based on the “same like same” principle. Indeed, the partitioning process of OPEs is more complex than those of classic semivolatile organic compounds, and it can hardly be explained with J-P adsorption or K_{OA} absorption models(Li et al., 2017a), which need further research considering both physical and chemical processes occurring on the particle.(Okeme et al., 2018; Suhring et al., 2016; Wu et al., 2020)

3.3.4 OPEs in Seawater

In this work, 37 high-volume seawater samples and 23 1L seawater samples were measured for OPEs. The detection frequencies of OPEs in the dissolved phase of the high-volume seawater samples is 100% for TCEP, TCIPP, TDCIPP, TIBP, TNBP, TBEP, TPhP and EHDPP. Exceptions are 84% for TPrP and 46% for TEHP (Table S3-10). TEP could break through the XAD-2 adsorption owing to its high solubility in water (1.1×10^4 mg/L), which is not applicable with high-volume water sampling. For 1L seawater samples, TEP showed a detection frequency of 92%, followed by TCIPP (71%) and TDCIPP (67%), and the detection frequencies were less than 50% for other OPEs. The average concentration of TCIPP and TDCIPP measured with high-volume water samples were 420 ± 381 pg/L (MDL 63 pg/L) and 47 ± 48 pg/L (MDL 1.5 pg/L), and they were slightly lower than the concentrations determined with 1 L water samples (TCIPP 1100 ± 790 pg/L (MDL, 500 pg/L), TCIDPP 70 ± 75 pg/L (MDL, 18 pg/L)). Except TEP and TDCIPP, the average concentrations of OPEs measured with 1 L water samples are close to their MDLs. Therefore, we focused on the results from high-

volume seawater samples and TEP from 1 L seawater for discussion, statistical analysis, and estimation of air-sea exchange.

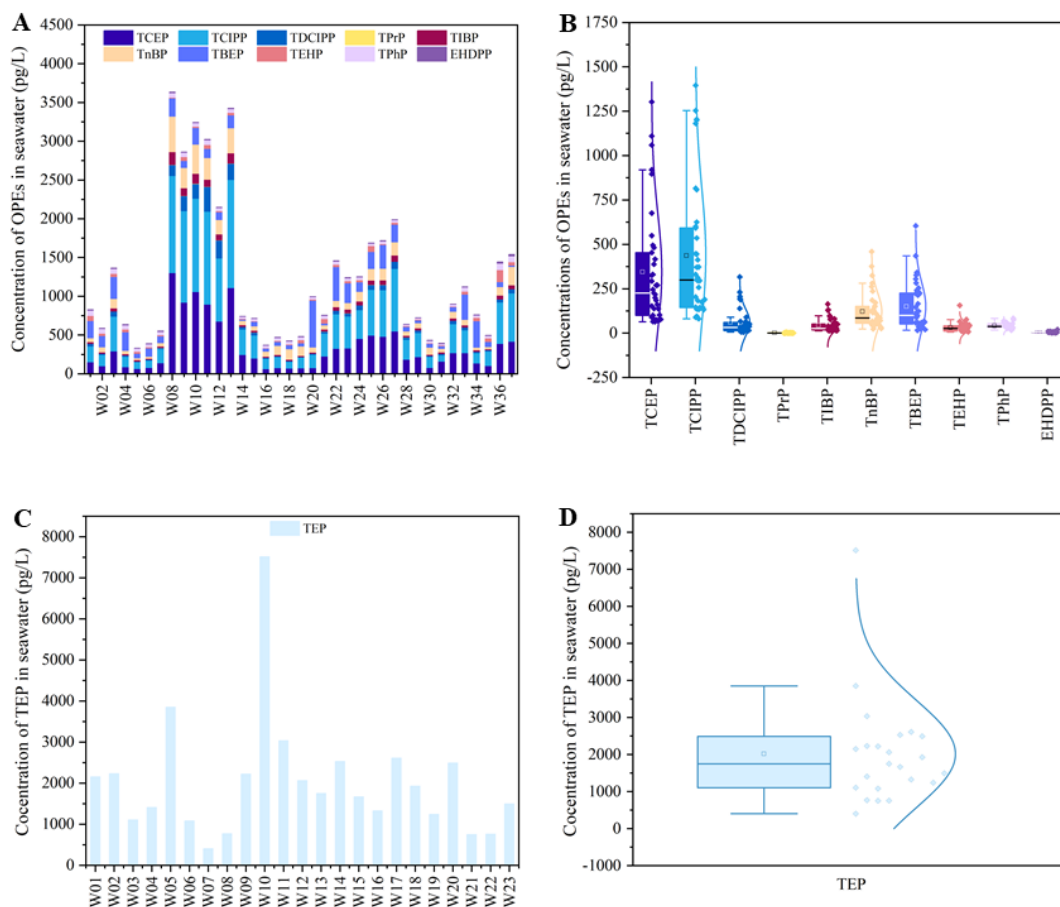


Figure 3-2 (A) Concentrations of OPEs (without TEP) in seawater of the South China Sea, measured with high-volume water samples. (B) Box chart of OPEs. (C) Distribution of TEP in seawater of the South China Sea, determined with 1 L water samples using liquid-liquid extraction. (D) Box chart of TEP.

The concentrations of OPEs have been determined in both dissolved and particle phases (Table S3-10). The total dissolved OPE concentrations (Σ_{10} OPEs without TEP) of all samples ranged from 300 to 3600 pg/L, with mean and median concentrations of 1180 ± 910 pg/L and 740 pg/L, respectively (Table S3-10, Figure 3-2). Three Cl-OPEs dominated the composition profile, with a mean contribution of 72%, followed by a 22% contribution of alkyl-OPEs and a 6% contribution of aryl-OPEs. Compared to previous studies for dissolved OPEs in marine and coastal areas, the results of this work showed relatively low levels, which are 2-3 orders of magnitude lower than those detected in the German Bight(Bollmann et al., 2012a), Amazon River mouth(Schmidt et al., 2019), Tokyo Bay(Lai et al., 2019a), and the Chinese marginal Seas.(Lian et al., 2021; Wang et al., 2015) In contrast, the OPE concentrations of this work are in line with those

measured in the East China Sea(Zhong et al., 2020), the Arctic(Li et al., 2017a), Pacific(Na et al., 2020; Xiao et al., 2021) and the South China Sea(Zhang et al., 2022a). The concentrations of TEP (measured with LLE) ranged from 400 to 7500 pg/L with an average of 2000 ± 1450 pg/L, which showed the highest concentration among the selected OPEs in this work. Previous studies have shown that TEP was the predominant OPE in the Bohai Sea, Laizhou Bay, Yellow River Estuary, Pearl River Estuary and the South China Sea in 2013,(Chen et al., 2019; Lian et al., 2021; Qi et al., 2022) while TEP concentrations in seawater measured in this work were usually 1-2 orders of magnitude lower than in those studies. A significant negative correlation was present between the concentration of TEP and the salinity of the seawater samples (-0.684 , $p < 0.001$), suggesting TEP is transported with the riverine plume and diluted by mixing with the Pacific oceanic waters. TEP has a solubility of 11,400 mg/L, which allows easy TEP transport from the estuary offshore.

3.3.5 Spatial Distribution of OPEs in Seawater

OPEs showed clear spatial variation in the research area (Figure 3-2). Relatively high OPE concentrations were measured nearshore, and declined following the distance from the coast to the open sea. The high levels of OPEs presented in the coastal water comprise the diluted plume of the Pearl River, which is evidenced by the low salinity of the seawater samples. For instance, the highest OPE concentrations were found in high-volume water samples W08 - W13 with salinities ranging from 26.77 to 32.02 psu. TEP measured from 1 L seawater samples showed a distribution trend similar to those of other OPEs in the high-volume water samples. The highest concentration was 7500 pg/L, found in the water sample with the lowest salinity of 27.25 psu among the 1 L seawater samples. The flow filed chart (Figure S3-5) shows that the diluted water plume extended eastward and westward from the Pearl River Estuary at the same time, forming a zonal distribution along the coast of Guangdong. Therefore, riverine discharged OPEs were transported southeastward along the coast and barred by the northward Pacific water intrusion, leading to a declining trend in the mixed water body of the South China Sea.(Zhu et al., 2022a)

3.3.6 Suspended Particulate Matter (SPM) Bound OPEs

The total concentrations of OPEs on SPMs ranged from 16 to 370 pg/L through all high-volume seawater samples, which accounted for 4.7% of the sum of dissolved and

SPM-bound OPEs. Therefore, sedimentation would not be a significant process for removing OPEs from water columns in the South China Sea. However, the SPM bound fraction is 56% for TEHP and 21.3% for TDCIPP, suggesting they may sink and accumulate in the coastal region. The sequence of mean concentrations of individual OPEs is as follow: TCIPP (17 ± 48 pg/L) \approx TEHP (17 ± 15 pg/L) > TDCIPP (13 ± 31 pg/L) > TNBP (3 ± 3 pg/L) > TCEP \approx TPhP > TBEP > EHDPP. This is consistent with OPE profiles in the sediments from the Gulf of Lion (Mediterranean)(Nigar, 2021), the Korean coast and Laizhou Bay,(Choi et al., 2020; Wang et al., 2017b) but differs to the OPEs determined in the Arctic sediments.(Ma et al., 2017)

3.3.7 Source Identification

Previous researches suggested that rivers efficiently transport OPEs from terrestrial sources to the marine environment.(Bollmann et al., 2012a; Wang et al., 2015) OPEs have been measured in the estuary of the Pearl River with concentrations of 630000 pg/L in 2013(Lai et al., 2019a) and 220000 pg/L in 2018(Shi et al., 2020), which are 2 orders of magnitude higher than those of this work, suggesting the riverine input has been significantly diluted by the oceanic water mass. The riverine pathway integrates various land sources, such as industrial release, effluents of wastewater treatment plants, and sewages and leakages of landfills.(Ye and Su, 2022) Besides, there are a few land-based sources, such as volatilization from consumer products and e-waste to the atmosphere and rivers, especially in the coastal areas of the east and southeast of China, Vietnam and Southeast Asia.(Ma et al., 2022; Ye and Su, 2022) The land-based emissions of OPEs can be transported to the offshore areas via riverine discharge, atmospheric deposition and precipitation.(Zeng et al., 2020b)

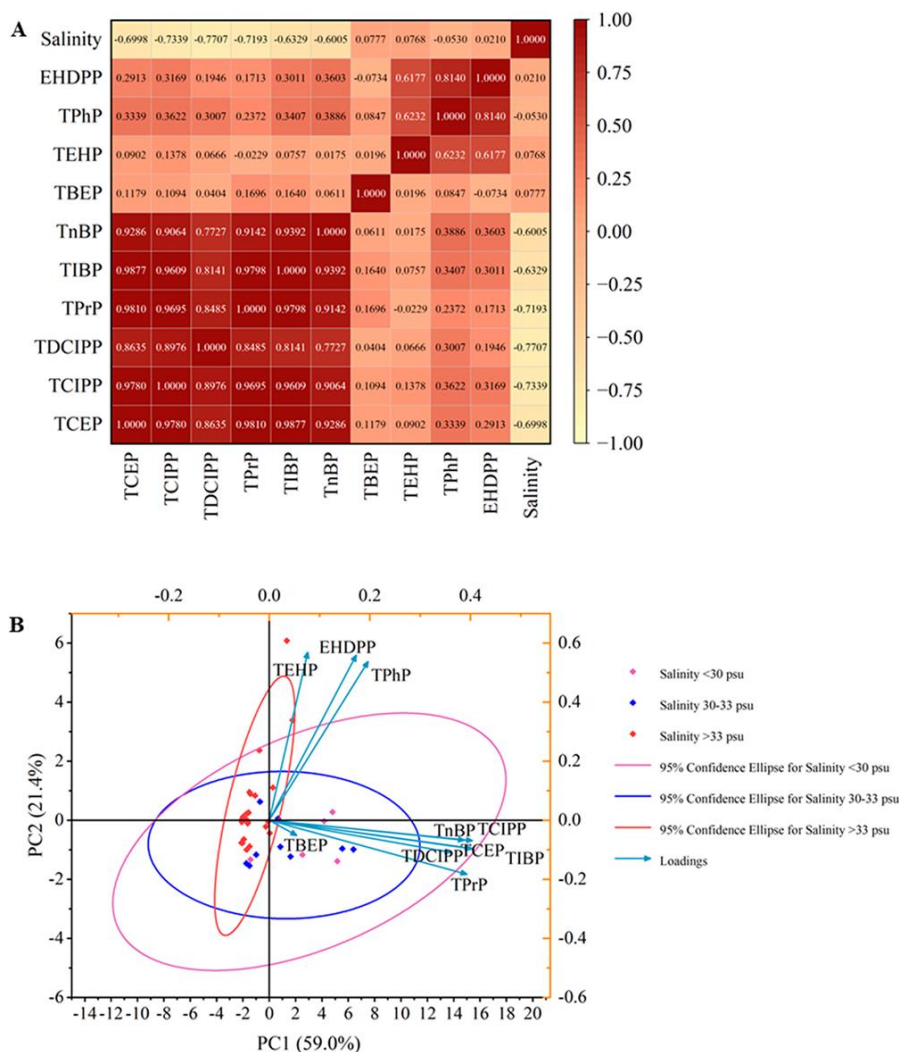


Figure 3-3 (A) Heat map for the correlation analysis of OPEs and salinity. (B) Source appointment based on the gradient of the salinities of seawater samples.

A correlation analysis of OPEs in air and seawater was conducted (Table S3-13 and S3-14). In seawater, Pearson correlation coefficient values ranged from 0.773 to 0.988 ($p < 0.01$) among TCEP, TCIPP, TDCIPP, TPrP, TIBP and TNBP (Table S3-14, Figure 3-3A), indicating significant correlations, with most likely similar sources and transport pathways. Besides, TCEP, TCIPP, TDCIPP, TPrP, TIBP and TNBP showed significantly negative correlation with the salinity of the seawater, suggesting riverine input and dilution by mixing with the oceanic waters. TPhP, EHDPP and TBEP may share similar sources based on their significant correlations to each other. However, chlorinated OPEs did not show any correlation with aryl-OPEs. Especially, PC1 was predominantly weighted by TCEP, TCIPP, TDCIPP, TPrP, TIBP and TNBP (Figure 3-3B), which can be attributed to the discharge of the wastewater treatment plants from the metropolitan area of the Pearl River Delta. In contrast, TEHP, EHDPP and TPhP

were only weighted less than 20% for PC 2, which might be attributed to atmospheric transport and deposition of OPEs occurring in the South China Sea. Industrial processes and e-waste treatment can be the major sources for these OPEs.

In air, three chlorinated OPEs showed significant correlations among the others. TPhP was significantly correlated with most OPEs except for TIBP and EHDPP. TEP had significant correlations with chlorinated OPEs, TPrP, TNBP and TPhP. TCEP, TCIPP and TDCIPP are usually used as flame retardants in textiles, electric products, and fire extinguishing foam. The relatively low $\log K_{OW}$ values of TEP (0.80), TCEP (1.70), and TCIPP (2.68) make them less removable by activated sludge particles, resulting in their discharge with effluents to the riverine. (Bester, 2005; Meyer and Bester, 2004) EHDPP and TEHP are correlated in both air (0.533, $p < 0.05$) and seawater (0.618, $p < 0.05$), indicating that they have similar sources and transport paths. As they both are often used as plastic additives in furniture and building materials, they might release into the ambient air and be transported via atmosphere from land to the sea. E-waste treatment can be an important source for OPEs transported to the South China Sea. (Zeng et al., 2020b) As most alkyl OPEs, such as TNBP, TEHP and TBEP, are physically added to engineering materials as plasticizers, they can release into the ambient environment during their life. (Hoang et al., 2022) Moreover, improper treatment for e-waste can directly release large quantities of plastic additives into the air and be transported offshore the South China Sea. (Li et al., 2019b) We suppose that OPEs have uniform sources for seawater, while OPEs in air might be highly affected by their original sources, monsoon, and atmospheric degradation and precipitation.

3.3.8 Air-Sea Exchange

Fugacity fractions (FFs) are used to determine the direction of the air-sea exchange and are calculated with equations 3-1 to 3-3 (Li et al., 2017a):

$$f_w = C_w H \quad (3-1)$$

$$f_A = C_A R T \quad (3-2)$$

$$FF = f_w / f_A \quad (3-3)$$

where f_w and f_A are the fugacities of OPEs in the water and air, and C_w (ng/m^3) and C_A (ng/m^3) are the concentrations of OPEs in the dissolved phase in seawater and the gaseous phase in air, respectively. FF is the ratio of f_w to f_A ; while $FF < 1$ indicates the direction of flux from air to water, $FF > 1$ indicates the flux from water to air and FF

= 1 represents an equilibrium between air and water. Given the uncertainties existing with H values, a range of 0.3 - 3 is adopted for FF , which shows a system at dynamic equilibrium. (Li et al., 2017a)

values of the air-sea exchange flux (F_{AW} , ng/m²/day) of OPEs are estimated using equation 3-4 and 3-5, (Li et al., 2017a)

$$F = K_{AW} (C_W - C_A RT/H) \quad (3-4)$$

$$1/K_{AW} = RT/K_A H + 1/K_W \quad (3-5)$$

where K_{AW} (m/s) is the overall mass transfer coefficient and contains contributions from the mass transfer coefficients of the water phase (K_W) and the air phase (K_A). $C_W - C_A RT/H$ describes the concentration gradient (ng/m³), where R is the gas constant (8.314 Pa m³/mol/K), T is the absolute temperature (K), and H is the Henry's law constant of OPEs, which is corrected by the temperature of seawater (T_W , K) and the average salt concentration (C_s , 0.5 mol/L). The calculation of K_W and K_A for OPEs refer to the equations recommended by Schwarzenbach et al. and Wanninkhoff's quadratic relationship. (Schwarzenbach et al., 2016; Wanninkhoff et al., 2004) The total propagation error in F was 45%, which is derived from an error propagation analysis from previous studies. A positive F value indicates seawater to air volatilization, while a negative F means that deposition is dominating the air-sea exchange flux.

The FF and F_{AW} values of air-sea exchange fluxes of 10 OPEs were estimated in the South China Sea. The results are shown in Figure 3-4, and the details are summarized in Table S3-15. For the chlorinated OPEs, the FF s of TCEP were mostly < 1, indicating that water to air volatilization is predominant. Six of 37 samples showed dynamic equilibria with FF s of 1.01 - 1.18. The F_{AW} of TCEP ranged from -0.16 to 19.43 ng/m²/day, with a mean of 2.99 ng/m²/day for all samples. The FF s of TCIPP and TCIDPP varied from site to site ranging 0.10 to 7.23, indicating the air-sea exchange directions are changing between volatilization to deposition according to the concentration gradients. The F_{AW} 's of TCIPP and TCIDPP varied between -20.25 and 43.04 ng/m²/day (mean: 4.41 ng/m²/day), and from -0.39 to 1.08 ng/m²/day (mean: 0.13 ng/m²/day), respectively. The FF of alkyl-OPEs showed that TIBP and TEHP were dominated by water to air volatilization, TEP was mainly from air to seawater deposition, and TPrP and TNBP varied between volatilization and deposition. The air-sea exchange fluxes of alkyl-OPEs are 0.32-94.93 (mean: 9.70 ± 15.61 ng/m²/day) for TEHP, -12.12 to 49.10 (mean: 4.82 ± 10.84 ng/m²/day) for TNBP, 0.34 - 38.74 (mean:

6.60 ± 7.39 ng/m²/day) for TIBP, -0.02 to 0.22 (0.03 ± 0.05 ng/m²/day) for TPrP and -10.51 to 12.40 (-1.99 ± 5.08 ng/m²/day) for TEP, respectively. Two aryl-OPEs, i.e. TPhP and EHDPP, showed clear water to air volatilization with mostly $FF < 1$, and their F_{AW} 's ranged from -4.09 to 13.41 ng/m²/day and from -0.01 to 14.81 ng/m²/day. The research area and the summer season affect the concentration gradients of most target OPEs insofar as OPEs are more favored to volatilization or reaching the dynamic equilibrium status. These results are consistent with the continual discharge of OPEs through the riverine area and persistence in the water phase. In contrast, OPEs in the gaseous phase are easily degraded or washed out by precipitation under the subtropical climate conditions during their transport in air.

In comparison with air-sea exchange fluxes of OPEs estimated from previous studies, the directions of air-sea exchange for OPEs are consistent with the estimation for OPEs in the North Atlantic and the Arctic,(Li et al., 2017a) where volatilization is predominant for OPEs. However, the air-sea exchange fluxes of OPEs obtained in this work are 2-3 orders of magnitude lower than those in the Arctic, e.g., 5 - 1075 ng/m²/day for TCEP, 61 to 12283 ng/m²/day for TCIPP, 12 - 2049 ng/m²/day for TIBP and 3 - 943 ng/m²/day for TNBP. (Li et al., 2017a) In the North Pacific Ocean and high Arctic Ocean,(Na et al., 2020) TCIPP and TCEP displayed net deposition, while TIBP showed net volatilization (0.19 to 0.72 ng/m²/day) which is comparable to this work. Air-sea exchange of OPEs reached dynamic equilibrium in the Farm Strait.(McDonough et al., 2018) Zhang et al. estimated air-sea exchange fluxes of OPEs in the South China Sea with gaseous OPEs calculated from particle-bound concentrations, which showed net air to sea deposition.(Zhang et al., 2022a) Air-sea exchange fluxes estimated in the coastal area of the Bohai Sea ranged from -395 ± 1211 ng/m²/day for TCIPP to 1414 ± 2093 ng/m²/day for TCEP, which are 2-3 orders magnitude high than those of this work.(Wang et al., 2018) Overall, the air-sea exchange of OPEs estimated in this work showed that the predominant volatilization can remove parts of OPEs from the water column in the near shore, and it reaches the dynamic equilibrium in the open area. We assume that the winter monsoon can transport high emissions from terrestrial sources and raise the OPE concentrations in air; thus, the equilibrium might be broken up with deposition being dominant. However, more investigation should be carried out to improve the understanding of the air-sea exchange process of OPEs in the South China Sea.

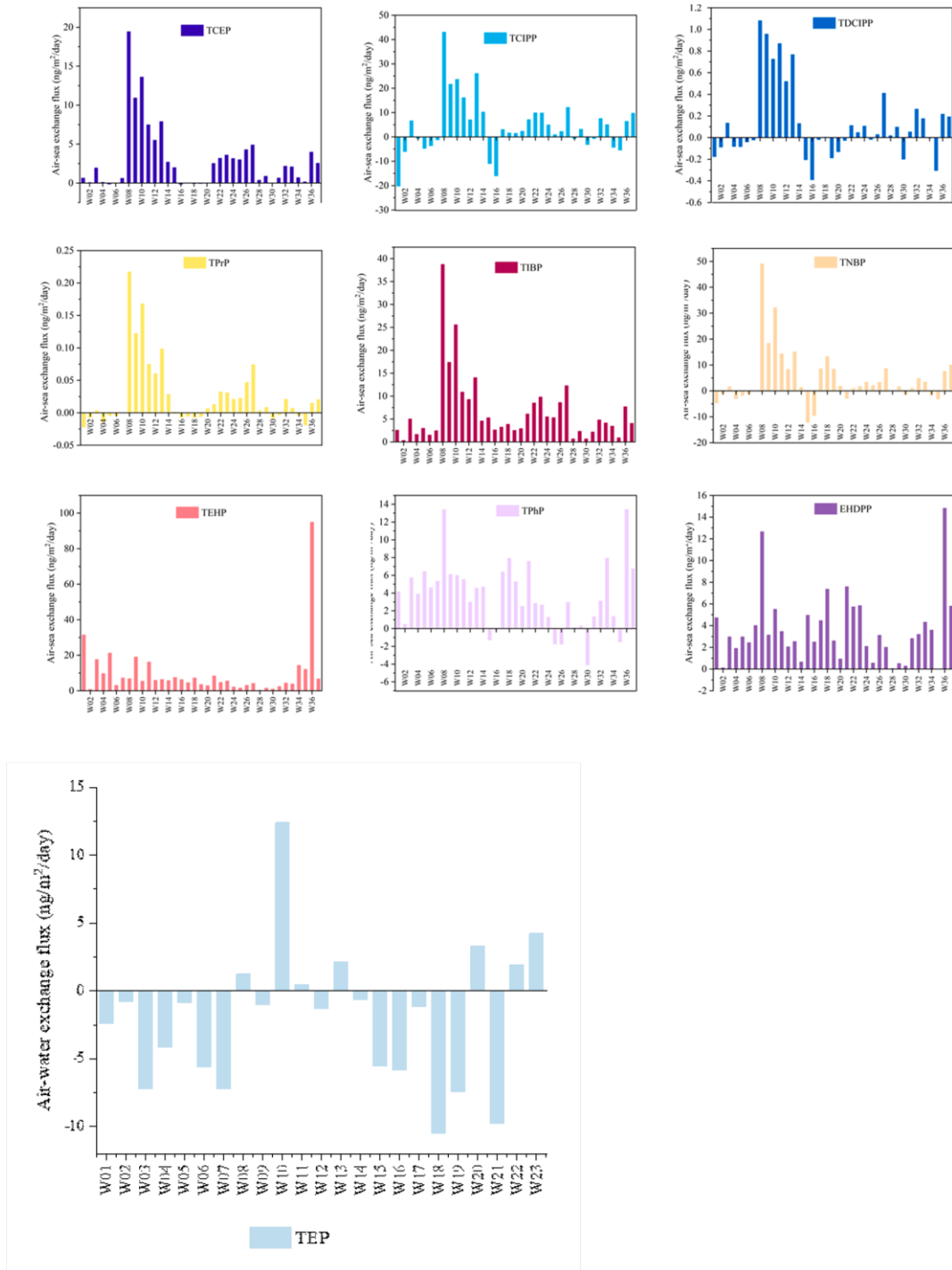


Figure 3-4 Air-sea exchange fluxes of OPEs (ng/m²/day) calculated with two-film fugacity mode using paired air/seawater concentrations. Positive (+) values indicate water to air volatilization, and negative (-) values mean air to water deposition.

3.3.9 Atmospheric Particle Dry Deposition Fluxes

The particle-bound dry deposition fluxes (F_D , ng/m²/day) were calculated via equation 3-6 (Schwarzenbach et al., 2016):

$$F_D = C_p \times V_D \quad (3-6)$$

where C_p is the concentration of particle phase OPEs (ng/m^3), and V_D is the deposition velocity (cm/s), which can be used to estimate the deposition fluxes of air pollutants. In this work, we used the dry deposition velocity of $0.2 \text{ cm}/\text{s}$, which was estimated for pollutants concentrated in fine particles over the South China Sea.(Gao et al., 2020)

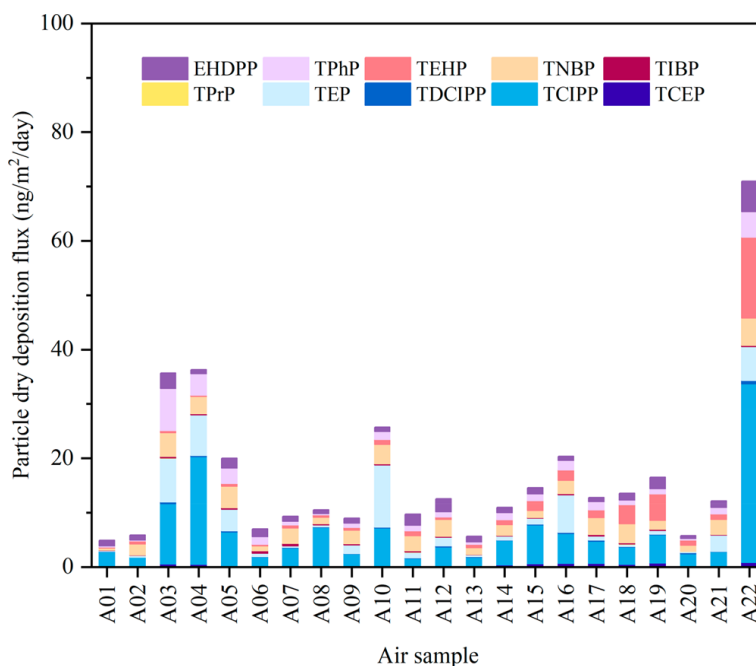


Figure 3-5 Dry deposition fluxes of particle-bound OPEs ($\text{ng}/\text{m}^2/\text{day}$) to the South China Sea.

The atmospheric particle dry deposition fluxes of 10 OPEs were shown in Figure 3-5 and Table S3-16, which ranged from 5 to $71 \text{ ng}/\text{m}^2/\text{day}$ with an average of $17 \pm 15 \text{ ng}/\text{m}^2/\text{day}$. The F_D was dominated by TCIPP ranging from 1.4 to $33 \text{ ng}/\text{m}^2/\text{day}$, followed by TEP, TNBP, TEHP, TPhP and EHDPP. TCEP, TDCIPP, TPrP and TIBP showed relatively low dry deposition fluxes owing to their concentrations in the atmospheric particle phase. In comparison to previous studies for OPEs in the South China Sea, the dry deposition obtained in this work was similar to the levels estimated for the year 2017 and 2018 at Yongxing Island(Zhang et al., 2022c), and those from 2012 in the northern South China Sea(Lai et al., 2015), while they were 4 times lower than those estimated by Zhang et al. (34.6 to $271 \text{ ng}/\text{m}^2/\text{day}$).(Zhang et al., 2022a) In the global ocean perspective, the dry deposition of OPEs was comparable to those estimated for the Arctic in 2014,(Li et al., 2017a) 3 times lower than in the North Pacific Ocean ($16.4 - 185 \text{ ng}/\text{m}^2/\text{day}$),(Na et al., 2020) 5-10 times lower than those estimated in the European seas, e.g., North Sea ($46 - 237 \text{ ng}/\text{m}^2/\text{day}$),(Moller et al., 2011) the

Mediterranean Sea (70 – 880 ng/m²/day), and the Black Sea (300 – 1060 ng/m²/day).(Castro-Jimenez et al., 2014)

As the OPEs measured in this work were at a lower level in comparison to most other marine environments and the Chinese marginal seas, the air-sea exchange and atmospheric dry deposition fluxes estimated in this work represent the baseline for air-sea interface interactions. Given the area of the South China Sea of 3500000 km², the annual atmospheric deposition flux of OPEs ranged from 6.3 - 91 tons/year with an average of 22 ± 19 tons/year (Figure 3-6A), which is consistent with the estimation based on the measurements from Yongxing Island, and previous studies in the South China Sea,(Lai et al., 2015; Zhang et al., 2022c) as well as comparable to those reported for the Bohai Sea (2.2-70.4 tons/year, 78000 km²)(He et al., 2023; Li et al., 2018a) but lower than those calculated for the Black Sea (50-170 tons/year, 440000 km²).(Castro-Jimenez et al., 2014) Meanwhile, the net air-sea gas exchange fluxes of OPEs were volatilization from water to air with an average of 44 ± 33 tons/year (Figure 3-6B). It is reported that the total riverine discharge of OPEs was 384 - 1225 tons/year from Pearl River Delta to the South China Sea,(Fang et al., 2020) which is ~10 times higher than the atmospheric net deposition estimated in this work, suggesting riverine input is prevailing for the levels of OPEs in the South China Sea. However, the volatilization of OPEs from water to air will interfere with the transport of OPEs from the coastal area to offshore and the open ocean.

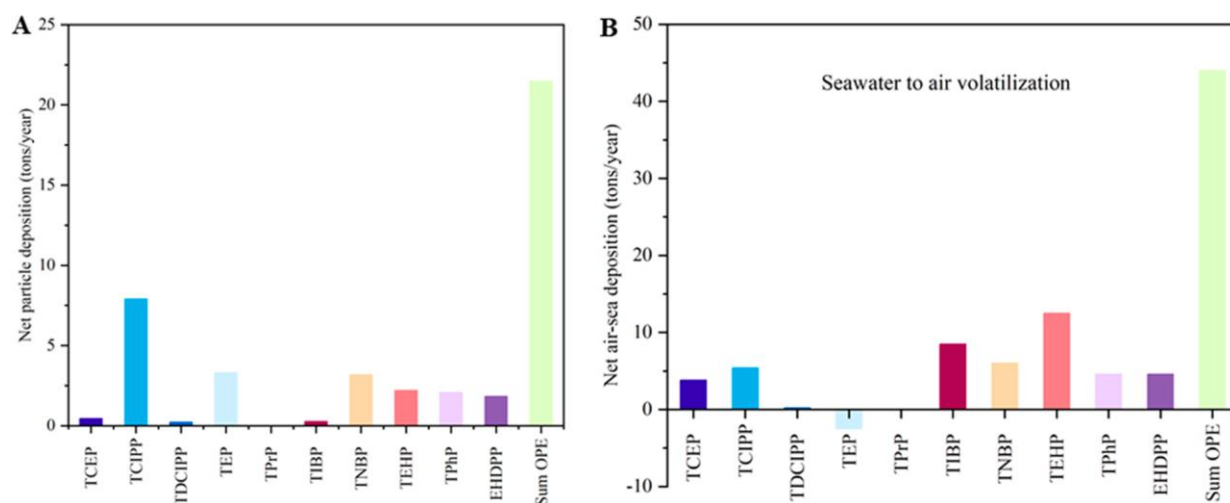


Figure 3-6 (A) Annual net dry deposition of particle-bound OPEs (tons/year). (B) Net air-sea deposition in the South China Sea (tons/year). TEP showed net deposition from air to water, while all other OPEs were dominated by water to air volatilization.

3.4 Implications

OPEs have been extensively detected in air and water in the South China Sea. They are persistent and mobile in the water column, while atmospheric particle bound OPEs are also subject to medium- and long-range transport. Emission of OPEs from industrial processes and wastewater treatment systems of the surrounding regions continually enter the South China Sea via riverine and atmospheric deposition. Besides, e-wastes in Asia are a significant source for OPEs released into the South China Sea. In 2019, 53.6 million tons (Mt) of e-wastes were generated worldwide, and are expected to increase to 74.7 Mt in 2030 and reach as much as 110 Mt in 2050.(Forti et al., 2020) The e-waste quantity from East and Southeast Asia has increased with 10% pro year from 2010 to 2015, and reached 24.9 million tons in 2019. Among them, only 12% of e-waste was documented to be environmentally soundly managed. Improper treatment and disposal of e-waste has amplified the emission of OPEs and acted as an important contamination source for the South China Sea.(Li et al., 2019b)

The effect of summer monsoon on the transport of OPEs in the South China Sea was shown, while the absence of data in winter limits the understanding of the input from East Asia, such as the mainland of China, Korea and Japan, driven by the winter monsoon. Besides, the vertical distribution of OPEs in the water column of the continental shelf and the deep sea need to be further explored to classify their transport with oceanic currents and bioaccumulation in diverse organisms. Nevertheless, the concentration levels of OPEs in both air and seawater have exceeded the levels of brominated flame retardants and most legacy POPs and have become an emerging concern for the protection of the marine environment. Consequently, more studies are required to investigate OPEs in wide areas of the South China Sea and point sources near the coast of Southeast Asia to improve the understanding for the transport, sink and bioaccumulation of OPEs in the South China Sea.

Supporting Information

Figure S 3-1 Air sampling stations in the South China Sea, with the blue dots marked at the end position of each air sample

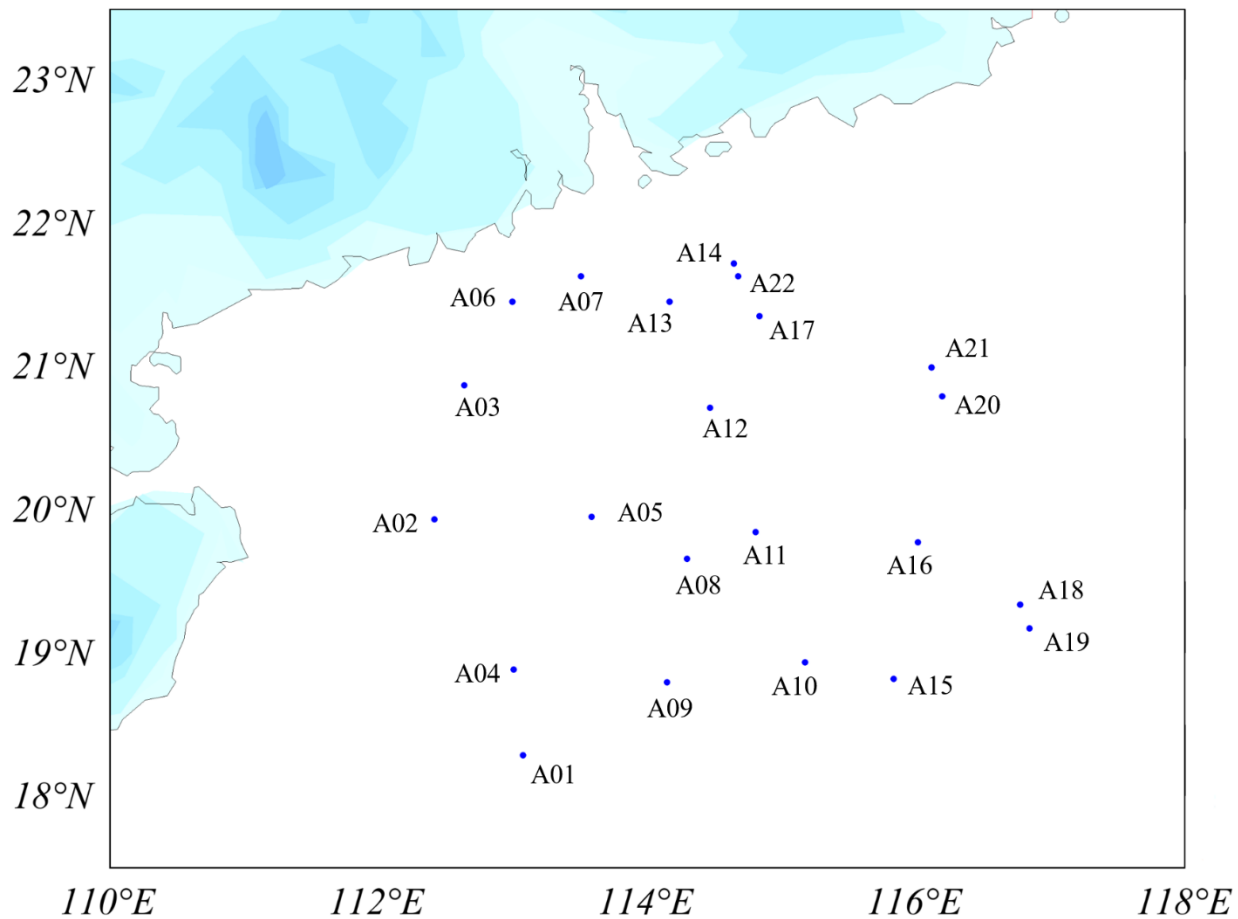


Figure S 3-2 High-volume Seawater sampling stations in the South China Sea, with the black dots marked at the starting position of each water sample.

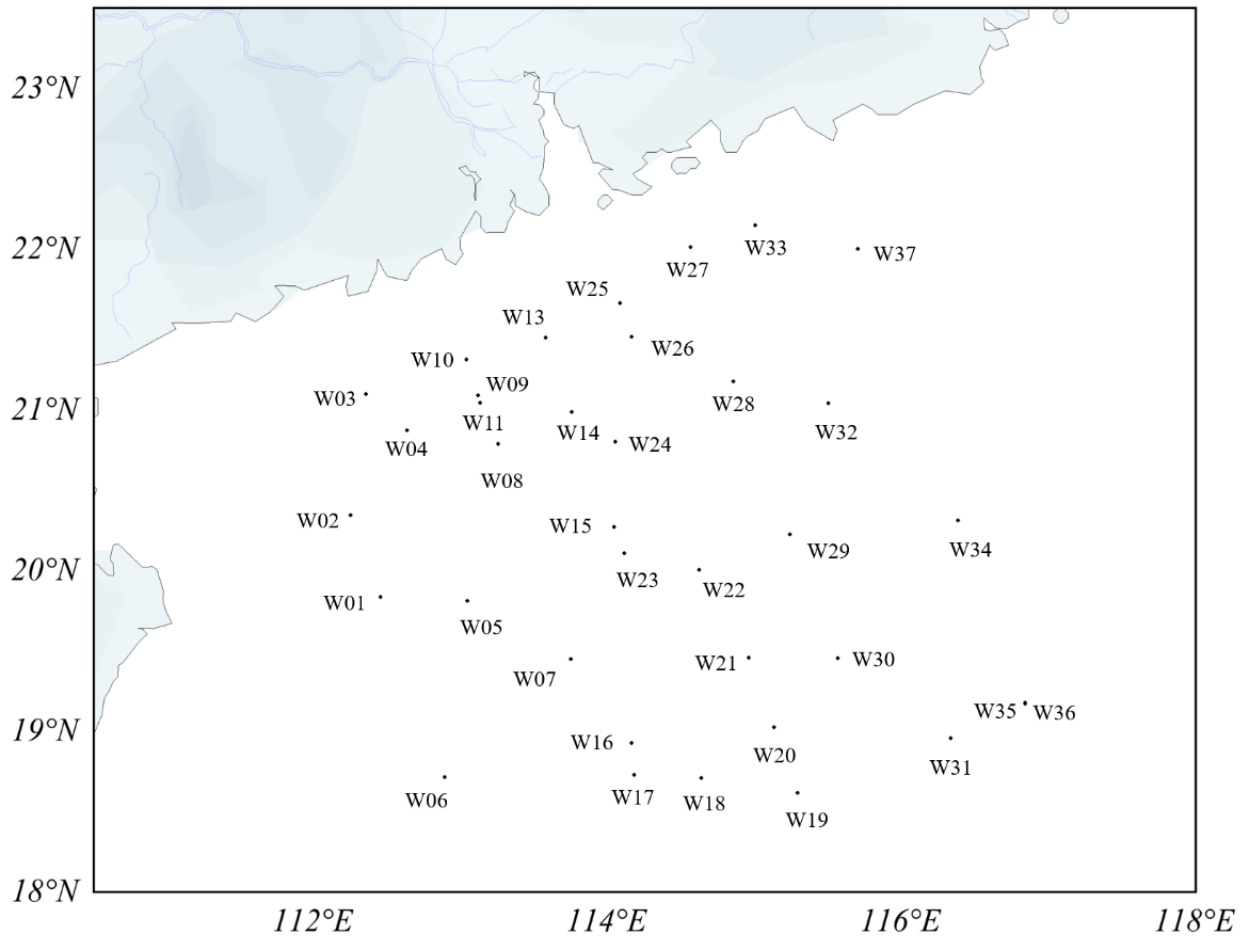


Figure S 3-3 Sampling station for 1-L seawater samples

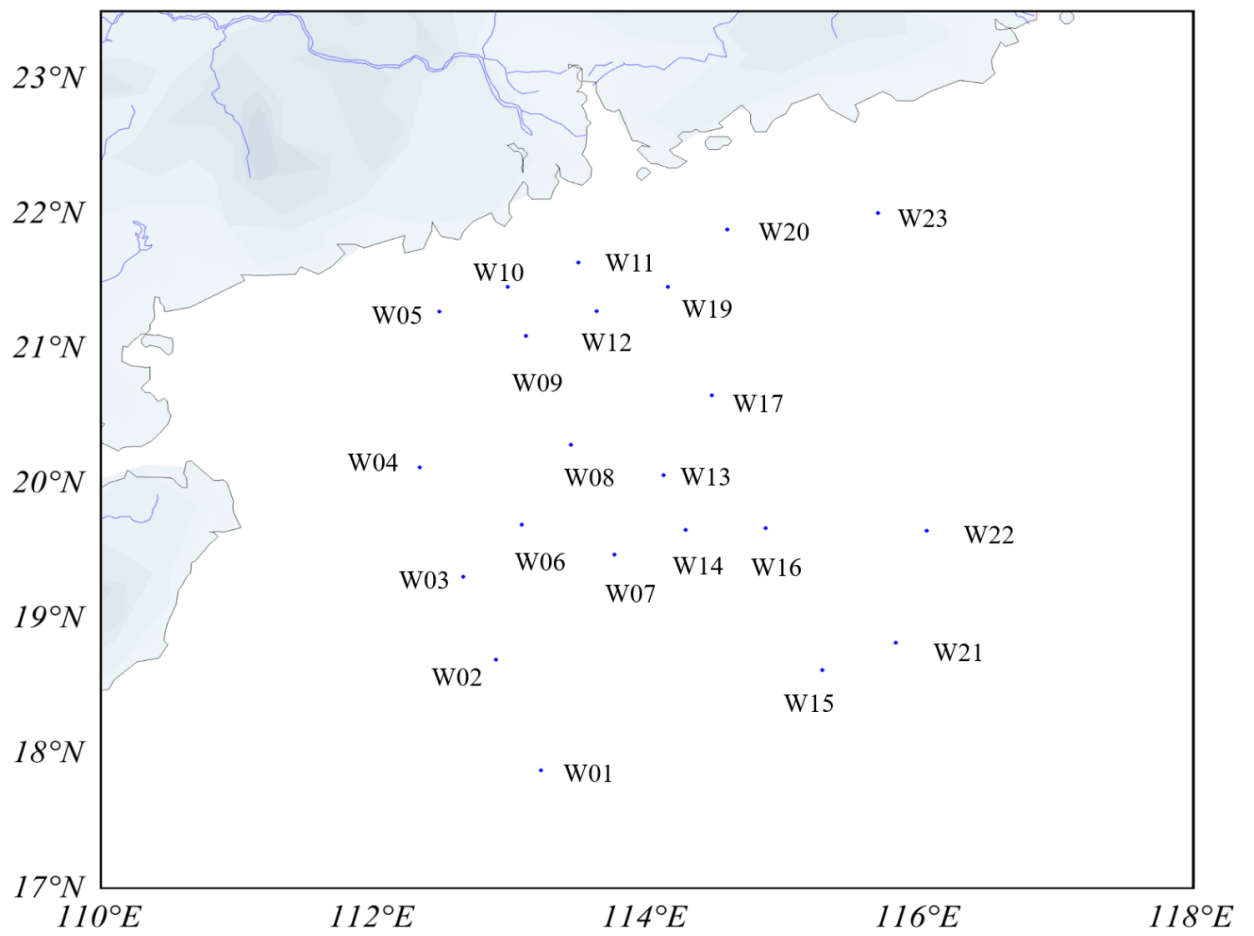
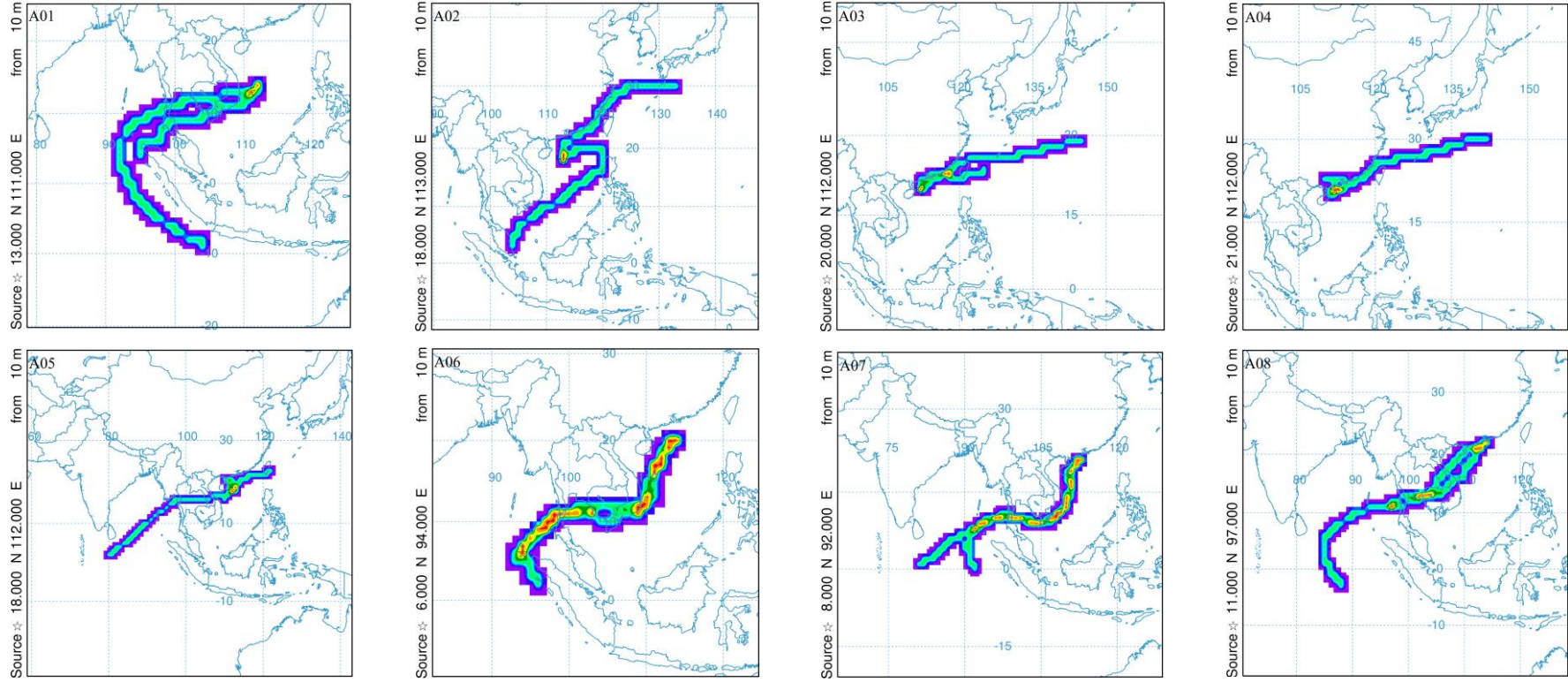
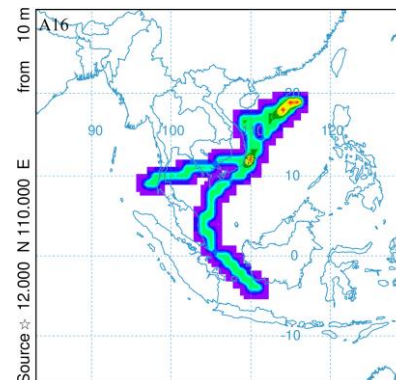
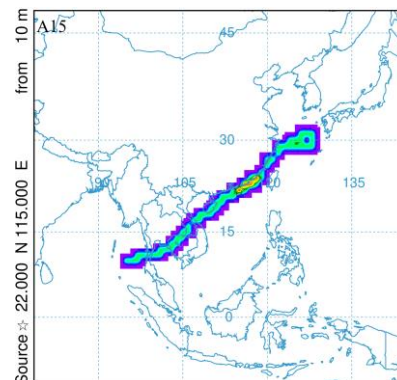
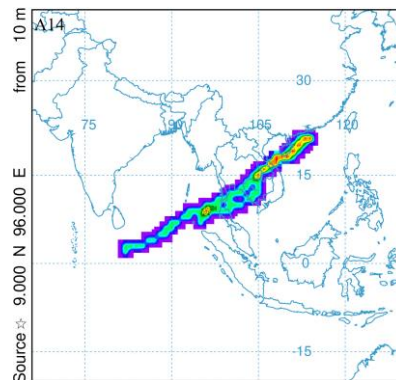
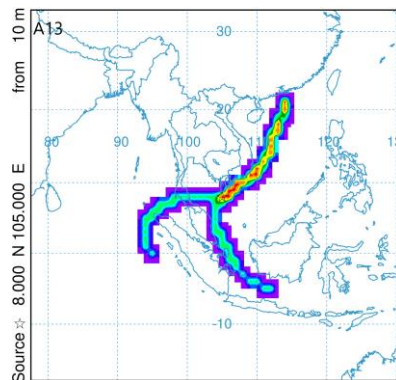
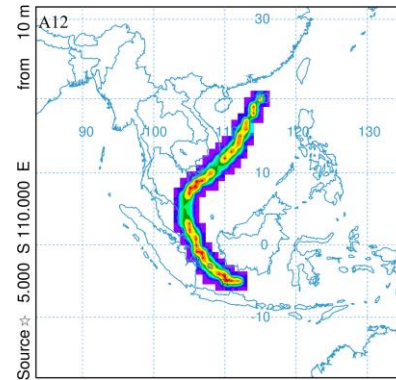
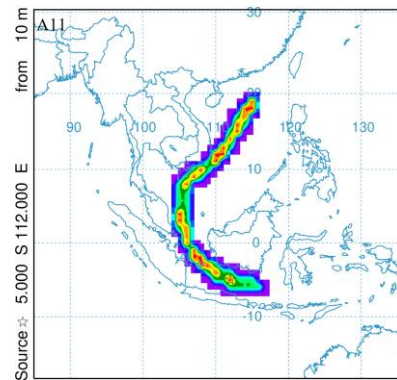
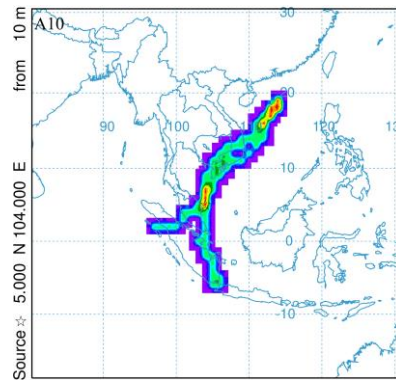
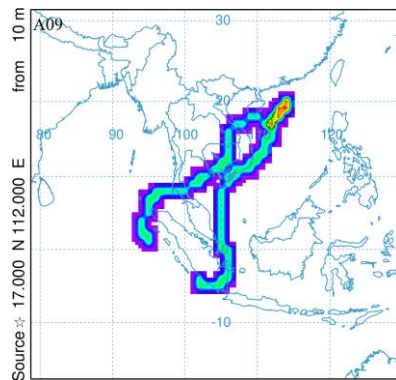


Figure S 3-4 Air mass back trajectories of air samples. Colors indicate the origin of the air mass parcels and their contribution to the air mass





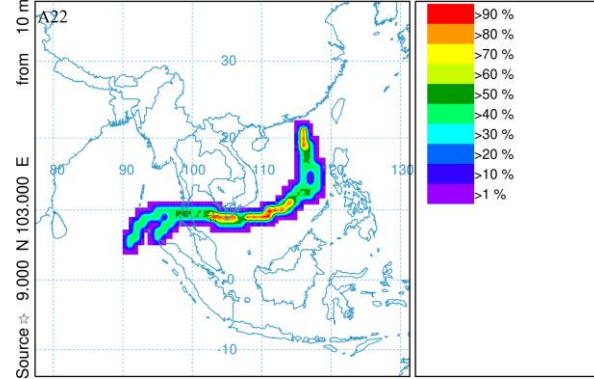
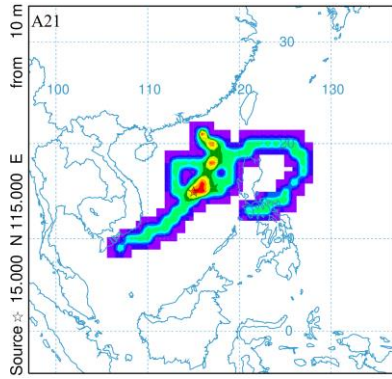
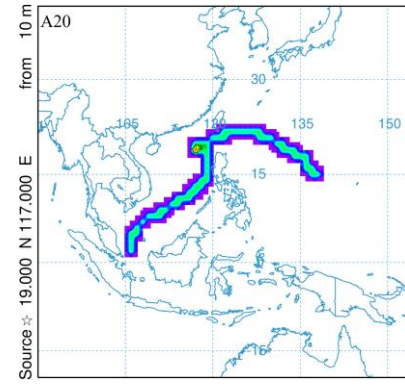
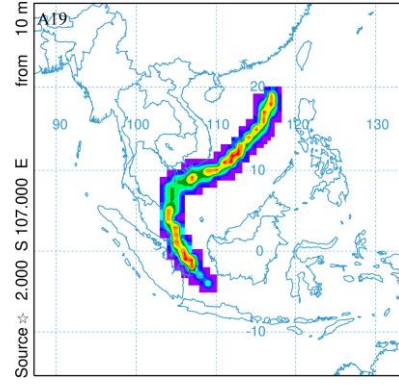
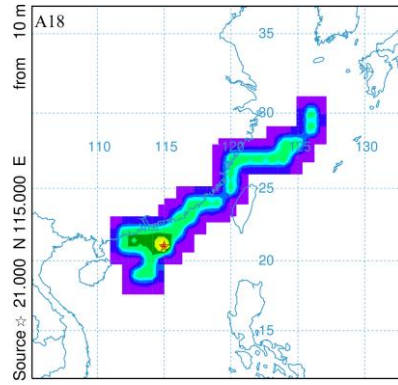
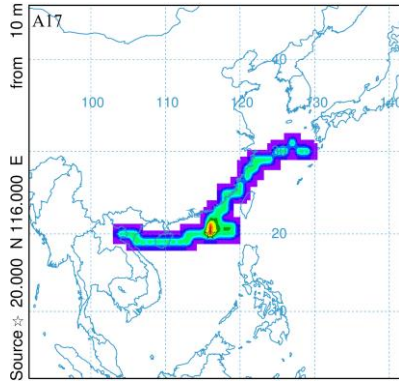


Figure S 3-5 The schematic diagrams of the flow field of the South China Sea on 10th August 2019

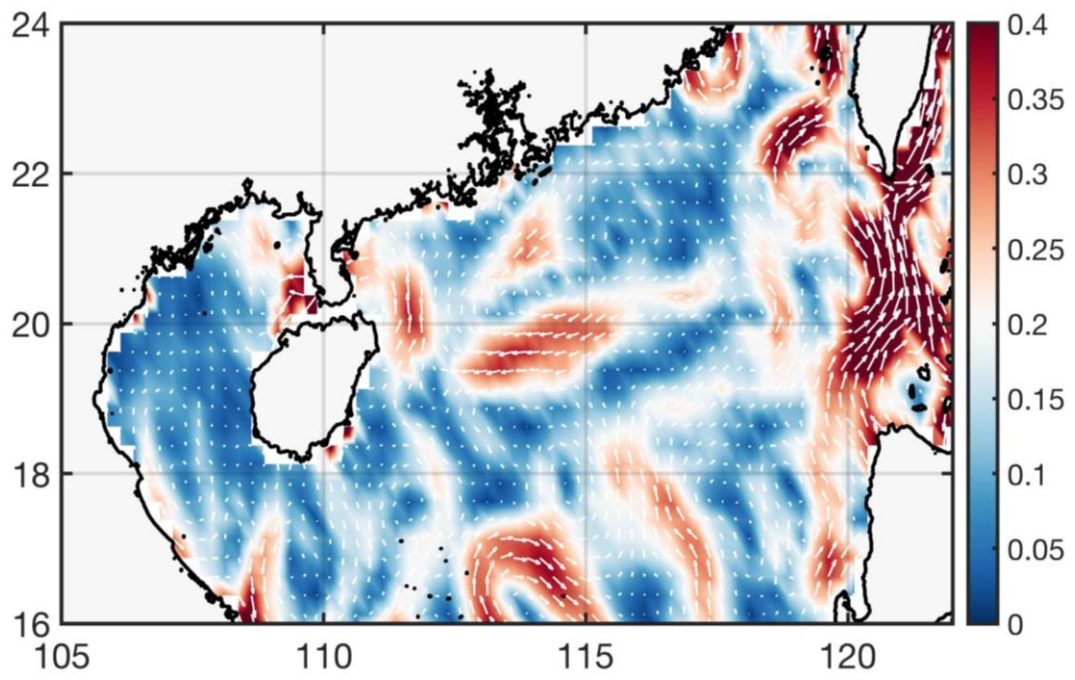


Table S 3-1. Detail information for air sampling

Air sample	Latitude (North, degree)	Longitude (East, degree)	Sampling Date	Time	Volume (m³)	Air temperature (°C)	Humidity (%)	Wind speed (m/s)	Wind direction (degree)
A01	18.278	113.070	6-Aug-2019	7:30	382	29	82.4	9.9	336.8
A02	19.927	112.414	7-Aug-2019	11:08	373	28.8	83.7	7.2	50.2
A03	20.867	112.632	8-Aug-2019	10:37	293	29.2	80.8	4.8	232.2
A04	18.875	112.997	9-Aug-2019	11:28	269	29.5	82.7	6.3	205
A05	21.453	112.986	11-Aug-2019	11:03	326	29.6	83.4	8.2	219.5
A06	21.631	113.505	12-Aug-2019	11:03	341	29.6	84.5	8.2	221.6
A07	19.651	114.290	13-Aug-2019	10:12	348	29.6	84.2	8.4	219.1
A08	18.787	114.142	14-Aug-2019	10:54	344	29.7	75.3	8.9	229.6
A09	18.926	115.167	15-Aug-2019	10:54	280	29.2	82.8	11.1	201.3
A10	19.839	114.797	16-Aug-2019	10:54	316	29.6	83	7.5	198.8
A11	20.708	114.456	17-Aug-2019	11:05	278	29.4	83.8	7.6	214.4
A12	21.452	114.160	19-Aug-2019	10:39	645	29.4	74.8	6	223
A13	21.720	114.644	20-Aug-2019	11:00	290	28.6	74.4	8.3	94.3
A14	18.813	115.830	22-Aug-2019	10:39	535	26.6	87	9.7	314.9
A15	19.766	116.008	23-Aug-2019	11:46	339	28.9	80.3	3.4	26
A16	21.351	114.831	24-Aug-2019	11:46	356	30.3	79.9	12.5	242.3
A17	19.332	116.770	26-Aug-2019	11:00	504	29.2	81.7	3.9	141.6
A18	19.166	116.840	27-Aug-2019	11:00	310	28.7	81.7	7.2	35.3
A29	20.791	116.190	29-Aug-2019	11:00	531	28.5	81.3	7.8	124.7
A20	20.993	116.111	30-Aug-2019	11:06	345	28.5	78.1	4.6	108.8
A21	21.630	114.665	31-Aug-2019	11:15	313	28.7	79.4	7.9	81.5
A22	21.087	113.12	1-Sep-2019	11:15	300	28.1	88	14.8	37.1

Table S 3-2. Detail information of high-volume seawater samples collected during the cruise SO269 in the South China Sea. Samples were collected through ship-intake system made with stainless steel

Seawater Sample	Latitude (North, degree)	Longitude (East, degree)	Sampling Date	Volume (L)	Ta (°C)	Tw (°C)	Conductivity (S/m)	Depth (m)
W01	19.83	112.45	7-Aug-2019	100	28.8	29.9	5.64	113.2
W02	20.34	112.25	7-Aug-2019	135	28.5	29.6	5.65	83.4
W03	21.09	112.35	8-Aug-2019	171	29	29.4	5.64	48.8
W04	20.87	112.63	8-Aug-2019	178	29.4	29.6	5.67	60
W05	19.81	113.04	9-Aug-2019	193	29.4	30	5.67	154
W06	18.71	112.89	9-Aug-2019	177	29.4	30	5.67	900
W07	19.45	113.75	10-Aug-2019	244	29.8	29.8	5.67	472.5
W08	20.78	113.25	10-Aug-2019	196	29.3	30	5.4	81.1
W09	21.09	113.12	11-Aug-2019	36	29.8	30.3	4.74	60
W10	21.31	113.04	11-Aug-2019	169	29.8	29.8	4.57	42
W11	21.04	113.13	12-Aug-2019	84	30.3	30.4	4.98	44.3
W12	21.04	113.13	12-Aug-2019	119	30.3	30.4	4.98	44.3
W13	21.44	113.57	12-Aug-2019	68	29.7	29.6	5.18	42.2
W14	20.98	113.75	12-Aug-2019	105	29.7	30.4	4.83	85.6
W15	20.27	114.04	13-Aug-2019	310	29.8	29.6	5.58	121.4
W16	18.92	114.16	13-Aug-2019	199	29.5	29.8	5.66	1348.3
W17	18.72	114.18	14-Aug-2019	198	29.5	29.8	5.66	1859.1
W18	18.70	114.64	14-Aug-2019	126	29.2	29.7	5.65	3510
W19	18.61	115.29	15-Aug-2019	247	29.2	29.4	5.62	3694.5
W20	19.02	115.13	15-Aug-2019	108	29.2	29.6	5.63	2276.6
W21	19.45	114.96	16-Aug-2019	195	29.9	29.7	5.62	1469.2
W22	20.00	114.62	16-Aug-2019	195	27.7	29.7	5.58	1469.2
W23	20.10	114.11	17-Aug-2019	165	29.6	29.8	5.61	187.5
W24	20.80	114.05	18-Aug-2019	165	29.6	30	5.68	89
W25	21.66	114.08	18-Aug-2019	217	27.7	29.6	5.45	51
W26	21.45	114.16	19-Aug-2019	210	29.2	29.9	5.42	55
W27	22.01	114.56	20-Aug-2019	143	28.4	29.2	5.3	40
W28	21.17	114.85	20-Aug-2019	158	28.4	29.7	5.46	95
W29	20.22	115.24	21-Aug-2019	185	26.7	29.4	5.35	468
W30	19.45	115.56	22-Aug-2019	258	28.7	29.3	5.56	2490
W31	18.95	116.33	23-Aug-2019	240	28.8	29.4	5.61	2732
W32	21.04	115.5	24-Aug-2019	220	29.4	29.8	5.34	125
W33	22.14	115	25-Aug-2019	250	27.5	29.9	5.44	51.8
W34	20.31	116.38	26-Aug-2019	138	29.2	29.4	5.58	961
W35	19.17	116.84	26-Aug-2019	180	29.2	29.5	5.6	3339
W36	19.17	116.84	27-Aug-2019	35	29.5	29.6	5.6	3340
W37	22.00	115.7	31-Aug-2019	100	29.2	29.9	5.54	80

Table S 3-3. Detail information of 1-L seawater samples collected in the South China Sea during the cruise SO269. Water samples were collected from ship intake system and from CTD stations

Seawater Sample	Date	Time	Latitude (N)	Longitude (E)	Ta (°C)	Tw (°C)	Salinity (psu)	Depth of Sea (m)
SO269-1L-W01	8/5/2019	23:55	17.8672	113.2291	29.2	29.9	33.89	1891
SO269-1L-W02	8/6/2019	15:21	18.6880	112.9000	29.0	29.3	33.91	952
SO269-1L-W03	8/7/2019	2:14	19.3010	112.6600	29.0	29.5	33.87	216
SO269-1L-W04	8/7/2019	13:32	20.1123	112.3402	28.8	29.6	33.88	90
SO269-1L-W05	8/8/2019	3:11	21.2684	112.4851	30.1	28.9	29.63	50
SO269-1L-W06	8/9/2019	2:20	19.6888	113.0900	29.4	29.8	33.90	181
SO269-1L-W07	8/10/2019	2:53	19.4660	113.7700	29.7	29.8	33.90	474
SO269-1L-W08	8/10/2019	12:44	20.2791	113.4500	29.6	29.8	33.55	102
SO269-1L-W09	8/10/2019	12:44	21.0870	113.1200	29.4	29.9	27.58	61
SO269-1L-W10	8/11/2019	8:47	21.4530	112.9860	30.0	29.1	27.25	35
SO269-1L-W11	8/12/2019	4:28	21.6309	113.5050	29.7	29.9	28.00	35
SO269-1L-W12	8/12/2019	14:54	21.2706	113.6395	29.4	29.6	29.13	57
SO269-1L-W13	8/13/2019	4:54	20.0563	114.1289	28.6	29.7	33.58	282
SO269-1L-W14	8/13/2019	10:12	19.6510	114.2901	29.6	29.9	33.24	825
SO269-1L-W15	8/15/2019	0:48	18.6110	115.2900	29.2	29.4	33.96	3695
SO269-1L-W16	8/16/2019	4:14	19.6632	114.8761	29.6	29.7	33.51	1466
SO269-1L-W17	8/17/2019	10:22	20.6466	114.4810	29.6	30.0	33.67	100
SO269-1L-W18	8/18/2019	10:52	21.4517	114.1600	27.0	30.0	32.08	50
SO269-1L-W19	8/19/2019	3:24	21.4517	114.1600	29.2	30.0	32.28	50
SO269-1L-W20	8/20/2019	9:46	21.8782	114.5952	28.9	29.3	32.18	58
SO269-1L-W21	8/22/2019	13:07	18.8128	115.8301	28.1	29.3	33.80	3217
SO269-1L-W22	8/23/2019	9:20	19.6426	116.0577	28.8	29.6	33.15	1787
SO269-1L-W23	8/31/2019	2:37	21.9979	115.7000	29.2	29.9	33.05	80

Table S 3-4. Physiochemical properties of organophosphate esters

Chemical Name	Abbreviation	CAS	MW	V _p (Pa)	S (mg/L)	H (pa.m ³ /mol)	logKow	logKoa	logKaw	Enthalpy of vaporization ΔH _{vap} (kJ/mol)	Half-life time (Air, h)	Half-life time (River, h)
Tris(2-chloroethyl) phosphate	TCEP	115-96-8	285.49	8.17	7000	0.333	1.44	5.311	-3.871	82.0	5.84	302
Tris(2-chloroisopropyl) phosphate	TCIPP	13674-84-5	327.57	7.53 x 10 ⁻³	51.85	0.0475	2.59	8.203	-5.613	85.2	2.87	1.778 x 10 ⁴
Tris (1,3-dichloro-2-propyl) phosphate	TDCIPP	13674-87-8	430.91	3.82 x 10 ⁻⁵	1.5	1.095 x 10 ⁻²	3.65	10.662	-6.972	91.3	7.098	4.657 x 10 ⁵
Triethyl phosphate	TEP	78-40-0	182.16	52.4	1.12 x 10 ⁴	0.359	0.80	6.632	-5.832	55.73	2.215	2.195 x 10 ⁴
Tripropyl phosphate	TPrP	513-08-6	224.24	3.08	827	0.0689	1.87	6.426	-4.556	70	1.721	1291
Tri-iso-butyl phosphate	TIBP	126-71-6	266.32	1.71	16.22	0.323	3.60	7.485	-3.885	73.13	1.629	301
Tri-n-butyl phosphate	TNBP	126-73-8	266.32	0.151	280	0.143	4.0	8.239	-4.239	80.57	1.628	679
Tris(2-ethylhexyl) phosphate	TEHP	78-42-2	434.65	1.1 x 10 ⁻⁵	1.46 x 10 ⁻⁵	9.69	9.49	14.983	-5.493	106	1.312	1.553 x 10 ⁴
Tris(2-butoxyethyl) phosphate	TBEP	78-51-3	398.48	1.65 x 10 ⁻⁴	1.96	0.0333	3.75	-9.309	13.059	112	0.997	9.739 x 10 ⁷
Triphenyl phosphate	TPHP	115-86-6	326.29	8.37 x 10 ⁻⁴	1.9	0.335	4.59	-3.869	8.459	92.8	11.838	321.4
2-Ethylhexyl diphenyl phosphate	EHDPP	1241-94-7	362.41	6.67 x 10 ⁻³	0.0666	5.49	5.73	-2.654	8.384	99.9	3.22	22.51

Table S 3-5. Agilent 7890 GC-MS/MS conditions

Parameter	Value
Analytical column	2 set Agilent HP5-ms, 250 μm \times 15 m, 0.25 μm
Sample injection mode	1 μL Pulsed splitless using Multimode Inlet (MMI)
Injection port liner	Agilent 200 μL dimpled, single-taper liner
Injection temperature program	20 $^{\circ}\text{C}$ (0.2 minutes), 300 $^{\circ}\text{C}/\text{min}$ to 300 $^{\circ}\text{C}$
Injection pulsed pressure	25 psi (1.9 minutes)
Purge flow to spit vent	50 mL/min (2.0 minutes)
Carrier gas	Helium
Carrier gas flow	1.2 mL/min
Oven temperature program	50 $^{\circ}\text{C}$ for 2 min, 20 $^{\circ}\text{C}/\text{min}$ to 80 $^{\circ}\text{C}$, 5 $^{\circ}\text{C}/\text{min}$ to 250 $^{\circ}\text{C}$, 15 $^{\circ}\text{C}/\text{min}$ to 300 $^{\circ}\text{C}$ (14 min)
Post run	310 $^{\circ}\text{C}$ for 3 min
Backflush	3.0 mL/min
Mass spectrometer	Agilent 7000C with electron impact ionization source operated in multiple reaction monitoring mode (MRM)
Ionization mode	Positive
Source temperature	280 $^{\circ}\text{C}$
Quadrupole 1 and 2 temperature	150 $^{\circ}\text{C}$
Transfer line temperature	280 $^{\circ}\text{C}$

Table S 3-6. The information for determination of OPEs using GC-MS/MS

OPE	Quantifier ions (m/z)	Collision energy (eV)	Retention time (min)
TCEP	249>187	10	23.11
TCIPP	99>81	25	23.88
TDCIPP	99>81	15	33.66
TEP	99>81	15	8.35
TPrP	99>81	15	14.50
TIBP	99>81	15	17.66
TNBP	99>81	15	20.65
TEHP	99>81	15	35.95
TBEP	153>97	15	35.0
TPHP	326>215	15	34.70
EHDPP	251>153	10	35.22
d27-TNBP	103>83	15	20.30
d12-TCEP	261>196	10	22.92
d15-TPHP	341>223	10	34.57
13C-PCB-208	476>406	20	38.66

Table S 3-7. The field blanks and the method detection limits of OPEs in PUF/XAD-2, XAD-2 columns, QFF and GFF filters

Sample material OPE	PUF/XAD-2 column (gas)		QFF (particle)		XAD-2 column (dissolved phase)		GFF (particular matter)	
	Blank (mean±SD) (pg/m ³)	MDL (pg/m ³)	Blank (mean±SD) (pg/m ³)	MDL (pg/m ³)	Blank (mean±SD) (pg/L)	MDL (pg/L)	Blank (mean±SD) (pg/L)	MDL (pg/L)
TCEP	0.99±0.46	2.37	0.36±0.19	0.93	2.51±0.58	4.25	0.61±0.15	1.06
TCIPP	0.88±0.24	1.60	4.2±0.8	6.5	25.51±12.59	63.29	4.86±2.09	11.14
TDCIPP	0.04±0.04	0.16	0.43±0.39	1.6	0.46±0.33	1.45	0.14±0.12	0.51
TEP	0.13±0.01	0.17	0.41±0.30	1.3	na	na	na	na
TPrP	0.02±0.005	0.04	0.16±0.09	0.44	0.13±0.07	0.34	0.04±0.01	0.08
TIBP	0.25±0.03	0.34	0.20±0.06	0.39	3.31±0.74	5.54	0.41±0.11	0.73
TNBP	2.5±0.4	3.72	0.36±0.17	0.87	6.95±1.14	10.37	0.77±0.09	1.03
TEHP	2.09±0.14	2.49	0.03±0.01	0.06	53.63±24.45	126.97	3.13±3.24	12.85
TBEP	10.8±3.4	20.9	0.39±0.29	1.26	4.57±0.74	6.79	0.47±0.29	1.33
TPHP	1.68±0.55	3.34	0.19±0.07	0.39	9.20±0.24	9.92	0.62±0.35	1.68
EHDPP	0.59±0.12	0.93	na	na	0.52±0.37	1.62	0.27±0.16	0.73

Table S 3-8. Concentrations of OPEs in the atmosphere over the South China Sea

OPE in gas phase (C_g , pg/m ³)													
	TCEP	TCIPP	TDCIPP	TEP	TPrP	TIBP	TNBP	TPeP	TEHP	TPhP	EHDPP	TBEP	Σ OPE
A01	0.43	49.46	0.55	5.68	0.01	1.10	8.84	10.94	36.74	10.94	85.88	23.16	211
A02	0.59	9.71	0.15	4.24	0.02	0.51	26.54	0.10	11.62	2.62	15.86	10.30	72
A03	4.46	8.90	0.15	10.09	0.01	0.33	4.34	0.20	10.10	4.17	6.56	18.82	49
A04	2.03	45.61	0.70	14.33	0.06	0.69	15.43	1.04	35.94	12.77	10.98	9.87	140
A05	1.56	7.10	0.34	11.73	0.04	0.47	12.26	0.19	10.49	6.99	10.81	16.11	62
A06	0.69	10.43	0.20	1.09	0.00	0.52	5.37	0.18	9.72	2.38	5.76	23.41	36
A07	0.66	25.88	0.27	7.84	0.02	1.29	8.22	4.38	10.89	6.57	10.30	11.42	76
A08	0.67	3.62	0.18	8.22	0.01	0.28	6.27	0.08	13.19	2.88	6.05	10.33	41
A09	0.74	25.60	0.60	24.75	0.01	0.60	21.12	0.54	8.16	10.89	5.50	14.68	99
A10	0.54	1.86	0.12	1.08	0.01	0.18	1.20	0.07	4.68	1.10	5.40	13.90	16
A11	0.83	4.49	0.28	8.16	0.02	0.45	5.90	0.06	27.27	5.15	9.08	9.21	62
A12	0.37	5.45	0.30	9.85	0.02	0.71	9.68	0.08	8.00	4.24	6.36	7.00	45
A13	0.45	6.53	0.32	9.27	0.02	0.49	8.92	0.10	11.72	7.98	5.74	5.65	52
A14	1.92	24.28	0.68	16.10	0.03	0.74	14.33	0.47	13.76	14.29	13.12	3.44	100
A15	0.49	15.57	0.20	11.01	0.02	0.27	7.02	0.40	4.55	4.02	6.22	13.21	50
A16	0.21	5.26	0.07	3.30	0.01	0.23	3.29	0.06	7.43	3.70	2.54	12.81	26
A17	0.54	14.12	0.63	8.13	0.03	2.56	15.06	0.38	27.83	21.43	18.52	12.29	109
A18	0.31	5.19	0.06	5.72	0.02	0.24	3.52	0.15	3.81	2.32	1.59	22.33	23
A19	0.44	11.88	0.19	6.98	0.02	0.48	6.62	0.22	14.67	7.22	6.00	1.01	55
A20	0.43	7.14	0.10	0.44	0.01	0.28	3.09	1.81	12.70	1.55	3.07	19.86	31
A21	0.79	11.89	0.30	13.26	0.03	0.39	5.87	1.93	16.44	3.89	9.32	19.12	64
A22	0.89	24.57	1.08	10.55	0.06	0.61	13.25	0.52	24.65	15.57	21.11	11.80	113
Mean (pg/m ³)	0.91	14.75	0.34	8.72	0.02	0.61	9.37	1.09	14.74	6.94	12.08	13.17	69.57
SD	0.93	12.96	0.26	5.53	0.02	0.51	6.24	2.41	9.60	5.31	17.22	6.16	44.96
Median	0.63	10.07	0.28	8.19	0.02	0.49	7.62	0.21	11.67	4.70	6.46	12.55	58.21
Min	0.21	1.86	0.06	0.44	0.00	0.18	1.20	0.06	3.81	1.10	1.59	1.01	16.23
Max	4.46	49.46	1.08	24.75	0.06	2.56	26.54	10.94	36.74	21.43	85.88	23.41	210.58
OPE in particle phase (C_p , pg/m ³)													
A01	0.49	15.93	0.27	1.00	0.03	0.22	2.31	4.08	0.89	1.34	5.99	0.62	33
A02	0.67	9.63	0.22	1.69	0.02	0.34	12.04	2.15	3.21	1.06	4.97	1.87	36
A03	3.11	64.20	2.11	46.49	0.10	1.87	24.97	11.35	2.40	44.91	16.23	0.58	218
A04	2.80	114.49	1.42	43.30	0.07	1.13	18.30	18.91	1.52	22.67	4.38	0.45	229
A05	1.50	35.89	1.09	23.03	0.08	1.38	22.90	6.69	3.14	16.19	10.56	2.05	122
A06	1.17	9.63	0.32	3.42	0.07	2.80	5.18	1.92	1.57	8.27	8.16	1.53	43
A07	1.51	18.85	0.46	1.68	0.06	2.59	16.28	3.39	3.36	3.75	5.43	1.03	57
A08	1.52	40.69	0.60	2.02	0.02	1.20	6.76	7.59	2.61	1.59	3.84	0.81	68
A09	0.67	13.17	0.42	9.14	0.04	1.21	14.45	2.41	3.06	4.63	5.09	1.66	54
A10	1.16	40.24	1.17	66.13	0.05	1.07	20.71	6.92	5.11	8.67	4.69	1.53	156
A11	1.06	8.04	0.64	6.00	0.06	1.47	16.00	1.73	5.15	5.94	11.73	1.29	58
A12	1.21	19.97	1.48	8.93	0.04	1.16	17.86	3.70	2.49	5.74	13.66	1.20	76
A13	0.58	9.66	0.90	1.91	0.01	0.40	7.03	1.99	3.82	2.59	5.87	1.03	35
A14	2.06	26.38	0.34	4.24	0.01	0.65	11.50	4.89	5.26	7.49	5.48	2.70	68

A15	3.56	41.27	0.86	6.25	0.01	0.65	7.63	7.71	10.30	7.43	6.29	3.31	92
A16	3.81	31.86	1.36	39.73	0.05	1.25	14.19	5.77	11.20	10.11	4.16	1.88	123
A17	3.83	23.53	1.31	4.23	0.04	1.82	17.96	4.18	8.17	8.87	4.16	0.70	78
A18	2.84	18.23	0.69	2.54	0.02	1.57	20.10	3.78	20.43	4.84	7.30	0.75	82
A19	4.18	30.17	0.75	3.74	0.03	1.34	9.31	6.22	28.46	5.47	11.94	3.50	102
A20	0.68	13.23	1.33	1.23	0.01	0.29	6.42	2.51	5.47	1.54	3.12	3.49	36
A21	1.05	15.14	0.52	17.11	0.04	0.81	15.92	2.81	5.82	6.99	6.83	1.14	73
A22	4.70	190.37	3.45	35.93	0.07	1.30	29.36	29.31	85.84	27.22	32.45	6.63	440
Mean (pg/m ³)	2.01	35.93	0.99	14.99	0.04	1.21	14.42	6.36	9.97	9.42	8.29	1.81	103.63
SD	1.34	41.84	0.74	18.88	0.03	0.67	6.97	6.43	18.17	10.32	6.44	1.43	92.62
Median	1.51	21.75	0.81	5.12	0.04	1.20	15.18	4.13	4.46	6.47	5.93	1.41	74.64
Min	0.49	8.04	0.22	1.00	0.01	0.22	2.31	1.73	0.89	1.06	3.12	0.45	32.57
Max	4.70	190.37	3.45	66.13	0.10	2.80	29.36	29.31	85.84	44.91	32.45	6.63	440.01
Sum OPE (C, pg/m ³)													
A01	0.92	65.39	0.82	6.68	0.04	1.32	11.16	15.03	37.63	12.28	91.87	23.78	243
A02	1.26	19.33	0.37	5.92	0.05	0.85	38.59	2.25	14.83	3.68	20.83	12.17	108
A03	7.57	73.10	2.26	56.59	0.11	2.20	29.31	11.55	12.50	49.08	22.78	19.40	267
A04	4.84	160.10	2.12	57.63	0.13	1.82	33.72	19.95	37.46	35.43	15.35	10.32	369
A05	3.06	43.00	1.43	34.76	0.12	1.84	35.16	6.88	13.64	23.17	21.37	18.16	184
A06	1.87	20.06	0.51	4.51	0.07	3.31	10.55	2.10	11.29	10.65	13.93	24.93	79
A07	2.17	44.73	0.73	9.53	0.08	3.89	24.51	7.77	14.25	10.32	15.73	12.45	134
A08	2.19	44.31	0.77	10.24	0.03	1.47	13.03	7.67	15.80	4.47	9.89	11.14	110
A09	1.42	38.76	1.02	33.89	0.06	1.81	35.57	2.95	11.22	15.52	10.60	16.34	153
A10	1.69	42.10	1.29	67.21	0.05	1.25	21.91	6.98	9.80	9.77	10.09	15.43	172
A11	1.89	12.53	0.92	14.17	0.08	1.92	21.91	1.80	32.42	11.09	20.81	10.49	120
A12	1.58	25.41	1.77	18.78	0.06	1.87	27.54	3.78	10.49	9.99	20.02	8.20	121
A13	1.03	16.19	1.22	11.17	0.04	0.89	15.96	2.10	15.54	10.57	11.60	6.68	86
A14	3.98	50.65	1.03	20.34	0.05	1.38	25.83	5.36	19.03	21.77	18.60	6.14	168
A15	4.05	56.84	1.06	17.26	0.03	0.92	14.65	8.12	14.84	11.45	12.50	16.52	142
A16	4.01	37.12	1.43	43.03	0.06	1.48	17.48	5.83	18.63	13.81	6.71	14.69	150
A17	4.37	37.65	1.94	12.36	0.07	4.38	33.02	4.57	35.99	30.31	22.67	12.99	187
A18	3.16	23.41	0.75	8.26	0.03	1.82	23.62	3.93	24.25	7.16	8.88	23.08	105
A19	4.62	42.05	0.94	10.71	0.05	1.82	15.93	6.44	43.13	12.69	17.94	4.52	156
A20	1.11	20.37	1.43	1.66	0.01	0.57	9.51	4.32	18.16	3.09	6.19	23.35	66
A21	1.84	27.03	0.81	30.36	0.07	1.20	21.79	4.73	22.26	10.89	16.15	20.26	137
A22	5.58	214.94	4.54	46.48	0.14	1.91	42.61	29.83	110.49	42.79	53.57	18.43	553
Mean (pg/m ³)	2.92	50.69	1.33	23.71	0.06	1.82	23.79	7.45	24.71	16.36	20.37	14.98	173
SD	1.75	47.77	0.88	19.51	0.03	0.94	9.73	6.65	21.67	12.48	18.66	6.03	109
Median	2.18	40.41	1.04	15.72	0.06	1.81	22.76	5.59	16.98	11.27	15.94	15.06	146
Min	0.92	12.53	0.37	1.66	0.01	0.57	9.51	1.80	9.80	3.09	6.19	4.52	66
Max	7.57	214.94	4.54	67.21	0.14	4.38	42.61	29.83	110.49	49.08	91.87	24.93	553

Table S 3-9. Particle-bound fractions (ϕ) of OPEs in air samples from the South China Sea

Air sample	TCEP	TCIPP	TDCIPP	TEP	TPrP	TIBP	TNBP	TEHP	TPhP	EHDPP
A01	29.1	24.4	33.0	14.9	76.2	16.6	20.7	2.4	10.9	6.5
A02	35.8	49.8	60.4	28.5	49.1	40.1	31.2	21.6	28.8	23.9
A03	41.1	87.8	93.3	82.2	92.8	84.9	85.2	19.2	91.5	71.2
A04	70.0	71.5	66.8	75.1	55.7	62.1	54.3	4.1	64.0	28.5
A05	55.5	83.5	76.1	66.3	65.8	74.8	65.1	23.0	69.8	49.4
A06	49.5	48.0	61.8	75.8	97.0	84.4	49.1	13.9	77.6	58.6
A07	55.8	42.1	62.5	17.7	77.3	66.7	66.4	23.6	36.3	34.5
A08	55.9	91.8	77.3	19.7	67.5	81.2	51.9	16.5	35.6	38.8
A09	36.0	34.0	41.3	27.0	74.1	67.0	40.6	27.2	29.8	48.1
A10	49.1	95.6	90.8	98.4	88.8	85.7	94.5	52.2	88.7	46.4
A11	46.9	64.2	69.5	42.4	77.0	76.4	73.0	15.9	53.6	56.4
A12	50.3	78.6	83.4	47.6	69.9	62.2	64.9	23.7	57.5	68.2
A13	32.6	59.7	73.6	17.0	33.2	45.0	44.1	24.6	24.5	50.6
A14	63.2	52.1	33.6	20.9	28.7	46.8	44.5	27.7	34.4	29.5
A15	74.8	72.6	81.2	36.2	31.7	70.8	52.1	69.4	64.9	50.3
A16	76.0	85.8	95.2	92.3	82.6	84.4	81.2	60.1	73.2	62.1
A17	76.2	62.5	67.5	34.3	54.3	41.5	54.4	22.7	29.3	18.3
A18	70.3	77.9	92.6	30.7	49.1	86.7	85.1	84.3	67.6	82.1
A19	77.7	71.7	80.3	34.9	65.9	73.4	58.4	66.0	43.1	66.5
A20	36.2	65.0	93.3	73.8	60.5	50.8	67.5	30.1	49.8	50.4
A21	46.7	56.0	63.7	56.3	55.5	67.3	73.0	26.1	64.2	42.3
A22	84.1	88.6	76.1	77.3	52.8	68.2	68.9	77.7	63.6	60.6
Mean (%)	55.1	66.5	71.5	48.6	63.9	65.3	60.3	33.3	52.7	47.4
SD	16.7	19.4	18.2	27.0	19.0	18.4	18.3	23.6	21.9	18.5
Median	52.9	68.2	74.8	39.3	65.8	67.7	61.6	24.2	55.5	49.9
Min	29.1	24.4	33.0	14.9	28.7	16.6	20.7	2.4	10.9	6.5
Max	84.1	95.6	95.2	98.4	97.0	86.7	94.5	84.3	91.5	82.1

Table S 3-10. Concentrations of OPEs in the seawater from the South China Sea

OPE (pg/L)	TCEP	TCIPP	TDCIPP	TPrP	TIBP	TnBP	TBEP	TEHP	TPhP	EHDPP	Sum OPE
W01	139	167	32	0.3	21	45	220	46	62	8	740.5
W02	94	132	14	0.2	15	54	146	20	55	4	535.4
W03	288	433	56	0.8	39	117	282	25	59	6	1305.3
W04	86	124	14	0.2	16	39	241	19	51	5	595.5
W05	61	80	6	0.2	17	20	58	18	36	3	299.9
W06	74	79	10	0.2	12	22	106	5	35	4	347.1
W07	135	175	14	0.3	19	39	87	10	40	6	527.2
W08	1302	1253	130	4.1	163	457	220	5	55	9	3597.9
W09	913	1160	144	2.9	95	251	86	17	45	4	2719.8
W10	1058	1204	111	3.6	127	374	214	5	44	6	3145.1
W11	894	1199	180	2.6	89	276	117	28	55	7	2847.7
W12	675	815	117	2.1	77	185	98	11	38	5	2022.3
W13	1108	1388	182	3.9	131	322	163	14	46	6	3364.2
W14	244	326	28	0.8	21	55	10	5	25	1	717.7
W15	199	298	34	0.3	24	56	59	5	28	4	706.3
W16	63	129	9	0.2	14	66	33	5	31	3	352.9
W17	74	139	8	0.2	19	114	50	5	37	5	452.8
W18	71	82	11	0.2	18	133	50	5	35	6	410.2
W19	72	138	5	0.2	13	123	40	5	37	3	436.1
W20	74	167	9	0.4	17	63	603	5	27	2	967.5
W21	221	275	24	0.5	26	49	22	5	37	5	664.1
W22	321	432	44	1.1	46	76	435	5	36	6	1401.0
W23	327	403	34	1.0	47	82	254	5	34	5	1191.2
W24	451	363	49	1.1	48	120	123	5	32	5	1196.9
W25	492	580	58	1.4	55	147	218	5	27	3	1586.8
W26	480	594	64	1.8	58	147	304	5	31	6	1691.7
W27	547	798	85	2.2	79	166	226	5	29	3	1940.3
W28	183	250	27	0.6	20	52	58	5	14	2	611.5
W29	215	306	32	0.7	27	61	36	5	14	2	698.8
W30	76	140	11	0.2	16	88	48	5	28	4	416.3
W31	160	79	16	0.2	20	45	32	5	18	5	381.0
W32	269	369	44	0.8	30	85	58	5	23	4	887.6
W33	270	291	32	0.5	28	70	326	5	52	5	1080.0
W34	136	126	17	0.2	21	32	341	14	29	4	719.4
W35	102	185	14	0.2	14	25	67	43	29	4	482.9
W36	386	235	35	0.4	50	100	61	109	78	17	1071.0
W37	416	614	52	0.9	50	234	18	22	73	19	1499.0
Average (pg/L)	343	420	47	1.0	43	119	149	14	39	5.4	1178.7
SD	329	381	48	1.1	37	103	133	19	15	3.5	913.6
Median	221	291	32	0.5	26	82	98	5	36	5.0	740.5
Min	61	79	5	0.2	12	20	10	5	14	1.4	299.9
Max	1302	1388	182	4.1	163	457	603	109	78	19	3598
Detection frequency	100	100	100	84	100	100	100	46	100	100	
SPM (pg/L)											

W01	14	36	0.3	0.04	1.8	6.4	2.5	20	6.4	0.4	87.0
W02	6.1	14	0.4	0.04	1.4	12.4	0.7	11	4.5	0.4	50.9
W03	4.9	15	9.4	0.04	1.3	6.0	0.7	16	4.1	1.2	57.9
W04	3.6	12	0.3	0.04	0.8	3.7	0.7	16	2.9	0.7	40.0
W05	4.2	5.5	0.3	0.04	0.9	3.4	0.7	8.9	3.3	0.4	27.6
W06	4.5	16.3	0.6	0.04	1.0	3.4	0.7	8.2	2.4	1.0	38.0
W07	2.9	8.2	1.0	0.04	0.7	2.1	0.7	5.4	2.1	0.4	23.4
W08	0.5	5.5	9.1	0.04	0.4	2.2	13.2	6.6	3.2	0.4	41.2
W09	6.7	20.4	50	0.04	3.2	11.5	4.3	33	9.8	2.4	141.2
W10	1.1	5.5	77	0.04	1.1	2.3	0.7	11	2.8	0.7	102.0
W11	2.2	5.5	136	0.04	2.3	4.6	0.7	22	5.4	1.2	180.1
W12	0.5	5.5	114	0.04	0.6	0.5	1.8	6.4	1.7	0.4	131.4
W13	1.8	5.5	24	0.04	0.7	2.5	2.3	19	3.6	1.0	60.3
W14	0.9	5.5	3	0.04	0.5	1.3	5.4	6.4	0.8	0.4	24.7
W15	0.5	5.5	2	0.04	0.1	0.5	0.7	6.4	0.8	0.4	17.3
W16	1.3	5.5	0.8	0.04	0.6	1.3	3.7	6.4	2.0	0.4	22.0
W17	1.2	5.5	0.4	0.04	0.4	1.4	1.2	6.4	0.8	0.4	17.7
W18	0.5	5.5	0.5	0.04	0.2	0.5	0.7	6.4	1.9	0.4	16.7
W19	0.5	5.5	0.9	0.04	0.1	0.5	0.7	38	0.8	0.4	47.5
W20	0.6	5.5	2.3	0.04	0.4	1.4	0.7	14	1.9	0.4	27.4
W21	4.6	20.9	2.4	0.04	1.2	4.5	0.7	51	3.9	0.4	89.4
W22	4.1	12.3	1.6	0.04	1.3	4.4	0.7	24	4.6	0.4	53.7
W23	3.2	10.1	5	0.04	1.0	3.8	0.7	21	3.8	0.8	49.6
W24	3.0	5.5	11	0.04	1.1	4.2	0.7	19	3.8	0.4	49.3
W25	3.4	12.1	2.8	0.04	1.0	4.1	0.7	70	3.3	0.4	98.1
W26	1.7	5.5	1.1	0.04	0.6	3.5	0.7	6.4	2.4	0.4	22.4
W27	2.2	5.5	5.0	0.04	0.9	4.8	0.7	18	3.1	0.8	40.6
W28	1.7	5.5	2.5	0.04	0.8	4.0	0.7	6.4	3.2	0.4	25.2
W29	2.1	5.5	0.9	0.04	0.7	3.5	0.7	6.4	2.5	0.4	22.7
W30	1.2	5.5	0.2	0.04	0.4	2.4	0.7	6.4	0.8	0.4	18.0
W31	0.6	5.5	1.3	0.04	0.4	0.5	0.7	6.4	0.8	0.4	16.6
W32	0.8	5.5	0.7	0.04	0.4	0.5	0.7	6.4	0.8	0.4	16.2
W33	0.5	5.5	2.4	0.04	0.4	0.5	0.7	34	0.8	0.4	45.6
W34	1.1	5.5	0.3	0.04	0.4	1.1	0.7	28	2.4	0.4	39.4
W35	1.0	5.5	1.1	0.04	0.4	0.5	0.7	6.4	0.8	0.4	16.8
W36	2.1	300	2.4	0.04	1.2	10.0	1.1	48	5.6	1.8	371.9
W37	0.6	11	0.3	0.04	0.4	1.9	2.2	20	2.2	0.8	39.5
Average (pg/L)	2	17	13	0.0	1	3	2	17	3	0.6	58.6
SD	3	48	31	0.0	1	3	2	15	2	0.4	65.5
Median	2	6	2	0.0	1	3	1	11	3	0.4	40.0
Min	0	6	0	0.0	0	0	1	5	1	0.4	16.2
Max	14	300	136	0.0	3	12	13	70	10	2	372

Table S 3-11. Concentrations of OPEs in air of the marine environment (pg/m³)

Region	TCEP	TCIPP	TDCIPP	TEP	TPrP	TIBP	TNBP	TBEP	TEHP	TPhP	EHDPP
South China Sea (this study)	2.9±1.8 (0.92-7.6)	50±48 (12.5-215)	1.33±0.88 (0.37-4.5)	23±20 (1.7-67)	0.06±0.03 (0.01-0.14)	1.8±0.94 (0.57-4.38)	24±9.7 (9.5-43)		25±22 (9.8-110)	25±22 (3.1-49)	20±19 (6.2-92)
South China Sea(Lai et al., 2015)	46±29 (14-107)	25±6.0 (15-38)	2.6±1.2 (1.3-4.5)			2.3±1.0 (1.1-3.8)	2.7±1.2 (1.4-4.8)		5.1±4.2 (2.3-16)	8.1±4.3 (3.4-16)	
South China Sea(Zhang et al., 2022a)	93-780	53-319	3-14			n.d.-176	18-169	2-17	n.a.	32-283	n.a.
South China Sea (Yongxing Island)(Zhang et al., 2022d)	40-741	19-973	0.3-45			2-75	3-78	0.1-132	3-158	15-265	n.a.
South China Sea (Yongxing Island)(Liu et al., 2022)	39.2-8944	63.9-1405	n.d.-2.55	n.d.-3.305	n.d.-0.002	n.a.	n.d.-5.975	n.d.	n.d.-2.045	n.d.-6.32	n.d.-1.8
North Atlantic(Castro- Jimenez et al., 2016)	150 (n.d.-1230)	770 (n.d.-1310)	110 (n.d.-430)			90 (10-380)	270 (10-1710)		180 (60-490)	10 (n.d.-50)	70 (20-1730)
South Atlantic(Castro- Jimenez et al., 2016)	190 (10-540)	590 (n.d.-980)	170 (n.d.-540)			110 (30-280)	390 (120-1180)		20 (50-890)	10 (n.d.-30)	540 (n.d.-1020)
Indian Ocean(Castro- Jimenez et al., 2016)	160 (50-620)	460 (30-1250)	60 (n.d.-290)			50 (n.d.-110)	280 (70-940)		230 (n.d.-630)	10 (n.d.-10)	380 (n.d.-630)
South Pacific(Castro- Jimenez et al., 2016)	150 (30-370)	470 (50-790)	180 (n.d.- 1000)			60 (10-160)	360 (50-2170)		160 (40-350)	10 (n.d.-40)	430 (0.26-800)
North Pacific(Castro- Jimenez et al., 2016)	100 (n.d.-310)	660 (110-1460)	130 (n.d.-500)			30 (3-100)	430 (20-2500)		120 (60-380)	10 (n.d.-30)	360 (100-1210)
North Sea(Moller et al., 2011)	46.6±37.7 (6-163)	357.2±283.1 (38-1200)	9.0±17.9 (0-78)			47.4±34.1 (0-150)	33.2±34.6 (0-150)	20.1±23.5 (0-80)	6.8±8.0 (0-31)	45.1±62.0 (4-290)	
Western Mediterranean(Castro- Jimenez et al., 2014)	328.2 (69.7-853.9)	849.6 (126.4- 1797.8)	80.2 (n.d.- 115.1)			247.3 (4.2-532.1)	295.4 (56.5-498.2)		167.0 (85.1- 268.4)	22.2 (2.7-44.0)	539.8 (n.d.- 834.0)
Ionian Sea-Sicily(Castro- Jimenez et al., 2014)	366.5 (102.8-841.0)	1113.7 (301.2- 2338.8)	230.6 (n.d.- 459.6)			118.2 (60.0- 329.9)	263.0 (77.5-508.4)		189.5 (55.8- 307.4)	24.3 (n.d.-42.8)	433.2 (n.d.- 762.5)
South-East Mediterranean(Castro- Jimenez et al., 2014)	242.0 (119.5-478.9)	1003.6 (560.1- 1903.0)	116.5 (n.d.- 298.5)			375.8 (95.6- 643.6)	343.1 (226.1- 598.6)		100.3 (56.7- 176.4)	40.5 (20.4- 79.5)	294.2 (n.d.- 435.4)

Black Sea(Castro-Jimenez et al., 2014)	868.5 (308.0-2417.3)	1158.7 (538.8-2722.4)	80.4 (n.d.-96.9)		139.4 (66.5-190.7)	298.1 (202.4-369.0)		144.1 (36.3-190.7)	27.5 (2.7-40.1)	183.5 (n.d.-310.0)
North Atlantic and the Arctic Ocean(Li et al., 2017a)	71	17	0.01		4.5	5.7		0.12	0.21	
Bohai and Yellow Seas(Li et al., 2018a)	76(27-150)	131 (43-530)	5.31		78(19-210)	13.7(3.0-37)		3.4	7.0	

Table S 3-12. Concentrations of OPEs in surface seawater from previous studies (pg/L)

Region	TEP	TCEP	TCIPP	TDCIPP	TPrP	TIBP	TNBP	TBEP	TEHP	TPhP	EHDPP
This study	2016±145 5 (403-7510)	345±329 (64-1300)	436±379 (81-1400)	60±74 (5.7-320)	1±1.1 (0.1-4)	44±37 (13-160)	122±103 (24-460)	150±133 (16-600)	31±28 (6.1-160)	42±16 (16-83)	6±3.7 (1.7-20)
Pearl River Estuary(Lai et al., 2019b)	280000	88000	100000	25000		27000		9400		2400	
South China Sea (Lai et al., 2019b)	10000	1600	13000	510		1500	1500	420		360	
Yellow River Estuary(Lai et al., 2019b)	130000	260000	49000	13000		12000	12000	1000		760	
north Atlantic and Arctic(Li et al., 2017a)		695 (n.d.-2401)	1843 (279-5773)	7 (n.d.-43)		258 (39-638)	122 (n.d.-412)		6 (n.d.-69)	n.d.	
north Atlantic(Schmidt et al., 2019)		479 (n.d.-1600)	445214 (74-1300000)	n.d.		1135 (n.d.-38000)	n.d.		n.d.	1236 (n.d.-6900)	900 (n.d.-5400)
north Atlantic(McDonough et al., 2018)		81 (n.d.-390)	36 (n.d.-54)	3.5 (1.6-7.1)			10 (n.d.-63)		0.61 (n.d.-1.5)	0.6 (n.d.-1.2)	0.21 (0.06-0.33)
Canadian Arctic(McDonough et al., 2018)		1300 (n.d.-3800)	180 (n.d.-570)	140 (n.d.-400)			27 (n.d.-48)		n.d.-	4.7 (0.99-8.2)	1.7 (n.d.-4.8)

Barrow Strait(McDonough et al., 2018)		1400 (820-2000)	3100 (930-5700)	620 (n.d.-960)		430 (170-630)		23 (n.d.-47)	570 (410-790)	290 (n.d.-630)
Bohai Sea(Zhong et al., 2017)		8305±4625 (2460-23140)	10574±5692 (2930-314000)	1204±595 (390-3240)		9033±2474 (n.d.-10910)			227±165 (100-750)	
Yellow Sea(Zhong et al., 2017)		7801±2497 (2930-11380)	12600±4489 (5540-21950)	863±365 (280-1710)		n.d.			326±139 (130-680)	
Lianyungang Coastal(Hu et al., 2014)		230000	150000	190000						
Qingdao Coastal(Hu et al., 2014)	n.d.	50000	19000	34000						
Xiamen Coastal(Hu et al., 2014)	n.d.	56000	42000	58000				n.d.		
NW Pacific and Arctic(Na et al., 2020)		11691	4169	1248	n.d.	4106.6	20.4	881	795	1088
West Pacific Ocean(Xiao et al., 2021)		11000	1600	5000			6300		n.d.	740
California Coast(Alvarez et al., 2014)		7600	410000	43000				11000		1200
coastal areas of New York State(Kim and Kannan, 2018)	1350 (760-1770)		31900 (25800-36300)	15700 (8910-25400)		880 (n.d.-2630)		3270 (n.d.-7740)	n.d.	530 (n.d.-1600)
Mirs Bay and Daya Bay(Lai et al., 2019b)	33000	7900	17000	960		2700	2800	110		n.d.
Tokyo Bay (Lai et al., 2019b)	17000	51000	81000	18000		3800	3800	180		n.d.
German Bight (Bollmann et al., 2012b)	42000	23000	150000	22000		34000		50000		n.d.

Table S 3-13. Correlation analysis of OPEs in air

	TCEP	TCIPP	TDCIPP	TEP	TPrP	TIBP	TNBP	TEHP	TPhP	EHDPP
TCEP	1(0.000***)	0.576(0.005***)	0.596(0.003***)	0.496(0.019**)	0.546(0.009***)	0.255(0.252)	0.356(0.104)	0.4(0.065*)	0.83(0.000***)	0.013(0.953)
TCIPP	0.576(0.005***)	1(0.000***)	0.818(0.000***)	0.536(0.010**)	0.669(0.001***)	0.044(0.846)	0.474(0.026**)	0.781(0.000***)	0.719(0.000***)	0.414(0.055*)
TDCIPP	0.596(0.003***)	0.818(0.000***)	1(0.000***)	0.539(0.010***)	0.635(0.002***)	0.103(0.648)	0.518(0.014**)	0.75(0.000***)	0.771(0.000***)	0.283(0.202)
TEP	0.496(0.019**)	0.536(0.010**)	0.539(0.010***)	1(0.000***)	0.605(0.003***)	-0.083(0.715)	0.447(0.037**)	0.158(0.483)	0.618(0.002***)	-0.052(0.818)
TPrP	0.546(0.009***)	0.669(0.001***)	0.635(0.002***)	0.605(0.003***)	1(0.000***)	0.386(0.076*)	0.663(0.001***)	0.462(0.030**)	0.783(0.000***)	0.2(0.372)
TIBP	0.255(0.252)	0.044(0.846)	0.103(0.648)	-0.083(0.715)	0.386(0.076*)	1(0.000***)	0.217(0.331)	0.086(0.704)	0.321(0.145)	0.015(0.949)
TNBP	0.356(0.104)	0.474(0.026**)	0.518(0.014**)	0.447(0.037**)	0.663(0.001***)	0.217(0.331)	1(0.000***)	0.351(0.109)	0.578(0.005***)	0.073(0.748)
TEHP	0.4(0.065*)	0.781(0.000***)	0.75(0.000***)	0.158(0.483)	0.462(0.030**)	0.086(0.704)	0.351(0.109)	1(0.000***)	0.492(0.020**)	0.533(0.011**)
TPhP	0.83(0.000***)	0.719(0.000***)	0.771(0.000***)	0.618(0.002***)	0.783(0.000***)	0.321(0.145)	0.578(0.005***)	0.492(0.020**)	1(0.000***)	0.267(0.229)
EHDPP	0.013(0.953)	0.414(0.055*)	0.283(0.202)	-0.052(0.818)	0.2(0.372)	0.015(0.949)	0.073(0.748)	0.533(0.011**)	0.267(0.229)	1(0.000***)

Note: ***, **, *means significant 0.01, 0.05, 0.1

Table S 3-14. Correlation analysis of OPEs in seawater

	TCEP	TCIPP	TDCIPP	TPrP	TIBP	TnBP	TBEP	TEHP	TPhP	EHDPP
TCEP	1(0.000***)	0.978(0.000***)	0.864(0.000***)	0.981(0.000***)	0.988(0.000***)	0.929(0.000***)	0.118(0.487)	0.09(0.595)	0.334(0.043**)	0.291(0.080*)
TCIPP	0.978(0.000***)	1(0.000***)	0.898(0.000***)	0.97(0.000***)	0.961(0.000***)	0.906(0.000***)	0.109(0.519)	0.138(0.416)	0.362(0.028**)	0.317(0.056*)
TDCIPP	0.864(0.000***)	0.898(0.000***)	1(0.000***)	0.849(0.000***)	0.814(0.000***)	0.773(0.000***)	0.04(0.812)	0.067(0.695)	0.301(0.071*)	0.195(0.248)
TPrP	0.981(0.000***)	0.97(0.000***)	0.849(0.000***)	1(0.000***)	0.98(0.000***)	0.914(0.000***)	0.17(0.316)	-0.023(0.893)	0.237(0.157)	0.171(0.311)
TIBP	0.988(0.000***)	0.961(0.000***)	0.814(0.000***)	0.98(0.000***)	1(0.000***)	0.939(0.000***)	0.164(0.332)	0.076(0.656)	0.341(0.039**)	0.301(0.070*)
TnBP	0.929(0.000***)	0.906(0.000***)	0.773(0.000***)	0.914(0.000***)	0.939(0.000***)	1(0.000***)	0.061(0.720)	0.018(0.918)	0.389(0.017**)	0.36(0.028**)
TBEP	0.118(0.487)	0.109(0.519)	0.04(0.812)	0.17(0.316)	0.164(0.332)	0.061(0.720)	1(0.000***)	0.02(0.908)	0.085(0.618)	-0.073(0.666)
TEHP	0.09(0.595)	0.138(0.416)	0.067(0.695)	-0.023(0.893)	0.076(0.656)	0.018(0.918)	0.02(0.908)	1(0.000***)	0.623(0.000***)	0.618(0.000***)
TPhP	0.334(0.043**)	0.362(0.028**)	0.301(0.071*)	0.237(0.157)	0.341(0.039**)	0.389(0.017**)	0.085(0.618)	0.623(0.000***)	1(0.000***)	0.814(0.000***)
EHDPP	0.291(0.080*)	0.317(0.056*)	0.195(0.248)	0.171(0.311)	0.301(0.070*)	0.36(0.028**)	-0.073(0.666)	0.618(0.000***)	0.814(0.000***)	1(0.000***)

***, **, * means significant 0.01, 0.05, 0.1

Table S 3-15. Air-sea exchange fluxes of OPEs in the South China Sea. Positive value indicates water to air volatilization and negative value indicates air to water deposition

F (ng/m ² /day)	TCEP	TCIPP	TDCIPP	TPrP	TIBP	TNBP	TEHP	TPhP	EHDP P	TEP
W1	0.64	-20.25	-0.18	-0.02	2.56	-4.71	31.42	4.15	4.73	-2.39
W2	0.06	-6.02	-0.09	-0.01	0.34	-1.00	0.71	0.49	0.11	-0.77
W3	1.94	6.59	0.13	0.00	5.01	1.60	17.59	5.71	2.96	-7.21
W4	0.08	-0.66	-0.08	-0.01	1.66	-3.02	9.71	3.89	1.90	-4.14
W5	-0.14	-4.72	-0.08	0.00	2.98	-1.76	21.17	6.43	2.96	-0.88
W6	0.02	-3.62	-0.04	0.00	1.50	-1.19	3.01	4.59	2.44	-5.60
W7	0.60	-1.22	-0.02	0.00	2.44	-0.01	7.17	5.33	4.01	-7.23
W8	19.43	43.04	1.08	0.22	38.74	49.10	6.79	13.40	12.66	1.23
W9	10.92	21.63	0.96	0.12	17.37	18.38	19.02	6.09	3.14	-1.03
W10	13.61	23.61	0.72	0.17	25.58	32.08	5.41	5.99	5.52	12.40
W11	7.47	16.11	0.87	0.07	10.89	14.31	16.17	5.54	3.47	0.46
W12	5.49	7.02	0.52	0.06	9.27	8.34	5.88	2.97	2.05	-1.28
W13	7.88	26.05	0.77	0.10	14.03	15.09	6.32	4.56	2.53	2.14
W14	2.69	10.24	0.13	0.03	4.58	1.34	5.72	4.70	0.66	-0.62
W15	1.98	-11.00	-0.21	0.00	5.29	-12.12	7.50	-1.29	4.96	-5.56
W16	-0.16	-16.03	-0.39	-0.01	2.61	-9.57	6.26	-0.15	2.50	-5.84
W17	0.00	3.03	-0.02	-0.01	3.25	8.55	4.58	6.36	4.46	-1.13
W18	-0.05	1.63	0.00	-0.01	3.87	13.26	7.19	7.91	7.36	-10.51
W19	-0.06	1.45	-0.19	-0.01	2.53	8.42	3.56	5.28	2.60	-7.43
W20	-0.01	2.29	-0.13	0.01	2.90	1.77	2.82	2.51	0.93	3.31
W21	2.51	7.10	-0.03	0.01	6.11	-2.91	8.39	7.56	7.59	-9.79
W22	3.18	9.84	0.11	0.03	8.49	0.91	4.74	2.85	5.74	1.92
W23	3.59	9.80	0.05	0.03	9.80	1.70	5.53	2.66	5.85	4.23
W24	3.16	4.92	0.11	0.02	5.51	3.37	2.08	1.28	2.09	
W25	3.00	0.91	-0.02	0.02	5.31	2.05	1.57	-1.75	0.55	
W26	4.28	2.21	0.03	0.05	8.60	3.32	3.09	-1.76	3.12	
W27	4.89	12.11	0.41	0.07	12.28	8.57	4.17	2.94	2.01	
W28	0.37	-0.73	0.02	0.00	0.67	0.01	0.32	0.10	0.04	
W29	0.88	3.11	0.10	0.01	2.32	1.63	1.48	0.32	0.52	
W30	-0.01	-3.20	-0.20	-0.01	0.66	-1.41	0.90	-4.09	0.27	
W31	0.65	-0.76	0.05	0.00	2.18	1.05	2.42	1.34	2.81	
W32	2.17	7.53	0.26	0.02	4.80	4.82	4.33	3.10	3.20	
W33	2.07	5.01	0.18	0.01	4.14	3.43	3.86	7.93	4.32	
W34	0.70	-4.33	0.00	0.00	3.45	-1.63	14.32	1.37	3.59	
W35	0.15	-5.45	-0.31	-0.02	0.92	-3.08	12.03	-1.52	-0.01	
W36	3.98	6.35	0.22	0.01	7.68	7.55	94.93	13.41	14.81	
W37	2.54	9.72	0.19	0.02	4.05	10.01	6.68	6.73	5.80	

Table S 3-16. Particle dry deposition of OPEs in the South China Sea

Particle dry deposition flux (F_{dry} , pg/m ² /day)	TCEP	TCIPP	TDCIPP	TEP	TPrP	TIBP	TNBP	TEHP	TPhP	EHDPP
A-01	0.08	2.75	0.05	0.17	0.01	0.04	0.40	0.15	0.23	1.04
A-02	0.12	1.66	0.04	0.29	0.00	0.06	2.08	0.55	0.18	0.86
A-03	0.54	11.09	0.36	8.03	0.02	0.32	4.32	0.42	7.76	2.80
A-04	0.48	19.78	0.24	7.48	0.01	0.20	3.16	0.26	3.92	0.76
A-05	0.26	6.20	0.19	3.98	0.01	0.24	3.96	0.54	2.80	1.82
A-06	0.20	1.66	0.05	0.59	0.01	0.48	0.90	0.27	1.43	1.41
A-07	0.26	3.26	0.08	0.29	0.01	0.45	2.81	0.58	0.65	0.94
A-08	0.26	7.03	0.10	0.35	0.00	0.21	1.17	0.45	0.27	0.66
A-09	0.12	2.28	0.07	1.58	0.01	0.21	2.50	0.53	0.80	0.88
A-10	0.20	6.95	0.20	11.43	0.01	0.18	3.58	0.88	1.50	0.81
A-11	0.18	1.39	0.11	1.04	0.01	0.25	2.76	0.89	1.03	2.03
A-12	0.21	3.45	0.26	1.54	0.01	0.20	3.09	0.43	0.99	2.36
A-13	0.10	1.67	0.16	0.33	0.00	0.07	1.22	0.66	0.45	1.01
A-14	0.36	4.56	0.06	0.73	0.00	0.11	1.99	0.91	1.29	0.95
A-15	0.62	7.13	0.15	1.08	0.00	0.11	1.32	1.78	1.28	1.09
A-16	0.66	5.51	0.24	6.87	0.01	0.22	2.45	1.94	1.75	0.72
A-17	0.66	4.07	0.23	0.73	0.01	0.31	3.10	1.41	1.53	0.72
A-18	0.49	3.15	0.12	0.44	0.00	0.27	3.47	3.53	0.84	1.26
A-19	0.72	5.21	0.13	0.65	0.01	0.23	1.61	4.92	0.95	2.06
A-20	0.12	2.29	0.23	0.21	0.00	0.05	1.11	0.95	0.27	0.54
A-21	0.18	2.62	0.09	2.96	0.01	0.14	2.75	1.00	1.21	1.18
A-22	0.81	32.90	0.60	6.21	0.01	0.23	5.07	14.83	4.70	5.61
Mean	0.35	6.21	0.17	2.59	0.01	0.21	2.49	1.72	1.63	1.43
SD	0.23	7.23	0.13	3.26	0.00	0.12	1.21	3.14	1.78	1.11
Median	0.26	3.76	0.14	0.89	0.01	0.21	2.62	0.77	1.12	1.02
Min	0.08	1.39	0.04	0.17	0.00	0.04	0.40	0.15	0.18	0.54
Max	0.81	32.90	0.60	11.43	0.02	0.48	5.07	14.83	7.76	5.61

4 Occurrence and Spatial Distribution of Phthalate Esters in Sediments of the Bohai and Yellow Seas

This chapter has been published as:

Lijie Mi, Zhiyong Xie, Zhen Zhao, Mingyu Zhong, Wenying Mi, Ralf Ebinghaus, Jianhui Tang, 2019. Occurrence and Spatial Distribution of Phthalate Esters in Sediments of the Bohai and Yellow Seas. *Science of The Total Environment* 653, 792-800.

DOI:10.1016/j.scitotenv.2018.10.438.

The section includes the full manuscript of the published paper except for some editorial changes. Layout and numbering have been changed to this thesis document. Abstract is deleted. References and acknowledgements have been integrated into the separate chapters of this thesis document.

4.1 Introduction

Phthalate esters (PEs) are a class of synthetic chemicals and have been widely used as plasticizers in industrial products and households, such as in children's toys, food packaging, lubricants, adhesives, paints, building materials, pharmaceuticals, and personal care products (Staples et al., 1997b). Global PE production exceeds 8.0 million tons annually (Paluselli et al., 2018a). As PEs are not chemically bonded to plastic polymers, they are easily released into the environment during the processes of manufacturing and application via evaporation and leaching from domestic and industrial effluents (Fujii et al., 2003; Kastner et al., 2012; Liu et al., 2013b). Recently, PEs have been listed as priority control pollutants in the European Union (EU), by the Environmental Protection Agency (EPA) in the United States, and by the Chinese State Environmental Protection Administration. Moreover, PEs have shown developmental toxicity and estrogenic endocrine disrupting activity in biological toxicity tests (Chen et al., 2011; Staples et al., 1997a; Weir et al., 2014; Xu et al., 2013). Extensive application of PE-containing products in industry and households has led to PEs being ubiquitous in various environments (Fernandez et al., 2007; Kastner et al., 2012; Peijnenburg and Struijs, 2006; Xie et al., 2007). Aquatic transport is thought to be among the important transport routes for PEs in the marine environment (Ajdari et al., 2018; Paluselli et al., 2018a; Paluselli et al., 2018b; Xie et al., 2005). Once PEs reach the marine environment, they distribute in the water, particulates, and sediments. It has been proven that sediments are important sinks and sources for PE distribution and bioaccumulation in the marine environment (Chen et al., 2013; Huang et al., 2008; Peijnenburg and Struijs, 2006; Wang et al., 2014).

The Bohai and Yellow seas have a combined total area exceeding 450,000 km², with an average water depth of 18 m for the Bohai Sea and 50 m for the Yellow Sea (Chen, 2009). They are semi-closed shallow shelf seas, affected by the dynamic processes of tides, waves, and regional oceanic currents. Hundreds of rivers in China as well as the Korean Peninsula discharge industrial and domestic effluents into this region. This

leads to high concentrations of total suspended sediment matter. The annual sediment load from the Yellow River to the Bohai Sea is 1.08 billion tons annually. Of this, approximately 40 to 100 mt/year sediment are transported into the Yellow Sea through the Bohai Strait. Moreover, the Yellow Sea receives high suspended matter discharge from the Yangtze River (5×10^8 tons/year), Huaihe ($\sim 1 \times 10^7$ tons/year) and Korean rivers ($< 1 \times 10^7$ tons/year) as well(Qiao et al., 2017; Wang et al., 2016; Yang et al., 2003). During the last few decades, the Bohai and Yellow seas have attracted increasing concern because of their natural variations caused by global climate change and land applications in China and Korea(Liu et al., 2004). Particularly, elevated environmental pressures from manufactured chemicals have threatened the biological productivities of their marine ecosystems(Meng et al., 2017). Recently, many organic contaminants have been found in the sediment and seawater of the Bohai and Yellow seas(Hu et al., 2009; Li et al., 2018c; Zhao et al., 2013; Zhong et al., 2015), which indicated the synthetic organic chemicals can be an emerging concern for the marine ecosystem of the Chinese marginal seas.

Several studies have investigated PEs in large rivers and estuaries along the Chinese coast, while studies in the open sea are still limited(Sha et al., 2007; Sun et al., 2013; Wang et al., 2014; Zhang et al., 2017; Zhang et al., 2018b). Sha et al.(Sha et al., 2007) reported PEs in sediments of the Yellow River ranging from 30.5 to 85.2 mg/kg. Zhang et al.(Zhang et al., 2018b)recently reported 16 PEs in the sediments from Bohai and Yellow seas (1.24 to 15.8 mg/kg), which are comparable to those measured in the sediment samples of Yangtze River Estuary and its adjacent area (0.48-29.94 mg/kg)(Zhang et al., 2018b), but much higher than those reported in 2017 (0.00079-0.0348 mg/kg)(Zhang et al., 2017). Furthermore, these studies demonstrated that PE concentrations in sediment are several orders of magnitude higher than other emerging organic contaminants, e.g. polybrominated diphenyl ethers (PBDE)(Pan et al., 2010), polyfluorinated alkyl substances (PFAS)(Gao et al., 2014), and organophosphate esters

(OPEs)(Zhong et al., 2018). Obviously, more research is necessary to provide reliable data for carrying out risk assessment of PEs in the Chinese coast.

The objective of this work was to conduct a systematic survey to determine the spatial distribution and pattern of six major PEs in sediments in the Bohai and Yellow seas. The chemical and physical properties of the selected PEs are listed in Table S4-1. The impact of total organic carbons (TOCs) on the accumulation of PEs in the sediments was also investigated. Furthermore, the PE inventories in sediment were estimated for the Bohai and Yellow seas.

4.2 Materials and Methods

4.2.1 Sample Collection

Marine sediment samples were collected onboard the research vessel Dongfanghong 2 during the Chinese Natural Science Foundation Expedition of 2009. The sampling stations approximately followed west-east transects and covered the Southern Yellow Sea, Northern Yellow Sea and Bohai Sea. Briefly, 54 surface sediment samples (from the top 10 cm) were collected using a stainless-steel box corer, scooped using a pre-cleaned stainless-steel scoop, and placed into aluminum containers that had been baked at 450 °C for 8 h and solvent-rinsed prior to use. All samples were stored at -20 °C until further treatment. Sediments were freeze-dried, grinded, and then sieved using 100-mesh. The homogenized sediment was packed into a 50 - mL brown vial and stored at -20 °C for analysis.

4.2.2 Extraction, Clean-Up, and Analysis

Ten grams of sediment were mixed with 10 g of anhydrous Na₂SO₄ and then packed into a 100-mL Soxhlet extractor and spiked with 40 μL of deuterated surrogate standards of 125 pg/μL of d₄-TEP, d₄-TnBP, and d₄-DEHP extracted with DCM for 16 h at a flow rate of 5 mL/min. Ten pieces of copper beads were added into the extract to remove elemental sulfur. Extracts were evaporated to 1-2 mL using hexane as a keeper and further cleaned on a silica column (2.5 g, 10% water deactivated) topped

with 3 g of anhydrous granulated sodium sulfate. The extract was purified by eluting with 20 mL of n hexane (fraction 1) and 20 mL of DCM/acetone (1, 1V/V) (fraction 2). Fraction 2 was concentrated to 200 μ L by roti-evaporation and nitrogen blower. Ten microliters of 50 pg $^{13}\text{C}_6$ -PCB 208 (Cambridge Isotope Laboratories) were added to the sample as an injection standard.

The samples were analyzed using an Agilent 6890 N gas chromatographer (GC) coupled to an Agilent 5975 mass spectrometer (MS) (Agilent Technologies, Avondale, PA, USA), in electron impact mode (EI), equipped with an HP-5MS column (30 m \times 0.25 mm i.d. \times 0.25 μ m film thickness, J&W Scientific). The injector was operated in the pulsed-splitless mode with an inlet temperature program as follows, 60 $^\circ\text{C}$ for 0.1 min then 300 $^\circ\text{C}/\text{min}$ until 280 $^\circ\text{C}$ and then held for 10 min. The GC oven temperature program was as follows, initially 60 $^\circ\text{C}$ for 2 min, then 30 $^\circ\text{C}/\text{min}$ until 130 $^\circ\text{C}$, followed by 2 $^\circ\text{C}/\text{min}$ until 240 $^\circ\text{C}$, then 30 $^\circ\text{C}/\text{min}$ until 300 $^\circ\text{C}$ and finally held for 4 min. The temperature of the MS transfer line, MS source, and quadrupole were 280, 230, and 150 $^\circ\text{C}$, respectively.

4.2.3 Quality Assurance and Quality Control

Four method blanks were used in this work. Mean blank values of the PEs were 0.38, 0.37, 0.32, 0.066, 0.005, and 2.1 ng/g for diethyl phthalate (DEP), di-isobutyl phthalate (DiBP), di-n-butyl phthalate (DnBP), benzylbutyl phthalate (BBP), dicyclohexyl phthalate (DCHP) and di (2-ethylhexyl) phthalate (DEHP), respectively. Method detection limits (MDLs) were defined as three times the standard deviation (σ) derived from the method blanks. The MDLs were 0.83, 0.12, 0.19, 0.037, 0.005, and 1.32 ng/g for DEP, DiBP, DnBP, BBP, DCHP, and DEHP, respectively. Ten microliters of PE standard mixture (10 ng/ μ L in acetone) were spiked in three parallel sediment samples and extracted simultaneously with other sediment samples. The recoveries were 118 ± 23 , 77 ± 4 , 81 ± 3 , 103 ± 15 , 80 ± 6 and $81 \pm 23\%$ for DEP, DiBP, DnBP, BBP, DCHP, and DEHP, respectively. Extraction efficiency was further checked with twice extraction for three sediment samples, which showed that the proportion of 6 PEs in

first extraction ranged from 76 to 98%. Quantification was performed using the internal calibration method based on a seven-point calibration curve for individual PEs. The coefficients of correlation (R^2) were 0.9998, 0.9985, 0.9989, 0.9925, 0.9942, and 0.9974 for DEP, DiBP, DnBP, BBP, DCHP, and DEHP, respectively. If the PE concentrations in the samples were \leq MDLs, they were reported as not detected (nd.). Concentrations of the sediments were corrected with surrogate recoveries and subtracted with average blanks.

4.2.4 Total Organic Carbon (TOC) and Total Inorganic Carbon (TIC) Analysis

The total organic carbon (TOC) and total inorganic carbon (TIC) of the freeze-dried sediments were determined using a LECO® RC612 multiphase carbon and hydrogen/moisture analyzer as described in the literature (Chen et al., 2016). The TOC and TIC of the sediments in this study range from 0.03% to 0.90% (average, $0.37 \pm 0.23\%$) and 0.11% to 1.67% (average, $0.61 \pm 0.30\%$), respectively. There are no significant differences in the TOC and TIC among the Bohai, Northern Yellow, and Southern Yellow seas. The details of the TOC and TIC measurements are shown in the supporting information (Table S4-2).

4.2.5 Data Analysis

The data were subjected to statistical analysis using Microsoft Excel 2016 and Origin 2017G (OriginLab Corporation, Northampton, MA) software. Sediment sampling stations and oceanographic visualization of the Bohai and Yellow seas were plotted using Ocean Data View 4 software (Schlitzer). Spearman analysis for the correlation between different PE compounds was conducted by IBM SPSS 20.

4.3 Results and Discussion

4.3.1 Occurrences and Levels

The concentrations of the six PEs (DEP, DiBP, DnBP, BBP, DCHP, and DEHP) in the sediments from the Bohai and Yellow seas are summarized in Table 4-1 (see Table S4-2 for details). PEs were detected in all of the sediment samples analyzed, indicating that they are ubiquitous contaminants in the studied marine environment. The sum of the six selected PE concentrations ($\Sigma_6\text{PE}$) obviously varied, ranging from 1.37 to 24.6 ng/g dry weight (dw), with an average of 9.1 ng/g and a median of 8.1 ng/g. Among the six PEs, DEP, DiBP, DnBP, and DEHP were detected in > 90% of the sediment samples, while BBP and DCHP were detectable in 66 and 26% of the sediment samples. The highest PE concentrations in the sediment samples were those of DEHP with a median concentration of 3.77 ng/g, followed by DiBP (1.60 ng/g), DnBP (0.91 ng/g), DEP (0.32 ng/g), BBP (0.03 ng/g) and DCHP (0.01 ng/g).

Table 4-1 Concentrations of PEs (ng/g) in sediment of Bohai, northern and southern Yellow Seas.

PE (ng/g)	Bohai Sea				North Yellow Sea				Southern Yellow Sea			
	mean	median	min	max	mean	median	min	max	mean	median	min	max
DEP	0.40	0.33	0.08	1.12	0.06	0.04	n.d.	0.29	0.80	0.59	n.d.	2.50
DiBP	1.66	1.67	0.77	2.58	2.10	2.13	0.72	4.08	1.99	1.52	0.22	6.40
DnBP	1.04	1.00	0.35	2.24	2.72	1.05	0.55	6.79	1.07	0.83	n.d.	3.85
BBP	0.07	0.03	n.d.	0.43	0.07	0.06	n.d.	0.18	0.10	0.03	n.d.	1.55
DCHP	0.01	0.01	n.d.	0.03	0.01	0.01	n.d.	0.05	0.01	n.d.	n.d.	0.05
DEHP	8.63	8.34	0.04	15.9	5.83	3.53	1.93	15.6	3.43	n.d.	n.d.	10.4
$\Sigma_6\text{PE}$	11.8	11.8	1.83	18.5	10.8	8.87	4.59	24.6	7.40	7.18	1.4	16.7

4.3.2 Spatial Distributions

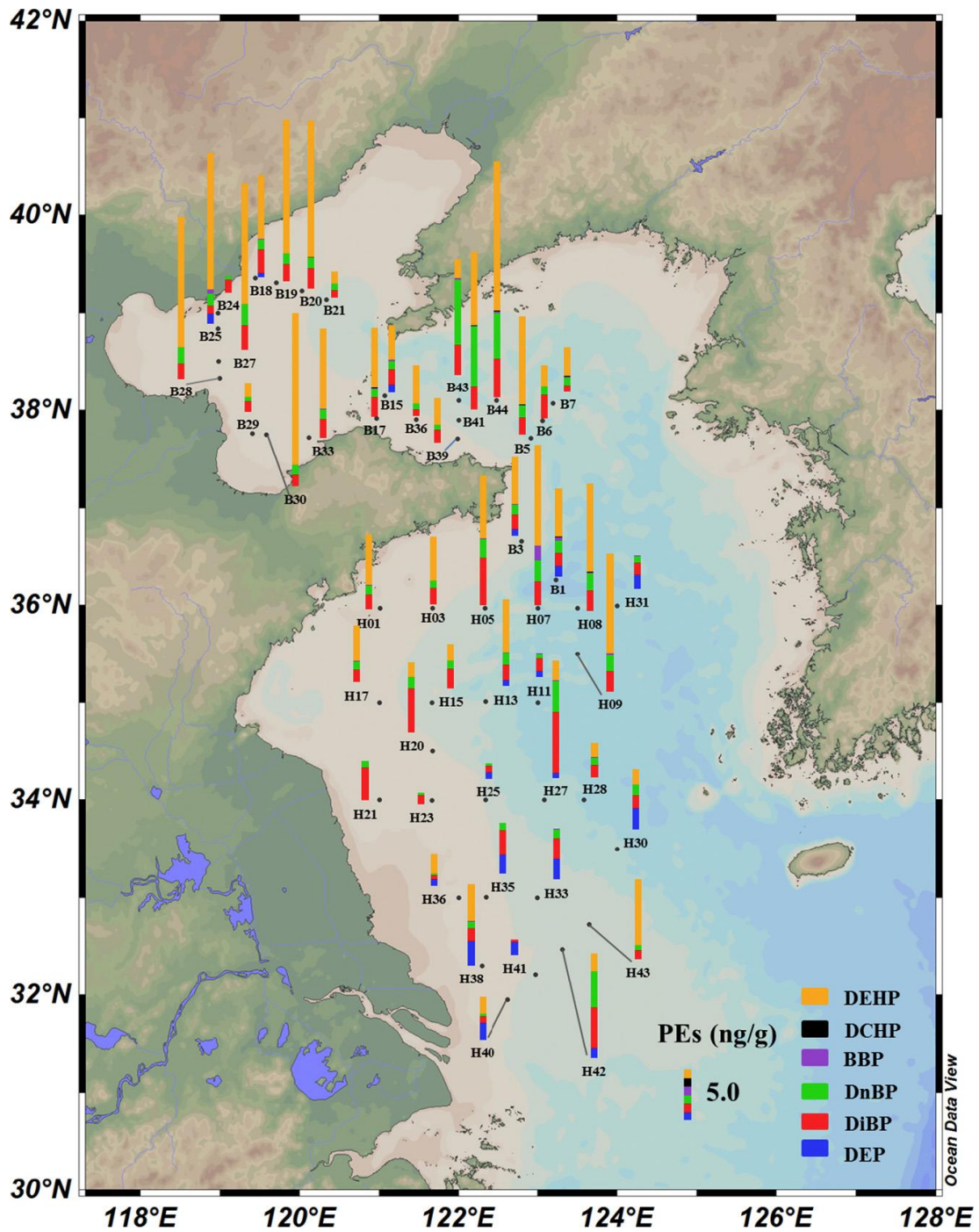


Figure 4-1 Spatial distribution of Σ_6 PEs (ng/g) in the surface sediment of the Bohai, Northern and Southern Yellow seas (BS, NYS and SYS)

The spatial distribution of Σ_6 PEs in the surface sediments of the Bohai and Yellow seas is shown in Figure 4-1. Σ_6 PEs observed in the Bohai Sea (mean, 11.8 ng/g, median, 11.8 ng/g) was slightly higher than those presented in the Northern Yellow Sea (mean, 10.8 ng/g, median, 8.9 ng/g) and Southern Yellow Sea (mean, 7.4 ng/g, median, 7.2

ng/g), suggesting PE accumulation discharged via riverine systems. Interestingly, the highest Σ_6 PEs concentration (24.6 ng/g-dw) was found at site B44, which is in the Northern Yellow Sea near the Bohai Strait. According to the study for the sedimentation rate in the Bohai and Yellow seas(Qiao et al., 2017), sediments from the Bohai coast can be transported along the Shandong Peninsula and form a mud zone in the Northern Yellow Sea. Consequently, the sediments originated from the highly contaminated Laizhou Bay may cause the high PE level at B44. The lowest Σ_6 PE concentration (1.4 ng/g-dw) was found at site H23 in the Southern Yellow Sea, which is located in a clayed sand area(Qiao et al., 2017; Shi, 2014). The hydrodynamics and currents of the east China seas are very complex and influenced by the monsoon, fluvial runoff, Kuroshio Current, tide-induced residual currents, sea contours and topography(Su, 2005). There are no obvious spatial PE trends along the west-east sampling transects, which could contribute to the complex dynamic conditions of the marginal seas.

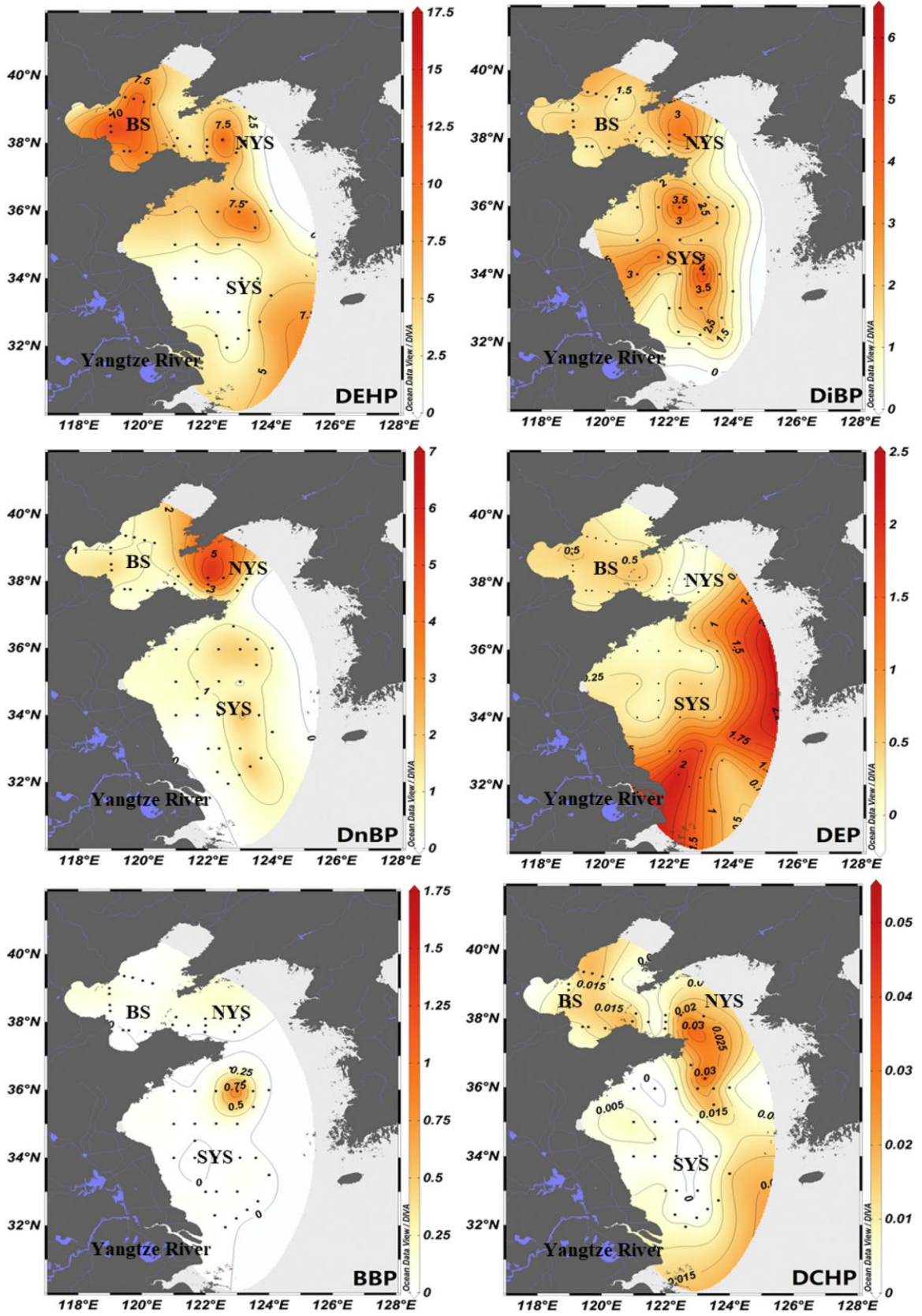


Figure 4-2 Distributions of DEP, DiBP, DnBP, BBP, DCHP and DEHP (ng/g) in sediment of the Bohai and Yellow seas

The spatial distributions of individual PEs are shown in Figure 4-2. DEHP obviously showed a decreasing trend from the Bohai Sea (median, 8.3 ng/g) to the Northern Yellow Sea (3.5 ng/g) and the Southern Yellow Sea (median, 2.0 ng/g). The DiBP and DnBP concentrations in the Northern Yellow Sea (median, 2.1, 1.0 ng/g) are slightly higher than those in the Bohai Sea (median, 1.7, 1.0 ng/g) and the Southern Yellow Sea (median, 1.52, 0.8 ng/g). However, a high level of DEP occurs in the Southern Yellow Sea (median, 0.59 ng/g) and which is approximately 2 times higher than that of the Bohai Sea (median, 0.33 ng/g) and > 10 times higher than that of the Northern Yellow Sea (median, 0.04 ng/g). The varying spatial distributions of the individual PEs were related to the PE discharge sources, regional oceanic circulation patterns, and mud areas in the Bohai and Yellow seas. Generally, organic contaminants can be transported into the marine environment from a riverine catchment as well as from atmospheric dry and wet deposition (Jurado et al., 2004; Xie et al., 2005). There are > 40 rivers flowing into the Bohai and Yellow seas, which discharge $\sim 782.2 \times 10^6$ ton/year of sediment into the Bohai Sea and 13.0×10^6 ton/year into the Yellow Sea (Qiao et al., 2017). The log octanol-water partition coefficient ($\log K_{ow}$) has been considered a key parameter for the measurement of organic pollutants in environmental fate modeling as it is correlated with water solubility and bioaccumulation (Schwarzenbach et al., 2002). DEHP, DCHP, and BBP have $\log K_{ow}$ values of 7.50, 6.20, and 4.59 (Staples et al., 1997a), respectively, suggesting they likely partition to particular matter and settle during the sedimentation process. Therefore, DEHP and DCHP may accumulate in coastal areas and transport with fine particles to remote areas, while DEP ($\log K_{ow}$, 2.38) (Staples et al., 1997b) is very soluble in water and can be transported with the water mass from the Bohai Sea to the Yellow Sea. Moreover, the northward water mass from the Yangtze estuary may also be responsible for the high PE concentrations occurring in the Southern Yellow Sea (Zhang et al., 2018b). Nevertheless, the distribution pattern of the PE components illustrates obvious fractionation of different PEs during transportation from emission sources to remote areas.

4.3.3 Comparison to Previous Studies

Table 4-2 Comparison of PEs concentrations (ng/g) in this study with those measured in global estuaries and coastal seas

Location	DEP	DiBP	DnBP	BBP	DCHP	DEHP	Reference
Bohai Sea	N.D.-1.12	0.77-2.54	1.00-2.24	N.D.-0.43	N.D.-0.02	N.D.-15.92	This work
Yellow Sea	N.D.-2.50	0.22-6.40	N.D.-6.79	N.D.-1.55	N.D.-0.55	N.D.-15.60	This work
Bohai Sea	10-90	200-6430	300-8850	N.D.-150	N.D.-10	330-3680	(Zhang et al., 2018c)
Yellow Sea	20-220	290-2540	630-8040	40-90	N.D.	420-1230	
East China Sea	49.4-355.0		55.6-4349.5				(Yang et al., 2016)
Laizhou Bay			2.00-43.89			4.37-4389.24	(Xiao et al., 2010)
Yellow River	1.60-7.70		18120-34080			9290-50690	(Sha et al., 2007)
HaiHe River			120-590			310-2730	(Chi, 2009)
Changjiang River Estuary	N.D.-1130	N.D.-7980	N.D.-7080			N.D.-8550	(Zhang et al., 2018b)
Changjiang River Estuary	N.D.-0.18	0.02-8.04	0.01-22.0			N.D.—4.55	(Zhang et al., 2017)
Changjiang River, Chongqing	15.4-34.2		557.4-1021.9	N.D.		729.2-1545.8	(Du et al., 2013)
Qiantang River	18	170	113	1.8	1.4	1555	(Sun et al., 2013)
Chaohu Lake	15	601	790	33	0.3	299	(Kang et al., 2016)
Quanzhou Bay	0.87	113.46	49.5			299.83	(Zhuang et al., 2011)
Kaohsiung Harbor, Taiwan	9.3-33.7	21.9-69.5	37.3-259	N.D.		574-21559	(Chen et al., 2017)
Pearl River Delta, Guangzhou	28-1050	970-71200	82-1260	N.D.-280	N.D.-220	210-14160	(Zeng et al., 2008)
Jiulong River, Southeast China	N.D.-5.8	10.2-116.8	1.6-92.8			4.3-394.7	(Li et al., 2017b)
Maowei Sea Littoral, Guangxi		0.013	0.0073	0.012		0.064	(Liao, 2015)
Kaveri River, India	16.5		35.5	2.6		278	(Selvaraj et al., 2015)
Freshwater Systems of Venda	160-320		190-6500			20-1120	(Fatoki et al., 2010)
Ogun river catchments, Nigeria	80-350		190-1420			20-820	(Adeniyi et al., 2011)
Anzali wetlands, Caspian Sea (Iran)			120-19020			250-43120	(Hassanzadeh et al., 2014)

Analysis of PEs in marine sediments is rare, though there are some data to describe the pollution status of PEs in the sediments of rivers and estuaries as shown in Table 4-2. In these previous studies, DnBP and DEHP were the most predominant compounds. DnBP and DEHP concentrations in sediments of the Bohai and Yellow seas were usually 1-3 orders of magnitude lower than those detected in riverine, estuarine and coastal sediments (Adeniyi et al., 2011; Du et al., 2013; Fatoki et al., 2010; Hassanzadeh et al., 2014; Li et al., 2017b; Sha et al., 2007; Stewart et al., 2014; Stoppa et al., 2017; Yang et al., 2016; Zhang et al., 2018b). Zhang et al. reported DEP, DiBP, DnBP, and DEHP in the Yangtze River estuary, which showed a comparable level in 2017 and a relatively high level in 2018 in comparison to values in this study (Zhang et al., 2017; Zhang et al., 2018b). BBP concentrations in sediment of the Bohai and Yellow seas

were comparable to those in the Maowei Sea and lower than those in the coastal zone of Qingdao, Changjiang River, and Kaohsiung Harbor(Chen et al., 2013; Liao, 2015; Zhang et al., 2018b). DCHP concentrations measured in the Chaohu Lake and Qiantang River are comparable to those in this work(Kang et al., 2016; Sun et al., 2013), while the DCHP reported in the Pearl River Delta and coastal zone of New Zealand are 2-3 orders of magnitude higher than that in this study(Stewart et al., 2014; Zeng et al., 2008). The PE concentrations in sediments of the Bohai and Yellow seas are 1-2 orders of magnitude lower than those measured in Laizhou and Quanzhou bays and the Haihe and Yellow rivers, suggested riverine catchment is a significant pathway for the transport of DnBP and DEHPs into the Bohai and Yellow seas(Chi, 2009; Sha et al., 2007; Xiao et al., 2010; Zhuang et al., 2011).

4.3.4 Correlation between PEs and Total Organic Carbon

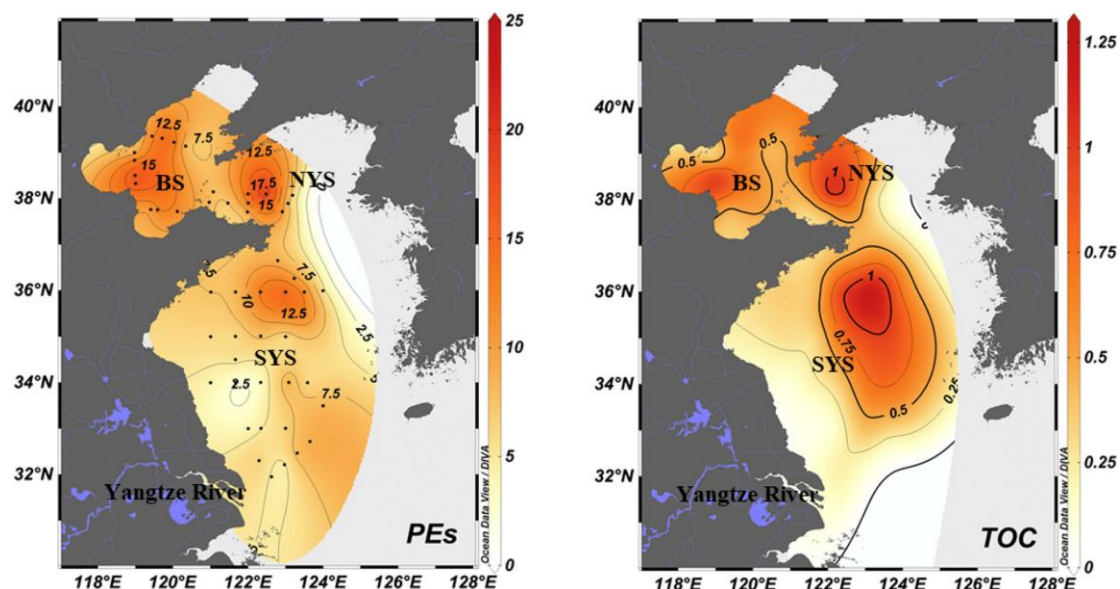


Figure 4-3 Distribution of PEs comparable to that of TOC in sediment of Bohai and Yellow seas

The mean value of TOC in the Bohai, North Yellow, and South Yellow seas was 0.33%, 0.41%, and 0.37%, respectively. The TOC contents were obviously higher in the clay regions, which is consistent with the PE horizontal distribution (Figure4-3). Significant positive correlations exist between concentrations of Σ_6 PEs and TOC ($r = 0.62$, $p < 0.001$) in the Bohai and Yellow seas (Figure S4-1). The TIC ranged from 0.11% to 1.67%

with a mean of $0.61 \pm 0.30\%$. The linear regression analysis showed no significant correlations between the PE concentrations and TIC contents ($p > 0.05$).

The correlations between TOC and individual PEs are shown in Table S4-3 and Figure S4-2. Significant positive correlations were observed between TOC and the concentrations of DiBP ($r = 0.44$, $p = 0.001$), DnBP ($r = 0.60$, $p < 0.001$), BBP ($r = 0.52$, $p < 0.001$), and DEHP ($r = 0.37$, $p = 0.01$), suggesting that TOC can be a factor affect the spatial distribution of major PEs. However, DCHP showed no significant correlation with TOC, which could be caused by its low concentration levels in the sediments. Relatively weak correlation was presented between DEP concentrations and TOC. This may be attributed to the high solubility and low K_{ow} value of DEP, which allows DEP can travel long distances with the oceanic current.

4.3.5 Source Identification of PEs

The PE concentrations in the Bohai and Yellow seas are generally 1-3 orders of magnitude lower than those determined in adjacent rivers and coastal areas, highlighting riverine catchments as an important source for the input of PEs in the Bohai and Yellow seas. Among the PE components, DiBP, DnBP, BBP, DCEP, and DEHP showed a significant coefficient among each other (Table S4-4), suggesting similar discharge sources and transport behavior. However, there was no significant correlation observed between DEP and the other five PEs in this study. According to information collected from the Anon(Anon, 2014), the industries producing DEP are mainly situated in Hubei, Jiangsu, and Shanghai along the Yangtze River. PE emissions via the Yangtze River estuary can be transported to the East China Sea and then move northward to the Southern Yellow Sea via the Taiwan Warm Current(Liu et al., 2004; Qiao et al., 2017).

Moreover, atmospheric transport and deposition is also an important source for organic contaminants in a marine environment(Xie et al., 2005). Recently, PEs have been found in PM_{2.5} and PM₁₀ in the ambient air of Tianjin, Beijing, and Shanghai(Chen et al.,

2018; Ma et al., 2014; Zhu et al., 2016). DnBP and DEHP are major components in atmospheric particles as well. The trade winds from the continent may steadily transport atmospheric particles to the Bohai and Yellow seas. Atmospheric deposition of particulate matter including organic carbon and black carbon into the Bohai and Yellow seas has been recently investigated (Fang et al., 2018). The area-integrated atmospheric particulate organic carbon (POC) and particulate black carbon (PBC) depositional fluxes to the Bohai Sea were 355 ± 8 and 68 ± 22 Gg/year, respectively, which accounts for nearly 50% of the input from riverine systems during 2013 (POC, 781.9, PBC, 150.4 Gg/year). Therefore, particle-bound PEs can be a significant input source for PEs in the sediments of the Bohai and Yellow seas.

Apart from long-range transport through riverine systems and the atmosphere, marine traffic, fishing boats, and mariculture can be direct sources of PEs in marine sediments (Akhbarizadeh et al., 2017; Fries et al., 2013). PEs containing solid waste generated from ship and fishing boats might be directly disposed into the sea. Microplastics have become a severe pollution issue in the Bohai and Yellow seas and which carry many chemical contaminants to the environment (Mai et al., 2018; Zhao et al., 2018). PEs, e.g., DEHP and DnBP, have been identified as major contaminants in microplastic samples collected along the coastal beach of the Bohai Sea (Zhang et al., 2018a). Once microplastics sink to the ocean floor, they can directly release organic contaminants, e.g., PEs, into the surrounding sediments (Bakir et al., 2016). Moreover, marine dumping sites for solid waste may form specific local sources for organic contaminants, e.g., PEs in the sea can spread on the ocean floor following oceanic currents. Although Chinese governments and authorities have also strengthened the protection of the marine environment, the overall situation of China's coastal water pollution remains a great challenge.

4.3.6 Inventory of PEs in the Marine Sediments

The inventories of PEs in the sediments for the Bohai and Yellow seas were calculated using the following equation (4-1) (Zhao et al., 2011):

$$\text{Inventory} = C \cdot \rho \cdot A \cdot D \cdot a \quad (4-1)$$

where C (ng/g) is the mean concentration of PEs in the sediment in this work and ρ (g/cm³) is the dry density of the sediment. A (cm²) represents the area of the sea, D (cm/y) is the sedimentation rate, and a (y) is the number of years considered in the inventory. In this work, the sedimentation rate and the dry bulk density of the Bohai and Yellow seas was estimated as 0.5 cm/y and 0.95 g/cm³, respectively (Qiao et al., 2017). Based on their total areas of 78,000 km² and 380,000 km², and five-year accumulation, it was estimated that the inventories of the Σ_6 PEs are 20.73 and 65.87 tons for the Bohai and Yellow seas, respectively. The uncertainties in the calculation of the inventories were propagated from analytical errors of C and the uncertainty in ρ , and D values. An analytical error was estimated to be 20% for C. The assumption of ρ of 0.95 g/cm³ and D value of 0.5 cm/y may contain an error of 20% and 50% for the mud areas of the Bohai and Yellow seas(Qiao et al., 2017). Therefore, a propagated uncertainty was ~57% for the estimated inventories.

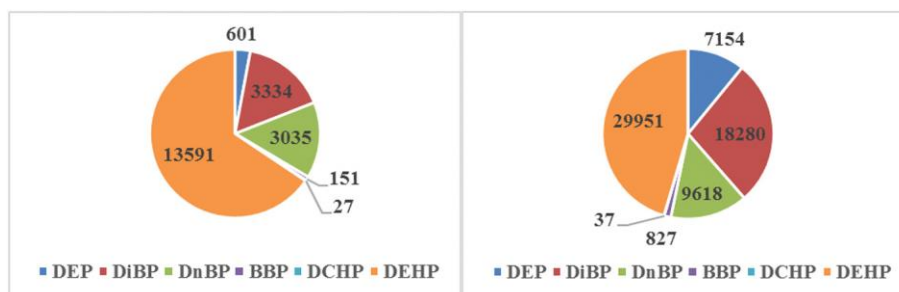


Figure 4-4 Inventory of PEs (ton) in sediment of Bohai (left) and Yellow (right) seas

The inventories of the individual PEs in the Bohai and Yellow seas are shown in Figure 4-4. The total inventory of DEHP was 43.54 tons, following by 21.61 tons of DiBP, 12.65 tons of DnBP and 7.76 tons of DEP. BBP and DCHP accumulation was < 1 ton in the Bohai and Yellow seas. The inventories of other organic contaminants have been estimated in the Bohai and/or Yellow Seas. A total of 11-19 t of BDE-209 and 1.3-1.9 t of seven PBDEs(Pan et al., 2010) were inventoried in the Bohai Sea, and 0.4-26 t of eight organophosphate esters (OPEs) in the Bohai and Yellow seas(Zhong et al., 2018).

Consequently, the inventories of the total PEs are comparable to those for BDE-209, and 10 times higher than those for PBDEs and OPEs.

4.4 Conclusion

This study focused on the concentrations, distributions, and source identifications of PEs in sediments of the Bohai and Yellow seas. High concentrations of PEs were detected with DEHP being the predominant compound in both the Bohai and Yellow seas. A positive correlation between TOC and PEs in the whole region implied a common source of TOC and organic pollutants. Riverine input and transport and deposition with suspended particles in mud areas might be the main factors that influence the distribution patterns of the PEs in the marine sediments while atmospheric deposition could be another notable input source of particle-bound PEs. Given that DEHP, DiBP, and DnBP are more persistent and bio-accumulative, more studies to investigate their level in marine organisms and the transformational products in biota are needed. As it is a great challenge to determine trace concentrations of PEs in marine sediments, more measurements are required to provide appropriate data for assessment of the environmental risk of PEs in marine environments.

Supporting Information

Table S 4-1 Physicochemical properties of PEs

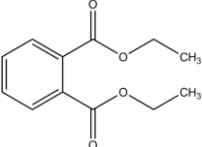
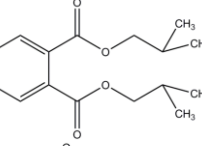
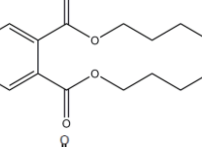
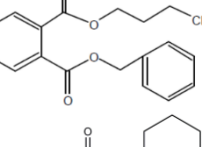
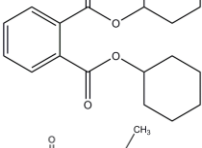
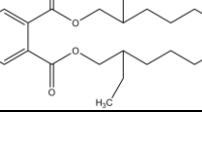
PEs	Structural	CAS	Solubility (mg/l)	V _P (Pa)	H ₀ (Pa m ³ mol ⁻¹)	Log K _{OW}	Log K _{OA}
DEP		84-66-2	591	0.0648	0.0244	2.38	7.55
DiBP		84-69-5	20	0.01	0.0185	4.46	8.5
DnBP		84-74-2	9.9	4.73 × 10 ⁻³	0.133	4.45	8.54
BBP		85-68-7	3.8	2.49 × 10 ⁻³	0.205	4.59	8.78
DCHP		84-61-7	0.2	2.95 × 10 ⁻⁴	4.924	6.20	11.59
DEHP		117-81-7	0.0025	2.52 × 10 ⁻⁵	3.95	7.50	10.53

Table S 4-2 PE concentration, TOC and TIC in the sediment of the Bohai, Northern Yellow and Southern Yellow seas

PE (ng/g)	DEP	DiBP	DnBP	BBP	DCHP	DEHP	ΣPE	TOC (%)	TIC (%)
Bohai Sea									
B15	0.88	1.59	0.87	0.14	0.01	3.51	7.0	0.21	0.53
B17	0.21	2.07	0.89	0.13	0.03	6.16	9.5	0.31	0.74
B18	0.47	2.54	1.00	0.06	0.02	6.62	10.7	0.48	0.42
B19	0.36	1.83	1.13	0.02	0.02	13.96	17.3	0.55	0.69
B20	0.31	2.10	1.12	0.05	0.02	14.28	17.9	0.40	0.47
B21	0.23	0.77	0.66	0.01	nd	1.29	3.0	0.15	0.33
B24	0.08	1.35	0.36	nd	nd	0.04	1.8	0.11	0.11
B25	1.12	0.84	1.25	0.43	0.01	14.18	17.8	0.22	0.37
B27	0.16	2.58	2.24	0.03	0.01	12.59	17.6	0.58	1.25
B28	0.35	1.67	1.60	0.01	0.02	13.68	17.3	0.53	1.51
B29	0.33	1.16	0.35	nd	nd	1.59	3.4	0.09	0.93
B30	0.33	1.20	0.99	nd	0.02	15.92	18.5	0.32	1.13
B33	0.37	1.93	1.07	0.03	0.01	8.34	11.8	0.31	0.85
Mean	0.40	1.66	1.04	0.07	0.01	8.63	11.82	0.33	0.72
Median	0.33	1.67	1.00	0.03	0.01	8.34	11.76	0.31	0.69
Min	0.08	0.77	0.35	nd	nd	0.04	1.83	0.09	0.11
Max	1.12	2.58	2.24	0.43	0.03	15.92	18.46	0.58	1.51
Northern Yellow Sea									
B5	0.02	1.77	1.24	0.06	0.05	9.27	12.4	0.40	0.62
B6	0.01	2.51	0.86	0.01	0.01	2.22	5.6	0.21	0.47
B7	0.06	0.75	0.78	0.12	0.02	3.00	4.7	0.15	0.34
B36	0.29	0.72	0.57	nd	nd	4.06	5.6	0.18	0.58
B39	nd	1.36	0.55	nd	nd	2.73	4.6	0.15	0.69
B41	0.06	2.49	6.18	0.05	0.01	7.81	16.6	0.44	0.42
B43	0.08	3.15	6.79	0.15	nd	1.93	12.1	0.90	0.46
B44	nd	4.08	4.80	0.18	0.03	15.60	24.6	0.87	0.50
Mean	0.06	2.10	2.72	0.07	0.01	5.83	10.79	0.41	0.51
Median	0.04	2.13	1.05	0.06	0.01	3.53	8.87	0.30	0.49
Min	nd	0.72	0.55	nd	nd	1.93	4.59	0.15	0.34
Max	0.29	4.08	6.79	0.18	0.05	15.60	24.60	0.90	0.69
Sothern Yellow Sea									
B1	1.07	1.34	1.28	0.37	0.05	5.10	9.2	0.81	0.46
B3	0.67	1.60	1.07	0.02	0.01	4.87	8.2	0.29	0.68
H01	0.05	1.52	1.03	0.05	nd	5.29	7.9	0.26	0.39
H03	0.11	1.74	0.83	nd	nd	4.51	7.2	0.17	0.30
H05	0.12	4.97	1.96	0.08	nd	6.59	13.7	0.68	0.54
H07	nd	2.59	2.13	1.55	0.02	10.43	16.7	0.81	0.40
H08	0.08	2.17	1.83	0.11	0.01	9.18	13.4	0.81	0.40
H09	0.09	2.06	1.74	0.11	0.03	10.44	14.5	0.75	0.38
H11	0.62	1.39	0.38	0.03	nd	0.60	3.0	0.50	0.55
H13	0.59	1.60	1.26	0.08	nd	5.45	9.0	0.50	0.47

H15	0.10	2.01	0.90	nd	nd	1.71	4.7	0.14	0.20
H17	0.41	1.33	0.80	0.07	0.01	3.72	6.3	0.25	0.60
H20	0.10	4.63	1.20	nd	0.01	1.50	7.4	0.16	0.84
H21	0.22	3.44	0.73	nd	nd	0.06	4.5	0.39	1.67
H23	0.18	0.94	0.25	nd	nd	nd	1.4	0.17	0.92
H25	0.74	0.62	0.29	nd	nd	nd	1.7	0.16	0.77
H27	0.56	6.40	3.20	0.07	nd	1.97	12.2	0.42	0.60
H28	0.23	1.26	0.77	0.03	nd	1.47	3.8	0.47	0.55
H29	1.82	0.77	0.57	0.04	0.03	7.99	11.2	0.48	0.54
H30	2.23	1.32	1.09	0.03	nd	1.71	6.4	0.48	0.61
H31	1.58	1.26	0.68	0.05	nd	0.35	3.9	0.35	0.61
H33	2.12	2.20	0.93	0.07	nd	0.18	5.5	0.28	0.70
H35	1.94	2.64	0.76	nd	nd	0.07	5.4	0.30	0.91
H36	0.72	0.39	0.17	nd	0.01	2.06	3.3	0.03	0.60
H38	2.50	1.40	0.67	0.08	nd	3.82	8.5	0.22	0.78
H40	1.83	0.61	0.25	0.01	0.01	1.78	4.5	0.16	0.59
H41	1.35	0.22	nd	nd	nd	nd	1.6	0.05	0.33
H42	1.01	4.28	3.85	0.01	nd	1.83	11.0	0.11	0.38
H43	0.10	0.93	0.50	0.02	0.01	6.91	8.5	0.68	0.46
Mean	0.80	1.99	1.07	0.10	0.01	3.43	7.40	0.37	0.59
Median	0.59	1.52	0.83	0.03	nd	1.97	7.18	0.30	0.55
Min	nd	0.22	nd	nd	nd	nd	1.4	0.03	0.20
Max	2.50	6.40	3.85	1.55	0.05	10.44	16.73	0.81	1.67

Table S 4-3 Correlation between TOC and PE compounds

Correlation between TOC (%) and log (compounds' concentrations (ng/g))							
	DEP	DiBP	DnBP	BBP	DCHP	DEHP	Σ ₆ PE
<i>r</i>	-0.29	0.44	0.60	0.52	0.30	0.37	0.62
<i>r</i> ²	0.09	0.19	0.35	0.27	0.09	0.13	0.38
<i>p</i>	0.04	0.001	<0.001	<0.001	0.06	0.01	<0.001

Table S 4-4 Correlations between different PE compounds

	DEP	DiBP	DnBP	BBP	DCHP	DEHP
DEP	1.000	-0.322*	-0.275	-0.052	-0.189	-0.275
DiBP	-0.322*	1.000	0.724**	0.278	0.077	0.221
DnBP	-0.275	0.724**	1.000	0.586**	0.339*	0.591**
BBP	-0.052	0.278	0.586**	1.000	0.419**	0.479**
DCHP	-0.189	0.077	0.339*	0.419**	1.000	0.726**
DEHP	-0.275	0.221	0.591**	0.479**	0.726**	1.000

*. Correlation is significant at the 0.05 level (2-tailed)

** . Correlation is significant at the 0.01 level (2-tailed)

Figure S 4-1 Correlations between Σ PES and TOC in research areas

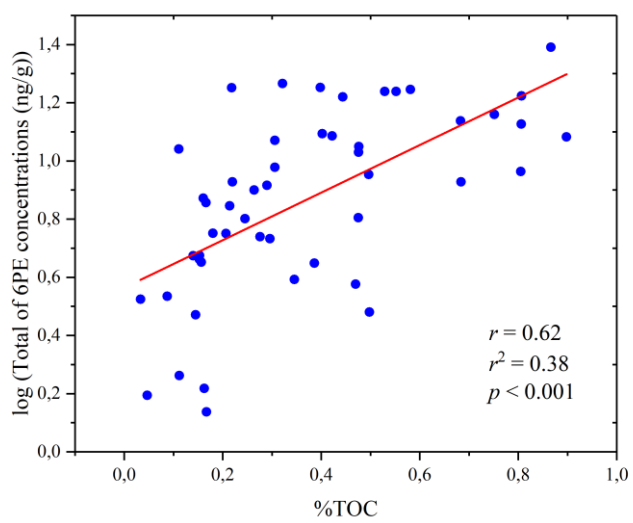
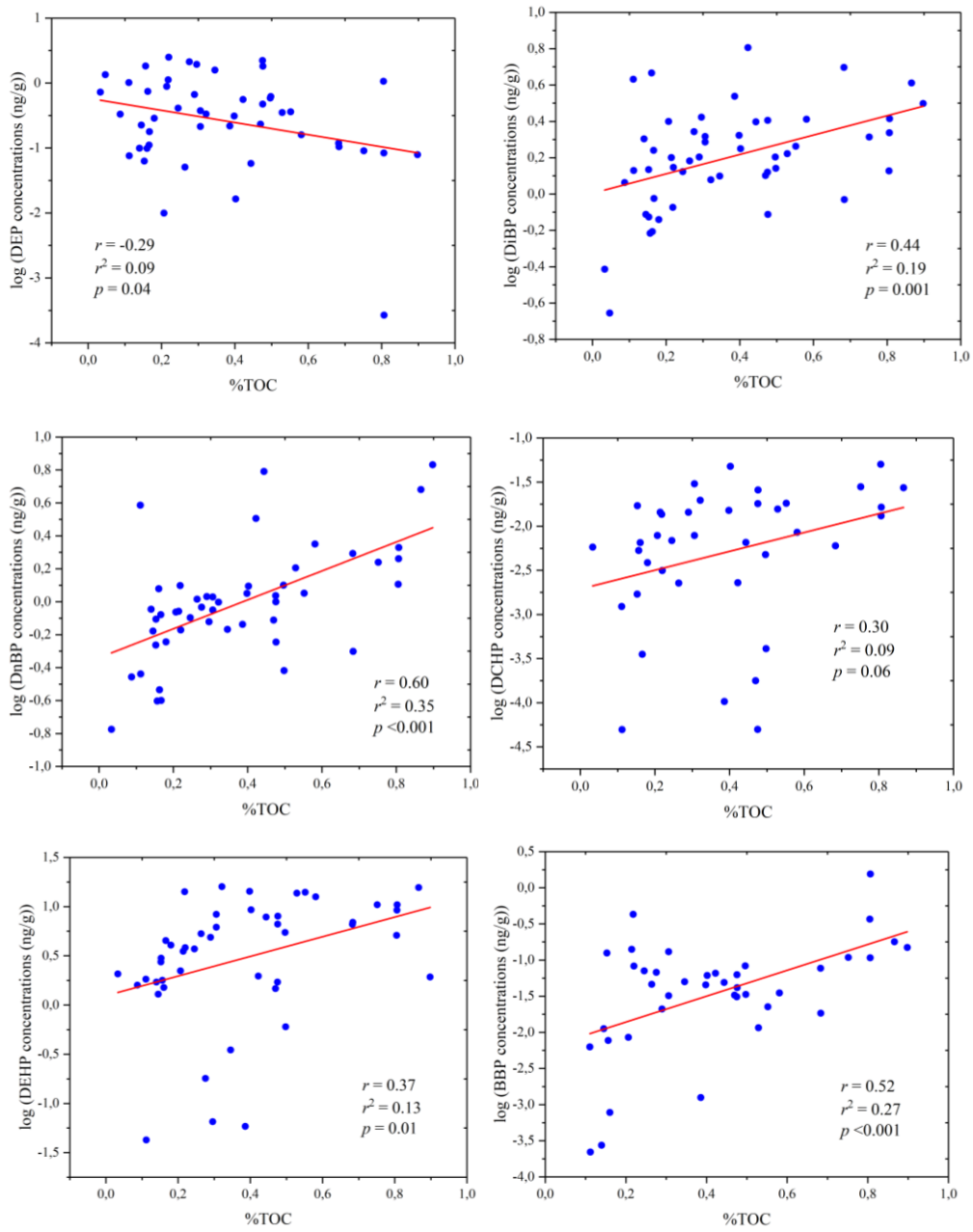


Figure S 4-2 Correlation between individual PEs and TOC in research areas



5 Air – Sea Exchange of Phthalate Esters in the Bohai and Yellow Seas

This chapter has been prepared to be published as:

Lijie Mi, Jianhui Tang, Wenying Mi, Thomas Pohlmann, Zhiyong Xie, 2024. Air – Sea exchange of phthalate esters in the Bohai and Yellow Seas

The section includes the full manuscript except for some editorial changes. Layout and numbering have been changed to this thesis document. Abstract is deleted. References and acknowledgements have been integrated into the separate chapters of this thesis document.

5.1 Introduction

Phthalate esters (PAEs), commonly referred to as phthalates, are a group of synthetic chemicals widely used as plasticizers in the manufacturing of flexible polyvinyl chloride (PVC) plastics. Due to their extensive use in a variety of consumer products such as packaging, toys, cosmetics, and medical devices, PAEs are prevalent in the environment, including marine air, seawater, and sediment.(Staples et al., 1997b; Xie et al., 2007) PAEs are known for their potential endocrine-disrupting effects, which can interfere with the hormonal systems of marine organisms(Norman et al., 2007; Sohn et al., 2016). They can affect reproductive and developmental processes in various aquatic species.(Seyoum and Pradhan, 2019) Some PAEs have been identified as endocrine disruptors, capable of interfering with hormone systems at relatively low concentrations.(Grindler et al., 2018) The extent of these effects often depends on the specific phthalate compound and its concentration.(Staples et al., 2011) Bioaccumulation of PAEs in the marine food web has become a concern, although the degree of bioaccumulation varies among different species and phthalate types.(Liu et al., 2024; Mondal et al., 2022)

In the marine environment, PAEs can undergo biotic and abiotic degradation processes. However, some PAEs are rather persistent, especially in anoxic conditions like those found in sediments.(Cao et al., 2022b) The rate of degradation varies based on environmental factors such as temperature, microbial activity, and sunlight exposure.(Chang et al., 2007; Feng et al., 2022) Given their potential ecological and health risks, monitoring and regulating the concentrations of PAEs in the marine environment is crucial. Various international and national regulations aim to reduce the release of PAEs into the environment.(Bai et al., 2024; EPA, 2019) However their widespread use and persistence pose ongoing challenges. Continuous monitoring is essential to assess the effectiveness of these regulatory efforts and to understand the distribution, fate and impact of the PAEs in the marine environment.(Mi et al., 2023)

PAEs are introduced through various routes, including direct discharge of industrial and domestic wastewater, runoff from land, atmospheric deposition, and marine traffic.(Hidalgo-Serrano et al., 2022; Ren et al., 2021; Wang et al., 2021) These compounds are hydrophobic and lipophilic, meaning they tend to associate with particulate matter and accumulate in sediments. The concentration of PAEs in marine environments varies widely depending on proximity to pollution sources, ocean

currents, and biogeochemical processes. They have been detected in various components of the marine ecosystem, including water, air, sediments, and biota.(Heo et al., 2020; Mi et al., 2023; Zhang et al., 2023)

PAEs are released into the marine atmosphere primarily through volatilization from plastic products and industrial emissions.(Chen et al., 2018; Wang et al., 2022a) Once in the air, they can be transported over long distances by winds. Their concentration in marine air is relatively low compared to water and sediment but can vary significantly based on factors like proximity to urban and industrial areas, weather conditions, and atmospheric deposition.(Cao et al., 2022d; Rafa et al., 2024; Zhang et al., 2020c) The presence of PAEs in marine air is a concern due to their potential for long-range transport, enabling them to impact regions far from their source of emission.(Xie et al., 2005; Xie et al., 2007) The introduction of PAEs into seawater mainly occurs through river runoff, direct industrial and municipal discharges, and atmospheric deposition. In seawater, PAEs are typically present in low concentrations, often in the range of nanograms to micrograms per liter.(Mi et al., 2023; Paluselli and Kim, 2020; Xie et al., 2007; Zhang et al., 2020d) However, these concentrations can be higher in areas close to urban or industrial discharges.(Gugliandolo et al., 2020a; Malem et al., 2019; Paluselli et al., 2018a) PAEs in seawater are subject to various environmental processes such as dilution, degradation, and adsorption onto particulates, influencing their distribution and concentration.

The Bohai and Yellow Seas, located off the eastern coast of China, facing significant environmental challenges due to industrialization, climate warming and chemical pollution.(Wang et al., 2023) The Bohai and Yellow Seas are surrounded by one of the most industrialized regions in China. A variety of industries, including petrochemical, metallurgical, textile, and electronic manufacturing, discharge effluents directly into the sea or nearby rivers, leading to the accumulation of hazardous chemicals like heavy metals, polycyclic aromatic hydrocarbons (PAHs), and persistent organic pollutants (POPs).(Wang et al., 2022b; Yoon et al., 2020) Besides, the extensive agricultural activities in the surrounding areas contribute to the pollution through runoff. Pesticides, herbicides, and fertilizers used in farming make their way into the seas, increasing the levels harmful chemicals that can lead to eutrophication and harmful algal blooms(Li et al., 2018b; Li et al., 2023b; Zheng and Zhai, 2021). Moreover, rapid urbanization has led to increased domestic sewage and urban runoff, which often carries a cocktail of

chemical pollutants, including pharmaceuticals, personal care products, and endocrine-disrupting chemicals such as PAEs. (Yang et al., 2020a; Zhang et al., 2021e) In addition, the Bohai and Yellow Seas are along with busy shipping lanes and harbors, and are used for wind parks and oil platforms. Maritime-related pollutants can be directly discharged into the seas (Shen et al., 2024). Additionally, discarded fishing gear and marine debris add to the plastic pollution in these waters, which act as significant vector for the PAEs in the marine environment. (Xu et al., 2021)

Global efforts to monitor and regulate the use and discharge of PAEs in the marine environment are ongoing. These efforts aim to understand the distribution, fate, and ecological impacts of these compounds to mitigate their potential risks to marine ecosystems and human health. Despite regulatory measures, the persistence and ubiquity of PAEs in the marine environment remain a challenge for environmental scientists and policymakers. This study focuses on investigating the concentrations, composition, and spatial distribution of PAEs in the air and seawater of the Bohai and Yellow Seas. It aims to assess the exchange fluxes crossing the interface of air and seawater for the PAEs. The research contributes new data, deepening our understanding of the transport behavior of PAEs in the marginal seas.

5.2 Materials and Methods

5.2.1 Research Area and Sample Collection

Sampling onboard the Chinese research vessel *Beidou* was carried out from April 6 to May 8, 2019, following a route from Qingdao-Shanghai-Qingdao. The expedition involved collecting 12 active air samples and 25 large-volume seawater samples along the cruise track in the Bohai and Yellow Seas (refer to Figure S5-1 and S5-2 for details). In brief, a substantial air volume ranging from 300 to 500 m³ was drawn in using an active pump at a rate of about 15 m³/h. Atmospheric particles were trapped using a quartz fiber filter (QFF, 150 mm diameter, 1.0 μm pore size), while the gaseous phase was collected through a PUF/XAD-2 column. To minimize the risk of contamination from the ship itself, air sampling was exclusively conducted upwind, thereby avoiding pollutants from the ship's emissions. For quality control, air sample blanks were prepared by briefly exposing PUF/XAD-2 columns and filters next to the air sampler. A substantial volume of seawater samples was collected using the pump system located in the wet laboratory. Suspended particulate matter (SPM) was collected via glass fiber

filters (GFF, 1.2 μm , 140 mm), and organic chemicals in the dissolved phase were captured using a XAD-2 column. It's crucial to acknowledge that chemicals adhered to SPM might be removed during the sampling process. To preserve the integrity of the samples, PUF/XAD-2, QFF, and GFF samples were stored at $-20\text{ }^{\circ}\text{C}$, while the XAD-2 column samples were kept at $5\text{ }^{\circ}\text{C}$. All samples were transported with cooling container from Yantai, China back to Helmholtz-Zentrum Hereon, Germany, in November 2019. The detailed information on air and water samples are provided as summaries in the Supporting Information (Tables S5-1 and 5-2).

5.2.2 Sample Preparation and Instrumental Analysis

Air and seawater samples were processed in a clean lab. PUF-XAD-2, XAD-2 columns, QFF and GFF spiked with internal standards, and extracted with a modified Soxhlet system using dichloromethane for 16 hours. The extracts were concentrated and purified via column chromatography with silica gel and anhydrous sodium sulfate. The elution was reduced to 190 μl under nitrogen stream, spiked with 10 μl 50 ng/mL $^{13}\text{C}_{12}$ -PCB 208 (Cambridge Isotope Laboratories). The samples were determined for 8 PAEs, including DMP, DEP, DiBP, DnBP, BBP, DEHP, DOP and DNP which are supplied by LGC (Wesel). The physicochemical properties of the PAEs are listed in Table S5-3. The analysis of PAEs utilized an Agilent 8890A gas chromatograph coupled to an Agilent 7010B triple quadrupole mass spectrometer (GC-MS/MS), featuring a programmed temperature vaporizer (PTV) multifunction injector. Two HP-5MS columns (15m x 0.25 μm x 0.25mm), connected in series and equipped with a mid-column backflush, facilitated compound separation. The mass spectrometer operated in Multiple Reaction Monitoring (MRM) mode to ensure precise detection. Comprehensive details on the GC-MS/MS setup, including qualitative and quantitative transitions, are provided in Tables S5-4 and S5-5.

5.2.3 Quality Assurance and Quality Control

GFF and QFF filters were pre-treated at 450°C and 600°C for 10 hours and 4 hours, respectively, to eliminate any PAE contamination. PUF/XAD-2 and XAD-2 columns underwent pre-extraction with methanol, acetone, and n-hexane sequentially for 72 hours. All organic solvents were distilled using equipment made entirely of glass. Despite rigorous efforts to remove PAEs from sampling materials and reduce background levels, DMP, DEP, DiBP, and DnBP and DEHP were often found in

procedure blanks. Other PAEs were generally undetectable or found at low levels. Method detection limits (MDLs) were established by adding three standard deviations to the mean concentrations in blanks. Details on blanks and MDLs are provided in Table S5-6. Recovery rates for internal standards d4-DMP, d4-DEP, d4-DnBP and d4-DEHP varied across different materials. PAE concentration findings in this study were reported without blank correction.

5.2.4 Data Analysis

The data of GC-MS/MS were analyzed using MassHunter B10 (Agilent). Statistical analyses were performed with Excel 2016 and Origin 2023 (OriginLab). Geographic maps were plotted with Ocean Data View 4.0.

5.2.5 Air Mass Back Trajectories (BTs)

The origins of the air samples were determined by tracing their air mass back trajectories (BT) using the Hybrid Single-Particle Lagrangian Integrated Trajectory (HYSPLIT) model. These back trajectories retraced the path of the air masses for 120 hours in 6-hour intervals at an altitude of 100 meters above sea level, as illustrated in Figure S5-3.(Stein et al., 2015b)

5.3 Result and Discussion

5.3.1 PAEs in Air

Eight PAEs were found in both the gaseous and particulate phases of air samples. Figure 5-1 displays the concentrations and spatial distribution of the PAEs, while Table S5-7 provides a summary. The total concentration of 8 PAEs (Σ_8 PAEs) ranged from 9.59 to 51.3 ng/m³ with average of 33.4 ± 10.3 ng/m³. The higher PAE concentrations were measured in air sample A11 followed by A03 and A09. However, the PAEs concentrations measured in A01, A02 and A04 were below the average level. The variation could be attributed to several factors including proximity to industrial areas, urban runoff, agricultural drainage, and air mass origins and ocean currents that can carry these pollutants over long distances.

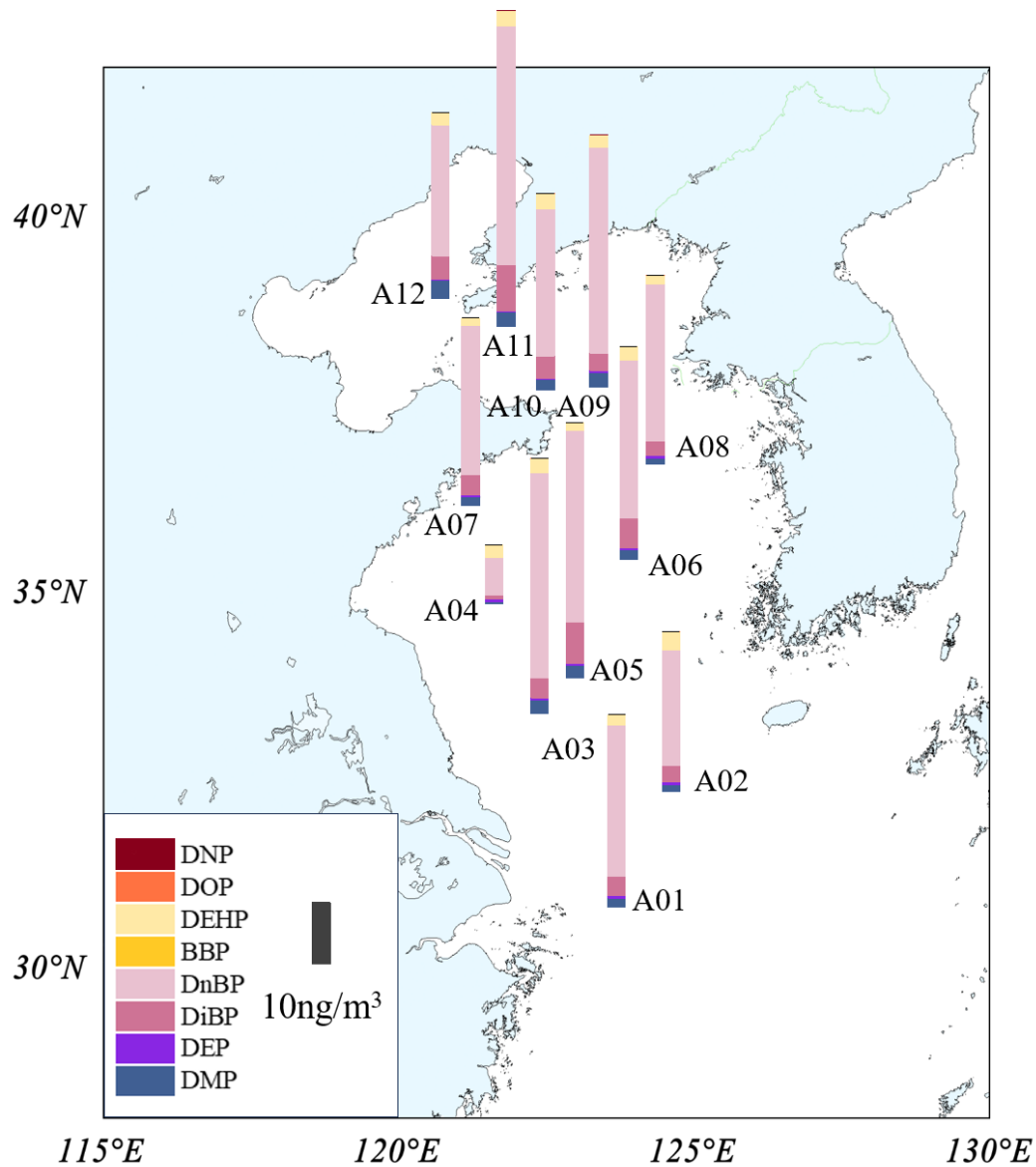


Figure 5-1 Spatial distribution of PAEs in the atmosphere (ng/m³) over the Bohai and Yellow Seas

Air mass back trajectories (Figure S5-3) show that most air masses came from the North or northwest of the mainland of China to the Bohai and Yellow Seas in spring 2019. Therefore, PAE measured in the air almost presented the overall land emissions transported to the marginal seas. Additionally, rain scavenging efficiently removes gaseous PAEs, particularly those with high solubility such as DMP, DEP, DiBP, and DnBP.(Mi et al., 2023) For instance, sample A04 was collected during rainfall, with relatively low concentrations of PAEs detected, indicating that precipitation scavenging can play a significant role in reducing PAEs from the atmosphere. Air samples such as A11, A10, and A09, which are closer to the shore or river mouths, show higher concentrations of certain PAEs, indicating possible sources from nearby human

activities.(Zhou et al., 2021) These air masses swept over the Bohai Economic Rim (BER) including Metropolis of Beijing and Tianjin, and Hebei, Liaoning and Shangdong provinces.(Lin et al., 2023) Plastic film application in agriculture, particularly in North China, has become an increasingly important technique due to its multiple benefits in improving crop production and efficiency.(Lin et al., 2023) As PAEs are the major plasticizers physically added in the plastic film, they can directly release into the air and transported with air masses to the seas(Maddela et al., 2023). Furthermore, a report from the Ministry of Ecology and Environment of China indicates that in 2017, 42% of electronic waste treatment facilities were situated in the coastal regions of North China (19%) and East China (33%) (<http://www.mee.gov.cn/hjzl/sthjzk/>). The air masses flowing through these regions have the potential to carry emissions to remote locations, thereby increasing the levels of PAE contamination in those areas. The overall spatial distribution of PAEs in this region reflects a combination of anthropogenic activities and environmental transport mechanisms. It highlights the need for continuous monitoring to understand the movement and impact of these pollutants in marine ecosystems.

5.3.2 PAE Composition Profile

DnBP emerged as the predominant PAE, with concentrations ranging from 6.0 to 38.6 ng/m³ (median: 25.0 ng/m³), representing 76.4% of the total of eight measured PAEs. This was followed by DiBP, which constituted 11.2% of the total, with levels between 0.65 and 7.47 ng/m³ (median: 3.21 ng/m³), DEHP at 6.0% with concentrations from 1.24 to 2.95 ng/m³ (median: 2.05 ng/m³), and DMP at 5.3%, ranging from 0.36 to 3.02 ng/m³. Other PAEs such as DEP, BBP, DOP, and DNP were detected at relatively low levels in this study, collectively making up only 1% of the total PAEs measured. DnBP, DiBP, and DEHP are commonly the most significant PAEs found in the environment and have been identified as prevalent PAEs in marine air as well.(Mi et al., 2023; Xie et al., 2007) Compared to findings from other regions, the levels of PAEs in the air over the Bohai and Yellow Seas are 2 to 10 times higher than those recorded in the South China Sea,(Mi et al., 2023) the German Bight(Xie et al., 2005), and the Arctic(Xie et al., 2007). This notably high concentration of DnBP may result from its use in nearby terrestrial activities. In 2017, China used 2,528,600 tons of agricultural plastic film, leading to 465,016 tons of plastic waste through recycling processes and water erosion.(Zhang et al., 2021c) DEHP, DnBP, and DiBP, which make up more than 90%

of the plasticizers incorporated into this film, can be emitted into the air, water, and soil throughout their lifecycle. Furthermore, plastic debris or microplastics originating from terrestrial sources can be carried by air to marine environments,(Lamichhane et al., 2023) serving as a direct source of PAEs in these areas. Certainly, the research ship may serve as a source of PAEs emissions during onboard air sampling, despite rigorous efforts to minimize background contamination. Nonetheless, the emissions from the ship during this cruise appear to be minimal, as evidenced by the low levels of DEP and DEHP found in the air samples.

5.3.3 Gas-Particle Partitioning

Table S5-8 illustrates the percentages of particle bound OPEs (Φ , %), ranging from $7.8 \pm 13.2\%$ for BBP to $31.1 \pm 11.2\%$ for DNP. The log octanol-air partition coefficients ($\log K_{OA}$) for PAEs extend from 7.01 for DMP to 11.03 for DNP. Lighter PAEs such as DMP, DEP, DiBP, and DnBP exhibit significantly higher volatility, with vapor pressures 3-6 orders of magnitude greater than those of DEHP, DOP and DNP, as detailed in Table S5-8. However, the Φ values for PAEs do not directly correlate with their $\log K_{OA}$ values and vapor pressures. Despite their higher volatility compared to lighter polycyclic aromatic hydrocarbon (PAHs)(Zhang et al., 2024) and Polychlorinated biphenyls (PCBs)(Iakovides et al., 2021), DMP and DEP have Φ values of $16.6 \pm 17.6\%$ and $17.3 \pm 14.5\%$, respectively, which are similar to those of DiBP, DnBP, and DEHP. In contrast, the Φ values identified in this study differ from those previously reported in the South China Sea(Mi et al., 2023) and the Arctic(Xie et al., 2007). The distribution of PAEs between the gaseous and particle phases is influenced not just by their physical and chemical properties but also by rapid degradation processes triggered by light intensity and radicals, as well as by scavenging processes. Meanwhile, the approximate atmospheric lifetimes were estimated to be 0.38 day for DEHP to 14.4 day for DMP (Table S5-3). PAEs are subject to various degradation processes, including photolysis, hydrolysis, and reactions with atmospheric oxidants such as hydroxyl radicals (OH), ozone (O₃), and nitrate radicals (NO₃). (Perterson, 2003) Photolysis, driven by sunlight, is a significant pathway for the degradation of phthalates in air, leading to the breakdown of their chemical structure and the formation of smaller products(Wang et al., 2019b). The reaction with hydroxyl radicals is considered the most dominant pathway for the atmospheric degradation of phthalates, resulting in their relatively short atmospheric lifetimes, typically ranging

from a few hours to several days(Feng et al., 2022). This rapid degradation limits the long-range transport potential of phthalates but leads to the formation of various oxidation products(Wang et al., 2019b), some of which may have unknown environmental and health impacts. Furthermore, the particle's thin liquid film may also capture certain PAEs, adhering to the principle of "like attracts like." The process of PAE partitioning is more intricate than that of traditional semivolatile organic compounds and cannot be fully described by conventional J-P adsorption or Koa absorption models(Iakovides et al., 2021). This indicates the need for more research to understand the physical and chemical interactions affecting PAEs on particles.

5.3.4 PAEs in Seawater

The levels of PAEs in seawater were measured in both the dissolved and particulate forms (refer to Table S5-9). The overall concentrations of dissolved PAEs (sum of 8 PAEs) varied between 132 and 542 ng/L, with average and median values being 257 ± 108 ng/L and 215 ng/L, respectively (Table S5-9). The predominant PAE was DnBP, with an average proportion of 66.8%, succeeded by DiBP at 19.1% and DEHP at 7.8%. These PAEs together constituted over 90% of the total PAEs in the seawater of the Bohai and Yellow Seas. When comparing with earlier research on dissolved PAEs in marine and coastal zones, the findings from this study align with those observed in the Pearl River Delta(Zhang et al., 2020b), the Mediterranean Sea(Paluselli et al., 2018a; Paluselli et al., 2018b), and the Southeast Coast Region of South Korea(Heo et al., 2020) (Table S5-10). However, the PAE levels reported in this study are significantly lower, by a factor of 5-10, than those found in the East China Sea(Zhang et al., 2018b), the Belgium Bight (North Sea), Barkley Sound in Canada(Keil et al., 2011), and the Tunisian coast(Jebara et al., 2021). In contrast, they are 2-3 orders of magnitude higher than levels reported in the Arctic, the German Bight, and the South China Sea.(Mi et al., 2023; Xie et al., 2005; Xie et al., 2007) It is clear that PAE pollution is notably high in estuaries and coastal regions that are influenced by river discharges.

The collective levels of PAEs detected on SPMs varied from 50 to 714 ng/L across all seawater samples, constituting approximately $39.9 \pm 12.9\%$ of the total PAE concentration (Table S5-11). Consequently, sedimentation emerges as a significant mechanism for PAE removal from water columns in marginal seas.(Neves et al., 2023) Nevertheless, the fraction bound to SPMs ranges from $2.6 \pm 1.4\%$ to $17.5 \pm 7.9\%$ for DMP, DEP, DiBP, and DnBP, indicating their propensity for transport toward the open sea

via ocean currents. Conversely, DEHP, DOP, and DNP likely adhere to particles, exhibiting particle fractions from $61.8 \pm 22.2\%$ to $88.1 \pm 4.8\%$, potentially leading to PAE accumulation in coastal sediment. Overall, DEHP dominates the particle-bound PAEs with concentrations ranging from 47.3 to 711 ng/L (averaging 217 ± 186 ng/L), followed by DnBP (90.4-410 ng/L) and DiBP (28.8-103 ng/L), consistent with PAE profiles observed in sediments from various regions including the Gulf of Lion (Mediterranean), the coast of Mahdia, Tunisia, the Korean coast, and the Bohai and Yellow Seas. (Lee et al., 2020; Schmidt et al., 2021; Souaf et al., 2023; Zhang et al., 2020d)

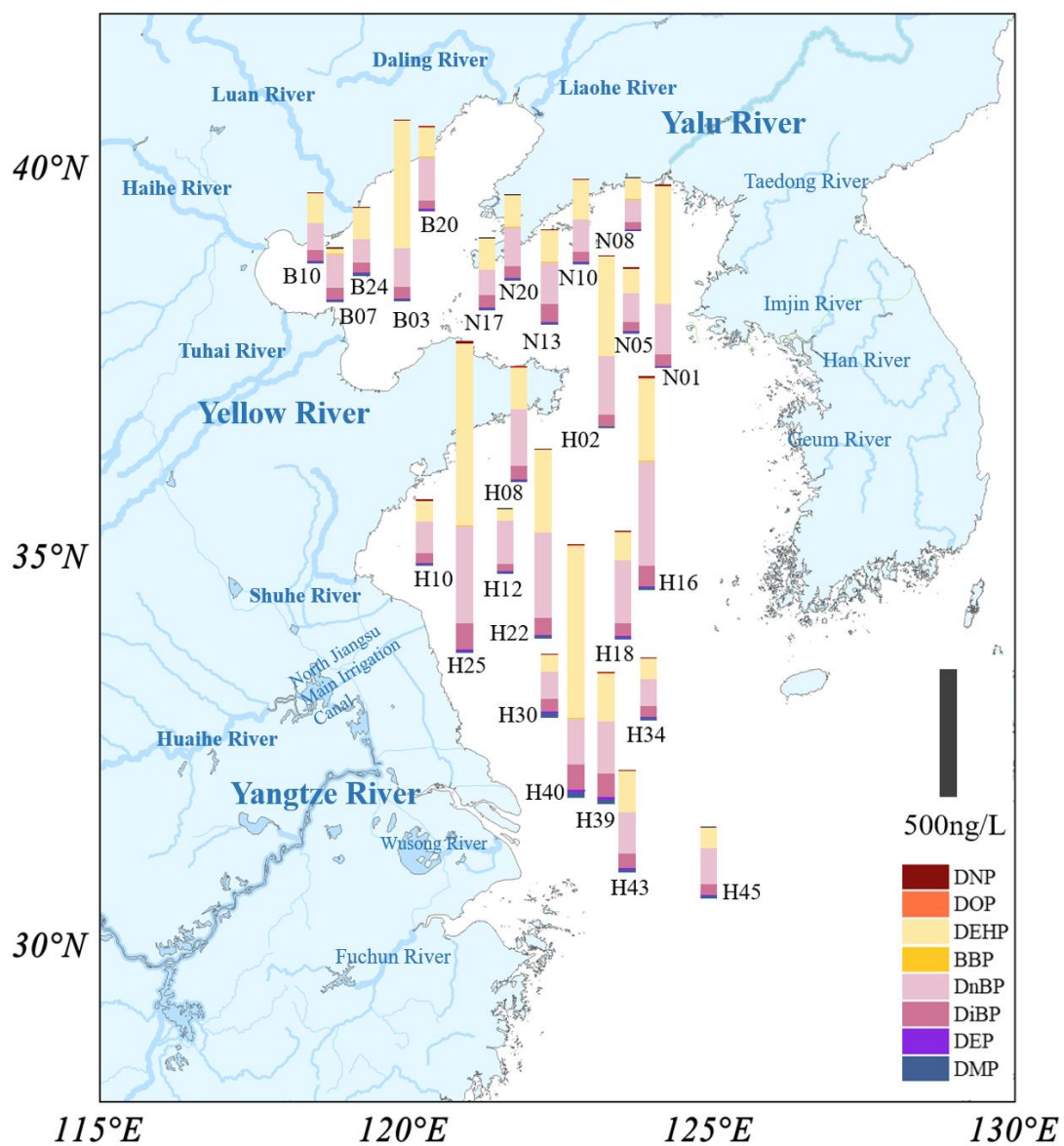


Figure 5-2 Spatial distribution of PAEs in seawater of the Bohai and Yellow Seas

5.3.5 Spatial Distribution of PAEs in Seawater

Figure 5-2 illustrates the spatial distribution of PAEs across the study area, highlighting significant variations. Notably, elevated PAE levels in coastal water are attributed to the diluted water masses from river discharges, as indicated by the reduced salinity in seawater samples. For example, the highest concentrations of PAEs were detected in samples H25, H40, H16, and B03, with salinity levels ranging between 26.77 and 32.59 psu. The salinity map provided in Figure S5-4 reveals numerous low-salinity zones along the coast, primarily due to the inflow from the Yellow River and Haihe River into the Bohai Sea, the Yangtze River into the Yellow Sea, and the Han River along the South Korean coast.(Fan et al., 2018) The Yangtze River plume stretches approximately 100 km into the Yellow and East China Seas, creating a significant low-salinity area.(Wei et al., 2021) As a result, PAEs discharged from rivers can be transported extensive distances to the central Yellow Sea, causing notable PAE contamination levels.(Chen et al., 2023) Predominantly, the Bohai Sea receives substantial contaminant loads through the Yellow, Haihe, and Liaohe Rivers.(Liu et al., 2023c) Similarly, smaller rivers, such as the Xiaoqing River in Shandong Province, are identified as critical contamination points.(Li et al., 2018c) PAE concentrations were recorded at 1170-15500 ng/L in the Haihe River, 500-28100 ng/L in the Pearl River, and 1590 – 6300 ng/L in the Yangtze River. (Li et al., 2016; Liu et al., 2023c; Xu et al., 2022; Zhu et al., 2022b) Consequently, the spatial distribution of PAEs in the Bohai and Yellow Seas are significantly impacted by river discharge and the seasonal dynamics of ocean currents.

5.3.6 Source Identification

Prior research indicates that rivers serve as effective sources for the transport of PAEs from land to sea.(Liu et al., 2023c) Measurements in the estuaries of the Haihe, Yellow, Yangtze, and Pearl Rivers revealed PAE concentrations ranging from 500-28100 ng/L, which are significantly higher by one to two orders of magnitude than seawater concentration reported in this study. This underscores the substantial role of riverine discharge in contributing to PAE pollution. For example, between 2018 and 2019, the Haihe River discharged an estimated 5.28 to 19.52 tons of PAEs into the Bohai Sea, marking it as a critical pollution source. (Liu et al., 2023c) Similarly, the Yangtze River delivers approximately 1060 tons of PAEs annually to the Yellow and East China

Seas,(Zhang et al., 2018b) further illustrating the significance of river pathways in transporting these contaminants. These riverine routes amalgamate diverse terrestrial sources, including industrial emissions, effluents from wastewater treatment facilities, sewage, and landfill leakages. Additionally, land-based sources such as the volatilization from consumer products and electronic waste contribute to the presence of PAEs in the atmosphere and rivers, particularly along the East China coast.(Ankit et al., 2021; Cleys et al., 2024) These emissions are transported to marine areas through rivers, atmospheric deposition, and precipitation, highlighting a complex network of pollutant pathways from land to sea.

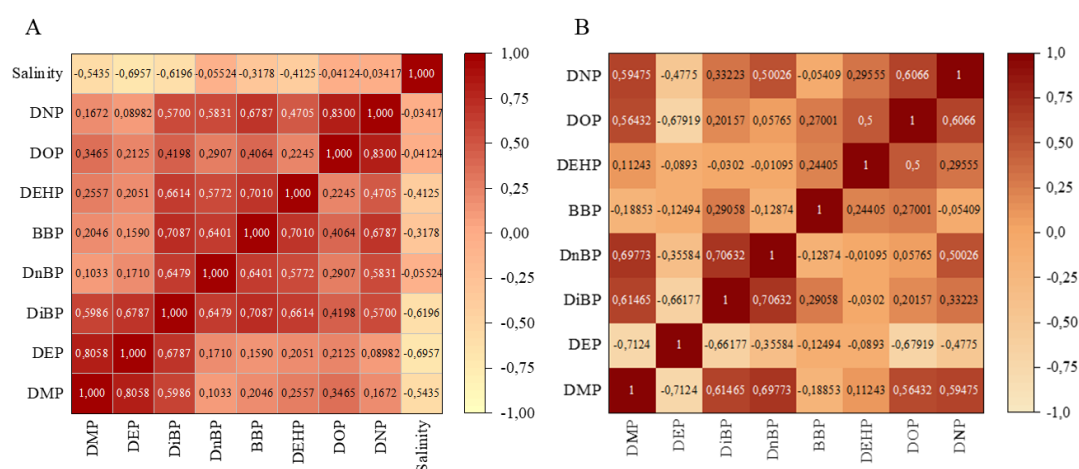


Figure 5-3 Heat map for the correlation analysis of PAEs and the salinity in seawater (A) and air (B)

Correlation analysis of PAEs in air and seawater was conducted (Figure 5-3A). In seawater, Pearson correlation coefficient values ranged from 0.5772 to 0.7087 ($p < 0.01$) among DiBP, DnBP, DEHP and BBP (Figure5-3A), which indicated the significant correlations, and attributed to similar sources and transport pathways. DMP and DEP may share similar sources based on their significant correlations to each other. For the two high molecular weight PAE, DNP shows significant correlation to most other PAEs, while DOP is only significantly correlated to DNP, which can be resulted from more common application of DNP than DOP in the household products and industrial processes.

The relationship between PAEs in the atmosphere is notably complex (Figure5-3B), primarily due to their rapid photo-degradation. Notably, DiBP and DnBP exhibit significant positive correlations, highlighting their interconnected presence in the air. DMP also shows a significant correlation with DiBP, DnBP, DOP, and DNP, yet it inversely correlates with DEP. DEHP's correlation is exclusively significant with DOP,

suggesting shared sources and environmental behaviors. Given their common application as plasticizers in flexible PVC, DEHP and DOP can volatilize into the atmosphere, facilitating their transport from terrestrial environments to marine areas.(Morgan and Mukhopadhyay, 2022) Furthermore, the processing of electronic waste emerges as a crucial pathway for PAEs to reach marine environments like the Bohai and Yellow Seas. Since PAEs are typically incorporated into polymers as plasticizers, they are prone to release into the environment throughout their lifecycle.(Maddela et al., 2023) Additionally, inadequate e-waste management practices can lead to significant emissions of these additives into the atmosphere, contributing to their translocation to marine areas off the Bohai and Yellow Seas.(Tembhare et al., 2022) It is hypothesized that PAEs share common sources in seawater, whereas the presence of PAEs in the atmosphere may significantly vary based on their original sources, atmospheric degradation, and precipitation patterns.

5.3.7 Air-sea Exchange

PAEs can undergo various processes at the air-seawater interface during the transportation from continental regions to the Bohai and Yellow Seas. The dynamics and magnitudes of PAEs' air-sea exchange are predominantly governed by their physicochemical characteristics, including Henry's Law Constants, and the respective concentrations in the air and seawater. These processes are also affected by meteorological conditions. In this study, the air-sea exchange fluxes of PAEs were determined using a modified version of Whitman's two-film fugacity model.(Xie et al., 2005) The calculations for volatilization and deposition fluxes (F_{vol} and F_{dep} , expressed in $ng/m^2/day$) follow the methodology outlined in equations 5-1 and 5-2.(Schwarzenbach et al., 2016)

$$F_{vol} = K_{OL} C_w \quad (5-1)$$

$$F_{dep} = K_{OL} C_a / H' \quad (5-2)$$

$$F = K_{OL} (C_w - \frac{C_a}{H'}) \quad (5-3)$$

$$K_{OL} = (\frac{1}{K_w} + \frac{1}{K_a * H'})^{-1} \quad (5-4)$$

The net diffusive gas exchange flux (F , measured in $ng/m^2/day$) is determined by calculating the difference between the deposition and volatilization fluxes. This

calculation is outlined in equation 5-3, where C_w (ng/m^3) represents the concentration of the dissolved phase in water, and C_a (ng/m^3) represents the concentration in the gas phase. The term $(C_w - C_a/H')$ signifies the concentration gradient (in ng/m^3), with H' being the dimensionless Henry's law constant. The overall mass transfer coefficient, K_{OL} (measured in m/s), incorporates contributions from both the water phase (K_w) and the air phase (K_a) mass transfer coefficients, as detailed in equation 5-4. For PAEs, the determination of K_w and K_a is based on the equations proposed by Schwarzenbach et al. and the quadratic relationship described by Wanninkhoff. (Schwarzenbach et al., 2016; Wanninkhoff, 1992) The Henry's law constant for PAEs is adjusted for the seawater temperature (T_w , in Kelvin) and the average salt concentration (C_s , at 0.5 mol/L). The total error in estimating F , which stands at 45%, was obtained from an error propagation analysis referencing prior research. (Xie et al., 2005) A positive F value indicates a net volatilization from seawater to air, whereas a negative F value suggests that deposition is the prevailing process in the air-sea exchange flux.

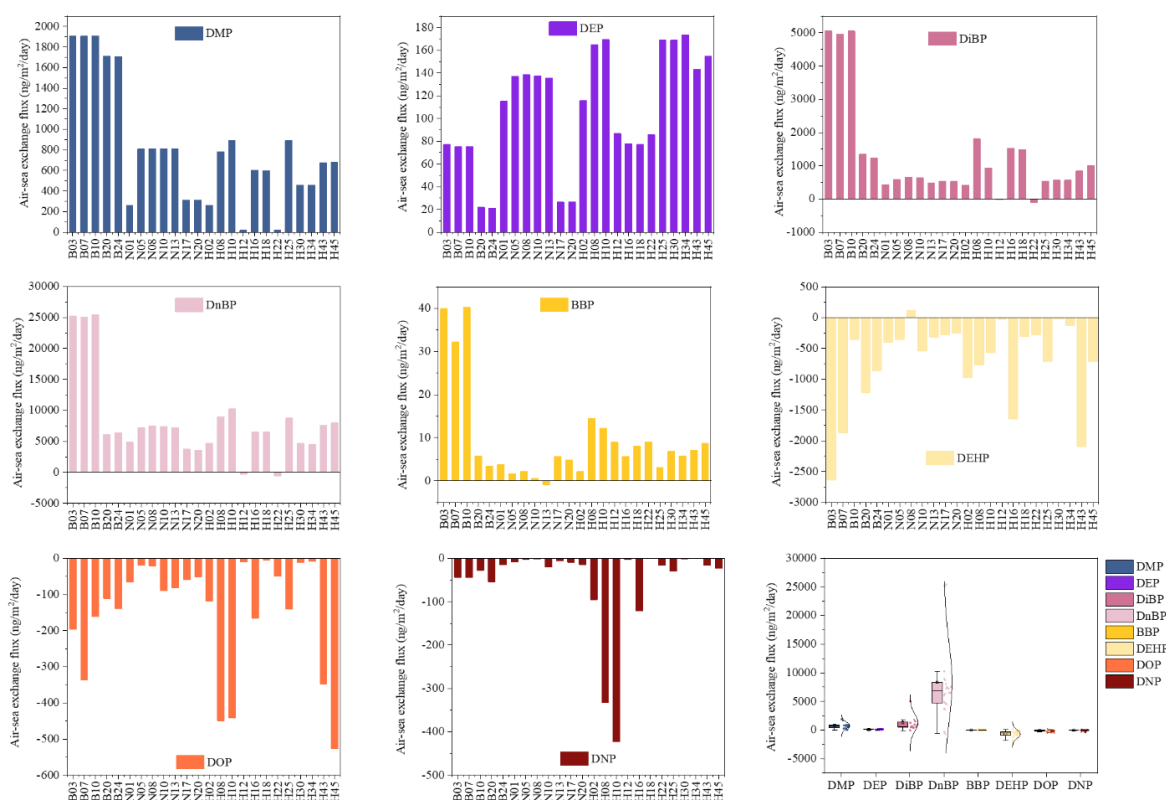


Figure 5-4 Air-sea exchange fluxes of PAEs ($\text{ng}/\text{m}^2/\text{day}$) calculated with two-film fugacity mode using paired air/seawater concentrations. The positive (+) value indicates water to air volatilization and the negative (-) value means air to water deposition

The estimation of air-sea exchange fluxes of Phthalate Esters (PAEs) was conducted using paired air and seawater samples from the Bohai and Yellow Seas. This analysis is shown in Figure 5-4, with comprehensive details provided in Table S5-12. The study found that for DMP, DEP, DiBP, and DnBP, there was a predominant volatilization with average fluxes ranging between 109 to 8280 ng/m²/day. Conversely, DEHP, DOP, and DNP experienced net deposition from the atmosphere to seawater, with mean fluxes ranging from -183 to -722 ng/m²/day. BBP was nearly at an equilibrium due to its minimal levels in both air and seawater. The air-sea exchange fluxes of PAEs assessed in this study revealed a complete reversal in direction compared to previous findings in the South China Sea (Mi et al., 2023), where DMP, DiBP, and DnBP were primarily deposited into seawater, while DEHP was predominantly volatilized from water to air. When compared to earlier assessments of air-sea exchange fluxes of PAEs in the North Sea and the Arctic, the directions of air-sea exchange were found to vary. (Xie et al., 2005; Xie et al., 2007) Nonetheless, the fluxes determined in this investigation were significantly higher, by two to three orders of magnitude, than those recorded in the Arctic, the North Sea, and the South China Sea.

The air-sea exchange of PAEs identified in this research indicates that significant volatilization is capable of removing parts of the dissolved PAEs from the water column in coastal areas, achieving dynamic equilibrium in open waters. It is theorized that air masses originating from land carry high emissions from terrestrial sources, thereby increasing PAE concentrations in the atmosphere and potentially disrupting the equilibrium, favoring deposition from air to seawater. However, to enhance our comprehension of the air-sea exchange processes of PAEs in the Bohai and Yellow Seas, further seasonal investigations are recommended.

5.3.8 Atmospheric Particle Dry Deposition Fluxes

Atmospheric deposition plays a crucial role in eliminating pollutants from the air, serving as the primary conduit for chemical contaminants to enter the marine ecosystem. Utilizing the measured concentrations of PAEs in the particulate phase, we calculated the particle-bound dry deposition fluxes (FD, expressed in ng/m²/day) using a specific equation (5-5) (Schwarzenbach et al., 2016):

$$F_D = C_p \times V_d \quad (5-5)$$

In this context, C_p represents the concentration of PAEs in the particulate phase (ng/m^3), and V_d denotes the deposition velocity (cm/s). In this work, we utilized a dry deposition velocity of $0.55 \text{ cm}/\text{s}$, as suggested by Gao et al. for pollutants contained within finer particles over the Yellow Sea, which was subsequently employed in the coastal regions of China. (Gao et al., 1992)

Figure 5-5 and Table S5-13 present the atmospheric particle dry deposition fluxes of 8 PAEs, which varied between 1540 to $5580 \text{ ng}/\text{m}^2/\text{day}$, averaging at $3470 \pm 1330 \text{ ng}/\text{m}^2/\text{day}$. The flux was primarily composed of DnBP, with values ranging from 1160 to $4960 \text{ ng}/\text{m}^2/\text{day}$ and was followed by DEHP and DiBP. DMP, DEP, BBP, DOP, and DNP exhibited lower dry deposition rates due to their lesser concentrations in the atmospheric particle phase. Compared to previous research conducted in the South China Sea and the North Sea, the dry deposition rates of DnBP in this study were found to be 1-2 orders of magnitude higher, whereas the levels of other PAEs were similar across the studied regions. (Mi et al., 2023; Xie et al., 2005)

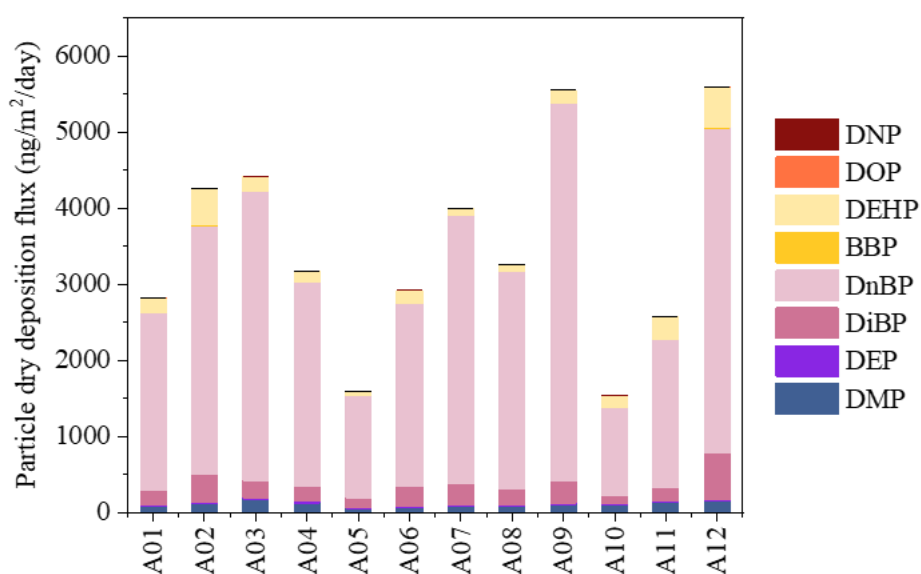


Figure 5-5 The dry deposition fluxes of particle bound PAEs ($\text{ng}/\text{m}^2/\text{day}$) to the Bohai and Yellow Seas

In this study, the PAEs levels were found to be comparatively in line with those observed in most other marine environments, including the Chinese marginal seas. Consequently, the air-sea exchange and atmospheric dry deposition fluxes of PAEs identified here set a benchmark for interactions at the air-sea interface. Covering an area of $457,000 \text{ km}^2$, the Bohai and Yellow Seas exhibited an annual atmospheric deposition flux of PAEs ranging between 257 and $932 \text{ ton}/\text{year}$, with an average of 579

± 222 ton/year (Figure 5-6A). This rate aligns with findings from the South China Sea, which recorded a flux range of 46 to 4,630 ton/year over a 3,500,000 km² area. (Mi et al., 2023) However, it is significantly higher by one to two orders of magnitude compared to the flux of organophosphate esters in the Bohai Sea, (Wu et al., 2022) which was calculated at 18.3 ± 12.5 ton/year for a 77,000 km² area. Additionally, the study revealed that the net air-sea gas exchange fluxes of PAEs primarily involved volatilization from water to air, averaging at 1540 ± 1430 ton/year as illustrated in Figure 5-6B. This volatilization process not only signifies the transfer of PAEs from water to air but also potentially impacts the transportation of PAEs from coastal regions to offshore and open ocean areas.

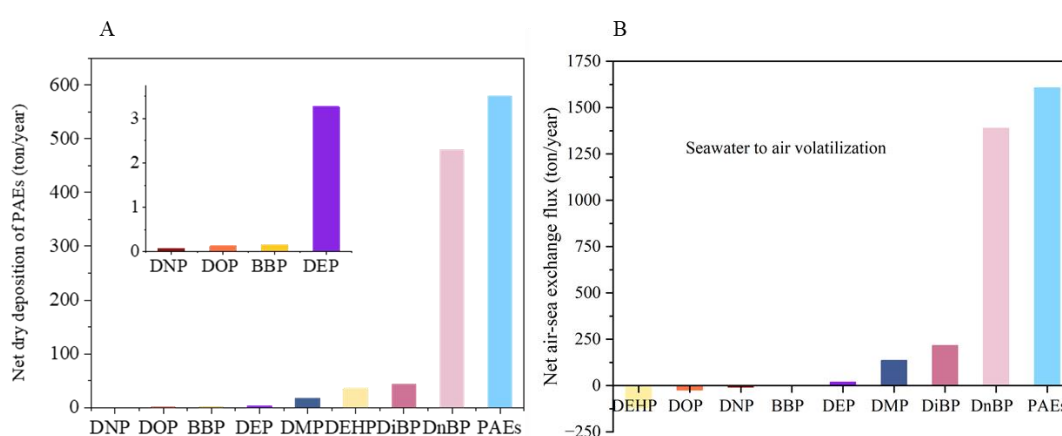


Figure 5-6 A: The annual net dry deposition of particle bound PAEs (ton/year), and B: the net air-sea deposition in the Bohai and Yellow Seas (ton/year)

5.4 Implication

PAEs have been found in significant quantities in both the air and seawater of the Bohai and Yellow Seas, demonstrating their persistence and mobility within aquatic environments. In contrast, atmospheric PAEs are subject to medium and long-range transport, exacerbated by the widespread use of PAE-containing materials, such as plastics, in urban and agricultural settings. Emissions from industrial activities and wastewater treatment processes in North and East China continuously introduce PAEs into these seas through both riverine flow and atmospheric deposition. Additionally, the improper disposal of plastic films used in greenhouse farming poses a significant environmental concern, not only due to microplastic pollution but also because of the leaching of toxic plastic additives into natural habitats. Consequently, plastic litter, along with micro and nano plastics, serves as critical carriers of PAEs, facilitating their

transport to distant marine regions. Moreover, the volume of electronic waste (e-waste) from East and Southeast Asia has been growing by 10% annually from 2010 to 2015, reaching 24.9 million tons in 2019. However, only 12% of this e-waste has been processed in an environmentally responsible manner. The improper handling and disposal of e-waste have significantly increased PAE emissions, making it a notable source of contamination for the marginal seas of China.

The influence of oceanographic factors on the distribution of phthalic acid esters (PAEs) in the seawater of the Bohai and Yellow Seas has been demonstrated. However, the lack of data across different seasons constrains our understanding of PAEs' full range. To elucidate the effects of river runoff on the spatial distribution of PAEs and their interactions between the Bohai and Yellow Seas, it is essential to implement frequent seasonal sampling. Furthermore, the vertical distribution of PAEs within the water column of the continental shelf warrants additional investigation to better understand their transport via ocean currents and their bioaccumulation in various marine organisms. Remarkably, the concentration levels of PAEs in both air and seawater have surpassed those of many traditional POPs and CECs, highlighting a growing issue for marine environmental protection. Therefore, further research is imperative to explore PAEs in the Bohai and Yellow Seas, including identifying point sources along the Chinese coast. This will enhance our comprehension of the transport, deposition, and bioaccumulation processes of PAEs in the marginal seas.

Supporting Information

Figure S 5-1. Air sampling sites in the Bohai and Yellow Seas are indicated by black dots, representing the initial location for each air sample collection. The voyage commenced from the ports Qingdao-Shanghai-Qingdao, proceeded to the Yellow Sea, and then continued north towards the Bohai Sea

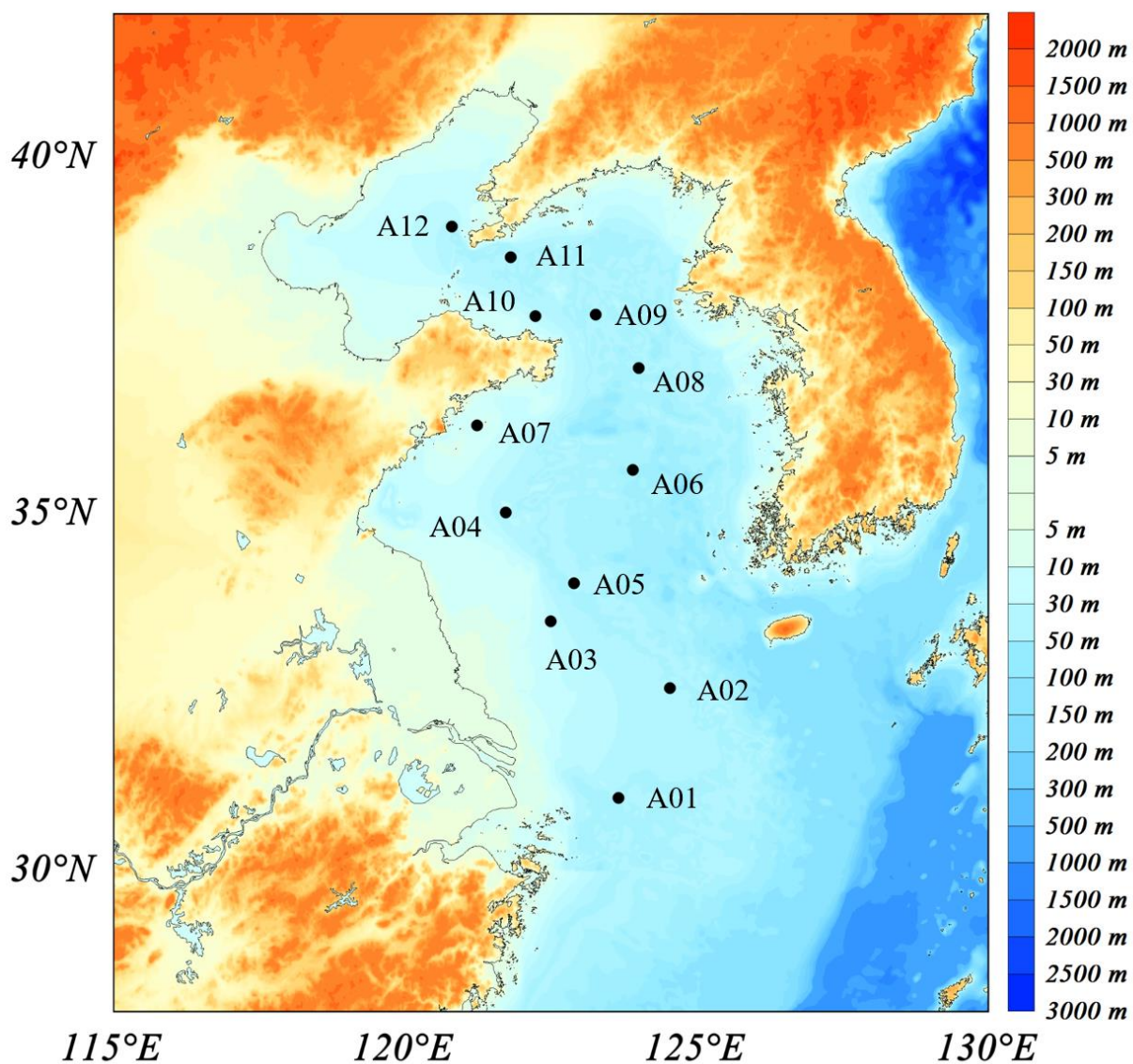


Figure S 5-2. Seawater collection points in the Bohai and Yellow Seas are denoted by black dots, marking the initial location of each water sample

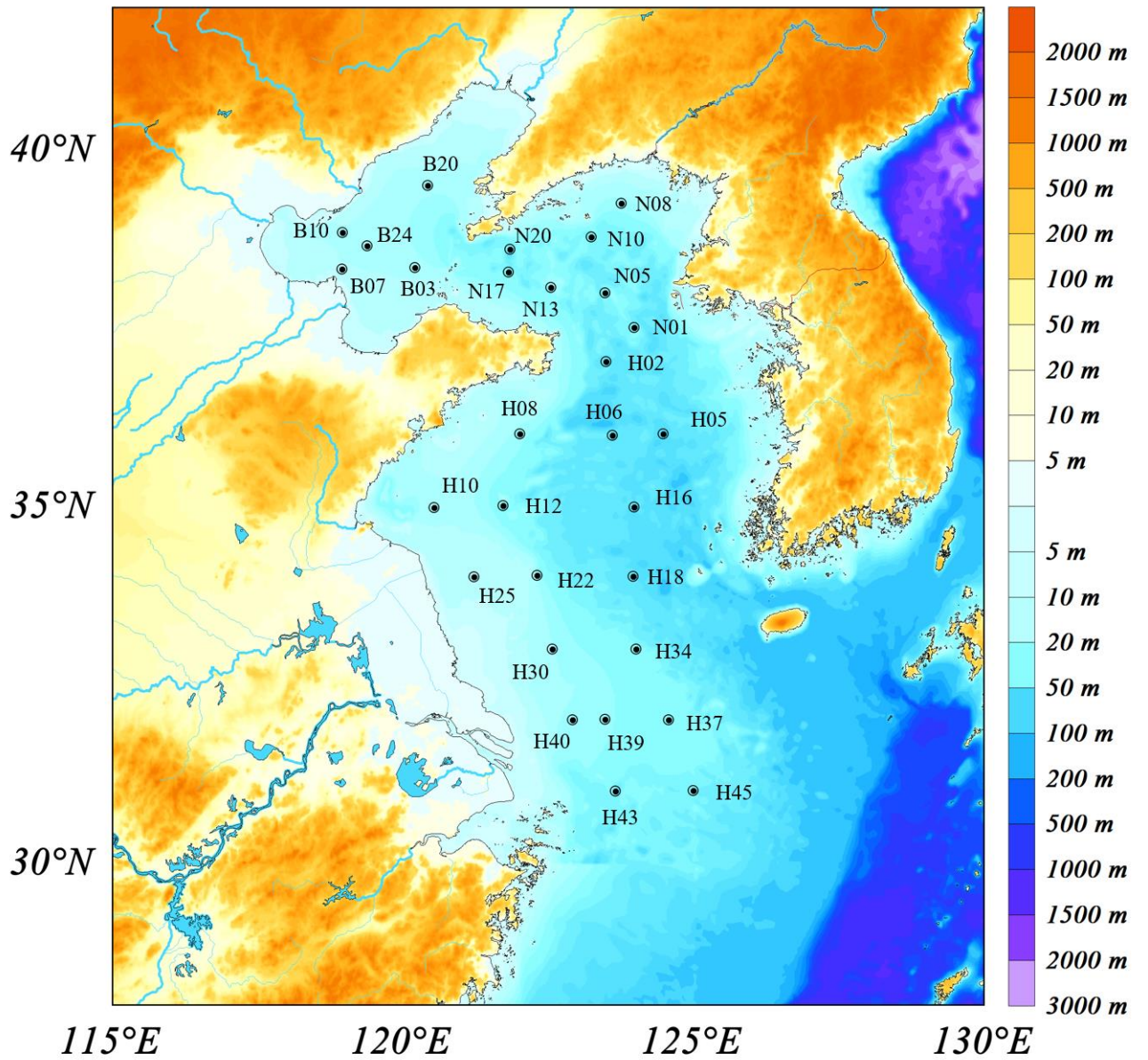


Figure S 5-3. Air mass back trajectories delineate the paths of air samples. Colors denote the source regions of the air mass parcels

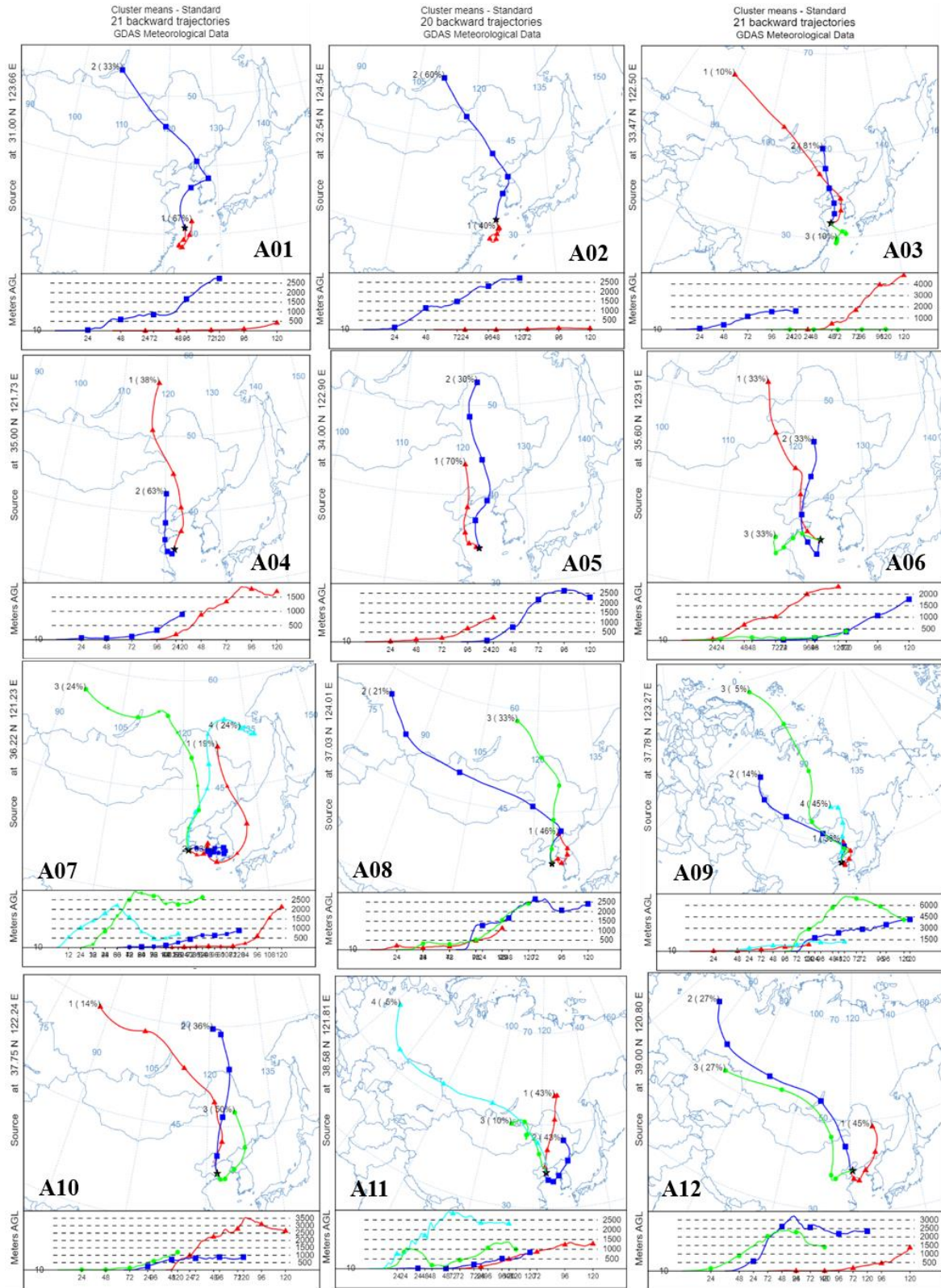


Figure S 5-4 The salinity of surface seawater in the Bohai and Yellow Seas during the cruise

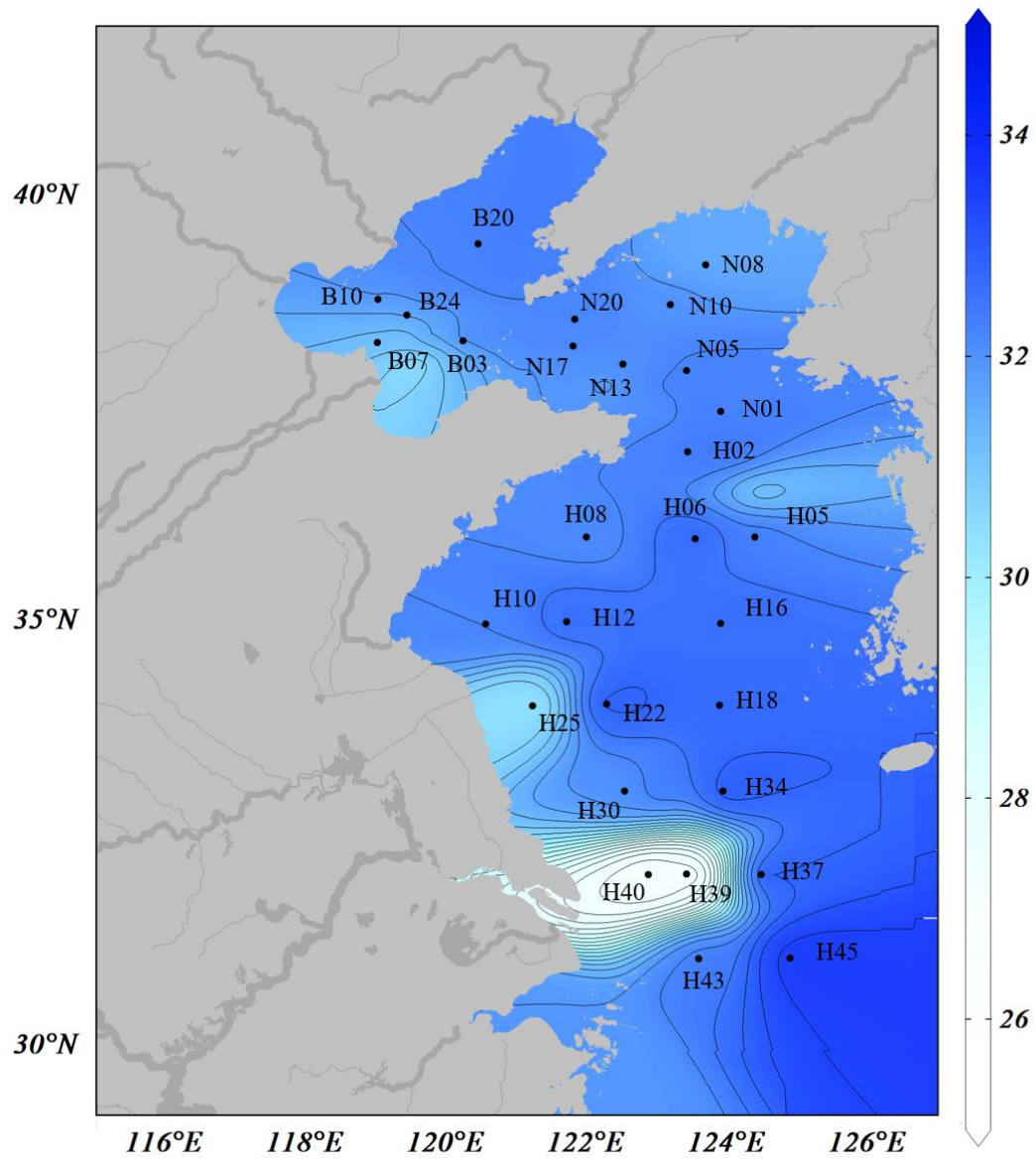


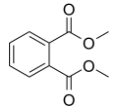
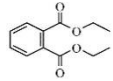
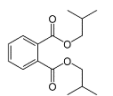
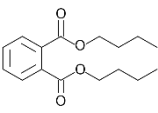
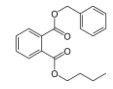
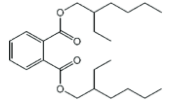
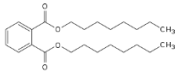
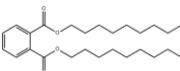
Table S 5-1. Detail information for seawater sampling Detail information for air sampling

Station	Longitude (°E)	Latitude (°N)	Date	Volume (L)	Temperature (C°)	Salinity
H02	123.50	37.02	4/29/2019	29.0	10.5	32.4
H08	122.02	36.00	4/17/2019	25.4	9.0	32.1
H10	120.55	34.97	4/14/2019	26.9	10.6	32.2
H12	121.73	35.00	4/14/2019	25.5	11.3	32.6
H16	123.98	34.98	4/16/2019	26.9	10.1	32.6
H18	123.96	34.01	4/15/2019	31.3	10.2	32.7
H22	122.32	34.02	4/15/2019	27.2	11.2	32.9
H25	121.23	34.00	4/14/2019	31.0	11.4	30.3
H30	122.58	32.99	4/13/2019	31.5	10.9	32.0
H34	124.01	32.99	4/12/2019	26.7	11.6	33.0
H37	124.57	32.00	4/12/2019	31.8	11.3	33.0
H39	123.49	32.00	4/8/2019	29.4	14.3	27.0
H40	122.92	32.00	4/7/2019	24.6	15.0	27.0
H43	123.66	31.00	4/11/2019	27.5	14.3	32.4
H45	125.00	31.00	4/11/2019	28.8	12.0	33.5
N01	123.98	37.49	4/28/2019	28.2	9.7	32.2
N05	123.48	37.98	4/29/2019	26.4	9.7	32.2
N08	123.76	39.24	4/30/2019	24.9	8.1	31.6
N10	123.25	38.76	4/30/2019	30.0	9.1	32.0
N13	122.56	38.06	4/30/2019	31.3	9.9	32.1
N17	121.82	38.28	5/1/2019	28.1	9.6	32.1
N20	121.85	38.59	5/1/2019	26.6	10.9	32.2
B03	120.21	38.33	5/2/2019	28.5	9.6	32.2
B07	118.96	38.32	5/2/2019	23.5	10.9	31.1
B10	118.97	38.83	5/3/2019	28.3	10.0	32.0
B20	120.43	39.48	5/3/2019	24.4	9.7	32.3
B24	119.40	38.64	5/4/2019	25.1	11.8	31.8

Table S 5-2. Detail information for air sampling (T: air temperature; WS: wind speed; WD: wind direction)

Air sample	Longitude (°E)	Latitude (°N)	Date	Volume (m ³)	T (°C)	WS (m/s)	WD (Degree)
A-01	31.00	123.66	11/04/2019	351.1	10.8	5.7	18
A-02	32.54	124.54	12/04/2019	250.5	11.4	5.7	359
A-03	33.47	122.50	13/04/2019	243.1	11.2	5.2	87
A-04	35.00	121.73	14/04/2019	222.1	11.0	1.3	218
A-05	34.01	122.90	15/04/2019	322.0	12.8	2.8	216
A-06	35.60	123.91	16/04/2019	281.6	12.6	6.1	153
A-07	36.22	121.23	27/04/2019	336.8	11.5	14.9	303
A-08	37.03	124.01	28/04/2019	199.0	10.8	2.9	127
A-09	37.78	123.27	29/04/2019	258.8	10.8	3.9	112
A-10	37.75	122.24	30/04/2019	265.0	12.0	1.4	106
A-11	38.58	121.81	1/05/2019	395.2	15.0	10.5	330
A-12	39.01	120.80	3/05/2019	503.5	12.3	7.5	14

Table S 5-3. Physiochemical properties of eight phthalate esters(Cousins and Mackay, 2000)

Chemical Name	Abbreviation	CAS	MW	Chemical formula	V _p (Pa)	S (mg/L)	H (pa.m ³ /mol)	logK _{ow}	logK _{oa}	logK _{aw}	Half-life time in air (d)	Chemical structure
Dimethyl phthalate	DMP	131-11-3	194.19	C ₁₀ H ₁₀ O ₄	0.263	5220	9.78x10 ⁻³	1.61	7.01	-5.4	14.4	
Diethyl phthalate	DEP	84-66-2	222.24	C ₁₂ H ₁₄ O ₄	6.48x10 ⁻²	591	2.44x10 ⁻²	2.54	7.55	-5.01	2.39	
Diisobutyl phthalate	DiBP	84-69-5	278.35	C ₁₆ H ₂₂ O ₄	4.73x10 ⁻³	9.9	0.13	4.27	8.54	-4.27	0.58	
Dibutyl phthalate	DnBP	84-74-2	278.34	C ₁₆ H ₂₂ O ₄	4.73x10 ⁻³	9.9	0.13	4.27	8.54	-4.27	0.89	
Benzylbutyl phthalate	BBP	85-68-7	312.37	C ₁₉ H ₂₀ O ₄	2.49x10 ⁻³	3.8	0.205	4.70	8.78	-4.08	0.75	
Bis(2-ethylhexyl) phthalate	DEHP	117-81-7	390.56	C ₂₄ H ₃₈ O ₄	2.52x10 ⁻⁵	2.49x10 ⁻³	3.95	7.73	10.53	-2.80	0.38	
Diocetyl phthalate	DnOP	117-84-0	390.56	C ₂₄ H ₃₈ O ₄	2.52x10 ⁻⁵	2.49x10 ⁻³	3.95	7.73	10.53	-2.80	0.52	
Dinonyl phthalate	DnNP	84-76-4	418.6	C ₂₆ H ₄₂ O ₄	6.81x10 ⁻⁶	3.08x10 ⁻⁶	9.26	8.60	11.03	-2.43	0.46	

V_p: vapor pressure at 25°C; S: water solubility at 25°C; H: Henry's law constants at 25°C; logK_{ow}: log Octanol-Air coefficient at 25°C; logK_{oa}: log Octanol-Air coefficient at 25°C; logK_{aw}: log air-water transfer coefficient; Half-life time in air (d) (exclude DiBP)(Perterson, 2003); Half-live time in air for DiBP: (Calculated by EPIWEB 4.1).

Table S 5-4. Agilent 7890 GC-MS/MS conditions

Parameter	Value
Analytical column	2 set Agilent HP5-ms, 250 μm \times 15 m, 0.25 μm
Sample injection mode	1 μL Pulsed splitless using Multimode Inlet (MMI)
Injection port liner	Agilent 200 μL dimpled, single-taper liner
Injection temperature program	20 $^{\circ}\text{C}$ (0.2 minutes), 300 $^{\circ}\text{C}/\text{min}$ to 300 $^{\circ}\text{C}$
Injection pulsed pressure	25 psi (1.9 minutes)
Purge flow to spit vent	50 mL/min (2.0 minutes)
Carrier gas	Helium
Carrier gas flow	1.2 mL/min
Oven temperature program	50 $^{\circ}\text{C}$ for 2 min, 20 $^{\circ}\text{C}/\text{min}$ to 80 $^{\circ}\text{C}$, 5 $^{\circ}\text{C}/\text{min}$ to 250 $^{\circ}\text{C}$, 15 $^{\circ}\text{C}/\text{min}$ to 300 $^{\circ}\text{C}$ (14 min)
Post run	310 $^{\circ}\text{C}$ for 3 min
Backflush	3.0 ml/min
Mass spectrometer	Agilent 7000C with electron impact ionization source operated in multiple reaction monitoring mode (MRM)
Ionization mode	Positive
Source temperature	280 $^{\circ}\text{C}$
Quadrupole 1 and 2 temperature	150 $^{\circ}\text{C}$
Transfer line temperature	280 $^{\circ}\text{C}$

Table S 5-5. The detail information for determination of PAEs using GC-MS/MS

PAE	Quantifier ions (m/z)	Qualifier ions (m/z)	Collision energy (eV)	Retention time (min)	Instrumental detection limit(pg)
DMP	163>77	163>135	15	16.963	0.02
DEP	149>93	149>121	15	20.258	0.03
DiBP	149>93	149>121	15	26.105	0.04
DnBP	149>93	149>121	15	27.956	0.04
BBP	149>93	149>121	15	34.854	0.1
DEHP	149>93	149>121	15	37.955	0.2
DOP	149>93	149>121	15	38.55	0.2
DNP	149>93	149>121	15	39.50	0.2
d4-DMP	167>81	167>139	15	16.933	-
d4-DEP	153>97	153>125	15	20.232	-
d4-DnBP	153>97	153>125	15	27.937	-
d4-DEHP	153>97	153>125	15	37.943	-

Table S 5-6 The field blanks and the method detection limits of PAEs in PUF/XAD-2, XAD-2 columns, QFF and GFF filters

Sample material	PUF/XAD-2 column (gas)		QFF (particle)		XAD-2 column (dissolved phase)		GFF (particular matter)	
	Blank (mean±SD) (ng/m ³)	MDL (ng/m ³)	Blank (mean±SD) (ng/m ³)	MDL (ng/m ³)	Blank (mean±SD) (ng/L)	MDL (ng/L)	Blank (mean±SD) (ng/L)	MDL (ng/L)
DMP	0.017±0.006	0.036	0.002±0.001	0.004	0.002±0.001	0.004	0.005±0.002	0.011
DEP	0.014±0.002	0.022	0.008±0.004	0.021	0.008±0.004	0.021	0.021±0.008	0.045
DiBP	0.020±0.007	0.042	0.005±0.001	0.007	0.005±0.001	0.007	0.045±0.011	0.077
DnBP	0.037±0.011	0.068	0.006±0.002	0.011	0.006±0.002	0.011	0.015±0.001	0.017
BBP	0.060±0.010	0.090	0.001±0.000	0.001	0.001±0.000	0.001	0.001±0.001	0.002
DEHP	0.14±0.002	0.15	0.074±0.031	0.166	0.074±0.031	0.17	0.17±0.099	0.47

Table S 5-7. Concentrations of PAEs in the atmosphere over the Bohai and Yellow Seas.

Name	DMP	DEP	DiBP	DnBP	BBP	DEHP	DOP	DNP	Σ_8 PAEs
Gaseous phase (C_g, ng/m³)									
A01	1.37	0.30	2.79	19.6	0.023	1.21	0.004	0.000	25.3
A02	0.95	0.35	1.92	11.9	0.020	1.92	0.003	0.001	17.1
A03	1.90	0.35	2.66	25.3	0.034	2.01	0.006	0.001	32.3
A04	0.11	0.43	0.23	0.36	0.057	1.74	0.006	0.001	2.93
A05	2.01	0.26	6.50	28.3	0.039	1.18	0.004	0.001	38.3
A06	1.47	0.30	4.27	20.6	0.036	1.81	0.007	0.002	28.5
A07	1.30	0.29	2.63	16.8	0.017	1.05	0.003	0.001	22.1
A08	0.85	0.36	2.01	19.4	0.023	1.26	0.002	0.001	23.9
A09	2.16	0.35	2.19	23.0	0.008	1.71	0.006	0.007	29.4
A10	1.56	0.13	3.47	21.4	0.036	2.11	0.010	0.003	28.8
A11	2.27	0.09	7.09	34.5	0.057	1.84	0.010	0.007	45.9
A12	2.71	0.04	2.60	12.2	0.012	0.92	0.004	0.003	18.5
Min	0.11	0.04	0.23	0.36	0.008	0.92	0.002	0.000	2.93
Max	2.71	0.43	7.09	34.5	0.057	2.11	0.010	0.007	45.9
Median	1.52	0.30	2.64	20.1	0.029	1.73	0.005	0.001	26.9
Average	1.55	0.27	3.20	19.5	0.030	1.56	0.005	0.002	26.1
SD	0.71	0.12	1.94	8.73	0.016	0.41	0.003	0.002	10.9
Particle phase (C_p, ng/m³)									
AF01	0.16	0.04	0.39	4.92	0.002	0.42	0.001	0.0002	5.93
AF02	0.23	0.05	0.77	6.88	0.004	1.03	0.001	0.001	8.97
AF03	0.36	0.04	0.48	7.99	0.001	0.42	0.001	0.0004	9.30
AF04	0.26	0.04	0.42	5.64	0.001	0.29	0.001	0.001	6.66
AF05	0.11	0.02	0.27	2.83	0.0002	0.10	0.000	0.0004	3.33
AF06	0.12	0.04	0.56	5.05	0.001	0.38	0.001	0.001	6.14
AF07	0.16	0.04	0.60	7.41	0.0004	0.19	0.001	0.001	8.39
AF08	0.17	0.04	0.42	6.04	0.001	0.17	0.001	0.001	6.84
AF09	0.22	0.04	0.61	10.4	0.0004	0.36	0.002	0.002	11.7
AF10	0.19	0.04	0.22	2.43	0.001	0.36	0.001	0.001	3.25
AF11	0.27	0.04	0.38	4.09	0.001	0.63	0.000	0.001	5.41
AF12	0.31	0.06	1.29	8.98	0.011	1.10	0.008	0.002	11.8
Min	0.11	0.02	0.22	2.43	0.0	0.10	0.000	0.000	3.25
Max	0.36	0.06	1.29	10.4	0.0	1.10	0.008	0.002	11.8
Median	0.20	0.04	0.45	5.84	0.0	0.37	0.001	0.001	6.75
Average	0.21	0.04	0.54	6.06	0.0	0.45	0.002	0.001	7.31
SD	0.08	0.01	0.28	2.41	0.0	0.32	0.002	0.001	2.80
Sum of C_g+C_p (ng/m³)									
A01	1.53	0.34	3.19	24.5	0.025	1.63	0.005	0.001	31.2
A02	1.18	0.40	2.69	18.8	0.023	2.95	0.005	0.002	26.0
A03	2.26	0.40	3.14	33.3	0.035	2.44	0.007	0.002	41.6
A04	0.36	0.48	0.65	6.00	0.058	2.04	0.007	0.001	9.59
A05	2.12	0.28	6.77	31.2	0.039	1.28	0.004	0.002	41.7
A06	1.60	0.34	4.82	25.6	0.037	2.18	0.008	0.003	34.6
A07	1.47	0.32	3.23	24.3	0.018	1.24	0.004	0.002	30.5
A08	1.02	0.40	2.43	25.4	0.023	1.43	0.003	0.003	30.8

A09	2.38	0.39	2.80	33.4	0.009	2.07	0.008	0.008	41.1
A10	1.75	0.18	3.69	23.9	0.037	2.47	0.011	0.005	32.0
A11	2.54	0.13	7.47	38.6	0.058	2.47	0.010	0.008	51.3
A12	3.02	0.10	3.89	21.2	0.022	2.02	0.013	0.005	30.3
Min	0.36	0.10	0.65	6.00	0.009	1.24	0.003	0.001	9.59
Max	3.02	0.48	7.47	38.6	0.058	2.95	0.013	0.008	51.3
Median	1.67	0.34	3.21	25.0	0.030	2.05	0.007	0.002	31.6
Average	1.77	0.31	3.73	25.5	0.032	2.02	0.007	0.003	33.4
SD	0.74	0.12	1.87	8.40	0.015	0.53	0.003	0.003	10.3

Table S 5-8. Particle-bound fractions (ϕ , %) of PAEs in air samples from the Bohai and Yellow Sea.

Air sample	DMP	DEP	DiBP	DnBP	BBP	DEHP	DOP	DNP
A01	10.5	12.2	12.3	20.1	7.2	25.7	21.5	34.3
A02	19.9	13.0	28.6	36.7	16.5	34.9	25.1	34.8
A03	15.9	11.0	15.3	24.0	2.4	17.3	14.3	24.7
A04	70.9	9.0	64.9	94.0	1.9	14.4	17.1	34.1
A05	5.2	8.5	4.0	9.1	0.4	7.7	11.1	23.1
A06	7.7	10.8	11.5	19.7	3.9	17.2	7.8	25.5
A07	11.0	11.1	18.5	30.5	2.1	15.4	21.5	42.1
A08	16.6	10.0	17.3	23.7	2.4	11.8	38.2	52.0
A09	9.2	10.2	22.0	31.3	4.8	17.2	28.5	22.7
A10	10.9	24.2	6.1	10.2	2.7	14.5	11.0	26.1
A11	10.6	29.0	5.1	10.6	2.1	25.7	3.6	10.9
A12	10.2	58.7	33.2	42.3	47.6	54.3	64.6	42.8
Min	5.2	8.5	4.0	9.1	0.4	7.7	3.6	10.9
Max	70.9	58.7	64.9	94.0	47.6	54.3	64.6	52.0
Median	10.7	11.1	16.3	23.9	2.6	17.2	19.3	30.1
Average	16.6	17.3	19.9	29.3	7.8	21.3	22.0	31.1
SD	17.6	14.5	16.8	22.9	13.2	12.7	16.5	11.2

Table S 5-9. Concentrations of PAEs in the seawater from the South China Sea. The MDLs of PAEs calculated with individual sampling volume are given in blankets for the calculated concentrations less than MDLs.

Sample	DMP	DEP	DiBP	DnBP	BBP	DEHP	DOP	DNP	Σ 8PAEs
Dissolved PAE (ng/L)									
B03	8.8	3.0	43.4	145.7	0.3	31.9	0.2	0.03	233
B10	9.2	3.6	39.7	101.1	0.2	12.1	0.2	0.03	166
B20	6.9	2.9	23.9	159.5	0.1	17.9	0.1	0.04	211
B24	13.1	2.7	31.2	80.9	0.3	10.3	0.2	0.02	139
N01	6.0	2.4	42.1	187.9	0.7	16.5	0.3	0.03	256
N05	7.4	2.5	35.2	111.8	0.3	18.3	0.2	0.02	176
N08	4.6	1.8	27.7	88.6	0.2	8.6	0.1	0.01	132
N10	7.5	2.9	31.9	121.8	0.6	21.7	0.3	0.05	187
N13	7.6	4.4	68.6	156.9	0.9	14.6	0.3	0.01	253
N17	7.1	3.6	46.9	95.3	0.4	20.6	0.2	0.02	174
N20	7.6	2.9	43.2	144.5	0.6	15.8	0.2	0.03	215
H02	7.7	1.6	41.0	219.2	1.1	27.2	0.6	0.38	299
H08	7.9	3.6	51.0	212.0	0.4	22.4	1.1	0.62	299
H10	8.2	4.8	36.9	118.6	0.4	16.3	0.9	0.55	187
H12	7.4	3.0	27.8	160.0	0.3	7.9	0.1	0.01	207
H16	11.5	5.4	76.3	402.5	1.3	43.4	0.7	0.40	542
H18	8.9	4.8	50.8	242.6	0.4	21.0	0.1	0.02	329
H22	11.3	4.7	63.0	322.8	0.3	14.7	0.2	0.04	417
H25	10.0	4.6	101.4	373.5	1.7	16.0	0.3	0.05	508
H30	17.9	8.5	48.5	99.9	0.2	8.5	0.1	0.01	184
H34	10.9	4.4	41.8	100.5	0.3	9.9	0.1	0.01	168
H39	17.6	11.0	82.1	196.8	0.4	29.7	2.5	1.17	341
H40	22.0	10.2	79.4	165.3	1.4	81.6	0.9	0.07	361
H43	12.3	6.6	46.1	152.3	0.3	17.1	0.6	0.02	235
H45	13.6	2.1	39.4	137.3	0.2	10.9	0.8	0.02	204
Min	4.6	1.6	23.9	80.9	0.1	7.9	0.1	0.0	132
Max	22.0	11.0	101	403	1.7	81.6	2.5	1.2	542
Median	8.8	3.6	43.2	152	0.4	16.5	0.2	0.0	215
Mean	10.1	4.3	48.8	172	0.5	20.6	0.5	0.1	257
SD	4.1	2.5	19.4	85.5	0.4	15.2	0.5	0.3	108
SPM (ng/L)									
B03	0.3	0.7	3.7	5.0	0.1	467	0.9	0.43	478
B10	0.3	0.8	3.4	3.8	0.2	103	0.7	0.17	113
B20	0.4	1.5	9.4	10.4	0.2	97.9	0.6	0.44	121
B24	0.3	1.2	8.0	9.5	0.1	112	0.6	0.22	132
N01	0.2	0.6	4.3	8.1	0.4	444	1.7	1.49	461
N05	0.3	0.7	0.8	2.9	0.1	76.8	0.3	0.06	82
N08	0.3	0.7	1.1	2.4	0.1	73.1	0.4	0.13	78
N10	0.4	0.8	8.1	5.5	0.1	132	0.6	0.23	148
N13	0.3	0.8	3.1	5.5	0.1	108	0.2	0.89	119
N17	0.2	0.9	2.0	3.1	0.2	105	0.8	0.28	112

N20	0.2	1.4	4.8	6.7	0.3	110	0.3	0.14	124
H02	0.2	0.6	3.8	8.9	0.3	363	0.7	1.50	379
H08	0.2	0.8	1.7	7.9	0.2	141	0.9	0.40	153
H10	0.1	0.6	1.4	3.8	0.2	64.9	0.3	0.14	71
H12	0.2	0.6	3.1	6.5	0.1	39.4	0.1	0.06	50
H16	0.2	0.7	2.3	7.9	0.2	280	1.6	1.95	295
H18	0.2	0.8	1.0	3.4	0.1	89.4	0.3	0.42	96
H22	0.3	0.9	2.3	9.8	0.2	311	0.5	0.39	325
H25	0.1	0.4	1.6	9.2	0.2	695	2.2	5.09	714
H30	0.2	0.5	2.1	3.9	0.1	57.6	0.4	0.22	65
H34	0.1	0.6	1.2	3.3	0.2	72.0	0.3	0.66	78
H39	0.2	0.9	8.7	7.9	0.1	156	0.4	0.12	174
H40	0.2	0.7	19.4	16.3	0.2	593	1.0	0.40	631
H43	0.2	1.0	9.6	11.6	0.2	143	0.9	0.22	166
H45	0.2	0.5	1.1	3.0	0.2	70	0.4	0.08	76
Min	0.1	0.4	0.8	2.4	0.1	39	0.1	0.1	50
Max	0.4	1.5	19.4	16.3	0.4	695	2.2	5.1	714
Median	0.2	0.7	3.1	6.5	0.2	110	0.6	0.3	124
Average	0.2	0.8	4.3	6.6	0.2	196	0.7	0.6	210
SD	0.1	0.3	4.2	3.4	0.1	181	0.5	1.0	185

Concentration of Sum PAE (ng/L)

B03	9.0	3.7	47.1	151	0.3	499	1.1	0.5	712
B10	9.4	4.3	43.0	105	0.4	115	0.9	0.2	279
B20	7.3	4.4	33.4	170	0.3	116	0.7	0.5	332
B24	13.4	3.9	39.1	90	0.5	122	0.8	0.2	270
N01	6.2	3.0	46.4	196	1.1	461	2.0	1.5	717
N05	7.7	3.2	36.0	115	0.4	95.1	0.5	0.1	258
N08	4.9	2.5	28.8	91	0.3	81.8	0.5	0.1	210
N10	8.0	3.7	39.9	127	0.7	154	0.9	0.3	335
N13	7.9	5.2	71.7	162	1.0	123	0.5	0.9	372
N17	7.4	4.5	48.9	98	0.5	125	1.0	0.3	286
N20	7.8	4.3	48.0	151	0.9	126	0.5	0.2	339
H02	7.9	2.1	44.8	228	1.4	390	1.2	1.9	677
H08	8.1	4.5	52.7	220	0.7	163	2.0	1.0	452
H10	8.4	5.4	38.3	122	0.5	81.2	1.2	0.7	258
H12	7.6	3.6	30.9	166	0.4	47.3	0.2	0.1	257
H16	11.7	6.1	78.6	410	1.5	323	2.3	2.3	836
H18	9.1	5.6	51.7	246	0.5	110	0.5	0.4	424
H22	11.7	5.6	65.4	333	0.5	325	0.7	0.4	742
H25	10.1	5.0	103.0	383	1.8	711	2.5	5.1	1222
H30	18.1	9.0	50.6	104	0.3	66.2	0.5	0.2	249
H34	11.1	4.9	43.0	104	0.5	81.8	0.3	0.7	246
H39	17.9	12.0	90.8	205	0.6	186	2.9	1.3	516
H40	22.2	10.9	98.8	182	1.6	674	1.9	0.5	992
H43	12.5	7.6	55.6	164	0.5	160	1.5	0.2	402
H45	13.8	2.6	40.6	140	0.4	81.3	1.2	0.1	280
Min	4.9	2.1	28.8	90.4	0.3	47.3	0.2	0.1	210

Max	22.2	12.0	103.0	410	1.8	711	2.9	5.1	1222
Median	9.0	4.5	47.1	162	0.5	125	0.9	0.4	339
Average	10.4	5.1	53.1	179	0.7	217	1.1	0.8	466
Standard deviation	4.1	2.5	20.5	86.8	0.4	190	0.7	1.1	268

Table S 5-10. Comparison with previous studies for the concentrations of 8 PAEs in seawater (ng/L)

Region	DMP	DEP	DiBP	DnBP	BBP	DEHP	DOP	DNP
Arctic(Xie et al., 2007)	n.d.- 0.3	n.d.-0.8	n.d.-0.2	0.008-0.4	n.d.-0.05	n.d.-3.3	-	-
North Sea (Germany)(Xie et al., 2005)	0.23	1.45	-	1.74	0.07	3.8	-	-
North Sea (Belgium)(Huysman et al., 2019)	-	< 25-753	-	< 5-2645	< 10-343	66-766	-	-
East China Sea, China(Wang et al., 2021; Zhang et al., 2018b; Zhang et al., 2020d)	0.08-830	0.25-2404	5-17256	11-17952	0.09-344	9- 9738	n.d. – 52.43	n.d. - 268
Bohai and Yellow Seas, China(Liu et al., 2020; Zhang et al., 2018c)	n.d.-160	1.18-85.9	89.3-2424	n.d.-2226	n.d.-7.8	51.4-3388	n.d.-3.86	-
Pearl River Delta, China(Cao et al., 2022b)	1.7-13.6	<5.1-34.8	<30.2-70.3	<33.2-358	n.d.	12.7-1050	n.d.	-
Mediterranean Sea(Castro-Jimenez and Ratola, 2020; Paluselli et al., 2018a; Sanchez-Avila et al., 2012)	1.4-140	6.9-870	56.5-383.4	63.4-466	1-100	30-5970	n.d.	-
Bay of Biscay, Spain(Prieto et al., 2007)	7.5±0.4	33±3	-	83±7	8±1	-	3.6-93	-
Barkley Sound, Canada(Keil et al., 2011)	-	-	-	18-3000	-	10-950	-	-
Puget Sound, USA(Keil et al., 2011)	-	-	-	-	-	60-640	-	-
Klang River estuary, Australia(Tan, 1995)	-	-	-	-	-	3100-64300	n.d. - 1500	-
South Korea(Heo et al., 2020)	20-100	20-150	-	40-360	-	30-300	-	-
Tropical western Pacific Ocean(Zhang et al., 2019a)	n.d.-7	n.d.-2.1	1.9-14	2.2-13	n.d.-5.5	2.0-9.2	n.d.-1.68	-
Caspian Sea, Iran(Hadjmohammadi et al., 2011)	490	520	-	-	-	-	-	-
Thailand(Malem et al., 2019)	-	-	-	230-770	-	310-1160	n.d.	-
Tunisia(Jebara et al., 2021)	-	< 10-17000	< 5-106000	< 29-30500	-	< 26-168000	-	-
South China Sea(Mi et al., 2023)	0.07-2.17	0.14-1.08	0.06-1.27	0.11-1.58	<n.d.-0.12	0.53-5.62	-	-
This study	4.9-22.2	2.1-12.0	28.8-103	90.4-410	0.3-1.8	47.3-711	0.2-2.9	0.1-5.1

Table S 5-11 Particle-bound fractions (ϕ) of PAEs in seawater from the Bohai and Yellow Seas

Sample	DMP	DEP	DiBP	DnBP	BBP	DEHP	DOP	DNP	Σ 8PAEs
B03	2.8	17.9	7.9	3.3	25.8	93.6	82.3	93.9	67.2
B10	2.8	17.8	7.8	3.7	45.4	89.5	77.9	87.0	40.4
B20	5.3	33.8	28.3	6.1	63.3	84.6	82.4	92.2	36.4
B24	2.5	31.3	20.4	10.6	27.5	91.6	73.8	93.4	48.7
N01	3.5	20.2	9.3	4.1	35.6	96.4	83.9	97.9	64.3
N05	4.2	22.7	2.2	2.5	29.5	80.8	61.6	69.9	31.8
N08	6.1	26.3	3.7	2.6	39.5	89.4	78.2	92.8	37.2
N10	5.2	22.2	20.2	4.3	16.4	85.9	65.8	80.6	44.2
N13	3.9	16.0	4.3	3.4	13.1	88.1	49.2	98.4	32.0
N17	2.9	19.3	4.1	3.1	29.8	83.6	79.0	94.0	39.1
N20	2.1	32.9	10.0	4.4	29.1	87.4	65.7	83.8	36.5
H02	2.0	26.5	8.5	3.9	21.3	93.0	53.6	79.8	55.9
H08	2.6	18.6	3.2	3.6	34.8	86.3	45.5	39.3	33.8
H10	1.6	10.4	3.6	3.1	31.9	79.9	26.1	20.4	27.7
H12	2.8	15.8	10.1	3.9	30.5	83.3	68.2	81.1	19.5
H16	1.5	10.7	2.9	1.9	11.8	86.6	70.0	83.2	35.2
H18	2.0	13.6	1.9	1.4	25.2	81.0	68.5	96.5	22.5
H22	2.9	15.9	3.6	3.0	36.1	95.5	72.6	91.5	43.8
H25	1.4	8.8	1.6	2.4	8.9	97.7	87.5	99.1	58.5
H30	0.9	5.7	4.2	3.7	29.4	87.1	82.8	94.9	26.1
H34	1.0	11.5	2.7	3.2	35.7	88.0	73.9	98.6	31.8
H39	1.4	7.9	9.5	3.9	26.1	84.0	13.3	9.0	33.8
H40	1.1	6.3	19.7	9.0	11.8	87.9	52.9	85.6	63.6
H43	1.9	13.0	17.2	7.1	45.5	89.3	57.3	91.2	41.4
H45	1.3	19.0	2.8	2.1	44.5	86.6	31.1	77.4	27.0
Min	0.9	5.7	1.6	1.4	8.9	79.9	13.3	9.0	19.5
Max	6.1	33.8	28.3	10.6	63.3	97.7	87.5	99.1	67.2
Median	2.5	17.8	4.3	3.6	29.5	87.4	68.5	91.2	36.5
Average	2.6	17.8	8.4	4.0	29.9	87.9	64.1	81.3	39.9
SD	1.4	8.0	7.2	2.1	12.5	4.8	19.2	23.7	13.2

Table S 5-12. Air-sea exchange fluxes of PAEs in the Bohai and Yellow Seas. Positive value indicates water to air volatilization and negative value indicates air to water deposition

F (ng/m²/day)	DMP	DEP	DiBP	DnBP	BBP	DEHP	DOP	DNP
B03	1909	77	5053	25226	40	-2640	-196	-44
B07	1907	75	4961	25064	32	-1867	-336	-44
B10	1908	75	5053	25464	40	-358	-162	-28
B20	1714	22	1342	6083	6	-1220	-111	-54
B24	1707	21	1232	6374	3	-864	-139	-15
N01	261	115	431	4860	4	-405	-66	-8
N05	808	137	596	7231	2	-352	-20	-2
N08	811	139	655	7502	2	117	-21	-2
N10	810	138	632	7392	1	-544	-89	-21
N13	810	136	480	7223	-1	-315	-82	-6
N17	313	27	540	3737	6	-278	-59	-9
N20	313	27	530	3593	5	-253	-51	-14
H02	260	116	420	4698	2	-977	-118	-95
H08	783	165	1812	8980	14	-765	-450	-332
H10	893	169	942	10234	12	-567	-442	-423
H12	19	87	-26	-291	9	-31	-10	-3
H16	602	78	1528	6526	6	-1646	-166	-121
H18	599	77	1493	6523	8	-313	-5	0
H22	18	86	-108	-650	9	-279	-50	-16
H25	891	169	538	8735	3	-711	-140	-30
H30	456	169	567	4669	7	-18	-12	-2
H34	458	174	567	4504	6	-128	-8	-1
H43	677	143	845	7557	7	-2095	-347	-16
H45	679	155	1004	8037	9	-711	-527	-23
Min	18	21	-108	-650	-1	-2640	-527	-423
Max	1909	174	5053	25464	40	117	-5	0
Median	731	115	643	6874	6	-475	-100	-16
Average	817	107	1295	8303	10	-718	-150	-55
SD	589	51	1510	7025	11	706	155	105

Table S 5-13. Particle dry deposition of PAEs in the Bohai and Yellow Seas

F_D (ng/m²/day)	DMP	DEP	DiBP	DnBP	BBP	DEHP	DOP	DNP	Σ₈PAE
AF01	76.5	19.8	186	2337	0.9	199	0.5	0.1	2820
AF02	111	24.9	365	3270	1.8	489	0.5	0.3	4263
AF03	171	20.8	228	3799	0.4	200	0.5	0.2	4420
AF04	123	20.4	199	2681	0.5	139	0.6	0.2	3164
AF05	52.7	11.5	129	1344	0.1	47	0.2	0.2	1585
AF06	58.6	17.3	264	2398	0.7	179	0.3	0.3	2918
AF07	76.9	17.0	284	3519	0.2	91	0.4	0.4	3989
AF08	80.5	18.9	200	2870	0.3	81	0.5	0.7	3252
AF09	104	19.1	292	4962	0.2	169	1.1	0.9	5548
AF10	90.4	20.3	106	1155	0.5	170	0.6	0.6	1543
AF11	128	18.3	181	1941	0.6	302	0.2	0.4	2572
AF12	146	27.2	615	4265	5.0	522	3.9	1.0	5585
Min	52.7	11.5	106.4	1155	0.1	47.0	0.2	0.1	1543
Max	171	27	615	4962	5	522	4	1	5585
Median	97.1	19.4	214.2	2776	0.5	174.0	0.5	0.3	3208
Average	102	20	254	2878	1	215	1	0	3472
Standard deviation	35.8	3.9	134.4	1146	1.4	150.8	1.0	0.3	1333

References

Addis, T.Z., Adu, J.T., Kumarasamy, M., Demlie, M. (2023) Assessment of Existing Fate and Transport Models for Predicting Antibiotic Degradation and Transport in the Aquatic Environment: A Review. *Water* 15.

Adeniyi, A.A., Okedeyi, O.O., Yusuf, K.A. (2011) Flame ionization gas chromatographic determination of phthalate esters in water, surface sediments and fish species in the Ogun river catchments, Ketu, Lagos, Nigeria. *Environmental Monitoring and Assessment* 172, 561-569.

Ajdari, B., Nassiri, M., Zahedi, M.M., Ziyaadini, M. (2018) Determination of phthalate esters in seawater of Chabahar Bay using dispersive liquid-liquid microextraction coupled with GC-FID. *Water Science and Technology* 77, 1782-1790.

Akhbarizadeh, R., Moore, F., Keshavarzi, B., Moeinpour, A. (2017) Microplastics and potentially toxic elements in coastal sediments of Iran's main oil terminal (Khark Island). *Environmental Pollution* 220, 720-731.

Alkan, N., Alkan, A., Castro-Jimenez, J., Royer, F., Papillon, L., Ourgaud, M., Sempere, R. (2021) Environmental occurrence of phthalate and organophosphate esters in sediments across the Gulf of Lion (NW Mediterranean Sea). *Science of the Total Environment* 760.

Alvarez, D.A., Maruya, K.A., Dodder, N.G., Lao, W.J., Furlong, E.T., Smalling, K.L. (2014) Occurrence of contaminants of emerging concern along the California coast (2009-10) using passive sampling devices. *Marine Pollution Bulletin* 81, 347-354.

Ankit, Saha, L., Kumar, V., Tiwari, J., Sweta, Rawat, S., Singh, J., Bauddh, K. (2021) Electronic waste and their leachates impact on human health and environment: Global ecological threat and management. *Environmental Technology & Innovation* 24.

Anon (2014) China plastics industry yearbook. ZHONG GUO SU LIAO JIA GONG GONG YE XIE HUI.

Arfaenia, H., Fazlzadeh, M., Taghizadeh, F., Saeedi, R., Spitz, J., Dobaradaran, S. (2019) Phthalate acid esters (PAEs) accumulation in coastal sediments from regions with different land use configuration along the Persian Gulf. *Ecotoxicology and Environmental Safety* 169, 496-506.

Armstrong, D.L., Rice, C.P., Ramirez, M., Torrents, A. (2018) Fate of four phthalate plasticizers under various wastewater treatment processes. *Journal of Environmental Science and Health Part a-Toxic/Hazardous Substances & Environmental Engineering* 53, 1075-1082.

Bai, X.Y., Pan, K.W., Shoaib, N., Sun, X.M., Wu, X.G., Zhang, L. (2024) Status of phthalate esters pollution in facility agriculture across China: Spatial distribution, risk assessment, and remediation measures. *Science of the Total Environment* 908.

Bakir, A., O'Connor, I.A., Rowland, S.J., Hendriks, A.J., Thompson, R.C. (2016) Relative importance of microplastics as a pathway for the transfer of hydrophobic organic chemicals to marine life. *Environmental Pollution* 219, 56-65.

Bamford, H.A., Ko, F.C., Baker, J.E. (2002) Seasonal and annual air-water exchange of polychlorinated biphenyls across Baltimore Harbor and the northern Chesapeake Bay. *Environmental Science & Technology* 36, 4245-4252.

Bamford, H.A., Offenberg, J.H., Larsen, R.K., Ko, F.C., Baker, J.E. (1999) Diffusive exchange of polycyclic aromatic hydrocarbons across the air-water interface of the Patapsco River, an urbanized subestuary of the Chesapeake Bay. *Environmental Science & Technology* 33, 2138-2144.

- Bao, L.J., Guo, Y., Liu, L.Y., Zeng, E.Y. (2017) Organic Contaminants in the Pearl River Delta, South China: Environmental Behavior and Human Exposure. *Progress in Chemistry* 29, 943-961.
- Bekele, T.G., Zhao, H.X., Wang, Q.Z., Chen, J.W. (2019) Bioaccumulation and Trophic Transfer of Emerging Organophosphate Flame Retardants in the Marine Food Webs of Laizhou Bay, North China. *Environmental Science & Technology* 53, 13417-13426.
- Bekele, T.G., Zhao, H.X., Yang, J., Chegen, R.G., Chen, J.W., Mekonen, S., Qadeer, A. (2021) A review of environmental occurrence, analysis, bioaccumulation, and toxicity of organophosphate esters. *Environmental Science and Pollution Research* 28, 49507-49528.
- Benson, N.U., Fred-Ahmadu, O.H. (2020) Occurrence and distribution of microplastics-sorbed phthalic acid esters (PAEs) in coastal psammitic sediments of tropical Atlantic Ocean, Gulf of Guinea. *Science of the Total Environment* 730.
- Bester, K. (2005) Comparison of TCPP concentrations in sludge and wastewater in a typical German sewage treatment plant - comparison of sewage sludge from 20 plants. *Journal of Environmental Monitoring* 7, 509-513.
- Bidleman, T.F. (1988) Atmospheric processes - wet and dry deposition of organic-compounds are controlled by vapor particle partitioning. *Environmental Science & Technology* 22, 361-367.
- Billings, A., Jones, K.C., Pereira, M.G., Spurgeon, D.J. (2024) Emerging and legacy plasticisers in coastal and estuarine environments: A review. *Science of the Total Environment* 908.
- Blum, A., Behl, M., Birnbaum, L.S., Diamond, M.L., Phillips, A., Singla, V., Sipes, N.S., Stapleton, H.M., Venier, M. (2019) Organophosphate Ester Flame Retardants: Are They a Regrettable Substitution for Polybrominated Diphenyl Ethers? *Environmental Science & Technology Letters* 6, 638-649.
- Bollmann, U.E., Moeler, A., Xie, Z., Ebinghaus, R., Einax, J.W. (2012a) Occurrence and fate of organophosphorus flame retardants and plasticizers in coastal and marine surface waters. *Water Research* 46, 531-538.
- Bollmann, U.E., Moler, A., Xie, Z.Y., Ebinghaus, R., Einax, J.W. (2012b) Occurrence and fate of organophosphorus flame retardants and plasticizers in coastal and marine surface waters. *Water Research* 46, 531-538.
- Cai, M.G., Duan, M.S., Guo, J.Q., Liu, M.Y., Qi, A.X., Lin, Y., Liang, J.H. (2018) PAHs in the Northern South China Sea: Horizontal transport and downward export on the continental shelf. *Marine Chemistry* 202, 121-129.
- Cao, D.D., Guo, J.H., Wang, Y.W., Li, Z.N., Liang, K., Corcoran, M.B., Hosseini, S., Bonina, S.M.C., Rockne, K.J., Sturchio, N.C., Giesy, J.P., Liu, J.F., Li, A., Jiang, G.B. (2017) Organophosphate Esters in Sediment of the Great Lakes. *Environmental Science & Technology* 51, 1441-1449.
- Cao, Y., Lin, H.J., Wang, Q., Li, J., Liu, M.Y., Zhang, K., Xu, S.P., Huang, G.L., Ruan, Y.F., Wu, J., Leung, K.M.Y., Lam, P.K. (2022a) Significant riverine inputs of typical plastic additives-phthalate esters from the Pearl River Delta to the northern South China Sea. *Science of the Total Environment* 849.
- Cao, Y.R., Li, J., Wu, R.B., Lin, H.J., Lao, J.Y., Ruan, Y.F., Zhang, K., Wu, J.X., Leung, K.M.Y., Lam, P.K.S. (2022b) Phthalate esters in seawater and sediment of the northern South China Sea: Occurrence, distribution, and ecological risks. *Science of the Total Environment* 811.
- Cao, Y.R., Lin, H.J., Wang, Q., Li, J., Liu, M.Y., Zhang, K., Xu, S.P., Huang, G.L., Ruan, Y.F., Wu, J.X., Leung, K.M.Y., Lam, P.K.S. (2022c) Significant riverine inputs of typical plastic additives-phthalate esters from the Pearl River Delta to the northern South China Sea. *Science of the Total Environment* 849.
- Cao, Y.R., Lin, H.J., Zhang, K., Xu, S.P., Yan, M., Leung, K.M.Y., Lam, P.K.S. (2022d) Microplastics: A major source of phthalate esters in aquatic environments. *Journal of Hazardous Materials* 432.

- Cao, Y.R., Xu, S.P., Zhang, K., Lin, H.J., Wu, R.B., Lao, J.Y., Tao, D.Y., Liu, M.Y., Leung, K.M.Y., Lam, P.K.S. (2022e) Spatiotemporal occurrence of phthalate esters in stormwater drains of Hong Kong, China: Mass loading and source identification. *Environmental Pollution* 308.
- Castro-Jimenez, J., Berrojalbiz, N., Pizarro, M., Dachs, J. (2014) Organophosphate Ester (OPE) Flame Retardants and Plasticizers in the Open Mediterranean and Black Seas Atmosphere. *Environmental Science & Technology* 48, 3203-3209.
- Castro-Jiménez, J., Berrojalbiz, N., Pizarro, M., Dachs, J. (2014) Organophosphate Ester (OPE) Flame Retardants and Plasticizers in the Open Mediterranean and Black Seas Atmosphere. *Environmental Science & Technology* 48, 3203-3209.
- Castro-Jimenez, J., Gonzalez-Gaya, B., Pizarro, M., Casal, P., Pizarro-Alvarez, C., Dachs, J. (2016) Organophosphate Ester Flame Retardants and Plasticizers in the Global Oceanic Atmosphere. *Environmental Science & Technology* 50, 12831-12839.
- Castro-Jiménez, J., González-Gaya, B., Pizarro, M., Casal, P., Pizarro-Alvarez, C., Dachs, J. (2016) Organophosphate Ester Flame Retardants and Plasticizers in the Global Oceanic Atmosphere. *Environmental Science & Technology* 50, 12831-12839.
- Castro-Jimenez, J., Ratola, N. (2020) An innovative approach for the simultaneous quantitative screening of organic plastic additives in complex matrices in marine coastal areas. *Environmental Science and Pollution Research* 27, 11450-11457.
- Castro-Jiménez, J., Sempéré, R. (2018) Atmospheric particle-bound organophosphate ester flame retardants and plasticizers in a North African Mediterranean coastal city (Bizerte, Tunisia). *Science of the Total Environment* 642, 383-393.
- Chang, B.V., Wang, T.H., Yuan, S.Y. (2007) Biodegradation of four phthalate esters in sludge. *Chemosphere* 69, 1116-1123.
- Chen, C.F., Chen, C.W., Ju, Y.R., Dong, C.D. (2017) Determination and assessment of phthalate esters content in sediments from Kaohsiung Harbor, Taiwan. *Marine Pollution Bulletin* 124, 767-774.
- Chen, C.T.A. (2009) Chemical and physical fronts in the Bohai, Yellow and East China seas. *Journal of Marine Systems* 78, 394-410.
- Chen, C.W., Chen, C.F., Dong, C.D. (2013) Distribution of Phthalate Esters in Sediments of Kaohsiung Harbor, Taiwan. *Soil & Sediment Contamination* 22, 119-131.
- Chen, M.Q., Gan, Z.W., Qu, B., Chen, S.B., Dai, Y.Y., Bao, X.M. (2019) Temporal and seasonal variation and ecological risk evaluation of flame retardants in seawater and sediments from Bohai Bay near Tianjin, China during 2014 to 2017. *Marine Pollution Bulletin* 146, 874-883.
- Chen, W.D., Chi, C.C., Zhou, C., Xia, M., Ronda, C., Shen, X.Y. (2018) Analysis of the influencing factors of PAEs volatilization from typical plastic products. *Journal of Environmental Sciences* 66, 61-70.
- Chen, W.L., Xie, Z.Y., Wolschke, H., Gandrass, J., Kötke, D., Winkelmann, M., Ebinghaus, R. (2016) Quantitative determination of ultra-trace carbazoles in sediments in the coastal environment. *Chemosphere* 150, 586-595.
- Chen, X.M., An, H., Ao, L., Sun, L., Liu, W.B., Zhou, Z.Y., Wang, Y.X., Cao, J. (2011) The combined toxicity of dibutyl phthalate and benzo(a)pyrene on the reproductive system of male Sprague Dawley rats. *Journal of Hazardous Materials* 186, 835-841.
- Chen, Y.L., Wang, Y.L., Tan, Y., Jiang, C.X., Li, T.Y., Yang, Y.Y., Zhang, Z.L. (2023) Phthalate esters in the Largest River of Asia: An exploration as indicators of microplastics. *Science of the Total Environment* 902.

Chen, Z.Y., Qiu, S., Zhang, C.C., Zhan, Y., Liu, L.R., Bao, Y.G., Chen, B., Bai, Y.J., Zheng, X.N., Huang, Y., Jin, K., Han, P., Wei, Q. (2022) Association of urinary organophosphate esters level with sex steroid hormones levels in adult males: A nationwide study, NHANES 2013-2014. *Andrology* 10, 567-575.

Chi, J. (2009) Phthalate acid esters in L. from Haihe River, China. *Chemosphere* 77, 48-52.

Choi, G., Keil, A.P., Villanger, G.D., Richardson, D.B., Daniels, J.L., Hoffman, K., Sakhi, A.K., Thomsen, C., Herring, A.H., Drover, S.S.M., Nethery, R., Aase, H., Engel, S.M. (2021) Pregnancy exposure to common-detect organophosphate esters and phthalates and maternal thyroid function. *Science of the Total Environment* 782.

Choi, W., Lee, S., Lee, H.-K., Moon, H.-B. (2020) Organophosphate flame retardants and plasticizers in sediment and bivalves along the Korean coast: Occurrence, geographical distribution, and a potential for bioaccumulation. *Marine Pollution Bulletin* 156.

Cleys, P., Hardy, E., Bamai, Y.A., Poma, G., Cseresznye, A., Malarvannan, G., Scheepers, P.T.J., Viegas, S., Porras, S.P., Santonen, T., Godderis, L., Verdonck, J., Poels, K., Martins, C., Silva, M.J., Louro, H., Martinson, I., Akülova, L., van Nieuwenhuysse, A., Graumans, M., Mahiout, S., Duca, R.C., Covaci, A. (2024) HBM4EU e-waste study: Occupational exposure of electronic waste workers to phthalates and DINCH in Europe. *International Journal of Hygiene and Environmental Health* 255.

Cong, B.L., Li, S., Liu, S.H., Mi, W.Y., Liu, S.F., Zhang, Z.H., Xie, Z.Y. (2022) Source and Distribution of Emerging and Legacy Persistent Organic Pollutants in the Basins of the Eastern Indian Ocean. *Environmental Science & Technology* 56, 4199-4209.

Cousins, I., Mackay, D. (2000) Correlating the physical-chemical properties of phthalate esters using the 'three solubility' approach. *Chemosphere* 41, 1389-1399.

Cristale, J., Dantas, R.F., De Luca, A., Sans, C., Esplugas, S., Lacorte, S. (2017) Role of oxygen and DOM in sunlight induced photodegradation of organophosphorous flame retardants in river water. *Journal of Hazardous Materials* 323, 242-249.

Ding, Y., Han, M.W., Wu, Z.Q., Zhang, R.J., Li, A., Yu, K.F., Wang, Y.H., Huang, W., Zheng, X.B., Mai, B.X. (2020) Bioaccumulation and trophic transfer of organophosphate esters in tropical marine food web, South China Sea. *Environment International* 143.

Ding, Y.C., Zou, X.Q., Wang, C.L., Feng, Z.Y., Wang, Y., Fan, Q.Y., Chen, H.Y. (2021) The abundance and characteristics of atmospheric microplastic deposition in the northwestern South China Sea in the fall. *Atmospheric Environment* 253, 118389.

Diss_Dreyer, (2009) Atmospheric Distribution and Seasonality of Airborne Polyfluorinated Compounds: Spatial and Temporal Concentration Variations from Ship-and Land-Based Measurements in Northern Germany, the Atlantic Ocean, and Polar Regions, Faculty of Biology, Chemistry and Earth Sciences. University of Bayreuth, Bayreuth.

Dong, C.D., Chen, C.W., Nguyen, T.B., Huang, C.P., Hung, C.M. (2020) Degradation of phthalate esters in marine sediments by persulfate over Fe-Ce/biochar composites. *Chemical Engineering Journal* 384.

Du, X., Li, X.H., Luo, T.L., Matsuura, N., Kadokami, K., Chen, J.W. (2013) Occurrence and aquatic ecological risk assessment of typical organic pollutants in water of Yangtze River estuary. 2013 International Symposium on Environmental Science and Technology (2013 Isest) 18, 882-889.

EPA (2019) Chemical Substances Undergoing Prioritization: High-Priority. United States Environmental Protection Agency.

F. Mohanty, S.K.S. (2017) Nanotechnology Applications in Food.

- Fan, H., Wang, X.J., Zhang, H.B., Yu, Z.T. (2018) Spatial and temporal variations of particulate organic carbon in the Yellow-Bohai Sea over 2002-2016. *Scientific Reports* 8.
- Fang, G.C., Ho, T.T., Kao, C.L., Zhuang, Y.J. (2021) Particle bound phthalate acid esters (PAEs) and total estimated ambient air PAEs concentrations study at a mixed (commercial, urban, and traffic) site in central Taiwan. *Environmental Forensics*.
- Fang, G.C., Ho, T.T., Kao, C.L., Zhuang, Y.J. (2022) Particle bound phthalate acid esters (PAEs) and total estimated ambient air PAEs concentrations study at a mixed (commercial, urban, and traffic) site in central Taiwan. *Environmental Forensics* 23, 482-490.
- Fang, X., Yang, S., Zhang, H., Gao, X., Yang, G. (2020) Review of organophosphate esters in oceans and atmospheres. *Marine Science* 44, 156-165.
- Fang, Y., Chen, Y.J., Tian, C.G., Wang, X.P., Lin, T., Hu, L.M., Li, J., Zhang, G., Luo, Y.M. (2018) Cycling and Budgets of Organic and Black Carbon in Coastal Bohai Sea, China: Impacts of Natural and Anthropogenic Perturbations. *Global Biogeochemical Cycles* 32, 971-986.
- Fatoki, O.S., Bornman, M., Ravandhalala, L., Chimuka, L., Genthe, B., Adeniyi, A. (2010) Phthalate ester plasticizers in freshwater systems of Venda, South Africa and potential health effects. *Water Sa* 36, 117-125.
- Fatoki, O.S., Noma, A. (2001) Determination of phthalate esters in the aquatic environment. *South African Journal of Chemistry-Suid-Afrikaanse Tydskrif Vir Chemie* 54, 1-15.
- Fauvelle, V., Garel, M., Tamburini, C., Nerini, D., Castro-Jimenez, J., Schmidt, N., Paluselli, A., Fahs, A., Papillon, L., Booth, A.M., Sempere, R. (2021) Organic additive release from plastic to seawater is lower under deep-sea conditions. *Nature Communications* 12.
- Feng, J.R., Deng, Q.X., Ni, H.G. (2022) Photodegradation of phthalic acid esters under simulated sunlight: Mechanism, kinetics, and toxicity change. *Chemosphere* 299.
- Fernandez, M.P., Ikonou, M.G., Buchanan, I. (2007) An assessment of estrogenic organic contaminants in Canadian wastewaters. *Science of the Total Environment* 373, 250-269.
- Forti, V., Baldé, C.P., Kuehr, R., (2020) The Global E-waste Monitor 2020: Quantities, flows and the circular economy potential. United Nations University (UNU)/United Nations Institute for Training and Research (UNITAR) – co-hosted SCYCLE Programme. International Telecommunication Union (ITU) & International Solid Waste Association (ISWA), Bonn/Geneva/Rotter.
- Fries, E., Dekiff, J.H., Willmeyer, J., Nuelle, M.T., Ebert, M., Remy, D. (2013) Identification of polymer types and additives in marine microplastic particles using pyrolysis-GC/MS and scanning electron microscopy. *Environmental Science-Processes & Impacts* 15, 1949-1956.
- Fu, J.M., Mai, B.X., Sheng, G.Y., Zhang, G., Wang, X.M., Peng, P.A., Xiao, X.M., Ran, R., Cheng, F.Z., Peng, X.Z., Wang, Z.S., Tang, U.W. (2003) Persistent organic pollutants in environment of the Pearl River Delta, China: an overview. *Chemosphere* 52, 1411-1422.
- Fu, L.F., Bin, L.Y., Cui, J., Nyobe, D.O.N., Li, P., Huang, S.S., Fu, F.L., Tang, B. (2020) Tracing the occurrence of organophosphate ester along the river flow path and textile wastewater treatment processes by using dissolved organic matters as an indicator. *Science of the Total Environment* 722.
- Fujii, M., Shinohara, N., Lim, A., Otake, T., Kumagai, K., Yanagisawa, Y. (2003) A study on emission of phthalate esters from plastic materials using a passive flux sampler. *Atmospheric Environment* 37, 5495-5504.
- Gao, Y., Arimoto, R., Duce, R.A., Lee, D.S., Zhou, M.Y. (1992) INPUT OF ATMOSPHERIC TRACE-ELEMENTS AND MINERAL MATTER TO THE YELLOW SEA DURING THE SPRING OF A LOW-DUST YEAR. *Journal of Geophysical Research-Atmospheres* 97, 3767-3777.

- Gao, Y., Fu, J.J., Zeng, L.X., Li, A., Li, H.J., Zhu, N.L., Liu, R.Z., Liu, A.F., Wang, Y.W., Jiang, G.B. (2014) Occurrence and fate of perfluoroalkyl substances in marine sediments from the Chinese Bohai Sea, Yellow Sea, and East China Sea. *Environmental Pollution* 194, 60-68.
- Gao, Y., Wang, L.F., Guo, X.H., Xu, Y., Luo, L. (2020) Atmospheric wet and dry deposition of dissolved inorganic nitrogen to the South China Sea. *Science China-Earth Sciences* 63, 1339-1352.
- Gholaminejad, A., Mehdizadeh, G., Dolatimehr, A., Arfaeina, H., Farjadfard, S., Dobaradaran, S., Bonyadi, Z., Ramavandi, B. (2024) Phthalate esters pollution in the leachate, soil, and water around a landfill near the sea, Iran. *Environmental Research* 248.
- Giam, C.S., Atlas, E., Chan, H.S., Neff, G.S. (1980) Phthalate-esters, PCB and DDT residues in the Gulf of Mexico atmosphere. *Atmospheric Environment* 14, 65-69.
- Greaves, A.K., Letcher, R.J. (2017) A Review of Organophosphate Esters in the Environment from Biological Effects to Distribution and Fate. *Bulletin of Environmental Contamination and Toxicology* 98, 2-7.
- Grindler, N.M., Vanderlinden, L., Karthikraj, R., Kannan, K., Teal, S., Polotsky, A.J., Powell, T.L., Yang, I.V., Jansson, T. (2018) Exposure to Phthalate, an Endocrine Disrupting Chemical, Alters the First Trimester Placental Methylome and Transcriptome in Women. *Scientific Reports* 8.
- Gugliandolo, E., Licata, P., Crupi, R., Albergamo, A., Jebara, A., Lo Turco, V., Potorti, A.G., Ben Mansour, H., Cuzzocrea, S., Di Bella, G. (2020a) Plasticizers as Microplastics Tracers in Tunisian Marine Environment. *Frontiers in Marine Science* 7.
- Gugliandolo, E., Licata, P., Crupi, R., Albergamo, A., Jebara, A., Lo Turco, V., Potorti, A.G., Ben Mansour, H., Cuzzocrea, S., Di Bella, G. (2020b) Plasticizers as Microplastics Tracers in Tunisian Marine Environment. *Frontiers in Marine Science* 7.
- Guo, J.H., Romanak, K., Westenbroek, S., Hites, R.A., Venier, M. (2017) Current-Use Flame Retardants in the Water of Lake Michigan Tributaries. *Environmental Science & Technology* 51, 9960-9969.
- Guo, Z.Y., Kodikara, D., Albi, L.S., Hatano, Y., Chen, G., Yoshimura, C., Wang, J.Q. (2023) Photodegradation of organic micropollutants in aquatic environment: Importance, factors and processes. *Water Research* 231.
- Hadjmohammadi, M.R., Fatemi, M.H., Taneh, T. (2011) Coacervative Extraction of Phthalates from Water and Their Determination by High Performance Liquid Chromatography. *Journal of the Iranian Chemical Society* 8, 100-106.
- Han, X., Hao, Y., Li, Y., Yang, R., Wang, P., Zhang, G., Zhang, Q., Jiang, G. (2020) Occurrence and distribution of organophosphate esters in the air and soils of Ny-Ålesund and London Island, Svalbard, Arctic. *Environmental Pollution* 263, 114495.
- Harris, P.T., Tamelander, J., Lyons, Y., Neo, M.L., Maes, T. (2021) Taking a mass-balance approach to assess marine plastics in the South China Sea. *Marine Pollution Bulletin* 171.
- Hassanzadeh, N., Sari, A.E., Khodabandeh, S., Bahramifar, N. (2014) Occurrence and distribution of two phthalate esters in the sediments of the Anzali wetlands on the coast of the Caspian Sea (Iran). *Marine Pollution Bulletin* 89, 128-135.
- He, J., Balasubramanian, R. (2009) A study of precipitation scavenging of semivolatile organic compounds in a tropical area. *Journal of Geophysical Research-Atmospheres* 114.
- He, J., Ma, H., Wang, Z., Li, H., Fan, H., Lian, L., Wu, M., Song, S., Zhang, J., Huang, H., Gao, H., Ma, J. (2023) Atmospheric deposition contributed mostly to organophosphorus flame retardant entering into the Bohai Sea, China. *iScience*.

- He, Y., Wang, Q.M., He, W., Xu, F.L. (2019) Phthalate esters (PAEs) in atmospheric particles around a large shallow natural lake (Lake Chaohu, China). *Science of the Total Environment* 687, 297-308.
- Heo, H., Choi, M.J., Park, J., Nam, T., Cho, J. (2020) Anthropogenic Occurrence of Phthalate Esters in Beach Seawater in the Southeast Coast Region, South Korea. *Water* 12.
- Hidalgo-Serrano, M., Borrull, F., Marce, R.M., Pocurull, E. (2022) Phthalate esters in marine ecosystems: Analytical methods, occurrence and distribution. *Trac-Trends in Analytical Chemistry* 151.
- Hoang, A.Q., Karyu, R., Tue, N.M., Goto, A., Tuyen, L., Matsukami, H., Suzuki, G., Takahashi, S., Viet, P.H., Kunisue, T. (2022) Comprehensive characterization of halogenated flame retardants and organophosphate esters in settled dust from informal e-waste and end-of-life vehicle processing sites in Vietnam: Occurrence, source estimation, and risk assessment. *Environmental Pollution* 310.
- Hou, R., Huang, Q.Y., Pan, Y.F., Lin, L., Liu, S., Li, H.X., Xu, X.R. (2022) Novel Brominated Flame Retardants (NBFRs) in a Tropical Marine Food Web from the South China Sea: The Influence of Hydrophobicity and Biotransformation on Structure-Related Trophodynamics. *Environmental Science & Technology* 56, 3147-3158.
- Hu, L.M., Zhang, G., Zheng, B.H., Qin, Y.W., Lin, T., Guo, Z.G. (2009) Occurrence and distribution of organochlorine pesticides (OCPs) in surface sediments of the Bohai Sea, China. *Chemosphere* 77, 663-672.
- Hu, M.Y., Li, J., Zhang, B.B., Cui, Q.L., Wei, S., Yu, H.X. (2014) Regional distribution of halogenated organophosphate flame retardants in seawater samples from three coastal cities in China. *Marine Pollution Bulletin* 86, 569-574.
- Hu, X.L., Gu, Y.Y., Huang, W.P., Yin, D.Q. (2016) Phthalate monoesters as markers of phthalate contamination in wild marine organisms. *Environmental Pollution* 218, 410-418.
- Huang, P.C., Tien, C.J., Sun, Y.M., Hsieh, C.Y., Lee, C.C. (2008) Occurrence of phthalates in sediment and biota: Relationship to aquatic factors and the biota-sediment accumulation factor. *Chemosphere* 73, 539-544.
- Huang, Y.Q., Zeng, Y., Wang, T., Chen, S.J., Guan, Y.F., Mai, B.X. (2022) PM_{2.5}-bound phthalates and phthalate substitutes in a megacity of southern China: spatioseasonal variations, source apportionment, and risk assessment. *Environmental Science and Pollution Research* 29, 37737-37747.
- Huo, C.Y., Li, W.L., Liu, L.Y., Sun, Y., Guo, J.Q., Wang, L., Hung, H., Li, Y.F. (2023) Seasonal variations of airborne phthalates and novel non-phthalate plasticizers in a test residence in cold regions: Effects of temperature, humidity, total suspended particulate matter, and sources. *Science of the Total Environment* 863.
- Huysman, S., Van Meulebroek, L., Janssens, O., Vanryckeghem, F., Van Langenhove, H., Demeestere, K., Vanhaecke, L. (2019) Targeted quantification and untargeted screening of alkylphenols, bisphenol A and phthalates in aquatic matrices using ultra-high-performance liquid chromatography coupled to hybrid Q-Orbitrap mass spectrometry. *Analytica Chimica Acta* 1049, 141-151.
- Iakovides, M., Apostolaki, M., Stephanou, E.G. (2021) PAHs, PCBs and organochlorine pesticides in the atmosphere of Eastern Mediterranean: Investigation of their occurrence, sources and gas-particle partitioning in relation to air mass transport pathways. *Atmospheric Environment* 244.
- Jambeck, J.R., Geyer, R., Wilcox, C., Siegler, T.R., Perryman, M., Andrady, A., Narayan, R., Law, K.L. (2015) Plastic waste inputs from land into the ocean. *Science* 347, 768-771.
- Jan, S., Chang, M.H., Yang, Y.J., Sui, C.H., Cheng, Y.H., Yeh, Y.Y., Lee, C.W. (2021) Mooring observed intraseasonal oscillations in the central South China Sea during summer monsoon season. *Scientific Reports* 11.

Jansen, M.A.K., Andrady, A.L., Bornman, J.F., Aucamp, P.J., Bais, A.F., Banaszak, A.T., Barnes, P.W., Bernhard, G.H., Bruckman, L.S., Busquets, R., Häder, D.P., Hanson, M.L., Heikkilä, A.M., Hylander, S., Lucas, R.M., Mackenzie, R., Madronich, S., Neale, P.J., Neale, R.E., Olsen, C.M., Ossola, R., Pandey, K.K., Petropavlovskikh, I., Revell, L.E., Robinson, S.A., Robson, T.M., Rose, K.C., Solomon, K.R., Andersen, M.P.S., Sulzberger, B., Wallington, T.J., Wang, Q.W., Waengberg, S.A., White, C.C., Young, A.R., Zepp, R.G., Zhu, L.P. (2024) Plastics in the environment in the context of UV radiation, climate change and the Montreal Protocol: UNEP Environmental Effects Assessment Panel, Update 2023. *Photochemical & Photobiological Sciences* 23, 629-650.

Jebara, A., Albergamo, A., Rando, R., Potortì, A.G., Lo Turco, V., Ben Mansour, H., Di Bella, G. (2021) Phthalates and non-phthalate plasticizers in Tunisian marine samples: Occurrence, spatial distribution and seasonal variation. *Marine Pollution Bulletin* 163.

Ju, X., Ma, C., Yao, Z.G., Bao, X.W. (2020) Case analysis of water exchange between the Bohai and Yellow Seas in response to high winds in winter. *Journal of Oceanology and Limnology* 38, 30-41.

Jurado, E., Jaward, F.M., Lohmann, R., Jones, K.C., Simó, R., Dachs, J. (2004) Atmospheric dry deposition of persistent organic pollutants to the Atlantic and inferences for the global oceans. *Environmental Science & Technology* 38, 5505-5513.

Kanaujija, D.K., More, A., Chhantyal, A.K., Karn, R., Pakshirajan, K. (2023) Biodegradation of low, medium and high molecular weight phthalate by *Gordonia* sp. in a batch system: Kinetics and phytotoxicity analyses. *Bioengineered* 14, 195-211.

Kang, L., Wang, Q.M., He, Q.S., He, W., Liu, W.X., Kong, X.Z., Yang, B., Yang, C., Jiang, Y.J., Xu, F.L. (2016) Current status and historical variations of phthalate ester (PAE) contamination in the sediments from a large Chinese lake (Lake Chaohu). *Environmental Science and Pollution Research* 23, 10393-10405.

Kastner, J., Cooper, D.G., Maric, M., Dodd, P., Yargeau, V. (2012) Aqueous leaching of di-2-ethylhexyl phthalate and "green" plasticizers from poly(vinyl chloride). *Science of the Total Environment* 432, 357-364.

Keil, R., Salemme, K., Forrest, B., Neibauer, J., Logsdon, M. (2011) Differential presence of anthropogenic compounds dissolved in the marine waters of Puget Sound, WA and Barkley Sound, BC. *Marine Pollution Bulletin* 62, 2404-2411.

Keith, L.H., Telliard, W.A. (1979) Priority Pollutants I-a Perspective View. *Environmental Science & Technology* 13, 416-423.

Kim, S., Lee, Y.S., Moon, H.B. (2020) Occurrence, distribution, and sources of phthalates and non-phthalate plasticizers in sediment from semi-enclosed bays of Korea. *Marine Pollution Bulletin* 151.

Kim, U.J., Kannan, K. (2018) Occurrence and Distribution of Organophosphate Flame Retardants/Plasticizers in Surface Waters, Tap Water, and Rainwater: Implications for Human Exposure. *Environmental Science & Technology* 52, 5625-5633.

Kim, U.J., Wang, Y., Li, W.H., Kannan, K. (2019) Occurrence of and human exposure to organophosphate flame retardants/plasticizers in indoor air and dust from various microenvironments in the United States. *Environment International* 125, 342-349.

Konstas, P.S., Hela, D., Giannakas, A., Triantafyllos, A., Konstantinou, I. (2019) Photocatalytic degradation of organophosphate flame retardant TBEP: kinetics and identification of transformation products by orbitrap mass spectrometry. *International Journal of Environmental Analytical Chemistry* 99, 297-309.

Kurt-Karakus, P., Alegria, H., Birgul, A., Gungormus, E., Jantunen, L. (2018) Organophosphate ester (OPEs) flame retardants and plasticizers in air and soil from a highly industrialized city in Turkey. *Science of the Total Environment* 625, 555-565.

- Kwan, W.S., Roy, V.A.L., Yu, K.N. (2021) Review on Toxic Effects of Di(2-ethylhexyl) Phthalate on Zebrafish Embryos. *Toxics* 9.
- Lai, N.L.S., Kwok, K.Y., Wang, X.-h., Yamashita, N., Liu, G., Leung, K.M.Y., Lam, P.K.S., Lam, J.C.W. (2019a) Assessment of organophosphorus flame retardants and plasticizers in aquatic environments of China (Pearl River Delta, South China Sea, Yellow River Estuary) and Japan (Tokyo Bay). *Journal of Hazardous Materials* 371, 288-294.
- Lai, N.L.S., Kwok, K.Y., Wang, X.H., Yamashita, N., Liu, G.J., Leung, K.M.Y., Lam, P.K.S., Lam, J.C.W. (2019b) Assessment of organophosphorus flame retardants and plasticizers in aquatic environments of China (Pearl River Delta, South China Sea, Yellow River Estuary) and Japan (Tokyo Bay). *Journal of Hazardous Materials* 371, 288-294.
- Lai, S.C., Xie, Z.Y., Song, T.L., Tang, J.H., Zhang, Y.Y., Mi, W.Y., Peng, J.H., Zhao, Y., Zou, S.C., Ebinghaus, R. (2015) Occurrence and dry deposition of organophosphate esters in atmospheric particles over the northern South China Sea. *Chemosphere* 127, 195-200.
- Lamichhane, G., Acharya, A., Marahatha, R., Modi, B., Paudel, R., Adhikari, A., Raut, B.K., Aryal, S., Parajuli, N. (2023) Microplastics in environment: global concern, challenges, and controlling measures. *International Journal of Environmental Science and Technology* 20, 4673-4694.
- Lange, J.P. (2021) Managing Plastic Waste-Sorting, Recycling, Disposal, and Product Redesign. *Acs Sustainable Chemistry & Engineering* 9, 15722-15738.
- Lao, J.Y., Wu, R.B., Cui, Y.S., Zhou, S.W., Ruan, Y.F., Leung, K.M.Y., Wu, J.X., Zeng, E.Y., Lam, P.K.S. (2022) Significant input of organophosphate esters through particle-mediated transport into the Pearl River Estuary, China. *Journal of Hazardous Materials* 438.
- Latini, G. (2005) Monitoring phthalate exposure in humans. *Clinica Chimica Acta* 361, 20-29.
- Lebreton, L., Egger, M., Slat, B. (2019) A global mass budget for positively buoyant macroplastic debris in the ocean. *Scientific Reports* 9.
- Lee, Y.M., Lee, J.E., Choe, W., Kim, T., Lee, J.Y., Kho, Y., Choi, K., Zoh, K.D. (2019) Distribution of phthalate esters in air, water, sediments, and fish in the Asan Lake of Korea. *Environment International* 126, 635-643.
- Lee, Y.S., Lim, J.E., Lee, S., Moon, H.B. (2020) Phthalates and non-phthalate plasticizers in sediment from Korean coastal waters: Occurrence, spatial distribution, and ecological risks. *Marine Pollution Bulletin* 154.
- Leistenschneider, C., Burkhardt-Holm, P., Mani, T., Primpke, S., Taubner, H., Gerdt, G. (2021) Microplastics in the Weddell Sea (Antarctica): A Forensic Approach for Discrimination between Environmental and Vessel-Induced Microplastics. *Environmental Science & Technology* 55, 15900-15911.
- Li, J., Liu, X.A., Zhang, G., Li, X.D. (2010) Particle deposition fluxes of BDE-209, PAHs, DDTs and chlordane in the Pearl River Delta, South China. *Science of the Total Environment* 408, 3664-3670.
- Li, J., Tang, J.H., Mi, W.Y., Tian, C.G., Emeis, K.C., Ebinghaus, R., Xie, Z.Y. (2018a) Spatial Distribution and Seasonal Variation of Organophosphate Esters in Air above the Bohai and Yellow Seas, China. *Environmental Science & Technology* 52, 89-97.
- Li, J., Wang, J., Taylor, A.R., Cryder, Z., Schlenk, D., Gan, J. (2019a) Inference of Organophosphate Ester Emission History from Marine Sediment Cores Impacted by Wastewater Effluents. *Environmental Science & Technology* 53, 8767-8775.
- Li, J., Xie, Z.Y., Mi, W.Y., Lai, S.C., Tian, C.G., Emeis, K.C., Ebinghaus, R. (2017a) Organophosphate Esters in Air, Snow, and Seawater in the North Atlantic and the Arctic. *Environmental Science & Technology* 51, 6887-6896.

- Li, Q.F., Lu, Y.L., Wang, P., Wang, T.Y., Zhang, Y.Q., Suriyanarayanan, S., Liang, R.Y., Baninla, Y., Khan, K. (2018b) Distribution, source, and risk of organochlorine pesticides (OCPs) and polychlorinated biphenyls (PCBs) in urban and rural soils around the Yellow and Bohai Seas, China. *Environmental Pollution* 239, 233-241.
- Li, Q.F., Zhang, Y.Q., Lu, Y.L., Wang, P., Suriyanarayanan, S., Meng, J., Zhou, Y.Q., Liang, R.Y., Khan, K. (2018c) Risk ranking of environmental contaminants in Xiaoqing River, a heavily polluted river along urbanizing Bohai Rim. *Chemosphere* 204, 28-35.
- Li, R.J., Gao, H., Hou, C., Fu, J., Shi, T.D., Wu, Z.L., Jin, S.C., Yao, Z.W., Na, G.S., Ma, X.D. (2023a) Occurrence, source, and transfer fluxes of organophosphate esters in the South Pacific and Fildes Peninsula, Antarctic. *Science of the Total Environment* 894.
- Li, R.L., Liang, J., Duan, H.L., Gong, Z.B. (2017b) Spatial distribution and seasonal variation of phthalate esters in the Jiulong River estuary, Southeast China. *Marine Pollution Bulletin* 122, 38-46.
- Li, R.L., Liang, J., Gong, Z.B., Zhang, N.N., Duan, H.L. (2017c) Occurrence, spatial distribution, historical trend and ecological risk of phthalate esters in the Jiulong River, Southeast China. *Science of the Total Environment* 580, 388-397.
- Li, T.Y., Bao, L.J., Wu, C.C., Liu, L.Y., Wong, C.S., Zeng, E.Y. (2019b) Organophosphate flame retardants emitted from thermal treatment and open burning of e-waste. *Journal of Hazardous Materials* 367, 390-396.
- Li, X.H., Yin, P.H., Zhao, L. (2016) Phthalate esters in water and surface sediments of the Pearl River Estuary: distribution, ecological, and human health risks. *Environmental Science and Pollution Research* 23, 19341-19349.
- Li, X.Y., Yu, R.C., Richardson, A.J., Sun, C.J., Eriksen, R., Kong, F.Z., Zhou, Z.X., Geng, H.X., Zhang, Q.C., Zhou, M.J. (2023b) Marked shifts of harmful algal blooms in the Bohai Sea linked with combined impacts of environmental changes. *Harmful Algae* 121.
- Li, Y.J., Wang, J.H., Ren, B.N., Wang, H.L., Qiao, L.P., Zhu, J.P., Li, L. (2018d) The characteristics of atmospheric phthalates in Shanghai: A haze case study and human exposure assessment. *Atmospheric Environment* 178, 80-86.
- Lian, M.S., Lin, C.Y., Wu, T.T., Xin, M., Gu, X., Lu, S., Cao, Y.X., Wang, B.D., Ouyang, W., Liu, X.T., He, M.C. (2021) Occurrence, spatiotemporal distribution, and ecological risks of organophosphate esters in the water of the Yellow River to the Laizhou Bay, Bohai Sea. *Science of the Total Environment* 787.
- Liang, K., Liu, J.F. (2016) Understanding the distribution, degradation and fate of organophosphate esters in an advanced municipal sewage treatment plant based on mass flow and mass balance analysis. *Science of the Total Environment* 544, 262-270.
- Liang, W., Wang, Y., Mu, J.L., Wu, N., Wang, J.Y., Liu, S.M. (2023) Nutrient changes in the Bohai Sea over the past two decades. *Science of the Total Environment* 903.
- Liao, R., Xv, Y., Zhong, Q., Xv, S. (2015) Distribution characteristics and ecological evaluation of chlorobenzene compounds in surface sediment of the Maowei Sea, Guangxi, China. *Ecol. Environ. Sci.* 24, 1342-1347.
- Ligocki, M.P., Leuenberger, C., Pankow, J.F. (1967) Trace organic compounds in rains-III. Particle scavenging of neutral organic compounds. *Atmospheric Environment* 19, 1619-1626.
- Lin, X.Q., Zhou, X., Wang, P.F. (2023) Spatial differentiation and influencing factors of industrial resource and environmental pressures in China. *Environment Development and Sustainability* 25, 9991-10015.

- Liu, B.L., Lv, L.Y., Ding, L.J., Gao, L., Li, J.J., Ma, X.Y., Yu, Y. (2024) Comparison of phthalate esters (PAEs) in freshwater and marine food webs: Occurrence, bioaccumulation, and trophodynamics. *Journal of Hazardous Materials* 466.
- Liu, F.B., Xu, Y., Liu, J.W., Liu, D., Li, J., Zhang, G., Li, X.D., Zou, S.C., Lai, S.C. (2013a) Atmospheric deposition of polycyclic aromatic hydrocarbons (PAHs) to a coastal site of Hong Kong, South China. *Atmospheric Environment* 69, 265-272.
- Liu, J.Y. (2013) Status of Marine Biodiversity of the China Seas. *Plos One* 8.
- Liu, K., Xiao, H., Zhang, Y.H., He, H., Li, S.Y., Yang, S.G., Li, H.M. (2023a) Gas-particle partitioning of organophosphate esters in indoor and outdoor air and its implications for individual exposure. *Environment International* 181.
- Liu, M.Y., Ding, Y.C., Huang, P., Zheng, H., Wang, W.M., Ke, H.W., Chen, F.J., Liu, L.H., Cai, M. (2021a) Microplastics in the western Pacific and South China Sea: Spatial variations reveal the impact of Kuroshio intrusion*. *Environmental Pollution* 288.
- Liu, S.M., Zhang, J., Li, D.J. (2004) Phosphorus cycling in sediments of the Bohai and Yellow Seas. *Estuarine Coastal and Shelf Science* 59, 209-218.
- Liu, S.Y., Xu, J.J., Tu, S.F., Zheng, M.Y., Chen, Z.Q. (2023b) Relationship between South China Sea Summer Monsoon and Western North Pacific Tropical Cyclones Linkages with the Interaction of Indo-Pacific Pattern. *Atmosphere* 14.
- Liu, Y., Chen, Z.L., Shen, J.M. (2013b) Occurrence and Removal Characteristics of Phthalate Esters from Typical Water Sources in Northeast China. *Journal of Analytical Methods in Chemistry* 2013.
- Liu, Y., Guan, Y.T., Yang, Z.H., Cai, Z.H., Mizuno, T., Tsuno, H., Zhu, W.P., Zhang, X.H. (2009) Toxicity of seven phthalate esters to embryonic development of the abalone. *Ecotoxicology* 18, 293-303.
- Liu, Y., Huang, L., Li, S.M., Harner, T., Liggio, J. (2014a) OH-initiated heterogeneous oxidation of tris-2-butoxyethyl phosphate: implications for its fate in the atmosphere. *Atmospheric Chemistry and Physics* 14, 12195-12207.
- Liu, Y., Liggio, J., Harner, T., Jantunen, L., Shoeib, M., Li, S.-M. (2014b) Heterogeneous OH Initiated Oxidation: A Possible Explanation for the Persistence of Organophosphate Flame Retardants in Air. *Environmental Science & Technology* 48, 1041-1048.
- Liu, Y., Tang, Y., He, Y., Liu, H.J., Tao, S., Liu, W.X. (2023c) Riverine inputs, spatiotemporal variations, and potential sources of phthalate esters transported into the Bohai Sea from an urban river in northern China. *Science of the Total Environment* 878.
- Liu, Y.C., Liggio, J., Harner, T., Jantunen, L., Shoeib, M., Li, S.M. (2014c) Heterogeneous OH Initiated Oxidation: A Possible Explanation for the Persistence of Organophosphate Flame Retardants in Air. *Environmental Science & Technology* 48, 1041-1048.
- Liu, Y.D., Li, Z.Z., Jalon-Rojas, I., Wang, X.H., Fredj, E., Zhang, D.H., Feng, L.J., Li, X.G. (2020) Assessing the potential risk and relationship between microplastics and phthalates in surface seawater of a heavily human-impacted metropolitan bay in northern China. *Ecotoxicology and Environmental Safety* 204.
- Liu, Y.E., Tang, B., Liu, Y., Luo, X.J., Mai, B.X., Covaci, A., Poma, G. (2019) Occurrence, biomagnification and maternal transfer of legacy and emerging organophosphorus flame retardants and plasticizers in water snake from an e-waste site. *Environment International* 133.
- Liu, Y.X., Gong, S., Ye, L.J., Li, J.H., Liu, C.S., Chen, D., Fang, M.L., Letcher, R.J., Su, G.Y. (2021b) Organophosphate (OP) diesters and a review of sources, chemical properties, environmental occurrence, adverse effects, and future directions. *Environment International* 155.

Liu, Z., Sun, Y.X., Zeng, Y., Guan, Y.F., Huang, Y.Q., Chen, Y.P., Li, D.N., Mo, L., Chen, S.J., Mai, B.X. (2022) Semi-volatile organic compounds in fine particulate matter on a tropical island in the South China Sea. *Journal of Hazardous Materials* 426.

Lohmann, R., Jaward, F.M., Durham, L., Barber, J.L., Ockenden, W., Jones, K.C., Bruhn, R., Lakaschus, S., Dachs, J., Booij, K. (2004) Potential contamination of shipboard air samples by diffusive emissions of PCBs and other organic pollutants: Implications and solutions. *Environmental Science & Technology* 38, 3965-3970.

Ma, J., Chen, L.L., Guo, Y., Wu, Q., Yang, M., Wu, M.H., Kannan, K. (2014) Phthalate diesters in Airborne PM and PM in a suburban area of Shanghai: Seasonal distribution and risk assessment. *Science of the Total Environment* 497, 467-474.

Ma, T.T., Christie, P., Luo, Y.M., Teng, Y. (2013) Phthalate esters contamination in soil and plants on agricultural land near an electronic waste recycling site. *Environmental Geochemistry and Health* 35, 465-476.

Ma, Y.L., Stubbings, W.A., Abdallah, M.A.E., Cline-Cole, R., Harrad, S. (2022) Formal waste treatment facilities as a source of halogenated flame retardants and organophosphate esters to the environment: A critical review with particular focus on outdoor air and soil. *Science of the Total Environment* 807.

Ma, Y.X., Xie, Z.Y., Lohmann, R., Mi, W.Y., Gao, G.P. (2017) Organophosphate Ester Flame Retardants and Plasticizers in Ocean Sediments from the North Pacific to the Arctic Ocean. *Environmental Science & Technology* 51, 3809-3815.

Mackintosh, C.E., Maldonado, J.A., Ikononou, M.G., Gobas, F. (2006) Sorption of phthalate esters and PCBs in a marine ecosystem. *Environmental Science & Technology* 40, 3481-3488.

Maddela, N.R., Kakarla, D., Venkateswarlu, K., Megharaj, M. (2023) Additives of plastics: Entry into the environment and potential risks to human and ecological health. *Journal of Environmental Management* 348.

Mai, L., Bao, L.J., Shi, L., Liu, L.Y., Zeng, E.Y. (2018) Polycyclic aromatic hydrocarbons affiliated with microplastics in surface waters of Bohai and Huanghai Seas, China. *Environmental Pollution* 241, 834-840.

Malem, F., Soonthondecha, P., Khawmodjod, P., Chunchakorn, V., Whitlow, H.J., Chienthavorn, O. (2019) Occurrence of phthalate esters in the eastern coast of Thailand. *Environmental Monitoring and Assessment* 191.

Marklund, A., Andersson, B., Haglund, P. (2003) Screening of organophosphorus compounds and their distribution in various indoor environments. *Chemosphere* 53, 1137-1146.

McDonough, C.A., De Silva, A.O., Sun, C.X., Cabrerizo, A., Adelman, D., Soltwedel, T., Bauerfeind, E., Muir, D.C.G., Lohmann, R. (2018) Dissolved Organophosphate Esters and Polybrominated Diphenyl Ethers in Remote Marine Environments: Arctic Surface Water Distributions and Net Transport through Fram Strait. *Environmental Science & Technology* 52, 6208-6216.

MEE, C. (2020) Ministry of Ecology and Environment of People's Republic of China. List of Chemicals under Priority Control (Second Batch).

Meng, J., Hong, S.J., Wang, T.Y., Li, Q.F., Yoon, S.J., Lu, Y.L., Giesy, J.P., Khim, J.S. (2017) Traditional and new POPs in environments along the Bohai and Yellow Seas: An overview of China and South Korea. *Chemosphere* 169, 503-515.

Meyer, J., Bester, K. (2004) Organophosphate flame retardants and plasticisers in wastewater treatment plants. *Journal of Environmental Monitoring* 6, 599-605.

- Mi, L.J., Xie, Z.Y., Xu, W.H., Wanick, J.J., Pohlmann, T., Mi, W.Y. (2023) Air-Sea Exchange and Atmospheric Deposition of Phthalate Esters in the South China Sea. *Environmental Science & Technology* 57, 11195-11205.
- Mi, L.J., Xie, Z.Y., Zhao, Z., Zhong, M.Y., Mi, W.Y., Ebinghaus, R., Tang, J.H. (2019) Occurrence and spatial distribution of phthalate esters in sediments of the Bohai and Yellow seas. *Science of the Total Environment* 653, 792-800.
- Mi, L.J., Xie, Z. Y., Zhang, L. L., Wanick, J. J., Pohlmann, T., Mi, W.Y., Xu, W. H. (2023) Organophosphate esters in air and seawater of the South China Sea: Spatial distribution, transport and air-sea exchange. *Environment & Health* 1(3), 12.
- Minh, N.H., Minh, T.B., Kajiwara, N., Kunisue, T., Iwata, H., Viet, P.H., Tu, N.P.C., Tuyen, B.C., Tanabe, S. (2007) Pollution sources and occurrences of selected persistent organic pollutants (POPs) in sediments of the Mekong River delta, South Vietnam. *Chemosphere* 67, 1794-1801.
- Mohammadian, S., Ghanemi, K., Nikpour, Y. (2016) Competitive adsorption of phthalate esters on marine surface sediments: kinetic, thermodynamic, and environmental considerations. *Environmental Science and Pollution Research* 23, 24991-25002.
- Möller, A., Sturm, R., Xie, Z.Y., Cai, M.H., He, J.F., Ebinghaus, R. (2012) Organophosphorus Flame Retardants and Plasticizers in Airborne Particles over the Northern Pacific and Indian Ocean toward the Polar Regions: Evidence for Global Occurrence. *Environmental Science & Technology* 46, 3127-3134.
- Moller, A., Xie, Z.Y., Caba, A., Sturm, R., Ebinghaus, R. (2011) Organophosphorus flame retardants and plasticizers in the atmosphere of the North Sea. *Environmental Pollution* 159, 3660-3665.
- Mondal, T., Mondal, S., Ghosh, S.K., Pal, P., Soren, T., Pandey, S., Maiti, T.K. (2022) Phthalates-A family of plasticizers, their health risks, phytotoxic effects, and microbial bioaugmentation approaches. *Environmental Research* 214.
- Morgan, A.B., Mukhopadhyay, P. (2022) A targeted review of bio-derived plasticizers with flame retardant functionality used in PVC. *Journal of Materials Science* 57, 7155-7172.
- Na, G.S., Hou, C., Li, R.J., Shi, Y.L., Gao, H., Jin, S.C., Gao, Y.Z., Jiao, L.P., Cai, Y.Q. (2020) Occurrence, distribution, air-seawater exchange and atmospheric deposition of organophosphate esters (OPEs) from the Northwestern Pacific to the Arctic Ocean. *Marine Pollution Bulletin* 157.
- Net, S., Sempere, R., Delmont, A., Paluselli, A., Ouddane, B. (2015) Occurrence, Fate, Behavior and Ecotoxicological State of Phthalates in Different Environmental Matrices. *Environmental Science & Technology* 49, 4019-4035.
- Neves, R.A.F., Miralha, A., Guimaraes, T.B., Sorrentino, R., Calderari, M., Santos, L.N. (2023) Phthalates contamination in the coastal and marine sediments of Rio de Janeiro, Brazil. *Marine Pollution Bulletin* 190.
- Newton, S., Sellstrom, U., de Wit, C.A. (2015) Emerging Flame Retardants, PBDEs, and HBCDDs in Indoor and Outdoor Media in Stockholm, Sweden. *Environmental Science & Technology* 49, 2912-2920.
- Nigar, A., Ali, Alkan, Javier Castro-Jiménez, Florian, Royer, Laure, Papillon, Mélanie, Ourgaud, Richard, Sempéré (2021) Environmental occurrence of phthalate and organophosphate esters in sediments across the Gulf of Lion (NW Mediterranean Sea). *Science of the Total Environment* 760, 143412.
- Norman, A., Börjeson, H., David, F., Tienpont, B., Norrgren, L. (2007) Studies of uptake, elimination, and late effects in atlantic salmon (*Salmo salar*) dietary exposed to di-2-ethylhexyl phthalate (DEHP) during early life. *Archives of Environmental Contamination and Toxicology* 52, 235-242.
- Okeme, J.O., Rodgers, T.F.M., Jantunen, L.M., Diamond, M.L. (2018) Examining the Gas-Particle Partitioning of Organophosphate Esters: How Reliable Are Air Measurements? *Environmental Science & Technology* 52, 13834-13844.

- Paluselli, A., Aminot, Y., Galgani, F., Net, S., Sempere, R. (2018a) Occurrence of phthalate acid esters (PAEs) in the northwestern Mediterranean Sea and the Rhone River. *Progress in Oceanography* 163, 221-231.
- Paluselli, A., Fauvelle, V., Galgani, F., Sempere, R. (2019) Phthalate Release from Plastic Fragments and Degradation in Seawater. *Environmental Science & Technology* 53, 166-175.
- Paluselli, A., Fauvelle, V., Schmidt, N., Galgani, F., Net, S., Sempere, R. (2018b) Distribution of phthalates in Marseille Bay (NW Mediterranean Sea). *Science of the Total Environment* 621, 578-587.
- Paluselli, A., Kim, S.K. (2020) Horizontal and vertical distribution of phthalates acid ester (PAEs) in seawater and sediment of East China Sea and Korean South Sea: Traces of plastic debris? *Marine Pollution Bulletin* 151.
- Pan, X.H., Tang, J.H., Li, J., Guo, Z.G., Zhang, G. (2010) Levels and distributions of PBDEs and PCBs in sediments of the Bohai Sea, North China. *Journal of Environmental Monitoring* 12, 1234-1241.
- Pantelaki, I., Voutsas, D. (2022) Occurrence and removal of organophosphate esters in municipal wastewater treatment plants in Thessaloniki, Greece. *Environmental Research* 214.
- Peijnenburg, W.J.G.M., Struijs, J. (2006) Occurrence of phthalate esters in the environment of the Netherlands. *Ecotoxicology and Environmental Safety* 63, 204-215.
- Perterson, D.R., Staples, C.A. (2003) Degradation of Phthalate Esters in the Environment. *The Handbook of Environmental Chemistry*. Springer-Verlag: Berlin/Heidelberg, Berlin.
- Preston, M.R., Alomran, L.A. (1986) Dissolved and Particulate Phthalate-Esters in the River Mersey Estuary. *Marine Pollution Bulletin* 17, 548-553.
- Prieto, A., Zuloaga, O., Usobiaga, A., Etxebarria, N., Fernandez, L.A. (2007) Development of a stir bar sorptive extraction and thermal desorption-gas chromatography-mass spectrometry method for the simultaneous determination of several persistent organic pollutants in water samples. *Journal of Chromatography A* 1174, 40-49.
- Qadeer, A., Anis, M., Warner, G.R., Potts, C., Giovanoulis, G., Nasr, S., Archundia, D., Zhang, Q.H., Ajmal, Z., Tweedale, A.C., Kun, W., Wang, P.F., Ren, H.Y., Jiang, X., Wang, S.H. (2024) Global environmental and toxicological data of emerging plasticizers: current knowledge, regrettable substitution dilemma, green solution and future perspectives. *Green Chemistry* 26, 5635-5683.
- Qi, Y.J., He, Z.S., Yuan, J.J., Ma, X.D., Du, J.Q., Yao, Z.W., Wang, W.F. (2021) Comprehensive evaluation of organophosphate ester contamination in surface water and sediment of the Bohai Sea, China. *Marine Pollution Bulletin* 163.
- Qi, Y.J., Yao, Z.W., Ma, X.D., Ding, X.L., Shangguan, K.X., Zhang, M.X., Xu, N. (2022) Ecological risk assessment for organophosphate esters in the surface water from the Bohai Sea of China using multimodal species sensitivity distributions. *Science of the Total Environment* 820.
- Qiao, S.Q., Shi, X.F., Wang, G.Q., Zhou, L., Hu, B.Q., Hu, L.M., Yang, G., Liu, Y.G., Yao, Z.Q., Liu, S.F. (2017) Sediment accumulation and budget in the Bohai Sea, Yellow Sea and East China Sea. *Marine Geology* 390, 270-281.
- Rafa, N., Ahmed, B., Zohora, F., Bakya, J., Ahmed, S., Ahmed, S.F., Mofijur, M., Chowdhury, A.A., Almomani, F. (2024) Microplastics as carriers of toxic pollutants: Source, transport, and toxicological effects. *Environmental Pollution* 343.
- Regnery, J., Puttmann, W. (2009) Organophosphorus Flame Retardants and Plasticizers in Rain and Snow from Middle Germany. *Clean-Soil Air Water* 37, 334-342.

- Ren, L., Wang, G., Huang, Y.X., Guo, J.F., Li, C.Y., Jia, Y., Chen, S., Zhou, J.L., Hu, H.Q. (2021) Phthalic acid esters degradation by a novel marine bacterial strain *Mycolicibacterium phocaicum* RL-HY01: Characterization, metabolic pathway and bioaugmentation. *Science of the Total Environment* 791.
- Ritsema, R., Cofino, W.P., Frintrop, P.C.M., Brinkman, U.A.T. (1989) Trace-level analysis of phthalate esters in surface-water and suspended particulate matter by means of capillary with electron-capture and mass-selective detection. *Chemosphere* 18, 2161-2175.
- Salamova, A., Ma, Y.N., Venier, M., Hites, R.A. (2014) High Levels of Organophosphate Flame Retardants in the Great Lakes Atmosphere. *Environmental Science & Technology Letters* 1, 8-14.
- Salamova, A., Pevery, A.A., Venier, M., Hites, R.A. (2016) Spatial and Temporal Trends of Particle Phase Organophosphate Ester Concentrations in the Atmosphere of the Great Lakes. *Environmental Science & Technology* 50, 13249-13255.
- Sanchez-Avila, J., Tauler, R., Lacorte, S. (2012) Organic micropollutants in coastal waters from NW Mediterranean Sea: Sources distribution and potential risk. *Environment International* 46, 50-62.
- Schlitzer, R., Ocean Data View. odv.awi.de.
- Schlitzer, R., (2023) Ocean Data View, odv.awi.de.
- Schmidt, C., Krauth, T., Wagner, S. (2017) Export of Plastic Debris by Rivers into the Sea. *Environmental Science & Technology* 51, 12246-12253.
- Schmidt, N., Castro-Jiménez, J., Fauvelle, V., Ourgaud, M., Sempéré, R. (2020) Occurrence of organic plastic additives in surface waters of the Rhone River (France). *Environmental Pollution* 257.
- Schmidt, N., Castro-Jimenez, J., Oursel, B., Sempere, R. (2021) Phthalates and organophosphate esters in surface water, sediments and zooplankton of the NW Mediterranean Sea: Exploring links with microplastic abundance and accumulation in the marine food web. *Environmental Pollution* 272.
- Schmidt, N., Fauvelle, V., Ody, A., Castro-Jimenez, J., Jouanno, J., Changeux, T., Thibaut, T., Sempere, R. (2019) The Amazon River: A Major Source of Organic Plastic Additives to the Tropical North Atlantic? *Environmental Science & Technology* 53, 7513-7521.
- Scholz, N. (2003) Ecotoxicity and biodegradation of phthalate monoesters. *Chemosphere* 53, 921-926.
- Schwarzenbach, R.O., Gschwend, P.M., Imboden, D.M. (2016) *Environmental Organic Chemistry*, 3rd Edition.
- Schwarzenbach, R.P., Gschwend, P.M., Imboden, D.M. (2002) *Environmental organic chemistry*, 2nd ed. John Wiley & Sons, New York.
- Selvaraj, K.K., Sundaramoorthy, G., Ravichandran, P.K., Girijan, G.K., Sampath, S., Ramaswamy, B.R. (2015) Phthalate esters in water and sediments of the Kaveri River, India: environmental levels and ecotoxicological evaluations. *Environmental Geochemistry and Health* 37, 83-96.
- Seyoum, A., Pradhan, A. (2019) Effect of phthalates on development, reproduction, fat metabolism and lifespan in *Daphnia magna*. *Science of the Total Environment* 654, 969-977.
- Sha, Y.J., Xia, X.H., Yang, Z.F., Huang, G.H. (2007) Distribution of PAEs in the middle and lower reaches of the Yellow River, China. *Environmental Monitoring and Assessment* 124, 277-287.
- Shaw, P.T., Chao, S.Y. (1994) Surface circulation in the South China Sea. *Deep-Sea Research Part I-Oceanographic Research Papers* 41, 1663-1683.

- Shen, Q., Yu, H.M., Cao, Y.B., Guo, Z.G., Hu, L.M., Duan, L., Sun, X.S., Lin, T. (2024) Distribution and sources of polycyclic aromatic hydrocarbons in surface sediments of the East China marginal seas: Significance of the terrestrial input and shelf mud deposition. *Marine Pollution Bulletin* 199.
- Shi, X., (2014) *China Coastal seas-marine sediment*. China ocean press, Beijing.
- Shi, Y.F., Zhang, Y., Du, Y.M., Kong, D.G., Wu, Q.H., Hong, Y.G., Wang, Y., Tam, N.F.Y., Leung, J.Y.S. (2020) Occurrence, composition and biological risk of organophosphate esters (OPEs) in water of the Pearl River Estuary, South China. *Environmental Science and Pollution Research* 27, 14852-14862.
- Shore, E.A., Huber, K.E., Garrett, A.D., Pespeni, M.H. (2022) Four plastic additives reduce larval growth and survival in the sea urchin *Strongylocentrotus purpuratus*. *Marine Pollution Bulletin* 175.
- Simcock, A., Halpern, B., Kirubakaran, R., Hossein, M., Polette, M., Smith, E., Inniss, L., Simcock, A. (2016) Coastal, riverine and atmospheric inputs from land. Inniss L, Simcock A, coordinators. *First Global Integrated Marine Assessment*. United Nations, 1-93.
- Sohn, J., Kim, S., Koschorreck, J., Kho, Y., Choi, K. (2016) Alteration of sex hormone levels and steroidogenic pathway by several low molecular weight phthalates and their metabolites in male zebrafish (*Danio rerio*) and/or human adrenal cell (H295R) line. *Journal of Hazardous Materials* 320, 45-54.
- Song, J.W., Zhao, Y., Zhang, Y.Y., Fu, P.Q., Zheng, L.S., Yuan, Q., Wang, S., Huang, X.F., Xu, W.H., Cao, Z.X., Gromov, S., Lai, S.C. (2018) Influence of biomass burning on atmospheric aerosols over the western South China Sea: Insights from ions, carbonaceous fractions and stable carbon isotope ratios. *Environmental Pollution* 242, 1800-1809.
- Souaf, B., Methneni, N., Beltifa, A., Turco, V.L., Danioux, A., Litrenta, F., Sedrati, M., Mansour, H.B., Di Bella, G. (2023) Occurrence and seasonal variation of plasticizers in sediments and biota from the coast of Mahdia, Tunisia. *Environmental Science and Pollution Research* 30, 48532-48545.
- Staples, A., Adams, W.J., Parkerton, T.F., Gorsuch, J.W., Biddinger, G.R., Reinert, K.H. (1997a) Aquatic toxicity of eighteen phthalate esters. *Environmental Toxicology and Chemistry* 16, 875-891.
- Staples, C.A., Guinn, R., Kramarz, K., Lampi, M. (2011) Assessing the Chronic Aquatic Toxicity of Phthalate Ester Plasticizers. *Human and Ecological Risk Assessment* 17, 1057-1076.
- Staples, C.A., Peterson, D.R., Parkerton, T.F., Adams, W.J. (1997b) The environmental fate of phthalate esters: A literature review. *Chemosphere* 35, 667-749.
- Stein, A.F., Draxler, R.R., Rolph, G.D., Stunder, B.J.B., Cohen, M.D., Ngan, F. (2015a) NOAA'S HYSPLIT ATMOSPHERIC TRANSPORT AND DISPERSION MODELING SYSTEM. *Bulletin of the American Meteorological Society* 96, 2059-2077.
- Stein, A.F., Draxler, R.R., Rolph, G.D., Stunder, B.J.B., Cohen, M.D., Ngan, F. (2015b) NOAA's HYSPLIT atmospheric transport and dispersion modeling system. *Bulletin of the American Meteorological Society* 96, 2059-2077.
- Stein, A.F., Draxler, R.R., Rolph, G.D., Stunder, B.J.B., Cohen, M.D., Ngan, F. (2015c) NOAA'S HYSPLIT Atmospheric Transport and Dispersion Modeling System. *Bulletin of the American Meteorological Society* 96, 2059-2077.
- Stewart, M., Olsen, G., Hickey, C.W., Ferreira, B., Jelic, A., Petrovic, M., Barcelo, D. (2014) A survey of emerging contaminants in the estuarine receiving environment around Auckland, New Zealand. *Science of the Total Environment* 468, 202-210.
- Stoppa, F., Schiavza, M., Pellegrini, J., Ambrosio, F.A., Rosatelli, G., D'Orsogna, M.R. (2017) Phthalates, heavy metals and PAHs in an overpopulated coastal region: Inferences from Abruzzo, central Italy. *Marine Pollution Bulletin* 125, 501-512.

- Su, J., Yuan, Y., (2005) Hydrology in China Coastal Sea. China ocean press, Beijing.
- Sudaryanto, A., Isobe, T., Takahashi, S., Tanabe, S. (2011) Assessment of persistent organic pollutants in sediments from Lower Mekong River Basin. *Chemosphere* 82, 679-686.
- Sühring, R., Diamond, M.L., Scheringer, M., Wong, F., Pucko, M., Stern, G., Burt, A., Hung, H., Fellin, P., Li, H., Jantunen, L.M. (2016) Organophosphate Esters in Canadian Arctic Air: Occurrence, Levels and Trends. *Environmental Science & Technology* 50, 7409-7415.
- Suhring, R., Wolschke, H., Diamond, M.L., Jantunen, L.M., Scheringer, M. (2016) Distribution of Organophosphate Esters between the Gas and Particle Phase-Model Predictions vs Measured Data. *Environmental Science & Technology* 50, 6644-6651.
- Sun, H., Mi, W., Li, X., Wang, S., Yan, J., Zhang, G. (2024) Organophosphate ester in surface water of the Pearl River and South China Sea, China: Spatial variations and ecological risks. *Chemosphere*, 142559.
- Sun, J.Q., Huang, J., Zhang, A.P., Liu, W.P., Cheng, W.W. (2013) Occurrence of phthalate esters in sediments in Qiantang River, China and inference with urbanization and river flow regime. *Journal of Hazardous Materials* 248, 142-149.
- Sun, S.B., Jiang, J.Q., Zhao, H.X., Wan, H.H., Qu, B.C. (2020) Photochemical reaction of tricresyl phosphate (TCP) in aqueous solution: Influencing factors and photolysis products. *Chemosphere* 241.
- Takeuchi, S., Kojima, H., Saito, I., Jin, K., Kobayashi, S., Tanaka-Kagawa, T., Jinno, H. (2014) Detection of 34 plasticizers and 25 flame retardants in indoor air from houses in Sapporo, Japan. *Science of the Total Environment* 491, 28-33.
- Tan, G.H. (1995) Residue Levels of Phthalate-Esters in Water and Sediment Samples from the Klang River Basin. *Bulletin of Environmental Contamination and Toxicology* 54, 171-176.
- Tan, X.-X., Luo, X.-J., Zheng, X.-B., Li, Z.-R., Sun, R.-X., Mai, B.-X. (2016) Distribution of organophosphorus flame retardants in sediments from the Pearl River Delta in South China. *Science of the Total Environment* 544, 77-84.
- Teil, M.J., Blanchard, M., Chevreuil, M. (2006) Atmospheric fate of phthalate esters in an urban area (Paris-France). *Science of the Total Environment* 354, 212-223.
- Tembhare, S.P., Bhanvase, B.A., Barai, D.P., Dhoble, S.J. (2022) E-waste recycling practices: a review on environmental concerns, remediation and technological developments with a focus on printed circuit boards. *Environment Development and Sustainability* 24, 8965-9047.
- Turner, A., Rawling, M.C. (2000) The behaviour of di-(2-ethylhexyl) phthalate in estuaries. *Marine Chemistry* 68, 203-217.
- van der Veen, I., de Boer, J. (2012) Phosphorus flame retardants: Properties, production, environmental occurrence, toxicity and analysis. *Chemosphere* 88, 1119-1153.
- Wang, A.M., Wang, H.J., Bi, N.S., Wu, X. (2016) Sediment Transport and Dispersal Pattern from the Bohai Sea to the Yellow Sea. *Journal of Coastal Research*, 104-116.
- Wang, C.J., Wang, Z.W., Hui, F., Zhang, X.S. (2019a) Speciated atmospheric mercury and sea-air exchange of gaseous mercury in the South China Sea. *Atmospheric Chemistry and Physics* 19, 10111-10127.
- Wang, C.Y., Zeng, T., Gu, C.T., Zhu, S.P., Zhang, Q.Q., Luo, X.P. (2019b) Photodegradation Pathways of Typical Phthalic Acid Esters Under UV, UV/TiO₂, and UV-Vis/Bi₂WO₆ Systems. *Frontiers in Chemistry* 7.

- Wang, F., Li, X.G., Tang, X.H., Sun, X.X., Zhang, J.L., Yang, D.Z., Xu, L.J., Zhang, H., Yuan, H.M., Wang, Y.T., Yao, Y.L., Wang, C.Z., Guo, Y.R., Ren, Q.P., Li, Y.L., Zhang, R.W., Wang, X., Zhang, B., Sha, Z.L. (2023) The seas around China in a warming climate. *Nature Reviews Earth & Environment* 4, 535-551.
- Wang, H.B., Yu, P.F., Schwarz, C., Zhang, B., Huo, L.X., Shi, B.Y., Alvarez, P.J.J. (2022a) Phthalate Esters Released from Plastics Promote Biofilm Formation and Chlorine Resistance. *Environmental Science & Technology* 56, 1081-1090.
- Wang, J., Bo, L.J., Li, L.N., Wang, D.J., Chen, G.C., Christie, P., Teng, Y. (2014) Occurrence of phthalate esters in river sediments in areas with different land use patterns. *Science of the Total Environment* 500, 113-119.
- Wang, L.Y., Gu, Y.Y., Zhang, Z.M., Sun, A.L., Shi, X.Z., Chen, J., Lu, Y. (2021) Contaminant occurrence, mobility and ecological risk assessment of phthalate esters in the sediment-water system of the Hangzhou Bay. *Science of the Total Environment* 770.
- Wang, Q.Z., Zhao, H.X., Wang, Y., Xie, Q., Chen, J.W., Quan, X. (2017a) Determination and prediction of octanol-air partition coefficients for organophosphate flame retardants. *Ecotoxicology and Environmental Safety* 145, 283-288.
- Wang, R.M., Tang, J.H., Xie, Z.Y., Mi, W.Y., Chen, Y.J., Wolschke, H., Tian, C.G., Pan, X.H., Luo, Y.M., Ebinghaus, R. (2015) Occurrence and spatial distribution of organophosphate ester flame retardants and plasticizers in 40 rivers draining into the Bohai Sea, north China. *Environmental Pollution* 198, 172-178.
- Wang, R.M., Zhang, J., Yang, Y.Y., Chen, C.E., Zhang, D.C., Tang, J.H. (2022b) Emerging and legacy per-and polyfluoroalkyl substances in the rivers of a typical industrialized province of China: Spatiotemporal variations, mass discharges and ecological risks. *Frontiers in Environmental Science* 10.
- Wang, X., Zhu, Q., Yan, X., Wang, Y., Liao, C., Jiang, G. (2020) A review of organophosphate flame retardants and plasticizers in the environment: Analysis, occurrence and risk assessment. *Sci Total Environ* 731, 139071.
- Wang, Y., Wu, X., Zhang, Q., Hou, M., Zhao, H., Xie, Q., Du, J., Chen, J. (2017b) Organophosphate esters in sediment cores from coastal Laizhou Bay of the Bohai Sea, China. *Science of the Total Environment* 607, 103-108.
- Wang, Y., Wu, X., Zhang, Q., Zhao, H., Hou, M., Xie, Q., Chen, J. (2018) Occurrence, distribution, and air-water exchange of organophosphorus flame retardants in a typical coastal area of China. *Chemosphere* 211, 335-344.
- Wang, Y., Zhu, H.K., Kannan, K. (2019c) A Review of Biomonitoring of Phthalate Exposures. *Toxics* 7.
- Wania, F., Mackay, D. (1996) Tracking the distribution of persistent organic pollutants. *Environmental Science & Technology* 30, A390-A396.
- Wanick, J.J., (2021) Megacity's fingerprint in Chinese marginal seas.
- Wanninkhof, R. (1992) Relationship between wind-speed and gas-exchange over the ocean. *Journal of Geophysical Research-Oceans* 97, 7373-7382.
- Wanninkhof, R. (2014) Relationship between wind speed and gas exchange over the ocean revisited. *Limnology and Oceanography-Methods* 12, 351-362.
- Wanninkhof, R., Sullivan, K.F., Top, Z. (2004) Air-sea gas transfer in the Southern Ocean. *Journal of Geophysical Research-Oceans* 109.

- Wei, G.L., Li, D.Q., Zhuo, M.N., Liao, Y.S., Xie, Z.Y., Guo, T.L., Li, J.J., Zhang, S.Y., Liang, Z.Q. (2015) Organophosphorus flame retardants and plasticizers: Sources, occurrence, toxicity and human exposure. *Environmental Pollution* 196, 29-46.
- Wei, Q.S., Wang, B.D., Zhang, X.L., Ran, X.B., Fu, M.Z., Sun, X., Yu, Z.G. (2021) Contribution of the offshore detached Changjiang (Yangtze River) Diluted Water to the formation of hypoxia in summer. *Science of the Total Environment* 764.
- Weir, S.M., Wooten, K.J., Smith, P.N., Salice, C.J. (2014) Phthalate ester leachates in aquatic mesocosms: Implications for ecotoxicity studies of endocrine disrupting compounds. *Chemosphere* 103, 44-50.
- Wolecki, D., Trella, B., Qi, F., Stepnowski, P., Kumirska, J. (2021) Evaluation of the Removal of Selected Phthalic Acid Esters (PAEs) in Municipal Wastewater Treatment Plants Supported by Constructed Wetlands. *Molecules* 26.
- Wu, J.H., Zhang, Y.F., Song, L., Yang, M., Liu, X., Yu, J.H., Liang, G.Z., Zhang, Y.M. (2022) Occurrence and dry deposition of organophosphate esters in atmospheric particles above the Bohai Sea and northern Yellow Sea, China. *Atmospheric Environment* 269.
- Wu, Y., Venier, M., Salamova, A. (2020) Spatioseasonal Variations and Partitioning Behavior of Organophosphate Esters in the Great Lakes Atmosphere. *Environmental Science & Technology* 54, 5400-5408.
- Xiao, K.Y., Lu, Z.B., Yang, C., Zhao, S., Zheng, H.Y., Gao, Y., Kaluwin, C., Liu, Y.G., Cai, M.H. (2021) Occurrence, distribution and risk assessment of organophosphate ester flame retardants and plasticizers in surface seawater of the West Pacific. *Marine Pollution Bulletin* 170.
- Xiao, X., Ma, Q., Cheng, H. (2010) Distribution of BDP and DEHP in superficial sediment of Laizhou Bay. *Mar. Environ. Sci* 29, 337-341.
- Xie, C.M., Qiu, N., Xie, J.L., Guan, Y.F., Xu, W.H., Zhang, L., Sun, Y.X. (2024) Organophosphate esters in seawater and sediments from the low-latitude tropical sea. *Science of the Total Environment* 907.
- Xie, Z. (2005) Development and validation of a method for the determination of trace alkylphenols and phthalates in sea water and air using GC-MS. *Leuphana University Lüneburg*.
- Xie, Z.Y., Ebinghaus, R., Temme, C., Caba, A., Ruck, W. (2005) Atmospheric concentrations and air-sea exchanges of phthalates in the North Sea (German Bight). *Atmospheric Environment* 39, 3209-3219.
- Xie, Z.Y., Ebinghaus, R., Temme, C., Lohmann, R., Caba, A., Ruck, W. (2007) Occurrence and air-sea exchange of phthalates in the arctic. *Environmental Science & Technology* 41, 4555-4560.
- Xie, Z.Y., Selzer, J., Ebinghaus, R., Caba, A., Ruck, W. (2006) Development and validation of a method for the determination of trace alkylphenols and phthalates in the atmosphere. *Analytica Chimica Acta* 565, 198-207.
- Xie, Z.Y., Wang, P., Wang, X., Castro-Jimenez, J., Kallenborn, R., Liao, C.Y., Mi, W.Y., Lohmann, R., Vila-Costa, M., Dachs, J. (2022a) Organophosphate ester pollution in the oceans. *Nature Reviews Earth & Environment* 3, 309-322.
- Xie, Z.Y., Zhang, P., Wu, Z.L., Zhang, S., Wei, L.J., Mi, L.J., Kuester, A., Gandrass, J., Ebinghaus, R., Yang, R.Q., Wang, Z., Mi, W.Y. (2022b) Legacy and emerging organic contaminants in the polar regions. *Science of the Total Environment* 835.
- Xu, H., Liu, Y., Xu, X., Lan, H.C., Qi, W.X., Wang, D.H., Liu, H.J., Qu, J.H. (2022) Spatiotemporal variation and risk assessment of phthalate acid esters (PAEs) in surface water of the Yangtze River Basin, China. *Science of the Total Environment* 836.

- Xu, H., Shao, X.L., Zhang, Z., Zou, Y.M., Chen, Y., Han, S.L., Wang, S.S., Wu, X.Y., Yang, L.Q., Chen, Z.L. (2013) Effects of Di-n-butyl Phthalate and Diethyl Phthalate on Acetylcholinesterase Activity and Neurotoxicity Related Gene Expression in Embryonic Zebrafish. *Bulletin of Environmental Contamination and Toxicology* 91, 635-639.
- Xu, L.L., Cao, L., Huang, W., Liu, J.H., Dou, S.Z. (2021) Assessment of plastic pollution in the Bohai Sea: Abundance, distribution, morphological characteristics and chemical components. *Environmental Pollution* 278.
- Xu, X.R., Li, X.Y. (2009) Sorption behaviour of benzyl butyl phthalate on marine sediments: Equilibrium assessments, effects of organic carbon content, temperature and salinity. *Marine Chemistry* 115, 66-71.
- Yadav, I.C., Devi, N.L., Zhong, G.C., Li, J., Zhang, G., Covaci, A. (2017) Occurrence and fate of organophosphate ester flame retardants and plasticizers in indoor air and dust of Nepal: Implication for human exposure. *Environmental Pollution* 229, 668-678.
- Yang, D., Feng, L., Li, M., Duan, X., Zhang, D., Li, X. (2016) Occurrence and distribution characteristics of phthalic acid esters (PAEs) in surface sediments of the East China Sea. *Periodical of Ocean University of China* 46, 74-81.
- Yang, L., Zhou, Y.Q., Shi, B., Meng, J., He, B., Yang, H.F., Yoon, S.J., Kim, T., Kwon, B.O., Khim, J.S., Wang, T.Y. (2020a) Anthropogenic impacts on the contamination of pharmaceuticals and personal care products (PPCPs) in the coastal environments of the Yellow and Bohai seas. *Environment International* 135.
- Yang, S.Y., Jung, H.S., Lim, D.I., Li, C.X. (2003) A review on the provenance discrimination of sediments in the Yellow Sea. *Earth-Science Reviews* 63, 93-120.
- Yang, W.L., Braun, J.M., Vuong, A.M., Percy, Z., Xu, Y.Y., Xie, C.C., Deka, R., Calafat, A.M., Ospina, M., Yolton, K., Cecil, K.M., Lanphear, B.P., Chen, A.M. (2022) Maternal urinary organophosphate ester metabolite concentrations and glucose tolerance during pregnancy: The HOME Study. *International Journal of Hygiene and Environmental Health* 245.
- Yang, X.L., Miao, X., Wu, J.L., Duan, Z.W., Yang, R., Tang, Y.H. (2020b) Towards Holistic Governance of China's E-Waste Recycling: Evolution of Networked Policies. *International Journal of Environmental Research and Public Health* 17.
- Ye, L.J., Su, G.Y. (2022) Elevated concentration and high Diversity of organophosphate esters (OPEs) were Discovered in Sediment from Industrial, and E-Waste Recycling Areas. *Water Research* 217.
- Yin, H.L., Luo, Y., Song, J.J., Li, S.P., Lin, S.Y., Xiong, Y.M., Fang, S.H., Tang, J. (2022) Pollution characteristics and emissions of typical organophosphate esters of a wastewater treatment plant. *Environmental Science and Pollution Research* 29, 25892-25901.
- Yong, J.L., Ren, S.M., Zhang, S.Q., Wu, G.X., Shao, C.X., Zhao, H.R., Yu, X.L., Li, M.K., Gao, Y. (2022) The Behavior of Moist Potential Vorticity in the Interactions of Binary Typhoons Lekima and Krosa (2019) in with Different High-Resolution Simulations. *Atmosphere* 13.
- Yoon, S.J., Hong, S., Kim, S., Lee, J., Kim, T., Kim, B., Kwon, B.O., Zhou, Y.Q., Shi, B., Liu, P., Hu, W.Y., Huang, B., Wang, T.Y., Khim, J.S. (2020) Large-scale monitoring and ecological risk assessment of persistent toxic substances in riverine, estuarine, and coastal sediments of the Yellow and Bohai seas. *Environment International* 137.
- Zeng, F., Cui, K.Y., Xie, Z.Y., Liu, M., Li, Y.J., Lin, Y.J., Zeng, Z.X., Li, F.B. (2008) Occurrence of phthalate esters in water and sediment of urban lakes in a subtropical city, Guangzhou, South China. *Environment International* 34, 372-380.

- Zeng, X., He, L., Cao, S., Ma, S., Yu, Z., Gui, H., Sheng, G., Fu, J. (2014) Occurrence and distribution of organophosphate flame retardants/plasticizers in wastewater treatment plant sludges from the Pearl River Delta, China. *Environmental Toxicology and Chemistry* 33, 1720-1725.
- Zeng, X.Y., Xu, L., Hu, Q.P., Liu, Y., Hu, J.F., Liao, W.S., Yu, Z.Q. (2020a) Occurrence and distribution of organophosphorus flame retardants/plasticizers in coastal sediments from the Taiwan Strait in China. *Marine Pollution Bulletin* 151.
- Zeng, Y., Ding, N., Wang, T., Tian, M., Fan, Y., Wang, T., Chen, S.J., Mai, B.X. (2020b) Organophosphate esters (OPEs) in fine particulate matter (PM_{2.5}) in urban, e-waste, and background regions of South China. *Journal of Hazardous Materials* 385.
- Zhang, F., Zhao, Y.T., Wang, D.D., Yan, M.Q., Zhang, J., Zhang, P.Y., Ding, T.G., Chen, L., Chen, C. (2021a) Current technologies for plastic waste treatment: A review. *Journal of Cleaner Production* 282.
- Zhang, F.R., Chen, H., Liu, Y.X., Wang, M.X. (2023) Phthalate acid ester release from microplastics in water environment and their comparison between single and competitive adsorption. *Environmental Science and Pollution Research* 30, 118964-118975.
- Zhang, G.Y., Zhang, Y.Y., Mi, W.Y., Wang, Z., Lai, S.C. (2022a) Organophosphate esters in atmospheric particles and surface seawater in the western South China Sea. *Environmental Pollution* 292.
- Zhang, H.B., Zhou, Q., Xie, Z.Y., Zhou, Y., Tu, C., Fu, C.C., Mi, W.Y., Ebinghaus, R., Christie, P., Luo, Y.M. (2018a) Occurrences of organophosphorus esters and phthalates in the microplastics from the coastal beaches in north China. *Science of the Total Environment* 616, 1505-1512.
- Zhang, H.K., Chao, Z., Huang, Y.F., Yi, X.H., Liang, X.J., Lee, C.G., Huang, M.Z., Ying, G.G. (2022b) Contamination of typical phthalate acid esters in surface water and sediment of the Pearl River, South China: Occurrence, distribution, and health risk assessment. *Journal of Environmental Science and Health Part a-Toxic/Hazardous Substances & Environmental Engineering* 57, 130-138.
- Zhang, L., Lohmann, R. (2010) Cycling of PCBs and HCB in the Surface Ocean-lower Atmosphere of the Open Pacific. *Environmental Science & Technology* 44, 3832-3838.
- Zhang, L., Lu, L., Zhu, W.J., Yang, B., Lu, D.L., Dan, S.F., Zhang, S.F. (2021b) Organophosphorus flame retardants (OPFRs) in the seawater and sediments of the Qinzhou Bay, Northern Beibu Gulf: Occurrence, distribution, and ecological risks. *Marine Pollution Bulletin* 168.
- Zhang, L., Xu, W., Mi, W., Yan, W., Guo, T., Zhou, F., Miao, L., Xie, Z. (2022c) Atmospheric deposition, seasonal variation, and long-range transport of organophosphate esters on Yongxing Island, South China Sea. *Science of the Total Environment* 806, 150673.
- Zhang, L.L., Xu, W.H., Mi, W.Y., Yan, W., Guo, T.F., Zhou, F.H., Miao, L., Xie, Z.Y. (2022d) Atmospheric deposition, seasonal variation, and long-range transport of organophosphate esters on Yongxing Island, South China Sea. *Science of the Total Environment* 806.
- Zhang, Q., Song, J.M., Li, X.G., Peng, Q.C., Yuan, H.M., Li, N., Duan, L.Q., Ma, J. (2019a) Concentrations and distribution of phthalate esters in the seamount area of the Tropical Western Pacific Ocean. *Marine Pollution Bulletin* 140, 107-115.
- Zhang, Q.Q., Ma, Z.R., Cai, Y.Y., Li, H.R., Ying, G.G. (2021c) Agricultural Plastic Pollution in China: Generation of Plastic Debris and Emission of Phthalic Acid Esters from Agricultural Films. *Environmental Science & Technology* 55, 12459-12470.
- Zhang, R., Yu, K., Li, A., Zeng, W., Lin, T., Wang, Y. (2020a) Occurrence, phase distribution, and bioaccumulation of organophosphate esters (OPEs) in mariculture farms of the Beibu Gulf, China: A health risk assessment through seafood consumption. *Environmental Pollution* 263, 114426.
- Zhang, R.J., Kang, Y.R., Yu, K.F., Han, M.W., Wang, Y.H., Huang, X.Y., Ding, Y., Wang, R.X., Pei, J.Y. (2021d) Occurrence, distribution, and fate of polychlorinated biphenyls (PCBs) in multiple coral

reef regions from the South China Sea: A case study in spring-summer. *Science of the Total Environment* 777.

Zhang, W.Z., Zheng, X.W., Gu, P., Wang, N., Lai, Z.N., He, J., Zheng, Z. (2020b) Distribution and risk assessment of phthalates in water and sediment of the Pearl River Delta. *Environmental Science and Pollution Research* 27, 12550-12565.

Zhang, X., Wang, Q., Qiu, T., Tang, S., Li, J., Giesy, J.P., Zhu, Y., Hu, X.J., Xu, D.Q. (2019b) PM_{2.5} bound phthalates in four metropolitan cities of China: Concentration, seasonal pattern and health risk via inhalation. *Science of the Total Environment* 696.

Zhang, Y.F., Liang, G.Z., Liu, Z.Q., Wu, J.H., Wang, Z.H., Liu, X., Yang, M., Wang, W.W. (2024) Gas-particle partitioning and dry deposition of atmospheric parent, alkylated, nitrated and hydroxyl polycyclic aromatic hydrocarbons over the Bohai sea and northern Yellow sea in autumn. *Atmospheric Environment* 318.

Zhang, Y.L., Kang, S.C., Allen, S., Allen, D., Gao, T.G., Sillanpää, M. (2020c) Atmospheric microplastics: A review on current status and perspectives. *Earth-Science Reviews* 203.

Zhang, Z.M., Wang, L.Y., Gu, Y.Y., Sun, A.L., You, J.J., Shi, X.Z., Chen, J. (2021e) Probing the contamination characteristics, mobility, and risk assessments of typical plastic additive-phthalate esters from a typical coastal aquaculture area, China. *Journal of Hazardous Materials* 416.

Zhang, Z.M., Zhang, H.H., Li, J.L., Yang, G.P. (2017) Determination of Phthalic Acid Esters in Seawater and Sediment by Solid-phase Microextraction and Gas Chromatography-Mass Spectrometry. *Chinese Journal of Analytical Chemistry* 45, 348-355.

Zhang, Z.M., Zhang, H.H., Zhang, J., Wang, Q.W., Yang, G.P. (2018b) Occurrence, distribution, and ecological risks of phthalate esters in the seawater and sediment of Changjiang River Estuary and its adjacent area. *Science of the Total Environment* 619, 93-102.

Zhang, Z.M., Zhang, H.H., Zou, Y.W., Yang, G.P. (2018c) Distribution and ecotoxicological state of phthalate esters in the sea-surface microlayer, seawater and sediment of the Bohai Sea and the Yellow Sea. *Environmental Pollution* 240, 235-247.

Zhang, Z.M., Zhang, J., Zhang, H.H., Shi, X.Z., Zou, Y.W., Yang, G.P. (2020d) Pollution characteristics, spatial variation, and potential risks of phthalate esters in the water-sediment system of the Yangtze River estuary and its adjacent East China Sea. *Environmental Pollution* 265.

Zhao, J.M., Ran, W., Teng, J., Liu, Y.L., Liu, H., Yin, X.N., Cao, R.W., Wang, Q. (2018) Microplastic pollution in sediments from the Bohai Sea and the Yellow Sea, China. *Science of the Total Environment* 640, 637-645.

Zhao, Z., Tang, J.H., Xie, Z.Y., Chen, Y.J., Pan, X.H., Zhong, G.C., Sturm, R., Zhang, G., Ebinghaus, R. (2013) Perfluoroalkyl acids (PFAAs) in riverine and coastal sediments of Laizhou Bay, North China. *Science of the Total Environment* 447, 415-423.

Zhao, Z., Zhong, G.C., Möller, A., Xie, Z.Y., Sturm, R., Ebinghaus, R., Tang, J.H., Zhang, G. (2011) Levels and distribution of Dechlorane Plus in coastal sediments of the Yellow Sea, North China. *Chemosphere* 83, 984-990.

Zheng, L.W., Zhai, W.D. (2021) Excess nitrogen in the Bohai and Yellow seas, China: Distribution, trends, and source apportionment. *Science of the Total Environment* 794.

Zhong, G.C., Tang, J.H., Xie, Z.Y., Mi, W.Y., Chen, Y.J., Möller, A., Sturm, R., Zhang, G., Ebinghaus, R. (2015) Selected current-use pesticides (CUPs) in coastal and offshore sediments of Bohai and Yellow seas. *Environmental Science and Pollution Research* 22, 1653-1661.

Zhong, M.Y., (2018) Studies on the toxicological effects of tris(1,3-dichloroisopropyl) phosphate in oyster *Crassostrea gigas*. Yantai Institute of Coastal Zone Research, Yantai.

Zhong, M.Y., Tang, J.H., Guo, X.Y., Guo, C., Li, F., Wu, H.F. (2020) Occurrence and spatial distribution of organophosphorus flame retardants and plasticizers in the Bohai, Yellow and East China seas. *Science of the Total Environment* 741.

Zhong, M.Y., Tang, J.H., Mi, L.J., Li, F., Wang, R.M., Huang, G.P., Wu, H.F. (2017) Occurrence and spatial distribution of organophosphorus flame retardants and plasticizers in the Bohai and Yellow Seas, China. *Marine Pollution Bulletin* 121, 331-338.

Zhong, M.Y., Wu, H.F., Mi, W.Y., Li, F., Ji, C.L., Ebinghaus, R., Tang, J.H., Xie, Z.Y. (2018) Occurrences and distribution characteristics of organophosphate ester flame retardants and plasticizers in the sediments of the Bohai and Yellow Seas, China. *Science of the Total Environment* 615, 1305-1311.

Zhou, B., Zhao, L.X., Sun, Y., Li, X.J., Weng, L.P., Li, Y.T. (2021) Contamination and human health risks of phthalate esters in vegetable and crop soils from the Huang-Huai-Hai region of China. *Science of the Total Environment* 778.

Zhu, J., Hu, J.Y., Zheng, Q.A. (2022a) An overview on water masses in the China seas. *Frontiers in Marine Science* 9.

Zhu, Q.Q., Xu, L.Y., Wang, W.Y., Liu, W.B., Liao, C.Y., Jiang, G.B. (2022b) Occurrence, spatial distribution and ecological risk assessment of phthalate esters in water, soil and sediment from Yangtze River Delta, China. *Science of the Total Environment* 806.

Zhu, Z.Y., Ji, Y.Q., Zhang, S.J., Zhao, J.B., Zhao, J. (2016) Phthalate Ester Concentrations, Sources, and Risks in the Ambient Air of Tianjin, China. *Aerosol and Air Quality Research* 16, 2294-2301.

Zhuang, W.-E., Yao, W.-S., Wang, X.-X., Huang, D., Gong, Z. (2011) Distribution and chemical composition of phthalate esters in seawater and sediments in Quanzhou Bay, China. *Journal of Environment and Health* 28, 898-902.